DOE/MC/21181-1950, Vol. 9
(DE88001007)
Distribution Category UC-132

Geological Evolution and Analysis of Confirmed or Suspected Gas Hydrate Localities

Volume 9. Formation and Stability of Gas Hydrates of the Middle America Trench

P. Finley
J. Krason

Work Performed Under Contract No.: DE-AC21-84MC21181

For
U.S. Department of Energy
Office of Fossil Energy
Morgantown Energy Technology Center
P.O. Box 880
Morgantown, West Virginia 26507-0880

By
Geoexplorers International, Inc.
5701 East Evans Avenue
Denver, Colorado 80222

December 1986

PREFACE

This document is Volume IX of a series of reports entitled "Geological Evolution and Analysis of Confirmed or Suspected Gas Hydrate Localities." Volume IX is a study titled "Basin Analysis, Formation and Stability of Gas Hydrates of the Middle America Trench." This report presents a geological description of the Pacific margin of Mexico and Central America, including regional and local structural settings, geomorphology, geological history, stratigraphy, and physical properties. It provides a the necessary regional and geological background for more in-depth research of the area. Detailed discussion of bottom simulating acoustic reflectors, sediment acoustic properties, and distribution of hydrates within the sediments are also included in this report. The formation and stabilization of gas hydrates in sediments are considered in terms of phase relations, nucleation, and crystallization constraints, gas solubility, pore fluid chemistry, inorganic diagenesis, and sediment organic content. Together with a depositional analysis of the area, this report is a better understanding of the thermal evolution of the locality. It should lead to an assessment of the potential for both biogenic and thermogenic hydrocarbon generation.

Project Manager
Gas Hydrates

CONTENTS

Executive summary 1

Introduction 4
Acknowledgements 5

Part I
Basin analysis 6
Location and geomorphology 6
Regional tectonics 9
Plate tectonic setting 10
Cocos Plate 10
Rivera Plate 12
North America Plate 12
Caribbean Plate 12
Structural development 12
Offshore of Mexico 13
Offshore of Guatemala 16
Offshore of Costa Rica 19
Caribbean-North America-Cocos Triple Junction 20
Tehuantepec Ridge 20
The Caribbean-North America Plate Boundary 21
Synthesis 23
Lithostratigraphy 27
DSDP Leg 66 27
Site 486 27
Site 487 27
Site 488 31
Site 489 31
Site 490 32
Site 491 32
Site 492 32
Site 493 33
DSDP Leg 67 33
Cocos Plate 33
Trench floor 37
Lower slope 38
Upper slope 39
DSDP Leg 84 40
Site 565 41
Site 566 41

Site 567 41
Site 568 42
Site 569 45
Site 570 45
Geothermal gradients 46
Hydrocarbon generation 46
DSDP Leg 66 47
DSDP Leg 67 48
DSDP Leg 84 49
Forearc basin 50
Source of hydrocarbons in metamorphic rocks 56
Slope sediments 59
Subducted sediments 59
Sub-thrust sediments 61
In situ generation 62

Part II
Formation and stability of gas hydrates 65
Direct evidence of gas hydrates 65
DSDP Leg 66 66
DSDP Leg 67 68
Site 495 68
Site 499 68
Site 500 68
Site 494 68
Site 498 69
Site 497 69
Site 496 69
DSDP Leg 84 71
Site 565 71
Site 566 74
Site 567 76
Site 569 76
Site 568 77
Site 570 91
Gas concentrations 91
Isotopic data 98
Summary 106
Seismic evidence of gas hydrates 107
Multichannel seismic lines 107
Offshore Mexico 107
Offshore Guatemala 118
Offshore Nicaragua and Costa Rica 127
Single channel seismic lines 129
Pore water chemistry 136
DSDP Leg 66 136
DSDP Leg 67 136
DSDP Leg 84 138
Discussion 141
Agreements with geological data 142
Gas volumes 143
Differences in chemical parameters 144

Multiple fractionation 150
Summary 158
Massive gas hydrate formation 160
Massive gas hydrate formation model 160
Dolomite cap rock 163
Descrition 164
Physical properties 167
Well logs 171
Summary 175
Tectonic uplift 177
Timing 177
Rate 178
Eustatic sea level change 181
Effect of uplift 181
Source of gas 193
Summary 198
Alternative massive gas hydrate formation model 198
Geological evidence for faulting 203
Geochemical evidence for faulting 204
Summary 211
Factors controlling gas hydrate formation 212
Host lithologies 212
Gas composition 213
Sedimentation rates 213
DSDP Leg 66 214
DSDP Leg 67 214
DSDP Leg 84 214
Structural geology 216
Fractures 216
Faults 218
Large-scale tectonics 218
Assessment of gas resources in gas hydrates 223
Offshore Mexico 223
Offshore Guatemala 225
Offshore Costa Rica and Nicaragua 227
Conclusions 228

References 230

ILLUSTRATIONS

Figure 1. Bathymetric map of the Middle America Trench study region west of 95°W longitude 7

2. Bathymetric map of the Middle America Trench study region east of 95°W longitude 8

3. Regional tectonic map of the Middle America Trench. 11

4. Seismic line MX-16 offshore Mexico and interpreted cross-section 15

5. Seismic line GUA-13 offshore Guatemala 18

6. Structure of the North America-Caribbean-Cocos Plate triple junction 22

7. Reconstruction of Middle America Trench before offset along Polochic Fault. 24

8. Structure of subducted Cocos Plate 25

9. Reconstruction of subducted Cocos Plate in late Miocene based on present Benioff zone geometry 26

10. Detailed bathymetric map of the continental margin of Mexico 28

11. Composite seismic section of Middle America Trench showing location of DSDP Leg 66 sites 29

12. Lithostratigraphy of DSDP Leg 66 sites 30

13. Location of DSDP sites offshore of Guatemala 34

14. Seismic line GUA-13 offshore of Guatemala showing locations of DSDP Leg 67 sites. 35

15. Lithostratigraphy of DSDP Leg 67 sites 36

16. Lithostratigraphy of DSDP Leg 84 sites 43

Figure 17. Part of seismic record GUA-13 showing the locations of Sites 496 and 568 and bottom simulating reflector 44

18. Total organic carbon content at DSDP Site 569 51

19. Organic carbon content and carbon isotopic composition of sediments from DSDP Site 568 52

20. Seismic line GUA-5 showing structure of forearc basin offshore Guatemala 53

21. Seismic line GUA-18 showing forearc basin sediments exposed by San Jose Canyon 55

22. Carbon isotope content of pore water methane and carbonate at DSDP Site 565 75

23. Concentration of heavy hydrocarbon gases in cores from DSDP Site 568 78

24. Concentration of heavy hydrocarbon gases in Miocene sediments of DSDP Site 568 81

25. Ratios of heavy to light hydrocarbons in core gases at DSDP Site 568 82

26. Pore water chlorinity and ratio of heavy to light hydrocarbons in core gases from DSDP Site 568 85

27. Results of compensation of heavy hydrocarbon ratio of DSDP Site 568 for downhole diagenetic gas buildup 87

28. Carbon isotope values from DSDP Leg 568 89

29. Discrepancies in reported isotopic values for carbon dioxide at DSDP Site 568 90

30. Propane, butane, and pentane content of core gases near massive gas hydrate at DSDP Site 570 93

31. Comparison of propane, butane, and pentane content of interstitial gas hydrate and surrounding sediments at DSDP Site 570 94

32. Comparison of isobutane, n-butane, and pentane content of massive gas hydrate, fracture-filling gas hydrate, and surrounding sediments at DSDP Site 570 96

Figure 33. Comparison of pentane isomer content of gas hydrates and surrounding sediments at DSDP Site 570 97

34. Carbon isotope content of methane from DSDP Site 570 cores 99

35. Carbon isotope content of carbon dioxide from DSDP Site 570 101

36. Carbon isotope content of methane, carbon dioxide, and total carbonate from DSDP Site 570 cores 104

37. Differences between carbon isotopic values for methane, carbon dioxide, and total carbonate from DSDP Site 570 cores 104

38. Distribution of bottom simulating reflectors from multichannel seismic lines offshore Mexico 108

39. Seismic line MX-16 offshore Mexico 109

40. Seismic line OM-7N offshore Mexico 110

41. Seismic line OM-4N offshore Mexico 111

42. Depth of bottom simulating reflectors offshore of Mexico compared to the depth of the base of the gas hydrate stability zone at different geothermal gradients 113

43. Segment of seismic line OM-7N showing relationship of bottom simulating relfector and DSDP Site 490 115

44. Location of bottom simulating reflectors offshore of Guatemala 119

45. Graph of water depth to subbottom depth of possible bottom simulating reflectors offshore of Guatemala 120

46. Segment of seismic line GUA-4 showing anomalous reflector 121

47. Seismic line GUA-14 offshore Guatemala 123

48. Display of individual seismic traces from seismic line GUA-14 124

49. Distribution of bottom simulating reflectors offshore of Nicaragua and Costa Rica 128

Figure 50. Location of bottom simulating reflectors on single channel seismic lines offshore of Mexico 131

51. Parallel single channel seismic lines offshore of Zihuatenejo, Mexico 132

52. Tectonic setting of bottom simulating reflectors in single channel seismic records 135

53. Pore water chemistry of gas hydrate bearing sites offshore Mexico 137

54. Pore water chemistry of possible gas hydrate bearing sites, DSDP Leg 67, offshore Guatemala 139

55. Chlorinity profiles of DSDP Leg 84 sites 140

56. Composite chlorinity profile for DSDP Sites 496, 568, and 570 151

57. Effect of multiple fractionation on isotopic composition of pore water at different levels of pore occupancy by hydrates 155

58. Effect of prior enrichment of pore water on multiple fractionation by gas hydrates 156

59. Effect of isotope replenishment on multiple fractionation by gas hydrate 159

60. Organic carbon content at DSDP Leg 84 sites 161

61. Proposed model of massive gas hydrate formation at DSDP Site 570 162

62. Lithostratigraphic summary of DSDP Site 570 165

63. Physical properties of sediments and rocks recovered from DSDP Site 570 168

64. Acoustic properties of sediments and rocks reported from DSDP Site 570 170

65. Acoustic velocity and bulk density logs from DSDP Site 570 172

66. Comparison of impedance, density, and velocity data from 1950 to 1980 m, DSDP Site 570 174

67. Deep resistivity and neutron porosity logs from DSDP Site 570 176

Figure 68. Biostratigrahic and paleobathymetric summary, DSDP Site 570 179

69. Distribution of water masses and benthic foraminiferal biofacies near DSDP Leg 84 sites 180

70. Solubility of methane in water at 10°C 187

71. Solubility of methane in water at 530 and 630 atm 189

72. Methane hydrate phase diagram at 25°C 190

73. Methane hydrate phase diagram at 25°C 192

74. Differences in ^{13}C content of CO_2 and ΣCO_2 at DSDP Site 570 as function of formation temperature 196

75. Detailed seismic record of continental slope near DSDP Site 570 200

76. Seismic section at DSDP Site 570 201

77. Seismic section near DSDP Site 570 202

78. Carbon isotope content of core gas from DSDP Sites 568 and 570 205

79. Hypothetical effect of normal faulting on carbon isotopic profile 206

80. Ratio of propane, butane and pentane to methane and ethane in sediments at DSDP Site 570 208

81. Ratio of n-butane and pentane to smaller hydrocarbons in core gases at DSDP Site 570 209

82. Mass sedimentation accumulation rates for DSDP Leg 66 sites 215

83. Map showing relationship of Colina Graben, Rivera Fracture Zone and bottom simulating reflectors 220

84. Seismic line from offshore Mexico near Colina Graben showing bottom simulating reflector 221

TABLES

Table 1. Summary data of basin analysis, formation and stability of gas hydrates in the Middle America Trench study region 3

2. Composition of hydrocarbon gases from igneous and metamorphic rocks, offshore Guatemala 57

3. Hydrocarbon gases evolved by heating serpentinite 64

4. Hydrocarbon ratios of serpentinite hosted gases 64

5. Suspected gas hydrate occurrences, DSDP Leg 66 67

6. Gas hydrate occurrences on DSDP Leg 67 70

7. Description of gas hydrates recovered on DSDP Leg 84 . . . 72

8. Analysis of gas hydrates recovered on DSDP Leg 84 73

9. Distribution of hydrocarbon gases, DSDP Site 566 76

10. Depth distribution of gas hydrates at DSDP Site 568 from core gas composition 79

11. Estimated reflection coefficients 125

12. Seismic velocity of sediments beneath bottom simulating reflector on seismic line GUA-14 125

13. Oxygen isotope content of pore water from DSDP Leg 84 145

14. Oxygen isotope content of pore water based on isotope content of gas hydrate and isotopic fractionation factor 147

15. Gas hydrate pore occupancy calculated from oxygen isotopes and chlorinity 148

16. Physical properties, DSDP Site 570 171

17. Equilibrium concentration of methane in pore water calculated using the method of Miller (1974) 185

BASIN ANALYSIS, FORMATION AND STABILITY OF GAS HYDRATES OF THE MIDDLE AMERICA TRENCH

By Patrick Finley and Jan Krason

EXECUTIVE SUMMARY

Geological factors controlling the formation, stability, and distribution of gas hydrates were investigated by basin analysis of the Middle America Trench region. Geological, geophysical, and geochemical data from the region were assembled and critically evaluated to develop consistent interpretations of the relationships of geological environments and gas hydrates. Preliminary estimates of the regional extent of the gas hydrates were derived.

This study was performed for the U.S. Department of Energy Morgantown Energy Technology Center by Geoexplorers International, Inc. as part of a worldwide evaluation of 24 offshore sites where the presence of gas hydrates has been confirmed or inferred. The results of this study are summarized in Table 1.

The Middle America Trench study region comprises the continental shelf, continental slope, trench, and abyssal plain offshore of the Pacific coasts of Mexico, Guatemala, El Salvador, Honduras, Nicaragua, and Costa Rica. Subduction of the Cocos Plate beneath Mexico and Central America has formed Middle America Trench and modified the topography, structure, and sedimentation patterns of other components of the study region.

The Middle America Trench is a product of the interaction of four lithospheric plates. The oceanic Cocos and Rivera Plates which are separated by a transform boundary are subducting beneath the North America and Caribbean Plates which are also in strike-slip contact. The complex interaction has produced strikingly different geological structure and topography of the trench and continental margins north and south of the Cocos-North America-Caribbean triple junction.

The trench north of the triple junction offshore of Mexico truncates onshore structures obliquely, producing a relatively shallow trench, with a compressionally deformed continental slope and a very narrow continental shelf. The continental margin along the northern segment of the trench has been actively growing since Miocene time by accreting trench sediments scraped from the subducting plate to the foot of the continental slope.

South of the triple junction, the trench parallels onshore geological features and is relatively deep. The continental slope is more gently dipping and regular. A broad continental shelf is underlain by a deep forearc basin.

Although the structure of the continental margin south of the triple junction is well documented only in one area, it appears to be very different from the structure of the margin to the north. The continental slope is composed of metamorphic and ultramafic rocks overlain by a thin veneer of sediments. In contrast to the northern segment, trench sediments are not accreted to the margin, but are entirely subducted.

Continental slope sediments in the study region are principally organic-rich mud and mudstone with abundant volcanic ash. Limestones and permeable beds of coarse-grained ash and sand from trench and canyon floor settings are minor constituents of the sedimentary sections.

Abundant organic matter in continental slope sediments indicates a high potential for microbial methane generation. The thin accumulations of sediments preclude thermal maturation of the organic matter. Sediments which have been subducted or accreted to the margin may be thermally mature as may sediments in the deep forearc basins landward of the southern segment of the trench. Hydrocarbons recovered from metamorphic basement rocks offshore of Guatemala may have been generated from any of these sources or by abiogenic processes.

Gas hydrates were recovered by coring at three widely separated areas of the Middle America Trench study region. The Deep Sea Drilling Project (DSDP) proved the existence of gas hydrates offshore of Acapulco, Mexico; San Jose, Guatemala; and the Nicoya Peninsula of Costa Rica. In each instance methane was the dominant component of the hydrates with minor amounts of carbon dioxide and heavier hydrocarbons. All occurrences are best categorized as resulting from bacterial methanogenesis, but unusual isotopic signatures indicate the possibility of thermogenic or abiogenic sources.

Seismic evidence indicates that gas hydrates are probably widespread throughout the study region. Bottom simulating reflectors (BSRs) are found in high quality seismic lines of the continental slope. Limited seismic coverage restricts mapping of BSR distribution to a few small areas. However, parts of the study region between areas surveyed probably also have abundant BSRs. A previously unreported area of abundant BSRs was discovered in this study.

A 4 m-thick zone of massive gas hydrate was drilled offshore of Guatemala. Massive gas hydrates can be formed in continental slope sediments given the proper conditions of pressure, temperature, hydrocarbon supply, and sediment permeability. Although various mechanisms to satisfy these conditions have been proposed, formation of the massive gas hydrate in a fault zone is the most consistent with available data.

Chemical composition of pore water from sediment cores in the study region varies regularly with depth. The change in pore water chemistry has been proposed to indicate gas hydrate presence. The relationship of gas hydrate formation and pore water chemistry is direct at some locations, but other processes have affected the pore water composition elsewhere in the study region.

Permeability of host sediments and abundant hydrocarbon supplies favor the formation of gas hydrates of the Middle America Trench. Gas hydrates have been recovered only from cores with highly permeable coarse lithologies, or from permeable fracture or fault systems in impermeable rocks. Permeability is necessary to deliver the large quantities of hydrocarbons required for gas hydrate formation. Sedimentation rate has no direct influence on gas hydrate distribution in the study region although it may affect methane generation processes. Structural deformation may have enhanced gas hydrate formation processes.

TABLE 1.

SUMMARY DATA OF BASIN ANALYSIS, FORMATION AND STABILITY OF GAS HYDRATES IN THE MIDDLE AMERICA TRENCH STUDY REGION

STUDY REGION / FACTOR / AREA	MIDDLE AMERICA TRENCH	
	Mexican Trench	Guatemalan Trench
BASIN ANALYSIS		
Location		
Longitude: latitude	95°W-107°W; 14°N-21°N	84°W-95°W; 9°N-16°N
Areal extent, km²	100,000 km²	100,000 km²
Geomorphology	Continental slope	Continental slope
Geology	Well defined	Well defined
Structural setting	Subduction zone/ accretionary prism	Subduction zone/ forearc basin
Stratigraphy	Upper Cretaceous-Quaternary	Upper Cretaceous-Quaternary
Lithology	Accreted trench fill, slope deposits	Slope deposits, deltaic forearc sediments
Sedimentary environments	Hemipelagic	Hemipelagic
Sediment source	Mexican Sierra Madre	Central America volcanic arc
Rate of sedimentation, m/m.y.	5 - 1,100	1 - 500
Sediment flux, mg/cm²/yr	0.5 - 500	Not determined
Geochemistry	Well defined	Very well defined
Total organic matter content, weight %	0.1 - 3%	0.2 - 6%
Source of organic matter	Terrestrial and marine	Terrestrial and marine
Depth of thermal maturity, m	Not determined	4,100 m in forearc basin
Geochemical anomalies	Pore water salinity	Hydrocarbon isotopes, pore water salinity
Physical and geophysical features		
Sediment thickness, m	0 - 4,000 m	0 - 6,000 m
Porosity, %	30 - 90%	21 - 90%
Geothermal gradient, °C/m	1.3 - 4.3°	1.8 - 3.8°
Heat flow, HFU (heat flow unit)	Not determined	Not determined
GAS HYDRATE FORMATION AND STABILITY		
Direct evidence	Hydrate recoveries	Hydrate recoveries
Type of gas hydrate occurrence	Disseminated, fracture filling	Disseminated, fracture filling, massive
Indirect evidence	Abundant	Abundant
Bottom simulating reflector(s), BSR	45 lines	23 lines
Areal extent of the bottom simulating reflector(s), km²	19,000 km²	23,000 km²
Quality of seismic data	Variable	Variable
Inferred evidence	Core gas, pore water chemistry	Core gas, pore water chemistry
Location	DSDP Leg 66	DSDP Legs 67 and 84
Sea water depth, m	700 - 4,000 m	1,500 - 4,000 m
Sub-sea bottom depth, m	0 - 640 m	0 - 450 m
Temperature at sea floor, °C	4°C	4°C
Gas hydrate host formation	Mudstone, ash	Mudstone, ash, serpentinite (?)
Age of gas hydrate host formation	Miocene-Pliocene	Eocene-Pliocene
Gas hydrate stability zone	300 - 800 m	300 - 800 m
Isotopic composition of gas, δ^{13}C ‰	Not determined	-37 to -90
Time of gas hydrate stabilization	Not determined	Not determined
Source of gas hydrates	Biogenic	Biogenic, thermogenic (?), abiogenic (?)
Evidence for free gas under gas hydrate zone	None	None
Estimated/inferred gas volume, at 25 °C/atm.		
In gas hydrates	12 TCF/m thickness	15 TCF/m thickness
In trapped free gas	Not determined	Not determined

INTRODUCTION

Gas hydrates are solid substances composed of gas molecules enclosed in a lattice of water molecules. Gas hydrates can be formed from gas and water at high pressures and low temperatures when a sufficiently high concentration of dissolved gas exists. Conditions favorable for gas hydrate formation and preservation are found in some continental margin and deep sea sediments where adequate hydrocarbon gases are available. Large quantities of natural gas with possible resource potential may be trapped in and beneath offshore gas hydrates.

This report presents the results of a study on the geological factors which control the distribution of gas hydrates in the sediments of the landward slope of the Middle America Trench off the western shore of Mexico and Central America. This study is a part of a project being performed for the U.S. Department of Energy (DOE) - Morgantown Energy Technology Center (METC) by Geoexplorers International, Inc. The main purpose of the project is to evaluate the geological environments of gas hydrate formation and stability and to make preliminary assessments of gas resources associated with gas hydrates.

Gas hydrates have been recovered in sediments from the continental margin of the Middle America Trench study region. Coring by the Deep Sea Drilling Project (DSDP) proved that gas hydrates exist in at least three widely separated areas of the study region: offshore of Mexico, offshore of Guatemala, and offshore of Costa Rica. Additionally, bottom simulating reflectors (BSRs) which mark the base of the gas hydrate stability zone are found in seismic reflection lines from throughout the study region. The combination of direct evidence of gas hydrates obtained from drilling and the abundant indirect seismic evidence of gas hydrates indicate that gas hydrates may be widespread in the continental slope sediments of the study region.

A large amount of information exists in the literature on the geology and gas hydrates of the Middle America Trench. Workers from the three DSDP cruises in the study region (Legs 66, 67, and 84) have published many relevant papers in the respective Initial Reports volumes (Watkins et al., 1982; Aubouin et al., 1982; von Huene et al., 1985) and in various journals. These papers present independent interpretations of the cruise data. In this study we compiled the data on the geologic environments and geochemistry of the sediments and gas hydrates of the study region from the reports of the separate research groups. Using this large integrated data base we analyzed and assessed the often contradictory interpretations presented by different authors to determine which are most consistent with the data. This critical review of previous work on the study region suggests that some widely held interpretations of the DSDP results should be revised.

This report is presented in two sections:

Part I - Basin Analysis examines structural geology and sedimentary environments of the Middle America Trench study region. Based on this information, the regional hydrocarbon generation potential is discussed.

Part II - Formation and Stability of Gas Hydrates presents the direct and indirect evidence of gas hydrate presence in the study region. Geochemistry of sediments, hydrocarbons, and pore water is examined in detail in light of the information presented in Part I to indicate which factors may control the distribution of gas hydrates of the Middle America Trench.

Acknowledgements

Geoexplorers International, Inc. and the authors are grateful to the U.S. Department of Energy - Morgantown Energy Technology Center for the opportunity to participate in the gas hydrate research program. Critical review of this report by Kathryn Dominic of DOE-METC is highly appreciated. Charles Komar and Rodney Malone expedited printing of this report.

Many people assisted the authors in assembling the geological and geophysical data used in this report. Bruce Grant, Kathy O'Day, and Dan Metzger from the National Geophysical Data Center assisted the authors in locating and retrieving seismic lines and navigation data. Don Marsee from Scripps Oceanographic Institution provided unpublished records from DSDP cruises in the study region. Kathy Litey of the Ocean Drilling Program provided core photographs.

The illustrations in this report were expertly drafted by Margaret Krason of Geoexplorers International, Inc. Joan Gross typed this paper.

PART I

BASIN ANALYSIS

The Middle America Trench study region includes the continental shelf and slope, the Middle America Trench, and the abyssal plain offshore of the Pacific coasts of Mexico and Central America. The study region has undergone extensive structural deformation due to the interaction of four lithospheric plates. Subduction of the Cocos and Rivera Plates beneath the North America and Caribbean Plates has continued to the present. The subduction process has been modified by lateral movement between the Cocos and Rivera Plates and between the North America and Cocos Plates. The subduction style varies greatly along the length of the Middle America Trench.

Sedimentary processes in the study region were investigated by drilling. Twenty sites on the Cocos Plate, the trench floor, and the continental slope were cored by the Deep Sea Drilling Project (DSDP). Continental slope deposits mainly consist of Tertiary and Quaternary muds and mudstones with very high concentrations of organic matter. The abundant sedimentary organic matter indicates a high potential for biogenic hydrocarbons, but the thermal maturity of the sediments is low.

Location and Geomorphology

The Middle America Trench is a narrow submarine depression which extends 2,500 km, 20 - 100 km offshore from the Pacific coasts of Mexico, Guatemala, El Salvador, Honduras, Nicaragua, and Costa Rica (Figures 1 and 2). The trench is continuous at greater than 4,500 m water depth offshore of Cabo Corrientes, Mexico (106°W, 21°N) to offshore of Costa Rica where it shoals rapidly, ending at about 85°W, 9°N. The trench is linear for most of its length, trending N40°W ± 5°. A short east to west segment at 15°5'N beneath the western Tehuantepec Gulf extends for about 150 km and divides the Middle America Trench into two segments with distinct geomorphological differences.

North of the inflection at 15°15'N, the Middle America trench averages 4,800 to 5,100 m deep at its axis (Figure 1). The northern segment is generally U-shaped with a fairly flat trench floor. The continental slope north of the Tehuantepec Gulf is very steep with only a narrow, poorly developed continental shelf. The continental slope is cut by many submarine canyons which follow irregular courses from the shelf to the trench. Onshore from the northern segment of the trench, rugged mountains of folded Paleozoic and Mesozoic sedimentary rocks and Cretaceous intrusives continue to very near the coast.

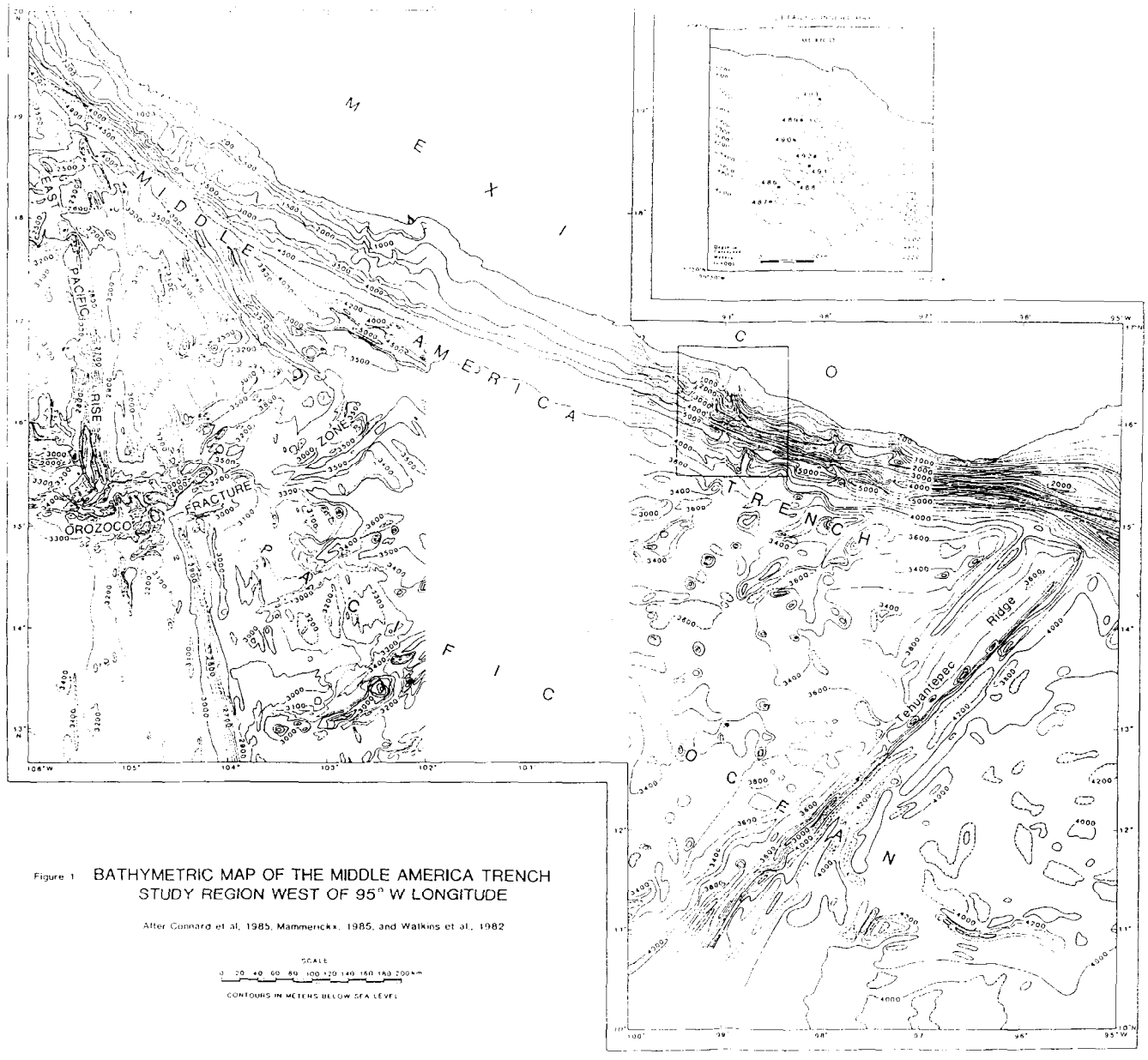

Figure 1 BATHYMETRIC MAP OF THE MIDDLE AMERICA TRENCH STUDY REGION WEST OF 95° W LONGITUDE

After Connard et al, 1985, Mammerickx, 1985, and Watkins et al, 1982

SCALE

0 20 40 60 80 100 120 140 160 180 200 km

CONTOURS IN METERS BELOW SEA LEVEL

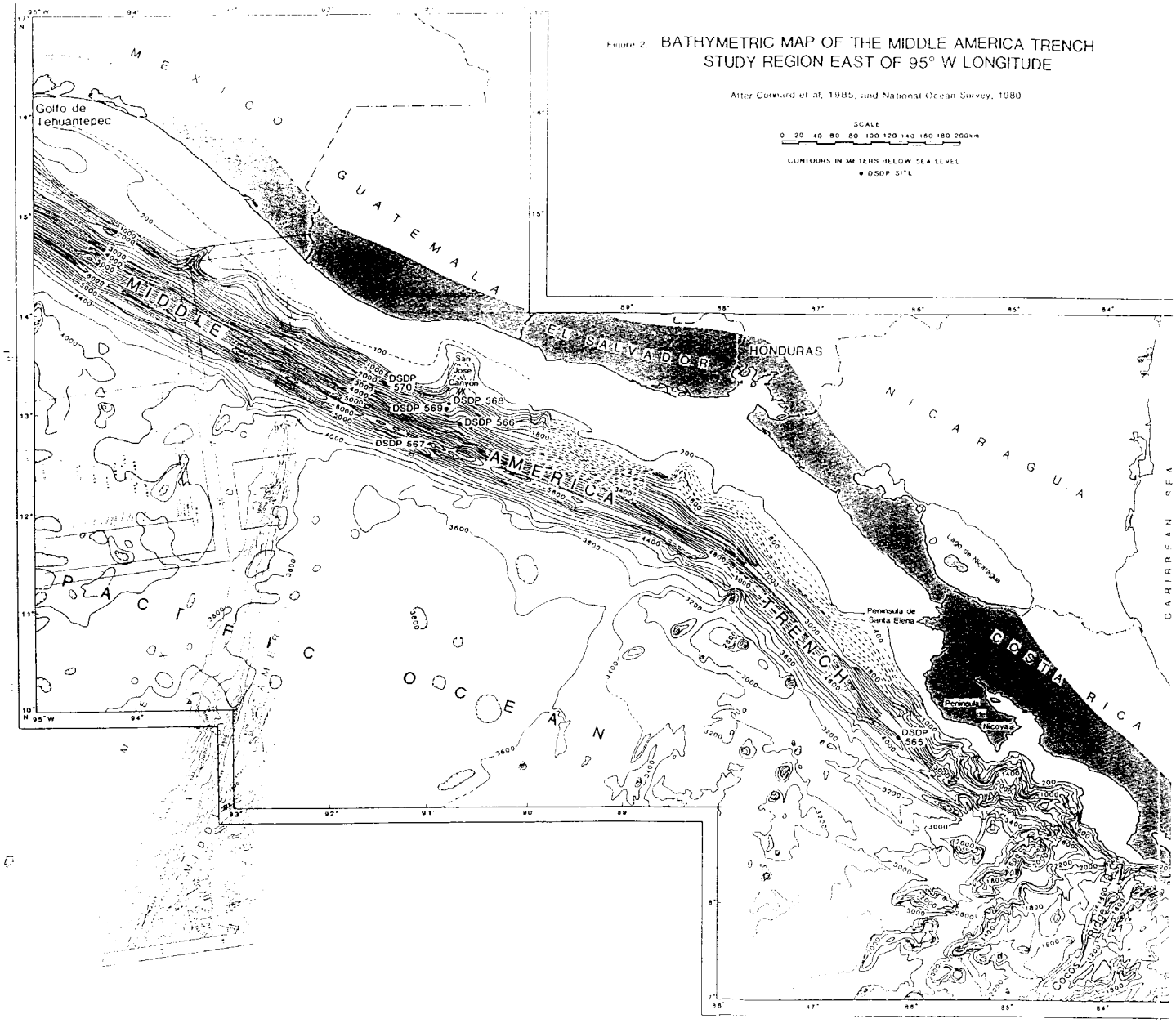

Figure 2. BATHYMETRIC MAP OF THE MIDDLE AMERICA TRENCH STUDY REGION EAST OF 95° W LONGITUDE

After Cornard et al. 1985, and National Ocean Survey, 1980

South of 15°15'N, the Middle America trench deepens and becomes more distinctly V-shaped in profile (Figure 2). The continental slope of the southern segment of the trench has a much gentler slope, and is much less rugged than the slope to the north. Only a few large submarine canyons transect the continental slope along the southern segment of the trench. A broad continental shelf occurs along the full length of the southern segment.

Onshore geology south of 15°15'N also contrasts with that to the north. The west coast of central America consists of a continuous chain of calcalkalic volcanoes which are historically active. The volcanic chain parallels the trend of the trench at a separation of about 200 km.

Southwest from the trench axis the sea floor rapidly rises 1,000 to 2,000 m to the flat abyssal plain of the eastern Pacific Ocean at 3,400 to 4,000 m depth (Figures 1 and 2). Several linear ridges cross the flat sea floor approximately normal to the trend of the Middle America Trench. The Rivera and Orozoco Fracture Zones abut the axis of the Middle America Trench offshore of Mexico, resulting in local irregularities in the depth and continuity of the trench floor. A major linear feature of the sea floor, the Tehuantepec Ridge, intersects the trench just southwest of the inflection at 15°15'N which marks the change in character between the northern and southern segments of the trench. The Cocos Ridge abuts the Middle America Trench at its southern boundary.

The "Middle America Trench study region" as used in this report includes the trench, the adjacent areas of the abyssal plain of the Cocos Plate, and the continental slope and shelf landward of the trench.

Regional Tectonics

The Middle America Trench is one of the most thoroughly studied deep sea trenches in the world. The detailed bathymetry, a distinct landward dipping seismic Benioff Zone, and abundant back arc volcanism in Mexico and Central America all indicate that the Middle America Trench is the site of subduction of Pacific oceanic crust beneath the North American continent. The abundance of geophysical and geological data available for the Middle America Trench has resulted in its being applied as a model for interpreting the subduction process and the formation of other circum-Pacific deep sea trenches.

Seely et al. (1974) proposed a general model for continental margin development over a subduction zone based on a multichannel seismic line from offshore of Guatemala. They proposed that sediments from the descending plate were scraped off by the overriding plate and incorporated into the continental slope. The offscraped sediments were accreted to the continental plate in the form of discrete wedges separated by imbricate thrust faults. Thus, continued subduction promotes seaward growth of the continental margin; progressive addition of thrust sheets from the toe of the slope also produces uplift of the continental margin resulting in an offshore structural high.

The marked difference in the sea floor topography on either side of the Tehuantepec Ridge which was noted by Fisher (1961) is also expressed in the structural geology of the two parts of the Middle America Trench. The

narrow accretionary complex, oblique relationship of back arc volcanism, and the apparent offshore extension of continental crust indicated that a different mode of subduction may be occurring along the Mexican Trench. The possibility of subduction erosion wherein the plunging oceanic plate eroded the leading edge and underside of the continental plate was considered as an alternative to Seely's (1974) accretionary model for the Middle America Trench north of the Tehuantepec Ridge (Karig et al., 1978).

Seismic surveys and coring by the DSDP on Legs 66 offshore of Acapulco, Mexico, and Legs 67 and 84 offshore of San Jose, Guatemala and Puntarenas, Costa Rica demonstrated that the previously developed models of Middle America Trench tectonics were inaccurate. Instead of subduction erosion, accretion appears to be occurring offshore of Mexico. However, little evidence of accretion since at least Eocene time was found offshore Guatemala near the location of the seismic line upon which Seely's accretionary model was based.

Plate Tectonic Setting

The Middle America Trench is a convergent boundary where the Cocos and Rivera Plates are being subducted beneath the North America and Caribbean Plates (Figure 3). The Rivera Plate is subducted only along the northernmost 200 km of the trench; the Cocos Plate is being subducted along the remaining 2,300 km of the trench. The North American and Caribbean Plates are in contact along the left-lateral Polochic-Montagua fault system which transects central Guatemala.

Cocos Plate. The Cocos Plate underlies about 2,000,000 km^2 of the eastern Pacific Ocean. The crust of the Cocos Plate was produced by sea-floor spreading at the East Pacific Rise; the plate is consumed beneath the North America and Caribbean Plates along the Middle America Trench.

The oldest parts of the Cocos Plate near the Middle America Trench are probably Eocene age based on magnetic lineations (Larson, 1972; Lynn and Lewis, 1976). However, DSDP drilling has identified basal sediments only as old as Miocene (von Huene et al., 1985).

The East Pacific Rise which currently separates the Pacific and Cocos Plates has resulted from progressive eastward ridge jumps from now extinct spreading centers in the last 3 to 10 m.y. (Mammerickx and Klitgord, 1982). The offset segments of the East Pacific Rise produce numerous transverse fracture zones (Trachan and Larson, 1973) which correspond with the east-west trending bathymetric lineations earlier noted by Fisher (1961). One of the most pronounced fracture zones near the Middle America Trench, the Orozoco Fracture Zone, is arcuate, concave to the north, and intersects the Middle America Trench offshore of Zihuatenejo, Mexico. Another major fracture zone with distinct topographic expression is the Tehuantepec Ridge which intersects the trench at its bend beneath the Gulf of Tehuantepec. In contrast to the parallel curvature of the traces of the Orozoco Fracture Zone and Tehuantepec Ridge, two fracture zones to the south have a more linear trend. The difference in trend of the east to west trending Siqueiros and Clipperton Fracture Zones and the curved trace of the Tehuantepec Ridge led Truchan and Larson (1973) to conclude that the Tehuantepec Ridge was not a fracture zone, but a large hinge fault. Truchan and Larson (1973) proposed that the

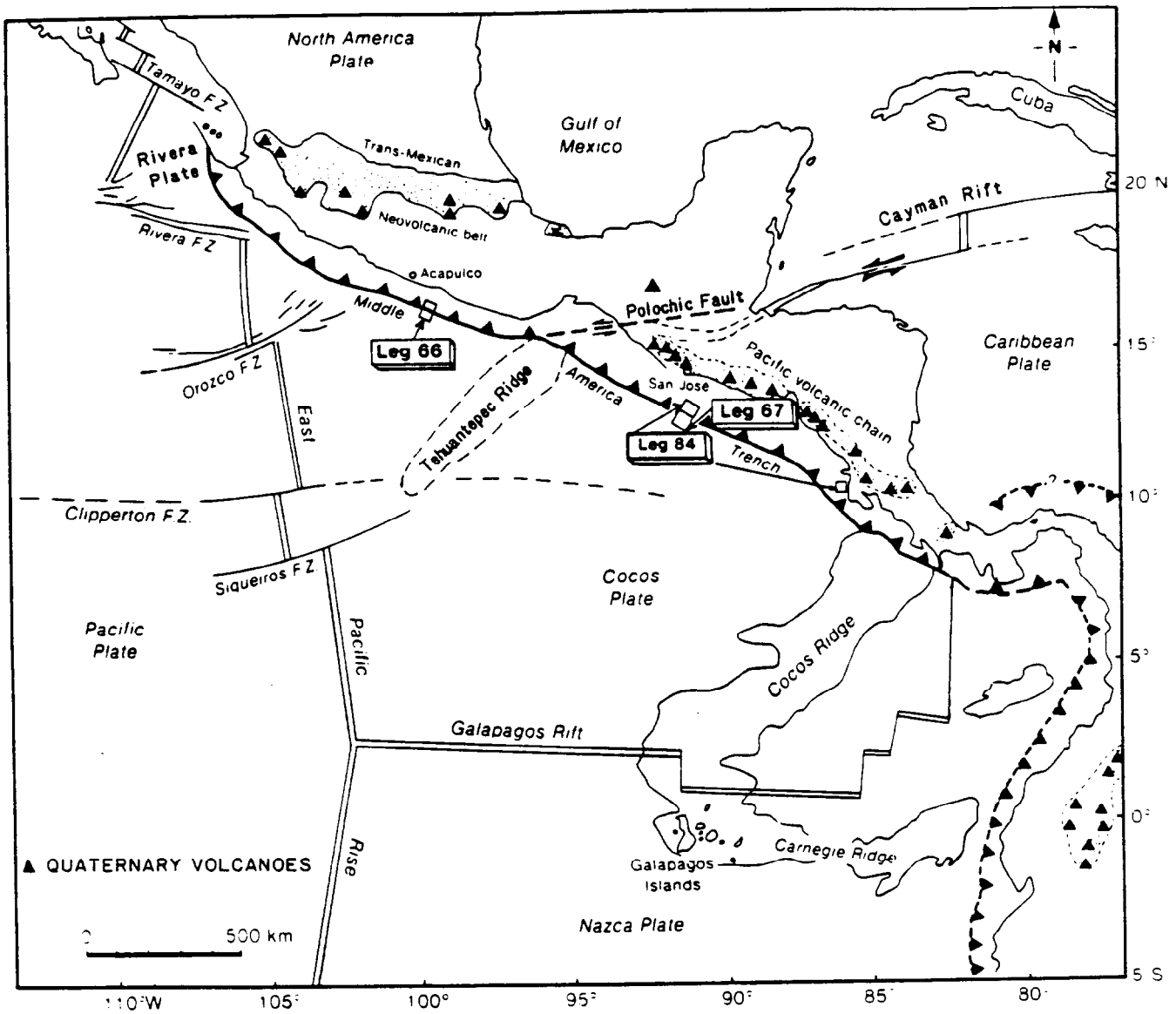

Figure 3. **REGIONAL TECTONIC MAP OF THE MIDDLE AMERICA TRENCH**

After Baltuck et al., 1985

fault was caused by flexure of the Cocos Plate to accommodate the different angles of subduction north and south of the ridge documented by Molnar and Sykes (1969). More detailed mapping by Mammerickx and Klitgord (1982) confirmed that the Tehuantepec Ridge was indeed a fracture zone, but that the angular relationship of fracture zones was due to a more complex spreading pattern where the Siqueiros Fracture Zone was intersected by an extinct spreading center.

The structural fabric of the Cocos Plate inherited from the sea-floor spreading process parallels the magnetic lineations on the plate. The zones of weakness are activated upon descending into the Middle America Trench resulting in horst and graben faulting of the trench floor. The relief of these structures reach up to 500 m (Ladd et al., 1982).

The Cocos Plate is bounded to the south by the Galapagos Rift and the aseismic Cocos Ridge. The border of the Cocos and Rivera Plates is the Rivera Fracture Zone which roughly parallels the Orozoco Fracture Zone and joins the Middle America Trench offshore of Manzanillo, Mexico.

Rivera Plate. The Rivera is a small, roughly triangular oceanic plate which intersects the North America Plate along the northernmost 200 km of the Middle America Trench. Whereas the Cocos Plate is moving northeast at 5 - 7 cm/year, the Rivera Plate moves southeast at less than 2 cm/year (Drummond, 1981).

North America Plate. The Middle America Trench marks the southwest boundary of the North America Plate for about 1,000 km along the Pacific margin of Mexico between 15° and 20°N. The onshore basement of Mexico consists of Precambrian schists and gneisses (Anderson, 1985) and late Cretaceous plutons. Rocks older than Cretaceous age are rare. Miocene volcanics parallel the trench. Quaternary volcanic activity is typically restricted to the Mexican volcanic belt which trends east-southeast at a 20° angle to the trench.

The North America Plate is moving southwest at 2.7 cm/year (Minster and Jordan, 1978).

Caribbean Plate. The Caribbean Plate is overriding the Cocos Plate along the southern 1,400 km of the Middle America trench. The Caribbean Plate contacts the North America Plate at a transform boundary which cuts due east to west through Guatemala. The Caribbean Plate is moving in the same direction as the North America Plate, but at less than 1 cm/year (Minster and Jordan, 1978). Thus the Polochic-Montagua fault system where the plates join experiences left-lateral movement of about 2 cm/year.

An ophiolitic complex apparently uplifted by Laramide compression crops out in Honduras and southern Guatemala. A very well developed Tertiary and Quaternary volcanic arc parallels the Middle America trench.

Structural Development

In view of the strikingly different shape and tectonic expression of the Middle America Trench north and south of the Tehuantepec Ridge, different models for the two sections have been proposed. The two sections of the trench complex typically were approached as two distinct trenches. Recently,

a more integrated view which relates the observed differences in the two segments of the trench to plate configurations has been proposed.

Offshore of Mexico. The continental margin of Mexico presented difficulties for understanding the tectonic development of the Middle America Trench. The onshore geology of Mexico does not display the features commonly associated with a convergent plate margin. The classical sequence of structures landward of a deep sea trench includes a broad wedge of sediments which have been accreted to the overriding plate forming a structural high (Dickenson and Seely, 1979). Landward of the uplifted accretionary prism terrigenous sediments are typically ponded to form a forearc basin. On land, an associated chain of plutons and volcanoes parallel to the trench is to be found according to the typical model of subduction-induced structures. Although many areas, e.g. offshore of Washington, the Aleutians, and Japan, follow this pattern, many workers noted that none of these factors are present along the Middle America Trench offshore of Mexico (e.g. Karig et al., 1978). No on-land accreted sediments or forearc basin are present; the metamorphic basement is exposed to the coast in some instances. The structural trends in the basement do not parallel the trench. The only Neogene back arc volcanism in Mexico is located in the Mexican volcanic belt which does not parallel the present subduction zone.

These structural inconsistencies suggested that the previously existing continental margin of Mexico had somehow been removed or truncated. Two mechanisms for the removal of the Mexican continental margin were proposed. One claimed that the present subduction zone had earlier been the site of strike-slip faulting. Both right-lateral and left-lateral faulting were proposed. Alternatively the possibility of subduction erosion was entertained as a possible means by which the subduction process itself could have truncated existing structures (Karig, 1974).

Analysis of magnetic and shallow core data indicated that the truncation of the continental margin occurred previous to the late Miocene. Shallow cores from the Mexican continental margin northwest of Acapulco contained indurated sedimentary rocks as old as late Miocene (Karig et al., 1978). Magnetic lineations showed that the characteristic magnetic stripes of the subducted Cocos plate could be resolved beneath the lower slope but were abruptly terminated about 30 km from the shoreline. The magnetic patterns of the nearshore areas matched well the regional trend of onland structures. Karig et al. (1978) considered the abrupt change in magnetic anomalies which also corresponded to a sharp slope break as marking the edge of the truncated continental basement. Karig et al. (1978) concluded that truncation had occurred previous to late Miocene, but the tectonic regime had later changed. The continental margin offshore of slope break from the projected edge of the continental crust was interpreted to be a small Neogene accretionary prism. The volume of sediment necessary to construct the small accretionary complex was calculated to have been within a range of what could reasonably be delivered to the trench in a subduction system. Karig et al. (1978) were not able to differentiate between the possible modes of continental truncation based on their results but favored a pre-Miocene regime of dextral strike-slip faulting. Sinistral slip along an extension of the Polochic-Montagua fault zone was held to be unlikely due to the extreme length of the observed truncation (1,000 km) and the small amount of documented slip along the Polochic-Montagua system (130 - 300 km). Karig et al. (1978) clearly favored a

tectonic regime analogous to the present San Andreas fault or one where subduction and right-lateral shear were concurrently active to produce a similar right-lateral separation. Karig et al. (1978) cited plate reconstructions and exotic terranes on the west coast of Baja California to support their choice.

Detailed seismic surveying and drilling on DSDP Leg 66 refined the view of Karig et al. (1978) that the continental margin of Mexico is composed of a small accretionary wedge seaward of shallowly buried, truncated continental crust. However, the DSDP results did not clarify the style of deformation which had truncated the continental crust.

Multichannel seismic lines collected as part of the pre-drilling site survey for Leg 66 showed accretionary features in the continental slope (Shipley et al., 1980). The seismic sections showed that the continental margin consists of two zones (Figure 4). Nearshore, thin slope sediments overlay a highly reflective acoustic basement beneath which no coherent reflections were seen. Farther seaward, the chaotic reflections of the acoustic basement abruptly were replaced by layered reflectors in which strong landward dipping reflectors could be resolved. The change in seismic response correlated with the edge of continental crust as proposed by Karig et al. (1978) from magnetic data. The slope seaward of the termination was identified as a small accretionary prism; the landward-dipping reflectors (LDRs) were interpreted to be imbricate thrust fault surfaces along which the trench sediments had been uplifted to the upper slope.

Drilling proved the existence of metamorphic basement rocks at shallow depths on the upper continental slope (Watkins et al., 1980). An inversion in the expected stratigraphic sequence was noted with older sediments (middle Miocene) drilled from the upper slope and Pleistocene sediments recovered from near the toe of the continental slope, as expected for an imbricately thrusted sequence. The LDRs were identified as coarse trench sands which had been accreted and uplifted rather than fault surfaces.

Small-scale structures in the slope sediments showed that most of the compressive deformation occurred near the toe of the continental margin. Additionally, the LDRs and the bedding planes rapidly attained a landward dip in the lower slope, but maintained the same dip as the imbrication continued and uplifted the sediments to an upslope position. The accretionary model (Seely et al., 1974) predicted that bedding and fault plane dips will progressively increase upslope as more sediments are offscraped at the trench and incorporated into the accretionary wedge. The upper slope had been uplifted more rapidly than predicted by the classical accretionary model.

These inconsistencies led the DSDP scientists to propose that accretion offshore of Mexico was occurring by two mechanisms: offscraping of sediments from the trench as predicted by the accretionary model and underplating of sediments (Moore et al., 1982). Underplating is a process by which sediments which have been subducted beneath the accretionary complex are transferred from the descending plate to the interior base of the accretionary prism (Figure 4).

Moore et al. (1982) calculated that 85% of the sediments which are input to the subduction zone are trench turbidites and slumps, the remainder being underlying pelagic and hemipelagic sediments deposited on the Cocos Plate prior to its approach to the trench. It was calculated that the incoming sediment is approximately equally divided into offscraped sediments

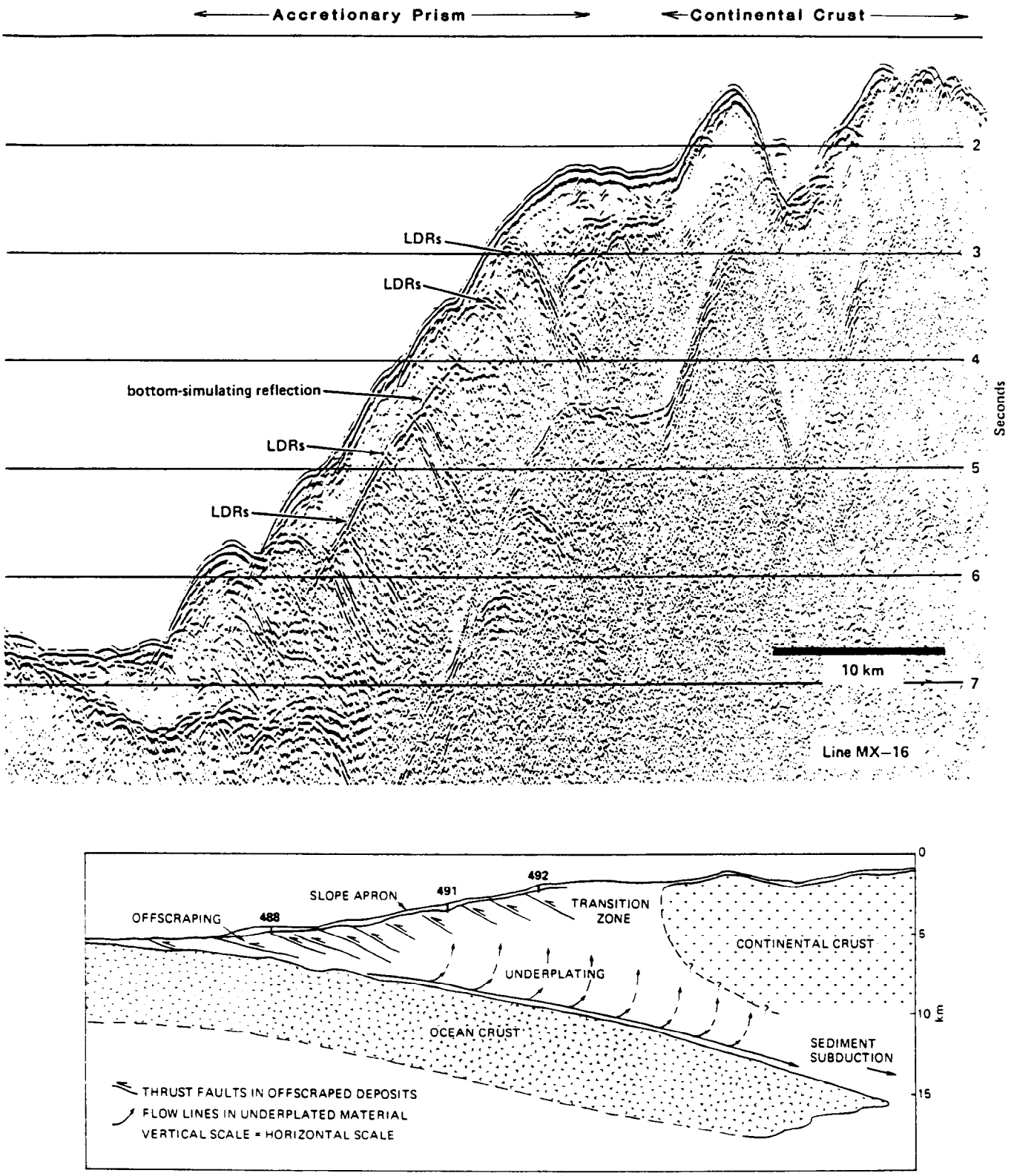

Figure 4. SEISMIC LINE MX-16 OFFSHORE MEXICO AND INTERPRETED CROSS-SECTION

After Shipley and Didyk, 1982, Moore et al., 1982, and Watkins et al., 1982

accreted to the toe of the margin in imbricate thrust slices, underplated sediments accreted to the base of the accretionary zone above the decollement zone, and sediments which are subducted. Since trench deposits constitute the upper 85% of the section, oceanic pelagic and hemipelagic sediments are entirely subducted; the sediments composing the accretionary wedge were proposed to be entirely trench deposits.

Watkins et al. (1982) proposed a detailed chronology of the tectonic development of the Mexican margin based on DSDP findings. Cessation of subduction at a previously existing subduction zone occurred no later than 23 m.y. ago. Truncation of the continental margin was projected to have begun 22 m.y. ago concurrently with rapid subsidence of the remaining continental crust. The lack of obvious accretionary deposits older than 10 m.y. indicated that the process responsible for marginal truncation was existent for up to 12 m.y. If the sediments drilled in the transition zone between the continental crust floored inner slope and the accretionary lower slope are also considered to have been deposited in an accretionary setting, the initiation of subduction could have been as early as 12 to 13 m.y. ago. For the last 10 m.y., accretion has apparently progressed continually.

Watkins et al. (1982) could not determine the type of tectonism which truncated the Mexican continental margin between 23 and 10 m.y. ago, but they favored sinistral slip lateral faulting. They noted that the crustal block upon which southern Guatemala and Honduras are currently found could have been juxtaposed to the present Mexican continental margin at 23 m.y. ago by invoking a revised estimate of the rate of sinistral slip along the Polochic-Montagua system of 4 cm/year. However, none of the direct results from DSDP Leg 66 favor any particular mode of early Miocene tectonism; dextral lateral faulting or subduction erosion could also have produced the observed results.

Offshore of Guatemala the trench and adjacent structures are oriented as expected for a Pacific Arc subduction system. Landward of the continental slope a deep, structural forearc basin underlies the broad continental shelf. A chain of Miocene to Holocene volcanic centers parallels the trench about 200 km landward from the trench axis. A well defined seismic Benioff zone dips 30° to 40° reflecting the position of the descending Cocos Plate.

A multichannel seismic section published by Seely et al. (1974) showed distinct landward dipping reflectors (LDRs) in the lower and middle continental slope offshore of Guatemala. The dip of the reflectors increased upslope. Seely et al. (1974) interpreted the LDRs to represent thrust fault surfaces. The geometry of the faults suggested that the continental slope was composed of trench floor sediments scraped from the descending plates and uplifted into place along the imbricate thrust faults seen on the seismic section. Drilling results from an Esso test hole near the outer edge of the continental slope and seismic stratigraphic analysis allowed Seely (1979) to extend the trench slope model to include the formation and deformation of the forearc basin beneath the shelf as a direct result of the accretion and uplift of trench sediments by thrusting. Seely (1979) included magnetic data into his model of the Guatemala margin which indicated that an uplifted slice of oceanic crust may have been emplaced beneath the shelf slope break.

Woodcock (1975) reported on gravity surveys which indicated that dense material, presumably oceanic crust, was present not only beneath the

continental shelf, but also beneath the continental slope along the full length of the southern Middle America Trench from the Tehuantepec Ridge to Nicoya Peninsula of Costa Rica.

Geophysical surveys prior to DSDP Leg 67 site selection indicated that the structure of continental slope of Guatemala is more complex than postulated by Seely et al. (1974). The GUA series of multichannel seismic lines from the Guatemala continental shelf and slope showed thin slope sediments (0 - 1,000 m thick) and an underlying seismic basement, the top of which is marked by strong diffractions (Figure 5). No bedding reflectors could be seen in the basement unit, but occasional strong landward dipping reflectors were resolved (Figure 5). Seismic refraction data collected prior to Leg 67 (Ibrahim et al., 1979) and earlier (Shor and Fisher, 1961) was combined by Ladd et al. (1982) to indicate that the acoustic basement on the reflection profiles had seismic velocities greater than 4.0 km/sec., compared to velocities of slope sediments of 1.5 to 2.5 km/sec. Furthermore, locally very high seismic velocities were recorded beneath the upper and lower continental slope. Ladd et al. (1982) concluded that the velocity structure indicated that one or more landward dipping slabs of oceanic crust were emplaced at shallow depths beneath the continental slope of Guatemala.

Drilling on DSDP Leg 67 and later on Leg 84 did not produce any evidence of the accretionary complex which had been assumed to comprise the continental slope of Guatemala. Rather than recently uplifted trench deposits predicted by Seely et al. (1974) to constitute the lower slope near the toe of the slope, a continuous sedimentary column was recovered with Cretaceous limestone at its base. The compressional features expected from the thrust faulted model were conspicuously absent. On Leg 84, the igneous and metamorphic basement rock predicted by geophysics to lie at shallow depths beneath the slope were drilled. The basement was found to extend beneath the veneer of slope sediments far beneath the lower continental slope (Figure 5). The conclusion derived from these unexpected discoveries was that no significant accretion of trench deposits had occurred in the study area at least since the very early Tertiary and probably not since the Late Cretaceous.

The lack of accreted sediments or any evidence for compressive deformation indicate a large degree of decoupling across the subduction decollement. Seismic sections showed that the descending Cocos Plate was broken into large horst and graben structures with an average relief of 500 m before being subducted. Just such an irregular surface of the descending plate had been proposed by Hilde (1983) to be ideal for subduction erosion rather than accretion. However, subduction erosion of the margin of the overriding plate by the descending plate should produce compressional structures in the upper plate. Von Huene (1985) reported that pore pressure in the subduction zone approached lithostatic. Elevated pore pressures were proposed to have allowed nearly total decoupling of the two plates allowing convergence between the plates concurrently with the formation of extensional features on the continental slope overlying the subduction zone.

Two interpretations of the mechanisms of emplacement of the Mesozoic ophiolitic basement beneath the continental slope of Guatemala have been put forward. Von Huene et al. (1985) proposed that the ophiolitic complex and the continental shelf are separated by a major strike-slip fault which was active in pre-Eocene time. The ophiolite mass was allegedly brought to its present site by left-lateral slip which von Huene et al. (1985) claimed to have

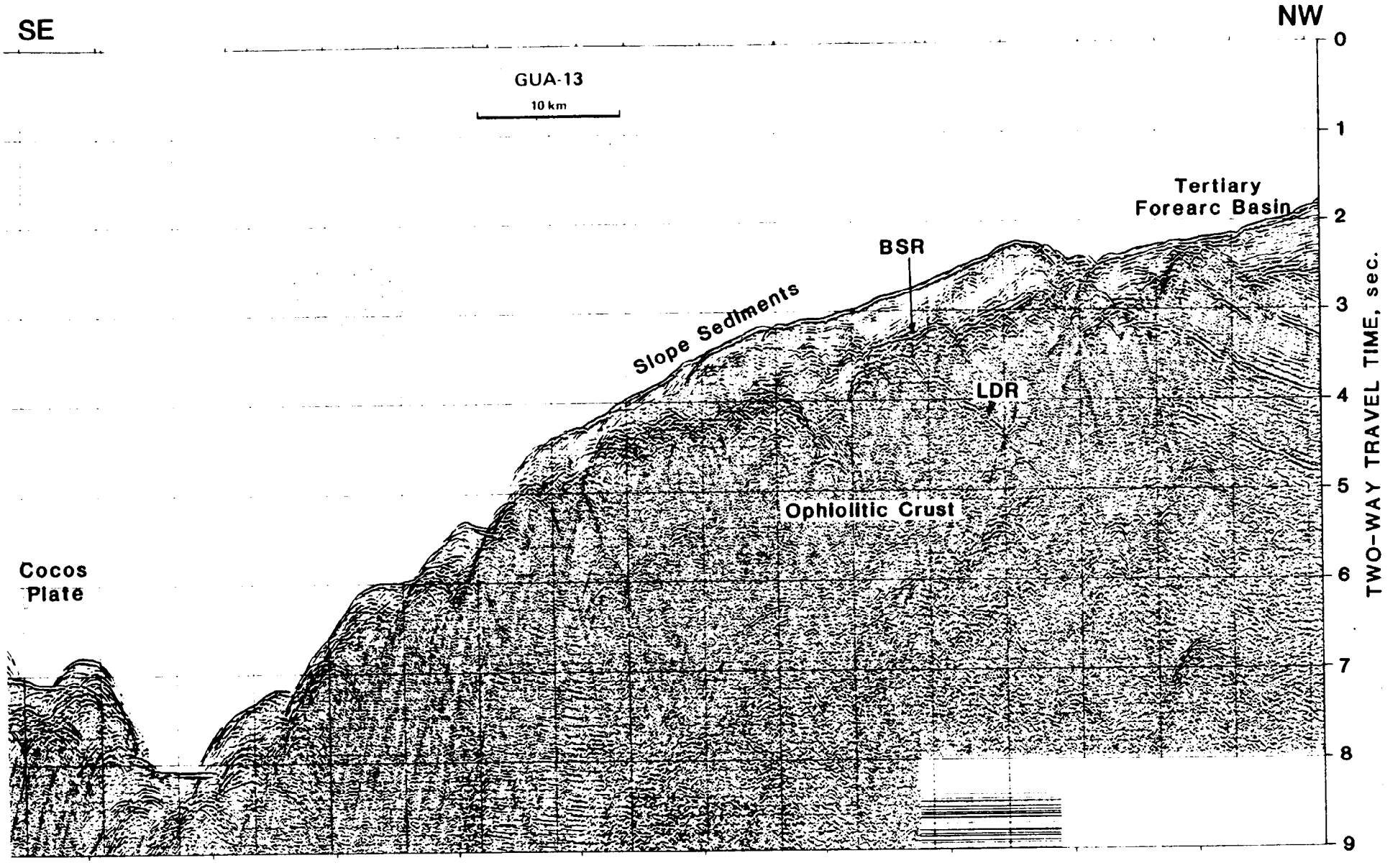

Figure 5. SEISMIC LINE GUA-13 OFFSHORE GUATEMALA

After Ladd et al., 1982

been similar in form to the well documented movement of the Polochic-Montagua fault system farther to the north. Ladd and Buffler (1985) cited a lack of evidence for lateral movement and stated that such a model did not explain the uplift of the ophiolitic complex. Ladd and Buffler (1985) favored the formation of the Guatemala margin by compressive failure of a passive margin in the Eocene. The stranded section of oceanic crust between the continental-oceanic crust transition and the nascent subduction zone was uplifted by sediment underplating and thrusting along landward dipping thrust faults. The Cretaceous and Paleocene sediments recovered on the lower trench slope were interpreted as fragmentary remnants of the pre-Eocene passive margin.

The lack of sediment accretion and compressional structures found in the Leg 67 and 84 cores has since been contradicted by seismic data. A tight grid of high resolution seismic profiles taken near the DSDP drilling sites shows distinct thrusts, folds, and accretion of trench sediments to the lower slope (Moore et al., 1986). Contrary to previous work, Moore et al. (1986) found no slumps, normal faults, or other extensional features. Moore et al. (1986) contended that the decollement fault is in fact 100 to 200 km deeper than had previously been assumed. The discrepancy between the DSDP results and the seismic profiles was attributed to differing degrees of accretion and sediment subduction along the trench. Certain places, e.g. the sites of DSDP drilling and surveying, experience total subduction of trench sediments with no appreciable sediment accretion; simultaneously a nearby location is experiencing minor sediment accretion at the foot of the continental slope.

Offshore of Costa Rica was investigated by seismic surveys and drilling of one hole on DSDP Leg 84.

The Nicoya and Santa Elena peninsulas of Costa Rica contain exposures of ophiolitic sequences similar to those drilled offshore of Guatemala on DSDP Leg 84. These sequences were apparently thrust over volcaniclastic and radiolarian cherts by north-south compressional Laramide forces (Azema et al., 1985). It was considered likely that the continental slope of Costa Rica is underlain by wedges of oceanic crust similar to that documented offshore of Guatemala.

The structure of the Middle America Trench offshore of Costa Rica is complicated by the Cocos Ridge. The ridge, which trends normal to the trench on the Cocos Plate, is apparently an aseismic buildup of subaqueous volcanic rock marking the passage of the Cocos Plate over the Galapagos hot spot (Krason and Ciesnik, 1986). The ridge has resisted subduction and now forms the southern terminus of the Middle America Trench. The exact mode of deformation due to the collision of the Cocos Ridge and the continental slope of Costa Rica is not well understood, although Azema et al. (1985) have suggested that the collision raised the Nicoya Peninsula to its present subaerial elevation.

Geophysical surveys and drilling performed in conjunction with DSDP Legs 67 and 84 were inconclusive in refining the structure of the Middle America Trench offshore of Costa Rica. The network of multichannel site survey seismic lines showed a thin cover of slope sediment over an acoustic basement. The intermediate seismic velocity of the rock underneath the acoustic basement could correspond either to serpentinite or thoroughly indurated accreted sediments (Crowe and Buffler, 1983). Drilling at Site 565

did not penetrate to depths necessary to sample the acoustic basement due to equipment problems. The recovered sediments consisted of late Miocene mudstones which were generally undeformed with no stratigraphic reversals. This lack of compressive structures and the general similarity in seismic sections between the offshore of Costa Rica and Guatemala led investigators to provisionally conclude that the same extensional convergent processes were occurring at both locations.

High resolution seismic profiles of the Costa Rica margin indicated that a combination of sediment accretion and sediment subduction is occurring (Shipley and Moore, 1986). Silver et al. (1985) used the Costa Rica margin as a type locale for the growth of accretionary wedges by duplex formation. In this process the accretionary complex is floored by a decollement thrust and is also separated from the overlying slope sediment by a thrust fault. By invoking a duplex structure to the Costa Rica margin, these investigators sought to reconcile the undeformed slope apron drilled at Site 565 with the abundant LDRs in seismic lines which they interpreted as imbricate thrusts.

Caribbean-North America-Cocos Triple Junction

From the above discussion, it is apparent that the topography, subduction style, and presubduction tectonic history of the two segments of the Middle America Trench separated by the Tehuantepec Ridge are very different. The Tehuantepec Ridge is a major topographic and structural feature of the Cocos Plate. The ridge has a sea-floor relief of 40 to 500 m. The ocean depth of the Cocos Plate southeast of the ridge is 400 m greater than to the northwest. The topography of the Tehuantepec Ridge is characteristic of a transform fracture zone (Larson and Truchan, 1972), and it separates crustal blocks of greatly different ages (Mammerickx and Klitgord, 1982). Due to these features of the Tehuantepec, it has been suggested that the subduction of the ridge has caused the differences in the observed structural features of the Middle America Trench and the onshore of Mexico and Central America.

The triple junction between the North America, Caribbean, and Cocos Plates coincides with the area where the Tehuantepec Ridge is subducted. The trench-trench-transform boundary is inherently unstable. It has been proposed that plate interactions at the triple junction are directly related to the contrasts in trench structure and morphology, and that the subduction of the Tehuantepec Ridge at the same point is coincidental. Recent work by Burkart (1983) and Burbach et al. (1984) applied an integrated approach to resolving the fundamental cause of the difference in the northern and southern segments of the Middle America Trench.

Tehuantepec Ridge. Truchan and Larson (1973) determined that the Tehuantepec Ridge is a transverse fracture zone based on seismic reflection profiling. Since Molnar and Sykes (1969) had not reported seismic activity on the Tehuantepec Ridge, the transform fracture zone was considered inactive. Truchan and Larson (1973) proposed that the structural weakness of the ridge resulted in the formation of a hinge fault upon subduction at the Middle America Trench. They claimed that the subduction of the Cocos Plate as two separate slabs with different dips could explain the lack of deep earthquakes in the Benioff Zone of Mexico noted by Molnar and Sykes (1969). The hinge fault was proposed to have caused the 800 m difference in the depth of the

trench axis north and south of the Tehuantepec Ridge, although that would seem to require initiation of hinge faulting considerably seaward of the trench axis rather than under the overriding plate as indicated by the authors. Truchan and Larson (1973) stated that the oceanic crust south of the ridge was older, cooler, and thicker than to the north and this allowed it to remain competent for a longer period following subduction resulting in the deeper Benioff zone beneath Central America.

Dean and Drake (1978) analyzed the focal mechanisms of Middle America Trench earthquakes and determined that the mean plunge of slip vectors was different north and south of the Tehuantepec Ridge. North of the ridge the motion of the subduction is oriented 15° below horizontal, whereas south of the ridge the subduction related earthquake slip vectors plunged 21°. This agrees with the difference in the azimuth of slip vectors, and the difference in dip of the Benioff zone reported by Molnar and Sykes (1969). Dean and Drake (1978) concluded that the sharp change in orientation of subduction indicated that the Cocos Plate was torn into two slabs upon subduction.

Nixon (1982) showed that there is a change in Benioff zone dip between Mexico and Central America, but the break does not correspond to the subducted trace of the Tehuantepec Ridge. Nixon (1982) located the change in Benioff zone orientation 200 to 300 km northeast of the Tehuantepec Ridge.

Burbach et al. (1984) demonstrated by precise location of reliably recorded seismic events that the subducted Cocos Plate is not faulted into two independently subduction slabs at the Tehuantepec Ridge. The Benioff zone showed no sharp discontinuity over the subducted Tehuantepec Ridge. The ridge did, however, have a measurable effect on the subduction of the Cocos Plate. Presumably due to the buoyancy and topographic relief of the ridge, the Benioff zone assumed a shallower dip over the ridge compared to the angle of subduction beneath Central America, but the change was in the form of a gentle arching rather than the distinct break envisioned by Truchan and Larson (1973) or Dean and Drake (1978). Burbach et al. (1984) reported a strike-slip event on the Tehuantepec Ridge seaward of the trench which indicated that the ridge is still somewhat active.

The Caribbean-North America Plate Boundary was provisionally identified as the landward extension westward of the Caribbean Cayman Trough by Molnar and Sykes (1969; Figure 3). It was stated that faults in eastern Guatemala subparallel to the Cayman Trough would be the likely site of the left-lateral movement, but no field evidence of strike-slip motion in southern Guatemala was known at that time.

Three arcuate faults, the Polochic, Montagua, and Jocotan were identified in southern Guatemala by field mapping and remote sensing (Figure 6). Evidence of substantial left-lateral movement along the Polochic and Montagua faults led to their assignment as the location of the North America-Caribbean Plate boundary (Muehlberger and Ritchie, 1975; Burkart, 1978).

Burkart (1983) contended that most of the Neogene movement along the transform plate boundary occurred on the Polochic Fault. By reconstruction of structures and drainage patterns on either side of the Polochic fault, Burkart (1983) accounted for 130 km of left-lateral movement within the last 10 m.y. Burkhart's (1983) reconstruction assumed a much more linear strike of the fault than previous representations (e.g. Case and Holcombe, 1980;

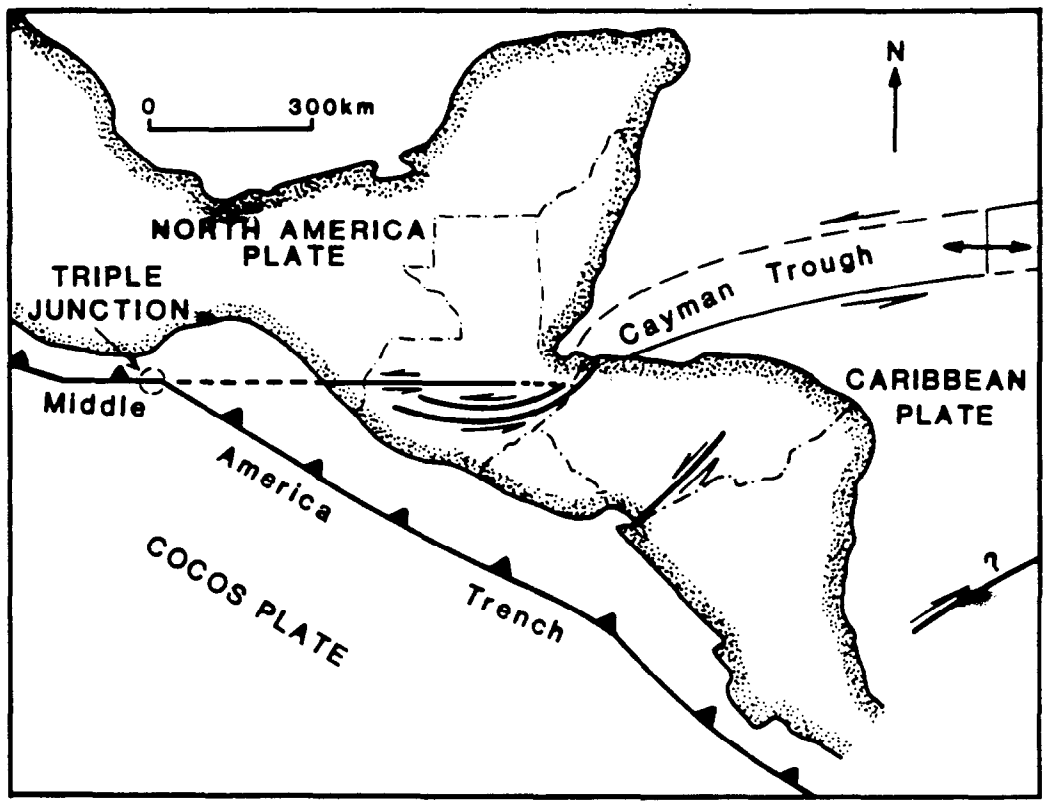

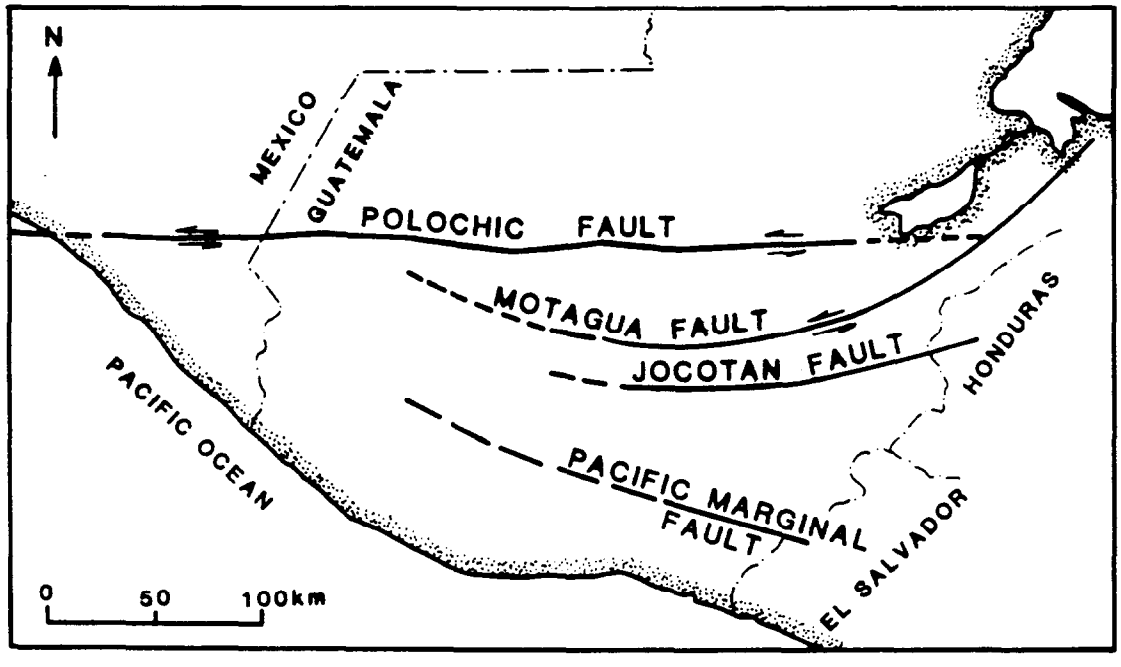

Figure 6. STRUCTURE OF THE NORTH AMERICA-CARIBBEAN-COCOS PLATE TRIPLE JUNCTION

After Burkart and Self, 1986

Drummond, 1983). A very important ramification of this more linear trace of the plate boundary is that when the Polochic fault is extended westward beneath the Pacific continental shelf and slope, it intersects the Middle America Trench at about 15°15'N. As seen on the bathymetric map (Figure 1), at 15°15'N the Middle America Trench is sinistrally offset and, for a short distance, the trench strikes almost due east-west. Burkart (1983) noted that the length of the trench offset (about 130 km) matched the offset which was documented along the Polochic fault in southern Guatemala. Thus, Burkart (1983) concluded that late Miocene to Holocene movement along the Polochic fault offset the Middle America Trench at the Tehuantepec Ridge intersection. The reconstruction of the area prior to movement of the fault shows that the Middle America Trench was a linear feature and that the accompanying back arc Miocene volcanic belt was continuous (Figure 7). The movement on the Polochic fault system could account for only about one half of the probable displacement of the North America and Caribbean Plates. Burkart (1983) proposed that large-scale extensional basin and range faulting in Central America south of the plate boundary absorbed the rest of the movement. Burkart (1983) suggested that the extensional forces in southern Guatemala could possibly explain the surprising finding of extensional rather than compressive features on the Guatemala continental slope by DSDP Legs 67 and 84.

Synthesis. The work which determined the true orientation of the Benioff zone landward of the trench and the character of the North America-Cocos-Caribbean triple junction suggests an explanation for the dual nature of the northern and southern segments of the Middle America Trench.

Burbach et al. (1984) and Nixon (1982) refined estimates of the orientation of the Middle America Trench Benioff zone. The Benioff zone beneath Central America is continuous, steep, and generally parallel to the trench (Figure 8). The distribution of Quaternary volcanics overlies the 150 km depth contour of the subducting plate. The Benioff zone is continuous across the Caribbean-North America plate boundary, but curves to assume a shallower dip to the north (Figure 8). One notable anomaly is that north of the Tehuantepec Ridge, the Benioff zone no longer parallels the Middle America Trench. Few seismic events occur to mark the Benioff zone beneath southwesten Mexico. Northeast of the seismic gap, a very shallow dipping Benioff zone oriented parallel to the Mexican volcanic belt has been mapped. Thus it is apparent that the oblique orientation of Quaternary volcanics in Mexico is a reflection of the present orientation of the subducted Cocos Plate.

Burbach et al. (1984) speculated that the present configuration of the Benioff zone beneath Mexico is a result of the Pliocene to Holocene movement of the Polochic-Montagua fault system documented by Burkart (1983). By superimposing the present Benioff zone contours on the probable arrangement of plates at the end of the Miocene (Figure 9), the segment of the subducted plate just north of the Polochic-Montagua fault can be aligned parallel to the trench axis. However, the present Benioff zone beneath Mexico landward of the northern part of the trench bears no relationship to the trench position at the Miocene-Pliocene boundary. Burbach et al. (1984) postulated that the subducted Cocos plate segment has become grounded in the mantle and is now being overridden by the westward moving North America Plate. The subducted Cocos plate beneath central Mexico has

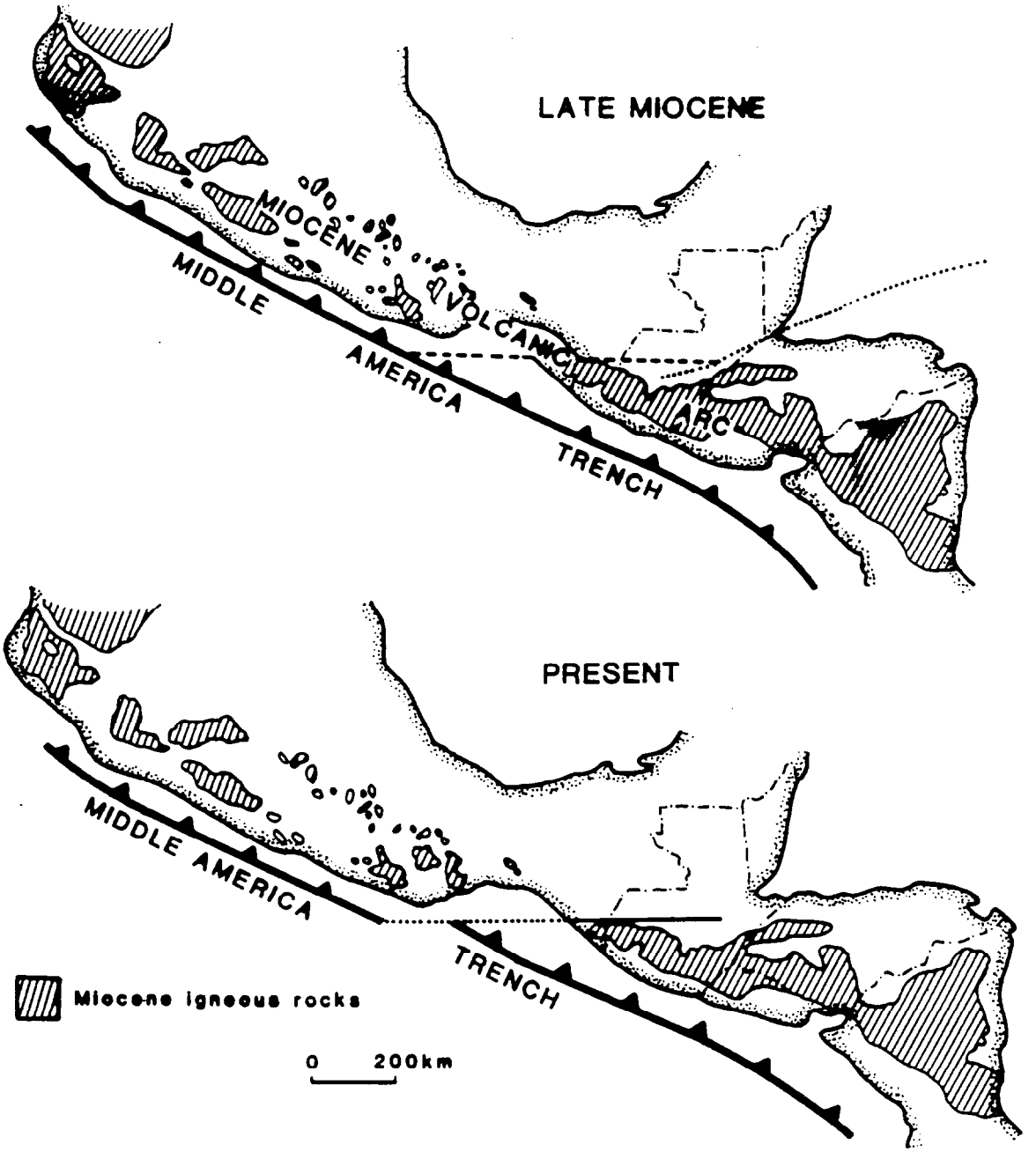

Figure 7. RECONSTRUCTION OF MIDDLE AMERICA TRENCH BEFORE OFFSET ALONG POLOCHIC FAULT

After Burkart, 1983

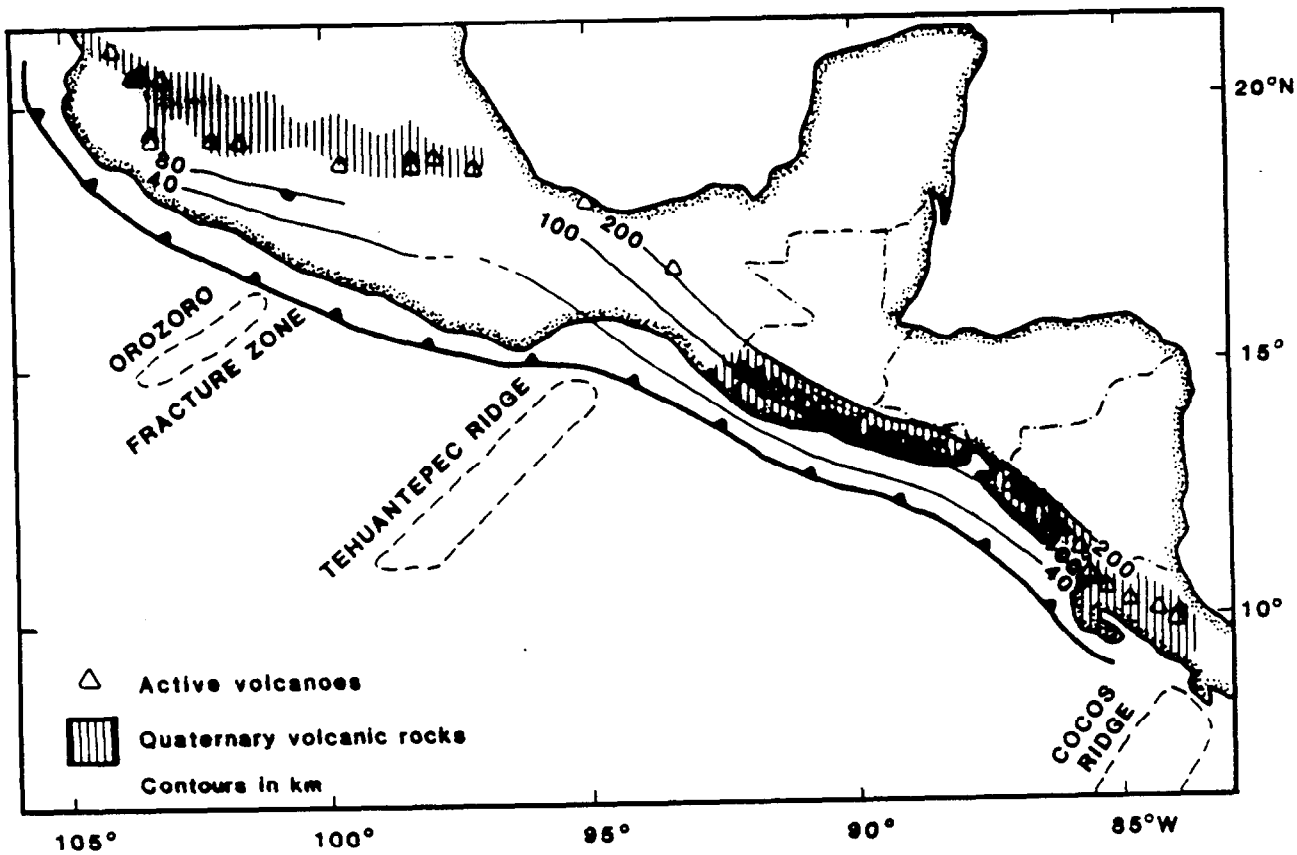

Figure 8. STRUCTURE OF SUBDUCTED COCOS PLATE

After Burbach et al., 1984

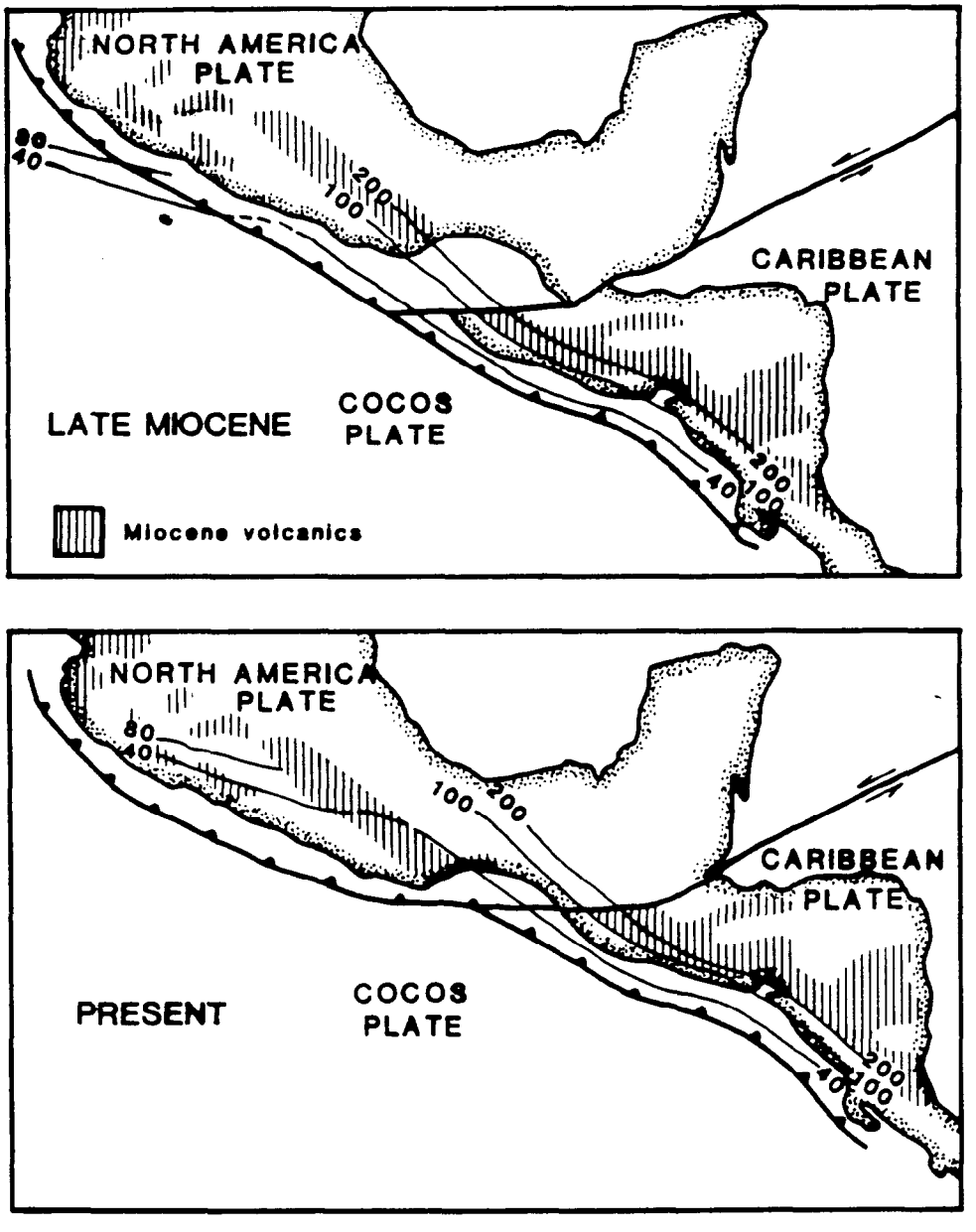

Figure 9. RECONSTRUCTION OF SUBDUCTED COCOS PLATE IN LATE MIOCENE BASED ON PRESENT BENIOFF ZONE GEOMETRY

After Burbach et al., 1984

become reconfigured to conform to the current plate motions. A similar scenario was discussed by Cross and Pilger (1982) using the plate velocity data of Jordan (1975). The North America Plate has been moving rapidly to the west-southwest in relation to the mantle, whereas the Caribbean Plate has been moving northwest at a much lower velocity. Cross and Pilger (1982) used the Middle America Trench as a type example of the effect of absolute motion of the overriding plate toward a trench; the angle of subduction flattens out greatly resulting in a magmatic gap near the arc. Precise mapping of the Benioff zone by Burbach et al. (1984) corroborate the effect of active overriding of the Cocos Plate by the North America Plate.

Lithostratigraphy

The sediments covering the Middle America Trench study region were sampled by coring during Deep Sea Drilling Project (DSDP) Legs 66, 67, and 84. A wide range of depositional environments is represented in the sites selected for drilling. Cores were recovered from the Cocos Plate, where pelagic and hemipelagic sediments document the migration of the plate from its formation at the East Pacific Rise. Sediments from the Middle America Trench axis showed the effect of submarine canyons in conveying coarse littoral and neritic sediments to the deep waters of the Trench. Cores from the Pacific continental slope of Mexico and Central America revealed pulses of rapid sedimentation separated by hiatuses along with abundant volcanic ash.

DSDP Leg 66

Eight locations offshore of the Mexican states of Oaxaca and Guerrero were drilled in Leg 66 (Figures 1, 10, and 11).

Site 486 was drilled 3 km seaward of the Middle America Trench axis in 5,140 m of water (Figures 10 and 11). Two holes offset 1 km were drilled at the location.

Coarse Quaternary sand was cored from the two holes at Site 486 (Figure 12). The recovered sediments were homogeneous in texture, unlike typical coarsening upward sediments expected in trench environments. It was proposed that the recovered sand was delivered to the site directly from the beach via a deep canyon cutting through the landward slope of the Trench. After coring 38 and 22 m of sand from Site 486, the location was abandoned for more prospective sites.

Site 487 was drilled on the Cocos Plate, 12 km seaward of Site 486 beneath 4,764 m of water (Figures 10 and 11). The location was selected to sample sediments on the oceanic plate to determine the rate and type of sediment delivery to the trench.

A sediment column of 171 m and 10 m of basalt basement was drilled at Site 487 (Figure 12). The hole was continuously cored from the sea floor. Sediments consisted of a 105 m Quaternary unit consisting of hemipelagic mud over a 66 m thick Miocene to Pliocene age section composed of pelagic clay.

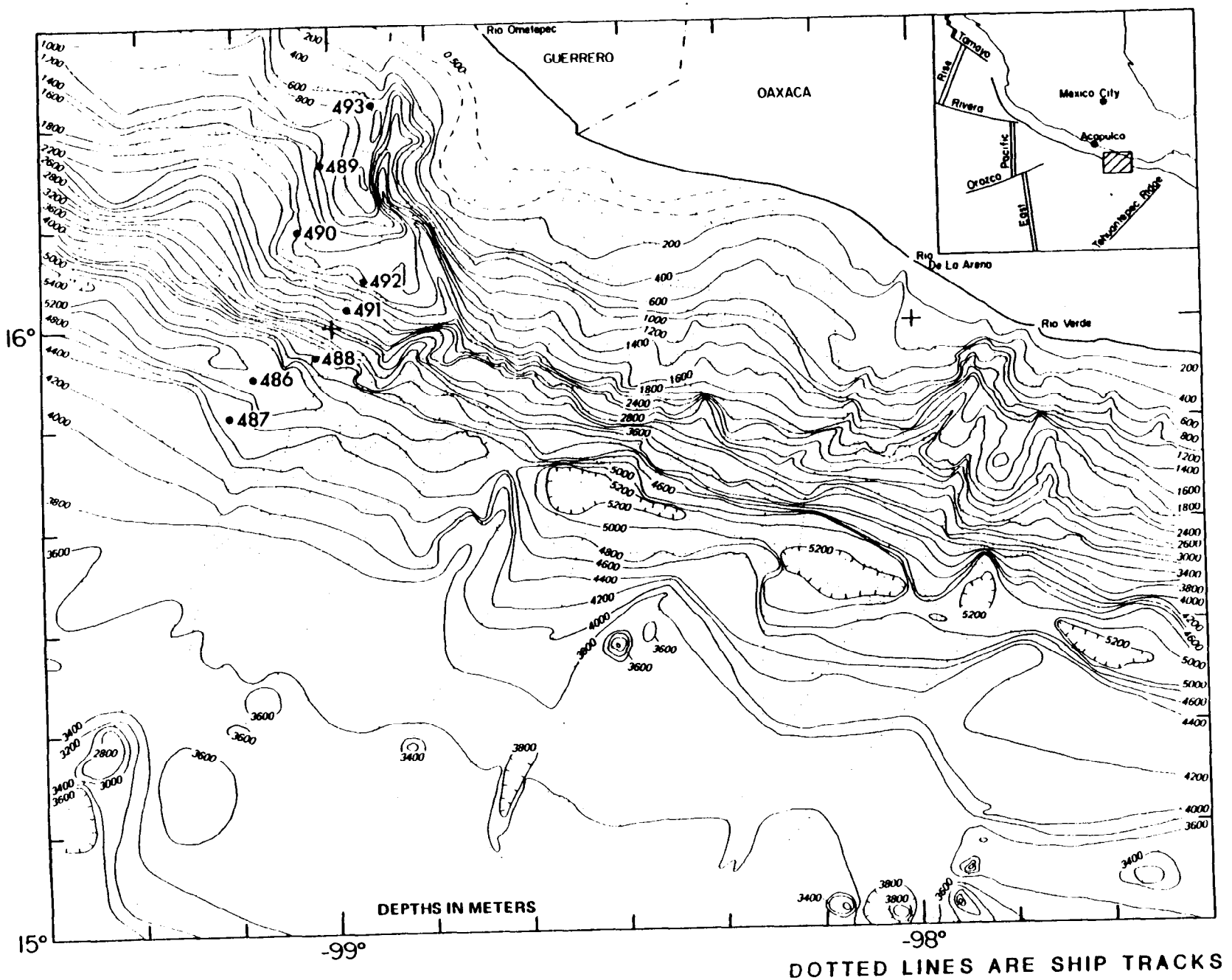

Figure 10. **DETAILED BATHYMETRIC MAP OF THE CONTINENTAL MARGIN OF MEXICO**

After Shipley, 1982

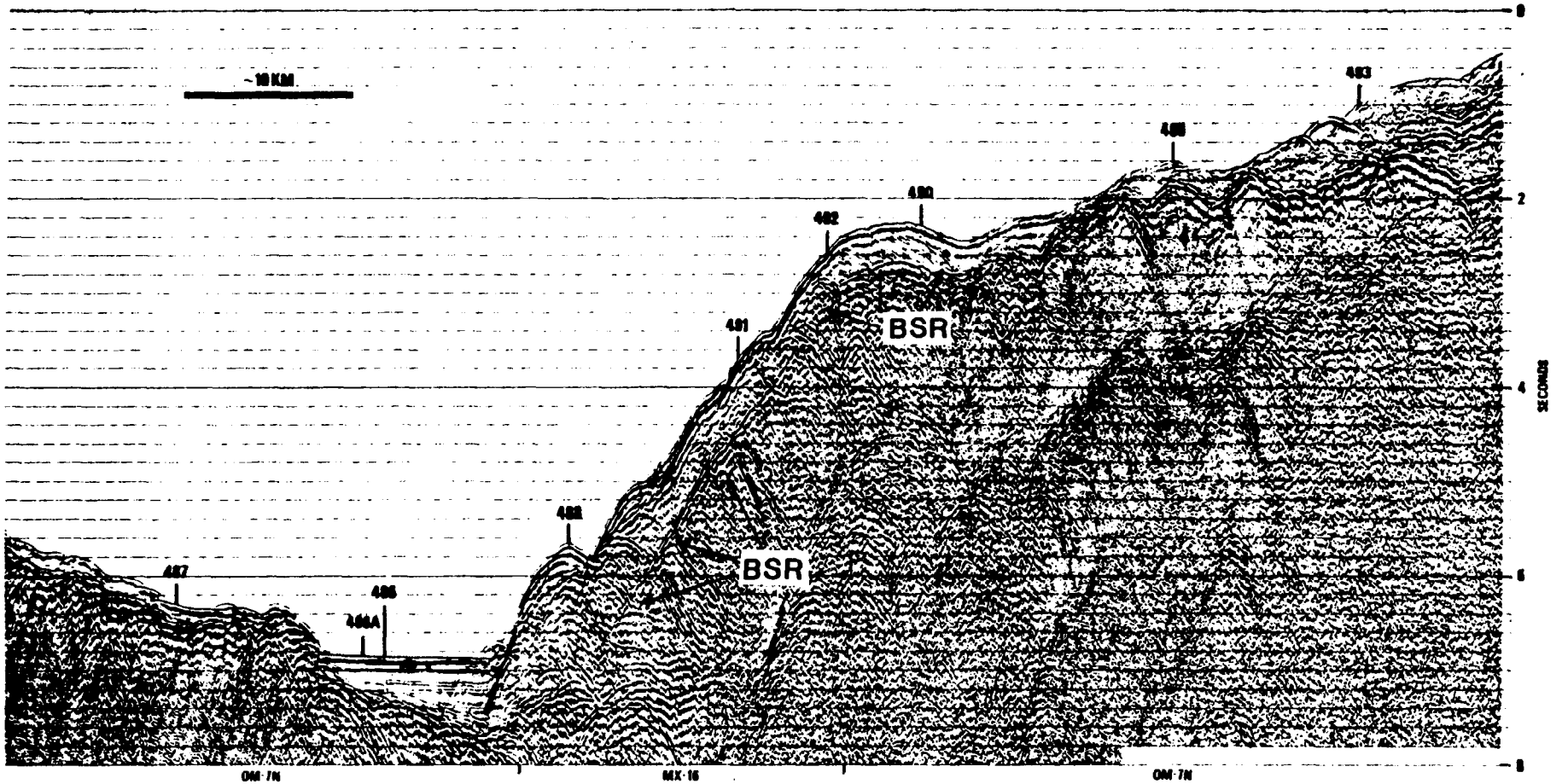

Figure 11. COMPOSITE SEISMIC SECTION OF MIDDLE AMERICA TRENCH SHOWING LOCATION OF DSDP LEG 66 SITES

After Watkins et al., 1982

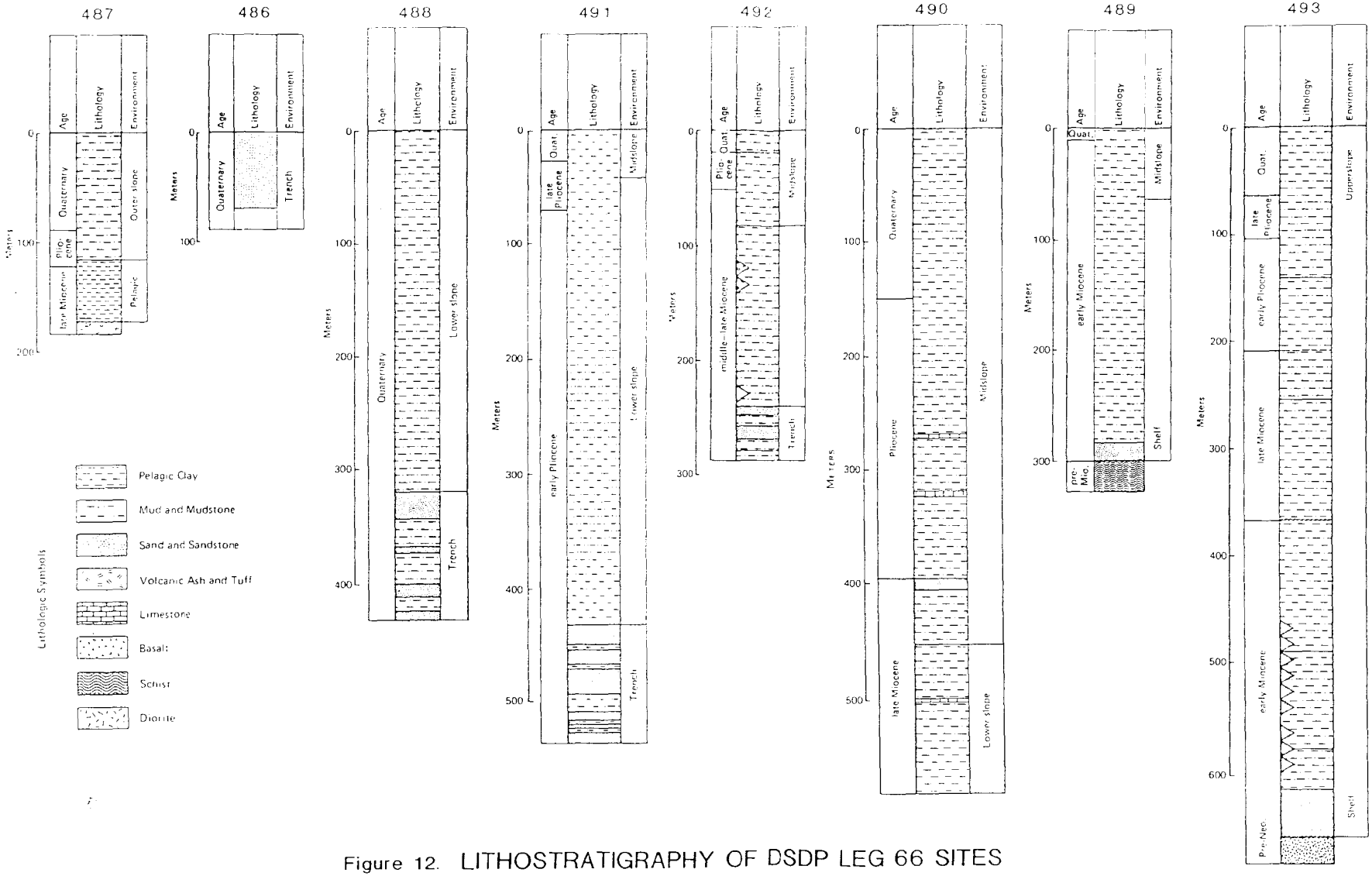

Figure 12. LITHOSTRATIGRAPHY OF DSDP LEG 66 SITES

After Stradner and Allran, 1982

The contact was fairly sharp between the two units, implying deposition of the upper unit by a gravity flow from the continental margin. The lower unit accumulated at a rate of 7 to 29 m/m.y.; the Pleistocene hemipelagic section accumulated at 28 to 129 m/m.y.

No evidence of gas hydrates or hydrocarbon gases were found at the site. Total organic carbon (TOC) ranged from 1.7% near the surface to 0 near the basalt contact.

Site 488 was drilled on the first structural high landward of the Middle America Trench in 4,254 m of water (Figures 10 and 11). Site 488 was located 12 km northeast of Site 486. The principal objective at Site 488 was to drill through a prominent landward dipping reflector (LDR) which had been interpreted as a thrust fault resulting from accretion of slope deposits to the continental margin.

A Quaternary sediment section was drilled to a depth of 429 m (Figure 12). The hole was continuously cored with 37% recovery. A unit composed of gray to gray-green mud and muddy silt was recovered from the sea floor to 303 m subbottom. A lower unit of sand and pebbly sand was drilled from 120 m before drilling was terminated.

The upper unit was tectonically deformed. The dips of bedding planes increased from horizontal at depths less than 210 m to 60° between 210 and 240 m. Fracturing was common below 20 m. Between 220 and 240 m, the fractures were healed producing blebs and stringers of silt in a mud matrix. In this interval, bulk density increased sharply, and water content dropped reaching a minimum at 240 m. Possible breccia was noted at 260 m. High levels of ethane also marked this zone. From this evidence, a fault was inferred to exist at a depth of near 240 m.

The landward dipping reflector was penetrated at 302 m. It was marked by a lithological change to coarser trench deposits. No direct evidence of thrusting was found coincident with the LDR.

Gases including methane, carbon dioxide, and ethane were recovered throughout the hole. No gas hydrate samples were found at Site 488. TOC values decreased from 2.6% at 38 m to 1.5% at total depth.

Site 489 was drilled on the upper continental slope beneath 1,240 m of water to determine the offshore extent of the metamorphic basement of western Mexico (Figure 10 and 11). A sediment section 302 m thick and 24 m of schist basement were drilled (Figure 12).

Four sedimentary units were recognized at Site 489. A thin veneer of Quaternary silt with abundant organic debris covered an unconformity at a depth of 5 m subbottom. Three underlying early Miocene units composed of silt and siltstone with rare calcareous limestone layers differed mainly in their clay content. The Miocene sediments were deposited rapidly, from 21 to 106 m/m.y.

Hydrocarbon gas was found throughout the sedimentary section. Methane predominated in the core gas. Ethane content increased with depth. A large increase in propane and heavier hydrocarbons was noted near the contact with the basement at 303 m. A maximum value of 4,362 ppm was measured at the contact. Organic carbon varied from 0.1 to 1.4%. No direct evidence of gas hydrates was noted at Site 489.

Site 490 was located on the lower continental slope 13 km south-southwest of Site 489 in 1,761 m of water (Figures 10 and 11). The location was selected to drill rocks thought to represent sediments accreted to the metamorphic continental crust drilled at Site 489. Miocene through Holocene sediments were drilled to a depth of 589 m (Figure 12).

The sedimentary sequence was divided into three units. Unit 1, extending from the sea floor to 142 m subbottom, consisted of muddy silt with rare limestone nodules. The sediments were locally glauconitic and bioturbated. Minor ash beds were found in Unit 1. More indurated siltstones of Pliocene to earliest Pleistocene age constituted Unit 2. Limestone and ash beds were common. Fractures and slickensides became more frequent near the base of the unit at 400 m. Unit 3 was more thoroughly indurated and deformed than Units 1 and 2.

Abundant hydrocarbon gas was recovered at Site 490. Ethane content increased downhole. Propane, butane, and pentane reached levels in excess of 800 m between 370 and 430 m corresponding to the most intensely faulted section of the hole. Organic carbon ranged from 1% to 3%, averaging 1.6% TOC.

Frozen sediments which released gas upon thawing were recovered at 139, 145, 166, and 370 m. These intervals seemed to be associated with vitric ash beds or faulted intervals. The shipboard scientists suspected that the icelike material was gas hydrate, but could not conclusively confirm hydrate presence.

Site 491 was located on the lower continental slope 13 km southeast of Site 490 beneath 2,890 m of water (Figures 10 and 11). The location was selected to permit drilling of a prominent landward dipping reflector (LDR) which had previously been interpreted to be a thrust fault resulting from accretion (Figure 11). The site selected was also directly over a distinct bottom simulating reflector (BSR).

A lower Pliocene to Holocene sedimentary section comprising three units was drilled to a depth of 542 m. Unit 1 was composed of silt and mud with ash layers and calcareous concretions (Figure 12). Unit 1 (0 - 67 m subbottom) was dated as late Pliocene to Holocene age. Unit 2, extending to 437 m subbottom was similar in composition, but more thoroughly indurated. Unit 3, lower Pliocene, consisted of muddy siltstone with beds of coarse pebbly sand.

The sequence at Site 491 was interpreted to represent depositional processes similar to those noted at Site 488. The lower coarse-grained deposits were considered to be trench deposits. The overlying finer-grained slope deposits accumulated after Site 491 was uplifted, apparently due to accretion. No evidence of faulting which would correlate with the seismic LDRs was identified.

Hydrocarbon gases were abundant in cores from Site 491. Small quantities of hydrocarbons heavier than methane were noted throughout the hole varying irregularly in concentrations.

Probable gas hydrates were recovered at 89 m, 163 m, and 168 m subbottom. Icelike nodules up to several centimeters in diameter were noted.

Site 492 was located 5 km upslope from Site 491 in 1,960 m of water (Figures 10 and 11). The drilling objectives were to again penetrate an LDR

and to determine if the trend of progressively older slope deposits over coarse trench sands noted at Sites 488 and 491 continued landward.

A sedimentary section 280 m thick was drilled at Site 492 (Figure 12). The upper 250 m was composed of upper Miocene to Holocene muddy silt and siltstone. Ash beds and glauconite-rich layers occured throughout the interval. Fracturing was noted especially in the lower 50 m of the interval. The lowermost 30 m of the hole is composed of sand and sandy gravel of late Miocene age.

Methane and minor amounts of heavier hydrocarbons were detected throughout the hole at Site 492. Carbon dioxide and hydrocarbons heavier than methane reached concentration peaks of 1.2% and 380 ppm respectively at 100 - 110 m depth. Organic carbon decreased downhole from 2.31% to 0.53%.

Frozen ash beds which released great quantities of gas were recovered from 140 m and 170 m. The shipboard scientists concluded that the ash samples contained interstitial gas hydrates.

Site 493 was located 37 km landward of Site 492, 16 km from the Mexican coast (Figure 10). The location was selected to provide a near shore reference point for the Mexican continental slope transect of Leg 66 (Figure 11). Site 493 is beneath 660 m of water.

A sedimentary section 652 m thick overlaid diorite continental basement at Site 493. The lithologies encountered in drilling were similar to those found at Site 489 (Figure 12). Quaternary silt up to 50 m thick with abundant wood debris, ash, and sand layers blanketed the site. An upper Miocene to Pliocene sequence (50 - 365 m subbottom) composed of silt, siltstone and mudstone with occasional fracturing was interbedded with ash and limestone. The basal sediments at Site 493 were lower Miocene siltstones and coarse sands. Slickensides document minor faulting.

Hydrocarbon gases were recovered below 30 m at Site 493. Shipboard scientists assumed a biogenic origin for the gas.

DSDP Leg 67

Seven locations offshore of San Jose, Guatemala were drilled during DSDP Leg 67. The sites comprised a transect of the Guatemala continental margin from the Cocos Plate (Site 495) through the trench axis (Sites 499 and 500), lower continental slope (Sites 494 and 498), and upper continental slope (Sites 496 and 497).

Cocos Plate. Site 495 was drilled 22 km seaward of the trench axis where seismic data indicated 0.4 sec of sediment overlying acoustic basement (Figures 13 and 14). The site was located on a horst in the normally faulted oceanic plate. The site yielded a 428 m hemipelagic and pelagic section overlying basalt basement (Figure 15).

The sediments of Site 495 recorded the changes in sedimentation which accompanied the evolution of an oceanic plate on its route from a spreading center to near a subduction zone. The basal sedimentary unit was a lower to middle Miocene pelagic carbonate layer over 228 m thick. The chalk was discolored in its lowermost 30 m by ferromagnesian minerals derived from hydrothermal circulation near the spreading center. The carbonate layer was deposited very rapidly for pelagic strata, 50 m/m.y. (Coulbourn et al., 1982),

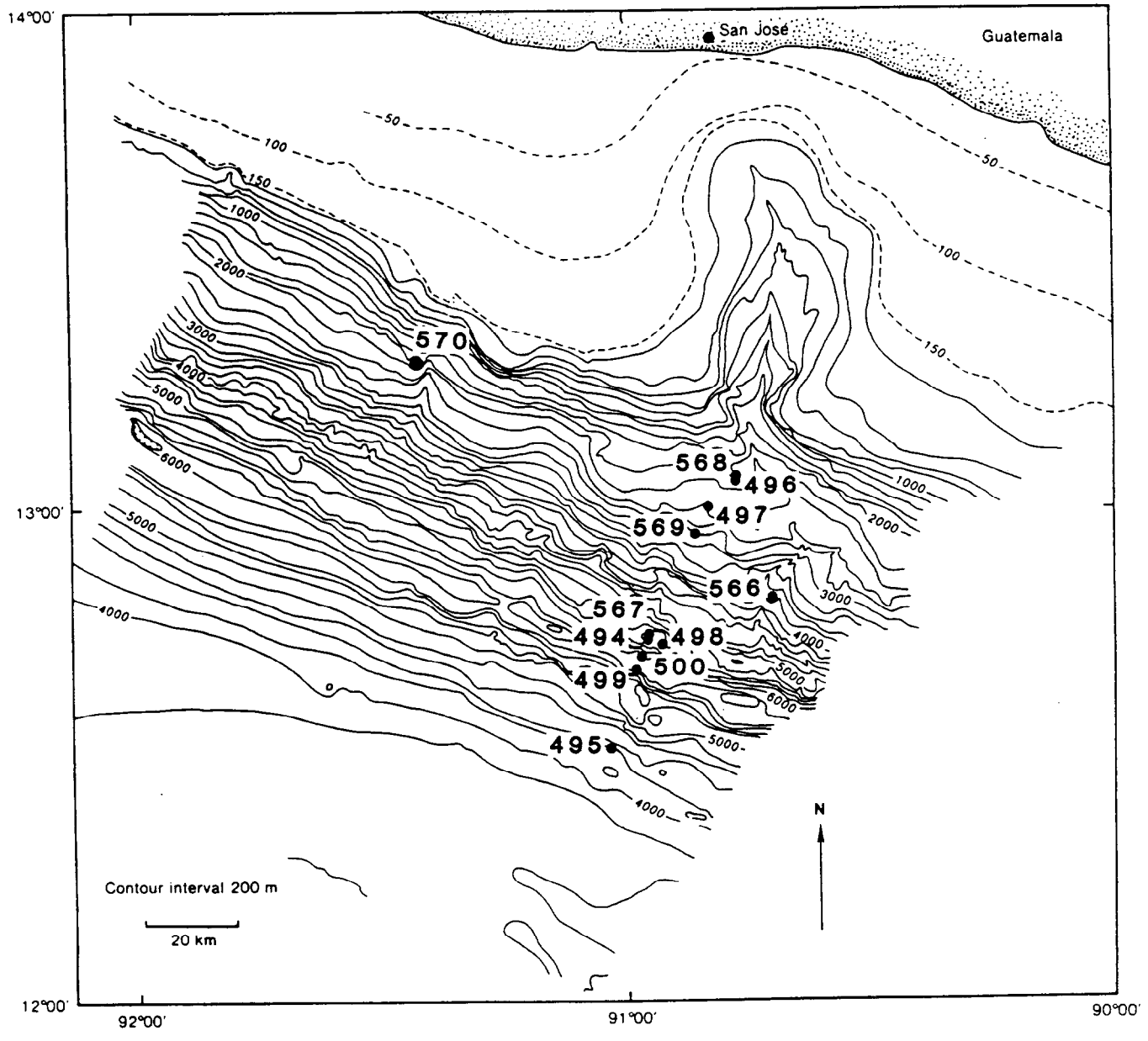

Figure 13. LOCATION OF DSDP SITES OFFSHORE OF GUATEMALA

After Ladd et al., 1982

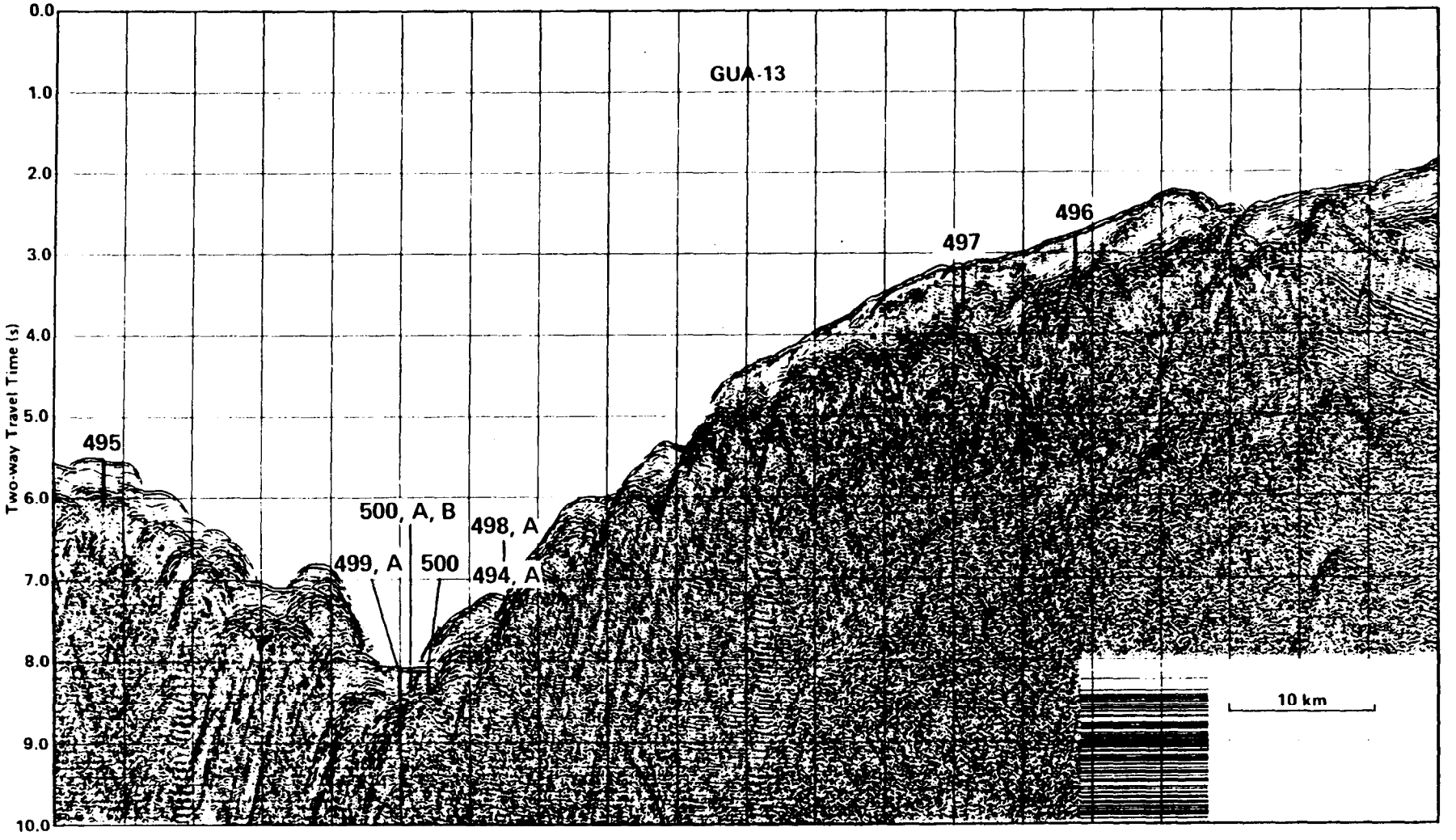

Figure 14. SEISMIC LINE GUA-13 OFFSHORE OF GUATEMALA SHOWING LOCATION OF DSDP LEG 67 SITES

After Colbourn, 1985

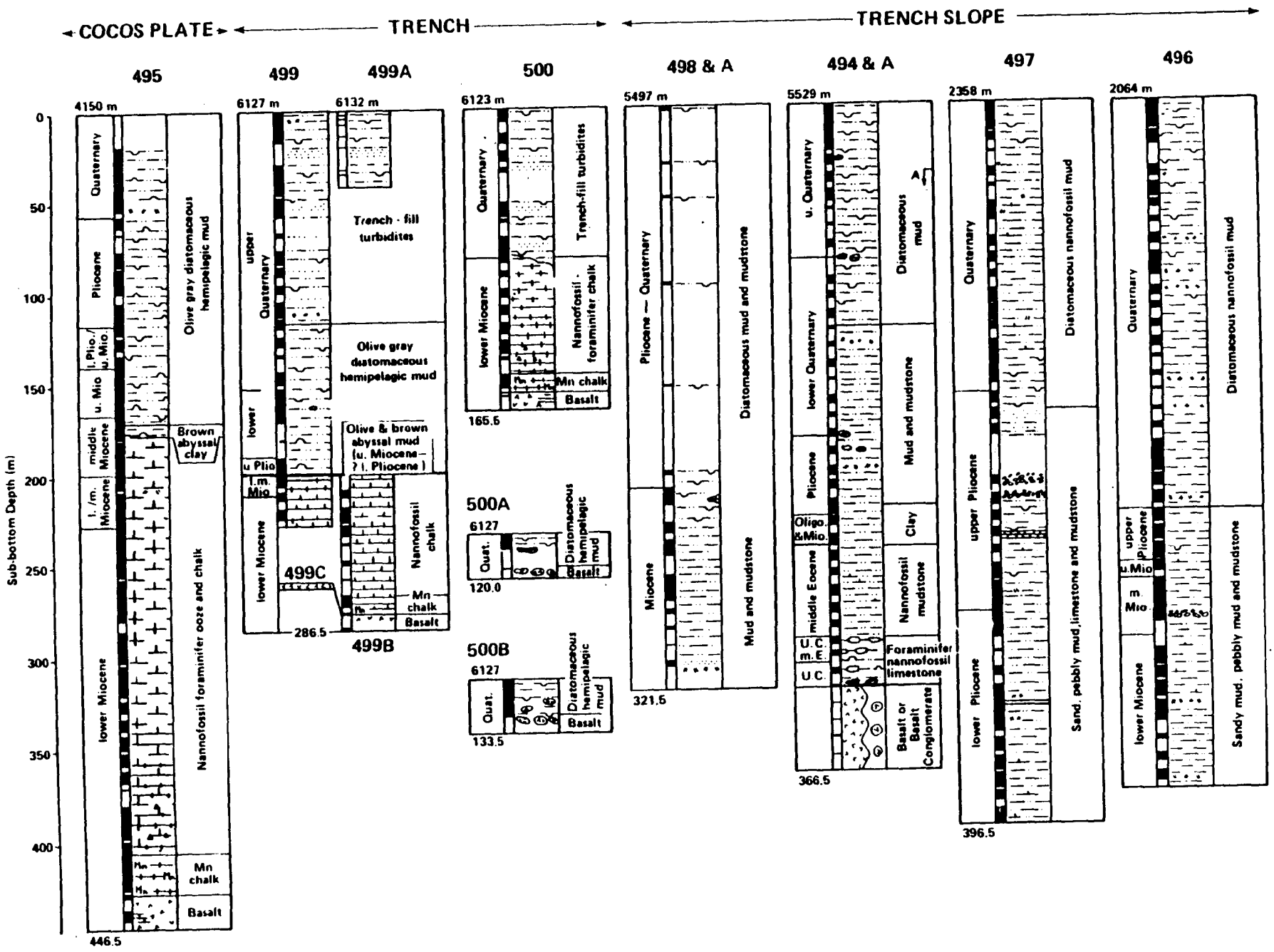

Figure 15. LITHOSTRATIGRAPHY OF DSDP LEG 67 SITES

After von Huene and Aubouin, 1982

reflecting the high primary productivity of the equatorial Pacific waters. An overlying layer of middle Miocene brown abyssal clay recorded the subsidence of the Cocos Plate below the carbonate compensation depth (CCD) as the plate moved southeastward away from the East Pacific Rise. Capping the 7 m pelagic clay sequence was a middle Miocene to Holocene section of green and gray hemipelagic mud 171 m thick.

Such a thick hemipelagic section at Site 495 was unexpected. The site is over 1,900 m shallower than the trench axis and is located on a prominent horst. Suspended sediments resulting from slumps and gravity flows down the continental slope have apparently traveled 22 km up the seaward slope of the trench. Since the site is currently converging on the trench at a rate of 9 cm/yr. (von Huene and Aubouin, 1982), the site would have been over 900 km from the trench when hemipelagic sediments were first deposited. Even if a much slower rate of convergence is assumed, the distance seaward that the terrigenous sediments traveled upslope from the trench axis is exceptional.

No hydrocarbon gases were in the sediments from Site 495.

Trench Floor. DSDP Sites 499 and 500 were drilled on the floor of the Middle America Trench (Figures 13 and 14). To adequately sample the trench deposits, four holes were drilled at Site 499 and three at Site 500.

Cores from Site 499 revealed a typical Cocos Plate oceanic pattern of hemipelagic sediments overlying pelagic carbonates resting on basalt (Figure 15). Capping the oceanic sequence, a 100 m trench fill unit composed of sandy turbidites separated by hemipelagic muds was cored. Probable water depth of deposition of the slope sediments of which the turbidites were composed increased with depth in the turbidites; shelf and upper slope debris dominate the upper parts of the turbidite units. Offset drill holes at Site 499 showed that the turbidite blanket was widespread on the trench floor.

The hemipelagic and pelagic oceanic sediments beneath the trench fill deposits were markedly thinner than similar deposits at Site 495. The reduced thickness of the pelagic carbonates at Site 499 relative to Site 495 (70 m vs. 210 m) was proposed to be due to deposition beneath the CCD. This possibility was borne out by a much greater degree of foraminifera dissolution in the cores from Site 499. The two sites were a mere 22 km apart, implying a large change in the lysocline depth over a short distance. Additionally, the brown pelagic clay found capping the carbonate section of Site 495 was not recovered at Site 499; hemipelagic mud directly overlaid the carbonates. The investigators did not have a comprehensive explanation for these discrepancies, but suggested removal of section at Site 499, or unequal rates of deposition due to position of the sites relative to the fault blocks making up the Cocos Plate.

Site 500 was drilled 2 km landward of Site 499 near the subduction front. A similar stratigraphic sequence was recognized at Site 500: turbidites, hemipelagic muds, pelagic carbonates, and basalt. The exact thickness of the various units was not determined. Basalt cobbles interrupted drilling on two holes. On the other hole, a normal fault which juxtaposed Quaternary turbidites and Miocene carbonates removed over 100 m of section from the cores. The turbidites drilled at Site 500 contained much organic debris including wood and plant materials.

No evidence of compressional deformation was seen in any of the cores from Sites 499 and 500.

In addition to the major normal fault drilled at Site 500, small normal faults were found in cores throughout the sedimentary section at both Sites 499 and 500.

Basaltic basement was reached more than 100 m shallower at Site 500 than at Site 499. Since Site 500 is the more landward location, it was expected that the basement would be deeper there than at Site 499 due to the 20° dip of the Cocos Plate into the trench. The shallow basalt at Site 500 could be interpreted as a thrusted, accreted sliver of Cocos Plate crust. However, in the absence of any evidence of small-scale deformation, and the presence of a major normal fault, such an accreted or underplated wedge was untenable. High resolution bathymetric surveys by Aubouin et al. (1984) showed that Site 499 is located in a graben of the Cocos Plate while Site 500 is located on the flank of a horst. Thus, the shallow basaltic basement drilled at Site 500 is a result of extensional deformation rather than compression.

Hydrocarbon gases were released from the cores of Sites 499 and 500. The gas was predominantly methane, with methane:ethane ratios of greater than 100,000 indicating biogenic origin (Aubouin et al., 1982). No quantitative estimate of the amount of gas contained in the cores is available. However, comments by shipboard personnel imply that the amount of gas diminished rapidly beneath the turbidite sediments at Site 499, while being measurable to total depth at Site 500.

Lower Slope. The lower part of the landward slope of the Middle America Trench is characterized by a series of three topographic benches separated by steeper steps (Figure 14). These topographic features suggest fault blocks. The steps and benches most closely resemble a set of normal fault scarps. However, the benches could also represent inbricate thrust sheets which would be expected at this position above the subduction zone according to the accretionary model of the Guatemala Margin proposed by Seeley (1979). By drilling into the bench on Leg 67 the accretionary model was to be tested. Evidence of compressional deformation or sediments in a reversed stratigraphic sequence (i.e. becoming younger with depth) would indicate thrusting and, by extension, support the accretionary model.

Two DSDP sites were drilled on the first bench landward of the trench during Leg 67.

Site 494, located 22 km landward of the trench axis (Figures 13 and 14) drilled a 320 m sediment section ranging in age from Upper Cretaceous to Holocene (Figure 15; Coulbourn et al., 1982). The hole bottomed in altered mafic igneous rocks which had a composition unlike typical oceanic crust. The 9 m basal sedimentary layer consisted of gray Upper Cretaceous mudstone deposited in open marine conditions. A 20 m Upper Cretaceous blue micritic limestone was unconformably overlain by 50 m of middle Eocene sandy mudstone. An overlying unit of Miocene bluish clay 20 m thick was also capped by an unconformity. The upper 210 m of Pliocene to Holocene sediments were gray diatomaceous mudstones derived principally from downslope transport of and redeposition of upper slope sediments.

Site 498 was offset 1.8 km from Site 494 along the strike of the slope. Seismic sections reviewed subsequent to drilling Site 494 suggested that Site 494 may have been located on a major transverse fault. Thus the missing time-equivalent strata interpreted as unconformities at Site 494 may have

been fault planes instead. Site 498 was drilled to determine whether the rocks not sampled at Site 494 were missing due to faults or erosional unconformities, and to attempt to drill through the overriding plate to sample subducted oceanic material.

The uppermost 200 m of sediment drilled at Site 498 was very similar to that sampled at Site 494, Pleistocene and Holocene diatomaceous mud and mudstone (Figure 15). The next lower 100 m of section was very different from the Cretaceous through Pliocene section at Site 494. A Miocene to Pliocene mudstone sequence with occasional limestone, ash, and sand layers was drilled between 210 and 310 m subbottom. The Miocene to Pliocene bluish clay found at Site 494 was not found. Indeed, the thick terrigenous Miocene sediments from Site 498 appeared to be missing or very thin at Site 494. The discrepancy in Miocene sediments between the two closely spaced locations may have been due to faulting or to different sediment depositional environments. Different paleobathymetry may have allowed hemipelagic sediments to accumulate at Site 498 during the Miocene, while Site 494 on a local high received only pelagic input or was exposed to current erosion.

Despite the plans to drill into the subduction zone at Site 498, drilling was terminated at 310 m in Miocene sediments. A large icy chunk of gas hydrate in a vitric pyroclastic sand matrix was recovered at Site 498. The hydrate was restricted to a volcanic ash layer; sediments above and below the coarse ash (lapilli) were barren of hydrate. Concurrently with the hydrate recovery, a large increase in the ethane content of core gas was noted. The elevated ethane concentrations were taken as an indicator of possible proximity to a thermogenic gas reservoir. In accord with DSDP safety conventions, drilling was stopped at Site 498.

Gas had been recovered from cores of Site 494. However, no gas hydrates were identified in the cores of Site 494. The coarse vitric ash layer from which gas hydrates were recovered at Site 498 were either not present in the sedimentary pile at Site 494 or were not sampled by the discontinuous coring employed at the sites.

Upper Slope. Two holes were drilled into the upper continental slope of Guatemala on DSDP Leg 67. Both Sites 496 and 497 were located near a major submarine canyon, the San Jose Canyon (Figure 13). The principal objective of drilling the upper slope sites was to penetrate and sample the acoustic basement. Drilling was terminated at holes 496 and 497 far short of their objective due to the possible presence of gas hydrates and the concomitant potential safety and pollution problems.

Site 496 was drilled beneath 2,049 m of water to a depth of 378 m. The site was located near the edge of the San Jose Canyon 4,000 m above and 47 km landward of the trench floor (Figures 13 and 14).

An indurated lower Miocene to Pliocene unit was found to be overlain by a 220 m Pleistocene to Holocene hemipelagic mud section (Figure 15). The lower unit was composed of overcompacted mudstone containing abundant volcanic debris throughout. Several layers of sand and silt were recovered; the sand was composed mainly of volcanic glass and biogenic debris rather than quartz. An intraformational conglomerate of mudstone clasts in a mud matrix was noted in the lower unit. Near the bottom of the drill hole, extensive sets of veins filled with clay were found and were interpreted as being due to rapid diagenetic dewatering. The Quaternary slope drape was remarkable for its thickness and high ash content.

Gas hydrates were inferred to have been drilled at Site 496 based on abundant methane and ethane in core gases and decreases in pore water salinity.

Site 497 was drilled 8 km downslope (SW) from Site 496 in an attempt to drill to basement without encountering the gas hydrates which caused abandonment of Site 496 (Figures 13 and 14). A hemipelagic sediment section of 396 m was drilled before abandoning the hole due to gas hydrate presence.

The recovered sediment was divided into three units of similar composition (Figure 15). The lowermost unit consisted of 180 m of olive gray mudstone of Pliocene age with sigmoidal veins and pervasive fractures. Overlying this indurated layer, a 70 m zone of ashy muds with an intraformational mudstone conglomerate was found. The sedimentary sequence was capped by a 150 m sequence of Quaternary mud with abundant vitric ash.

Gas hydrates were recovered in layers of coarse volcanic ash at Site 497. Additionally, high hydrocarbon gas content and pore water freshening suggested gas hydrate presence.

DSDP Leg 84

The results of drilling on Leg 67 were so surprising that the Glomar Challenger returned to drill the Guatemala continental margin during Leg 84. The cores recovered in Leg 67 showed no evidence to indicate that oceanic sediments from the descending Cocos Plate were accreted to the overriding Caribbean Plate. This was particularly surprising because the Pacific margin of Guatemala was presented as a type area for accretionary processes during subduction by Seely et al. (1974) and Seely (1979). All cores examined showed sediment beds in normal stratigraphic sequence and some displayed evidence of tensional faulting. These features are very different from that predicted by Seely's model. Safety considerations caused abandonment of several drill holes on Leg 67 before their principal drilling objectives were reached. Deep landward dipping seismic reflectors which were originally believed to be thrust faults were not cored. Thus, although many significant findings were obtained on Leg 67, much important work remained to be done.

Reprocessed existing data was used to plan the drilling program for Leg 84. Seismic sections which were collected and processed by the University of Texas Marine Science Institute (UTMSI) were the basis for selection of drilling sites for Legs 66 and 67. The multichannel seismic lines showed excellent details of the structure beneath the Guatemala continental shelf, but abundant diffraction features obscured features of the continental slope. Additionally, gas hydrates were recovered in cores in Leg 67, but no BSRs were seen in the seismic lines of the drilling sites. The original seismic records for 2 of the seismic lines collected by UTMSI, GUA-13 and GUA-18, were reprocessed using more sophisticated methods (von Huene et al., 1985). In these migrated sections BSRs could be resolved at 0.65 sec subbottom near Sites 496 and 497, both of which showed evidence of gas hydrate presence during the earlier cruise. Corrected acoustic velocity values for sediments within the gas hydrate stability zone were also available from Leg 67 data. Combining the seismic and drilling data, a probable depth of 550 m to the base of gas hydrates was obtained. The possibility of a free gas pool beneath the gas hydrate stability zone precluded drilling through the stability zone. Thus,

drilling sites for Leg 84 were chosen so that important horizons could be sampled at depths shallower than 550 m.

Site 565 was located 27 km landward of the Middle America Trench axis offshore of the Nicoya Peninsula, Costa Rica (Figure 2). The drill site is situated near the southern termination of the Middle America Trench, north of the Cocos Ridge. Site 565 was situated on a rise between two small submarine canyons dissecting the slope. The selection of the site was made so as to permit sampling of an acoustically turbid zone beneath slope sediments. This seismically indistinct zone was provisionally correlated with the well documented onshore accretionary terrane of the Nicoya Peninsula.

The hole was abandoned short of its objective after drilling 328 m of slope sediments due to drilling difficulties. The slope sediments consisted of dark greenish gray mudstones of Pliocene to Pleistocene age with occasional sand and ash layers. No evidence of accretion in the form of repeated or overturned strata was found. Paleontological age boundaries were not sharply defined, which, along with sedimentary structures, implied that much of the slope sediment was deposited from mass movements or density currents. The shear strength of the sediment increased rapidly for the first 30 m and remained approximately constant through the remainder of the hole. This indicates overcompacted shallow sediments and undercompaction at depths instead of the expected gradual increase in compaction with depth. Shipboard scientists speculated that the shallow sediment may have released incorporated gas or liquids while being redeposited, allowing more rapid lithification. One other possibility not addressed by the DSDP personnel is lower than expected shear strength at depth caused by core disruption due to gas hydrate dissociation.

Abundant hydrocarbon gas was found in the cores recovered from Site 565. The gas was interpreted as being of biogenic origin based on the preponderance of methane over other hydrocarbons. Samples of gas hydrates were recovered in atypically coarse sediments at Site 565. A 10 cm thick fractured fine-grained sandstone bed yielded small chunks of gas hydrates. Dissociation of the hydrate indicated that 133 volumes of gas were contained in a single volume of gas hydrates.

Site 566 was located on the lower slope of the Guatemala continental margin 22 km landward of the trench on the floor of the San Jose Canyon (Figure 13). The site was covered by 3,675 m of water. Four holes were drilled at Site 566, three of which penetrated to ophiolite basement. Drilling and equipment difficulties limited the quantity of recovered material. Offsets of approximately 3,000 m between holes resulted in a large variation in the thickness of sediment above the serpentinite basement from 6 m to 109 m. The sediments recovered were silty mudstones with occasional sand lenses. The igneous basement was cored to a depth of 136 m in hole 566C.

Only two core liner gas samples were taken at Site 566, both from serpentinite cores of hole 566C. The gas contained large quantities methane and anomalously large quantities of ethane-pentane. Also, reports from the shipboard crew stated that "Rubble associated with fractured serpentinite degassed vigorously" (von Huene et al., 1985).

Site 567 was located on the first bench of the lower slope landward from the trench axis (Figures 13 and 14). The location selected for Site 567 was offset 110 m from Site 494. Site 494 had drilled a nearly complete

section of Cretaceous to Holocene sediments demonstrating the absence of an accretionary prism on the Guatemalan slope. Drilling of Site 494 had been terminated due to technical problems. Thus, drilling at Site 567 was intended to confirm the unexpected findings of Site 494, and to penetrate closer to the underlying subduction zone itself.

Drilling at Site 567 penetrated 320 m of sediments and nearly 200 m of igneous basement (Figure 16). Only the section deeper than 180 m was cored. The Miocene through early Pliocene section was dominated by olive-green mud and mudstone. The mudstone was thoroughly fractured in places, resulting in cores with a brecciated appearance. Downward in the Tertiary section, the mudstone graded to an intraformational conglomerate with Cretaceous age pelagic limestone clasts. A 70 m interval of serpentinite was recovered beneath these conglomerates. Beneath the serpentinite, however, a thin layer of mixed sedimentary lithologies underlain by 20 m of possibly Late Cretaceous age limestone was found. Igneous and meta-igneous basement was drilled beneath the Cretaceous limestone. The basement exhibited the downhole lithological changes associated with ophiolite complexes of pillow basalts, through meta-diabase to serpentinized peridotite. Several faults were intercepted in the igneous rocks, but the tectonism was inferred to have occurred prior to the present subduction regime. Drilling was stopped at 501 m subbottom when the bit stuck. The extreme bottom hole overpressure (90% of lithostatic) and geophysical interpretations indicated that the hole came within 50 m of the underlying subduction zone. The displaced serpentinite-limestone section could not be completely explained. The concensus was that the upper serpentinite was an exotic block displaced from upslope. The rocks could have been dislocated by reverse faulting, but that possibility was discounted due to the lack of small-scale compressive features elsewhere in the adjacent cores.

Foraminifera indicated that the site had closely maintained its present depth of 5,500 m since the early Tertiary. Hydrocarbon gases were encountered throughout both the sedimentary and igneous portions of Site 567. There was no evidence of gas hydrate recovery or presence at Site 567.

Site 568 was located on the upper slope beneath 2,054 m of water (Figure 13). The site selected by DSDP was 1 km upslope from Site 496. Site 496 had been abandoned prior to reaching its drilling objective due to the possible presence of hydrates. Reprocessed seismic data showed a subtle BSR beneath Site 496 (Figure 17). With a confident estimate of the subbottom depth of the base of gas hydrates, a followup hole could be safely planned. Site 568 was drilled specifically to recover hydrates and to study their vertical distribution using onboard geochemical means which were not available on Leg 67.

Site 568 was drilled to a depth of 417 m, approximately 50 m above the calculated base of gas hydrates (Figures 16 amd 17). The sediments were very similar to those cored at Site 496 consisting of a very thick (220 m) Pleistocene section composed of dark olive-green mud with abundant volcanic ash layers. The thick Pliocene section of Site 496 was diminished by an unconformity at 206 m subbottom. Beneath the unconformity indurated ashy mudstone with varying amounts of calcite veins and thin limestone layers was recovered. The hole bottomed in late Oligocene mudstone.

Gas hydrates were indicated at Site 568 by abundant hydrocarbon gas. Depletion in the relative quantities of propane and butane led the scientific staff to infer the presence of dissociating Type I hydrate, since hydrocarbons

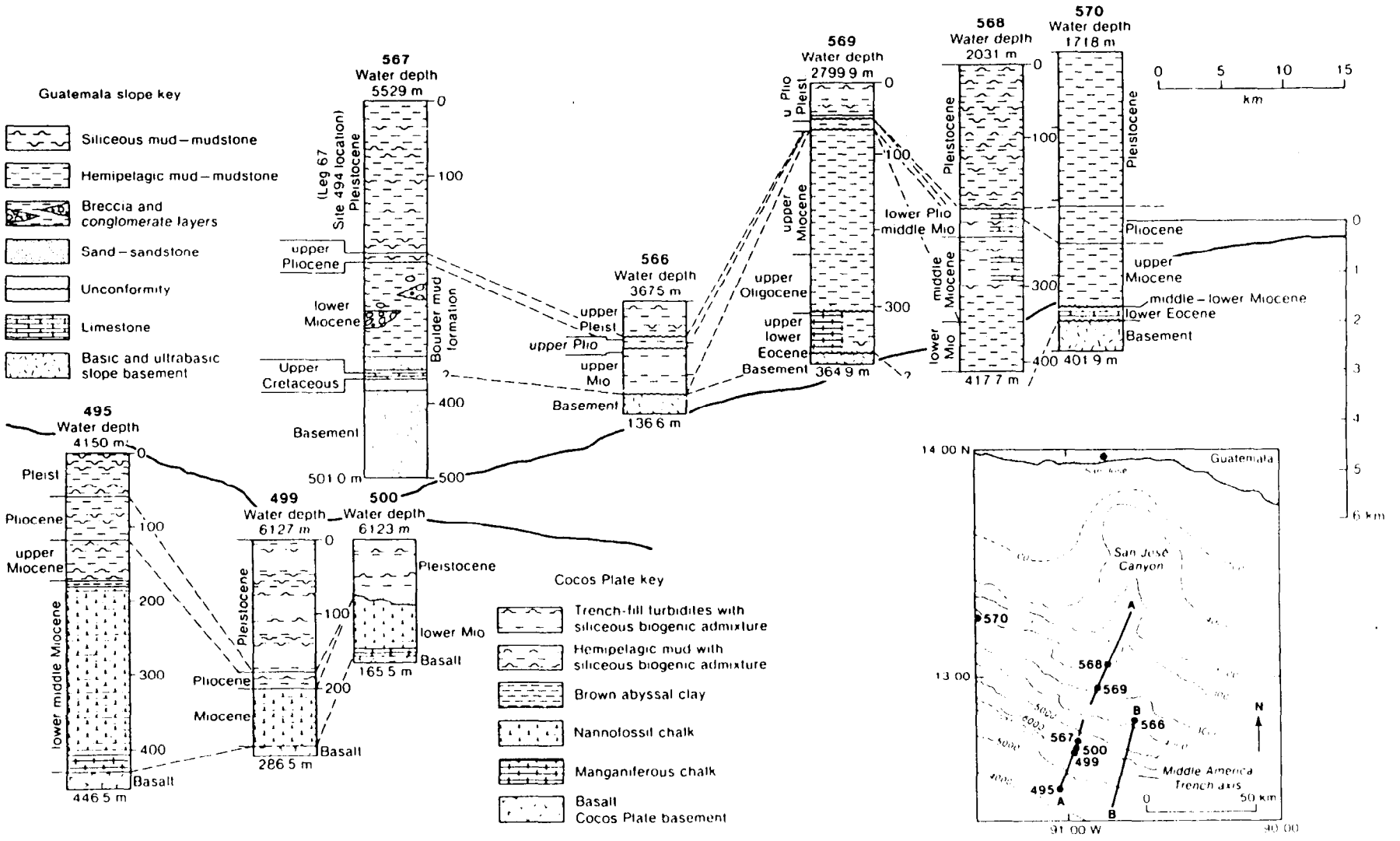

Figure 16. LITHOSTRATIGRAPHY OF DSDP LEG 84 SITES
After von Huene et al., 1985

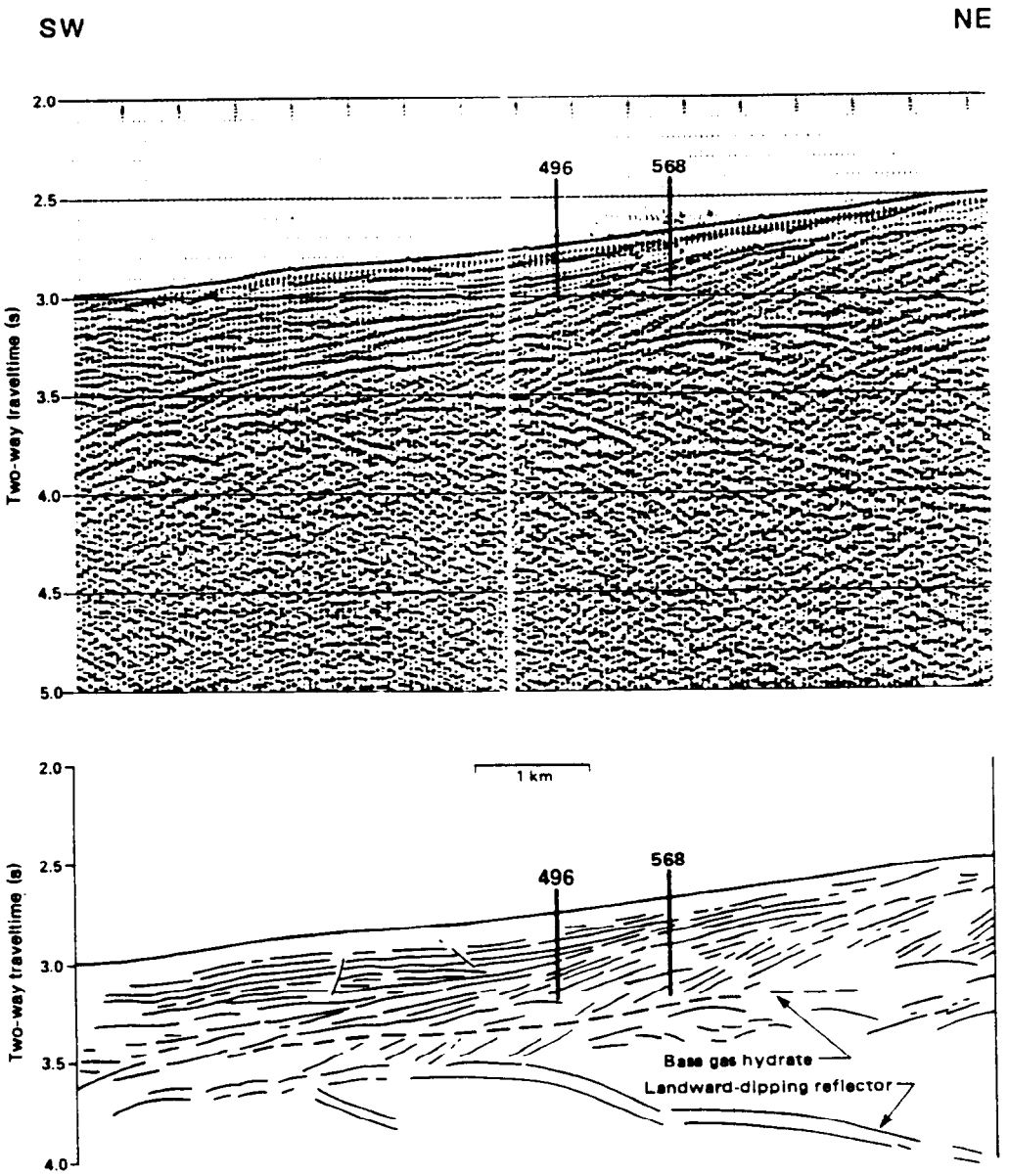

Figure 17. PART OF SEISMIC RECORD GUA-13 SHOWING THE LOCATIONS OF SITES 496 AND 568 AND BOTTOM SIMULATING REFLECTOR

After von Huene et al., 1985

larger than ethane are excluded from that hydrate structure. Gas hydrates were recovered from fractured mudstone and coarse vitric ash at 404 m subbottom. Based on hydrocarbon distribution and lack of observable samples, the scientific party concluded that the sediments from 410 to 417 m subbottom were not hydrated, even though the sediments were very gassy.

Site 569 was located beneath 2,800 m of water on the upper trench slope, 15 km downslope from Site 568 (Figure 13). The location of Site 569 was selected to permit sampling of the rock comprising the acoustic basement. Knowing that the probable maximum depth of gas hydrate stability on the slope was between 450 and 550 m, a site was chosen where the acoustic basement, as depicted on seismic line GUA-13, was elevated to within approximately 350 m from the sea floor. The site selected was thus on a basement rise, probably the result of faulting.

Green mud and mudstone totaling 351 m was found to overlie metamorphosed diabase or gabbro at Site 569 (Figure 16). Pliocene to Holocene age green-gray silty mud was separated from underlying Miocene mudstone by an unconformity at 57 m depth. Oligocene mudstone became more calcareous near the bottom of its 100 m thickness. A 20 m green and black siliceous Eocene mudstone directly overlaid the igneous basement.

Hydrocarbon gases were detected in cores recovered from Site 569. An overabundance of ethane relative to propane and butane was noted. Such a relationship at Site 568 was inferred to indicate gas hydrate presence. Pore water salinity diminished slightly with depth, also suggesting gas hydrate presence. No direct evidence of gas hydrates was found at Site 569.

Site 570 was located 70 km northeast from the closely spaced group of holes drilled on Legs 67 and 84 (Figure 13). The bathymetry of the immediate vicinity of Site 570 is complex. A divide between two submarine canyons, 100 to 120 m deep due east of a large conical high with a relief 700 m above the sea floor was selected for drilling. The principal objective of Site 570 was to sample basement rocks where seismic profiling indicated that the basement could be drilled at a shallower depth subbottom than the base of gas hydrate stability.

Eocene to Holocene sediments totaling 374 m and 28 m of serpentinized peridotite were drilled at Site 570 (Figure 16). The 208 m thick Pleistocene section consisted of gray-green mudstone with beds of volcanic ash and coarse sand. Unit II, from 208 to 255 m subbottom, was a Pliocene mudstone differentiated from unit 1 by its lithification and increased ash content. The base of unit 2 was marked by a sandy dolomite layer. Unit 3 was an 80 m Miocene sequence bounded on top and bottom by unconformities. The mudstone unit has thicker sand and ash layers and is fractured. The Lower Eocene unit 4 was composed of a variety of lithologies. The typical mudstone was interspersed with limestone layers, sandstones containing limestone clasts, pumice, conglomerate, and a basal serpentinite-rich carbonate mud. The basement at Site 570 was composed of serpentinite.

Hydrocarbon gas was pervasive throughout the Site 570 cores. The methane to ethane ratio diminished with depth. Gas mixtures rich in ethane and heavier hydrocarbons were measured from the serpentinite basement rock cores.

Gas hydrates were recovered from the sediments of Site 570 from a depth of 193 m to 374 m. The hydrates were found in sandstone and ash

layers and filling fractures in fine-grained mudstone. A 1.05-m core of massive gas hydrate was recovered from a depth of 249 m near the Miocene-Pliocene unconformity.

Geothermal Gradients

Although the Middle America Tranch region has been thoroughly drilled on three DSDP courses, the heat flow and geothermal gradients of the region are poorly known. Although many attempts were made to record down hole temperatures on DSDP Leg 66 offshore of Mexico, the only confident estimates made were 2.5°C/100 m for Site 490 and 2.2°/100 m for Site 492 (Shipley and Shephard, 1982). The values matched well with gradients calculated from BSRs in the same area (Shipley and Didyk, 1982).

Offshore of Guatemala, the thermal structure of the continental margin is similarly unknown. Von Huene et al. (1982) reported that the geothermal gradient of the Esso Petrel on the Guatemala continental shelf decreased with depth. From 3.4°C/100 m between the sea floor and 70 m depth, the geothermal gradient decreased to 1.4°C/100 m from 800 m to a depth of 2,000 m. A very low gradient of only 0.9°C/100 m was measured between 2,100 m and 3,800 m. Only two reliable values were obtained from Leg 67 (Watkins et al., 1982): 3.2°C/100 m at Site 497 on the upper slope and 2.2°C/100 m at Site 494 at the toe of the continental slope. At Site 568 a composite geothermal gradient was measured: 4.4°C/100 m from the sea floor to 90 m, 6.4°C/100 m from 90 m to 190 m, 3.5°C/100 m from 190 to 290 m, and 1.3°C/100 m from 290 m to the bottom of the hole at 417 m (von Huene et al., 1985). A gradient of 2.6°C/100 m was noted for Site 570.

The only geothermal gradient estimate available for the Costa Rica continental margin is 1.0 to 2.5°C/100 m from Site 565 (von Huene et al., 1985).

Yamano et al. (1982) calculated geothermal gradients of the continental slope of the Middle America Trench study region from the depth of bottom simulating reflectors (BSRs). Offshore of Acapulco, calculated geothermal gradients ranged from 2.22 to 3.13°C/100 m with a mean value of 2.82°C/100 m. Offshore of Nicaragua, Yamano et al. (1982) obtained values of 3.02 to 3.49°C/100 m with a mean of 3.25°C/100 m. Offshore of Costa Rica values of 2.01 to 4.42°C/100 m averaging 3.51°C/100 m were calculated.

Hydrocarbon Generation

The hydrocarbon generation potential of sediments recovered from the Middle America Trench study area has been investigated in at least seven published studies. The petrographic and geochemical studies of trench and slope sediments from DSDP Legs 66, 67, and 84 indicated good hydrocarbon generation potential due to abundant organic matter, but very low levels of thermal maturity.

DSDP Leg 66

Summerhayes and Gilbert (1982a) analyzed samples from the Cocos Plate and the continental slope offshore of Mexico. Optical examination revealed that organic matter derived from terrestrial sources was most abundant in the samples from the open ocean and sediments deposited near the trench axis. Organic material from the middle and upper slope sites was dominantly of marine origin. Total organic carbon (TOC) values were found to be extremely low (0.08%) for pelagic sediments deposited on the Cocos Plate. The TOC of slope and trench deposits was found to be quite high (0.70 to 4.32%). The TOC values tended to decrease with age, median values of 2.18%, 2.0%, 1.94%, and 0.9% were recorded for Pleistocene, Pliocene, upper Miocene, and middle Miocene samples respectively. The preponderance of marine organic matter was reflected in pyrolysis analyses where most of the sediment samples were found to be oil prone rather than gas prone. Optical analysis showed that all samples were thermally immature, as expected from their young age and shallow depth of burial. Benzene-methanol extraction of selected samples also indicated low levels of maturity. Total extractable organic matter (C_{15+}) averaged 434 ppm with saturates and aromatics amounting to only 2.7% and 2.5% respectively of the extracted organic material. Very high contents of polar material (95%) show that very little thermal breakdown of organic matter has occurred.

Summerhayes and Gilbert (1982a) identified four organic facies in samples from Leg 66. The low TOC Miocene pelagic clays contained entirely terrestrial organic matter. The very low rate of sediment accumulation on the Cocos Plate far from sediment sources resulted in complete consumption of incident marine organic material with only refractory terrestrial organic material being preserved. On the continental slope active amorphous and structured marine organic matter was prevalent. The high TOC and predominance of marine organic matter is unlike many other Pacific trench slopes, e.g. the Japan Trench.

Summerhayes and Gilbert (1982a) contended that three factors contributed to the anomalous preservation of organic matter on the trench slope offshore of Mexico: (1) high primary production, (2) deposition in a dysaerobic environment, and (3) rapid burial of organic-rich sediment. As with most of the east-central Pacific, the Middle America Trench study region is a well known upwelling area. The abundance of nutrients in upwelling zones results in a profusion of marine organisms. An oxygen minimum zone exists in the water columns along the west coast of North America and South America (Kester, 1975). Organic material deposited in oxygen deficient conditions is better preserved than when deposited under well oxygenated waters. Site 493 was probably within the oxygen minimum zone during deposition of upper Miocene and Pliocene sediments which had TOC values of 4.24% and 4.32%. Sites located lower on the slope (490, 491, and 492) were beneath the oxygen minimum zone, but were covered by oxygen deficient water. Preservation was good, averaging 1.8% TOC, but less than that at Site 493. Likewise, less marine and more terrestrial organic matter was preserved at Sites 490, 491, and 492 than at 493. Sedimentation rates of 10 to 300 m/m.y. resulted in rapid burial so that the deposited sediment passed quickly through the zone of oxidative decomposition, limiting depletion of reactive marine organic matter.

The trench and channel organic facies consisted of high TOC with abundant terrestrial organic matter. These facies were envisioned to have

been deposited in oxygenated shelf environments near terrestrial sediment sources. Subsequent slope failures and turbidity flows redeposited these sediments in deeper water in conditions of rapid burial resulting in good preservation of the detrital terrestrial organic matter.

Brassel et al. (1982) performed a wide range of geochemical analyses on organic material extracted from Quaternary sediment from two Leg 66 sites. The shallow samples from Site 498 near the trench and Site 491 on the upper slope were, as expected, very immature and composed of a mix of terrestrial and marine allogenic materials and compounds resulting from bacterial breakdown of the input organic matter. At Site 491 compounds indicating input of thermogenic hydrocarbons were detected. Since the core was from only 7 m subbottom depth, the presence of thermogenic organic compounds implies migration from a much deeper horizon. Site 491 is located near landward dipping reflectors which Shipley and Didyk (1982) interpreted as possible migrational conduits through which deep thermogenic gas was brought to the gas hydrate stability zone. Gas hydrates were recovered at Site 491, and a prominent BSR underlies it.

Chambers and Erdman (1982) measured the TOC and elemental composition of organic fractions of sediments from Sites 487, 488 and 490. The TOC measurements were consistent with those of Summerhayes and Gilbert (1982a) with slope deposits averaging 2% TOC, diminishing downhole. The pelagic sediments from the Cocos Plate averaged 0.12% TOC.

DSDP Leg 67

Summerhayes and Gilbert (1982b) analyzed the hydrocarbon generation potential of sediments cored in Leg 67 offshore of Guatemala. Optical character of the organic matter, TOC, and distribution of extractable organic matter were determined. As was the case offshore of Mexico, the sediments from Leg 67 were organic-rich and oil prone, but were thermally immature.

Summerhayes and Gilbert (1982b) distinguished 5 organic facies offshore of Guatemala. The number and terminology of the facies differ from those described offshore of Mexico (Summerhayes and Gilbert, 1982a), but the same general patterns persist.

Pelagic sediments from the Cocos Plate (Site 495) were characterized by very low TOC values (0.05%). The scarcity of organic matter precluded determination of its source.

The hemipelagic sediment overlying the barren pelagic sequence at Site 495 and trench-fill sediments (Sites 499 and 500) had similar characteristics, with the trench-fill having higher TOC (1.82% vs 1.14%) and more marine-derived organic matter. Slope sediments (Sites 494, 496, 497) had high organic content (2% TOC) and slightly more terrestrial organic matter than the trench-fill sediments.

Overall, the organic component of sediments offshore of Guatemala were found to be much more marine in character than those offshore of Mexico. Summerhayes and Gilbert (1982b) ascribed this to the much smaller watershed drained by rivers on the west coast of Guatemala. The same combination of factors was proposed to be responsible for the organic richness of the sediments: (1) high primary productivity due to upwelling currents, (2) presence of a distinct oxygen minimum zone in the water column, and (3) rapid sedimentation. The rates of sedimentation measured at Leg 67 sites were

about one half of those from Leg 66, but apparently still sufficient for efficient preservation.

The thermal maturity determined by spore coloration, pyrolysis, and composition of extracted organic matter was very low.

Wolf (1982) conducted a petrological study of sediments from three Leg 67 holes determining the source and maturity based on identification of coal macerals. Wolf (1982) found an increase in humic organic matter in the trench floor sediment compared with upper slope sediments. However, a great variability along the section was noted in both sedimentary environments with successive cores fluctuating from near totally liptinite (algal remains, resins, bitumen, etc.) to nearly all humite (land plant remains) to principally inertinite (charcoal). Thermal maturity measured by reflectance increased from R_o = 0.15% at the surface to 0.22% at 360 m at Site 496. These values are much below the generally accepted value of initiation of oil generation of 0.60%, but do show a steady increase with depth.

Curiale and Harrison (1982) measured ratios of two sterol molecules in three samples from Leg 67 without reaching conclusions significant for determining hydrocarbon generation potential.

DSDP Leg 84

The hydrocarbon generation potential of sediments drilled from the Guatemala continental slope on Leg 84 was investigated in two published studies. The results agree with studies from previous DSDP Middle America Trench legs, but the TOC values and marine organic matter content are generally lower.

Gilbert and Cunningham (1985) analyzed samples from four Leg 84 sites for TOC, organic matter type, and thermal alteration. Values obtained for TOC diminished with depth at Sites 567 and 568, but increased with depth at Site 569 from 0.66% at 1 m to 1.23% at 235 m. At Site 567 TOC dropped from 2.75% at 214 m to 0.84 at 325 m. Site 568 was characterized by a 200 m thick organic rich (2.4% TOC) marine Pleistocene section overlying a leaner terrestrial Miocene to Pliocene section averaging 0.9% TOC. Generally, terrestrial organic matter increased in abundance downslope.

Kennicutt et al. (1985) analyzed sediments from Leg 84 cores for TOC, isotopic content of organic matter, and composition of hexane extracts of organic matter. Some distinct trends are noted. Total organic carbon values of sediment samples decrease with depth. Depletion of ^{13}C also consistently occured with depth. A correlation therefore existed between TOC values and $\delta^{13}C$ values; samples with low TOC values tending to have lighter (more negative) $\delta^{13}C$ values. The quantity of organic material extracted from the sediment samples varied randomly. Kennicutt et al. (1985) ascribed the fluctuation in extractable organic matter to variations in biological inputs. An increase in extractable organic matter with depth due to thermal maturation was not seen; the level of maturity of the sediments is so low that the slight maturity increase at depth could not be detected.

In sediments of Oligocene to Pliocene age, Kennicutt et al. (1985) noted that TOC values are higher from the sites which are nearer to land. Since the sites near land are also under shallower water depths, this observation is equivalent to those of Summerhayes and Gilbert (1982a, 1982b) that sediments from locations overlain by shallow water tend to have higher TOC values. Summerhayes and Gilbert (1982a, 1982b) attributed the relationship to better

preservation at shallow sites due to closer proximity to the oxygen minimum zone in the water column; Kennicutt et al. (1985) did not speculate on a cause for their observed change in TOC with distance from shore.

Although TOC values are widely used to assess the hydrocarbon generation potential of sediments, they are not as precise nor as accurate as their widespread use would suggest (Dembecki, 1984). The values are sensitive to procedural irregularities between labs and selection of representative samples. Results from Leg 84 illustrate this point. For Site 569 Kennicutt et al. (1985) reported 14 TOC values which show a distinct decrease with depth. Gilbert and Cunningham (1985) report 6 TOC values for Site 569 which show a distinct increase with depth. A plot of both data sets on a common axis with regression lines from least squares correlation is shown in Figure 18. The trends of the two data sets are clearly opposite. However, the greater sample density of the data from Kennicutt et al. (1985) suggests that a trend of decreasing TOC values with depth is appropriate for Site 569.

The data on the character of the organic matter at Site 568 show a geochemical expression of an 8 m.y. unconformity. An unconformity between middle Miocene and Pleistocene sediments was found at 195 m at Site 568 (von Huene et al., 1985). Gilbert and Cunningham (1985) showed that the TOC values from Site 568 were distinctly bimodal with very high values (2.5%) in the Pleistocene sediments and lower values (1%) in the Miocene sediments (Figure 19). A difference in type of organic matter was seen across the unconformity; Pleistocene sediments had dominantly marine organic matter and Miocene sediments contained mainly terrestrial types. The TOC values of Kennicutt et al. (1985) were not as distinctly bimodal, but did show lower values in the older sediments. The Kennicutt et al. (1985) data on ^{13}C content were bimodal with all Pleistocene sediments having $\delta^{13}C$ values of greater than -22 per mil and all Miocene sediments having $\delta^{13}C$ values less than -22 per mil. Kennicutt et al. (1985) mentioned both the different types of organic matter and enhanced diagenesis at depth. They were apparently unaware of the unconformity at the time of writing. Recognition of this unconformity is important in interpreting data on gas hydrates at Site 568 to be addressed in the second part of this report.

Kennicutt et al. (1985) determined that the organic-rich sediments drilled on Leg 84 were thermally immature. However they detected aromatic compounds by fluorescence analysis which indicated that minor amounts of hydrocarbons of thermal origin were present. Kennicutt et al. (1985) did not discuss at which sites or at which depths the concentration of migrated thermogenic hydrocarbons was greatest.

Forearc Basin

The Middle America Trench south of the Tehuantepec Ridge is characterized by a broad continental shelf underlain by a forearc basin (Seely, 1979). The forearc basin is composed of thick accumulations of Cretaceous and Tertiary sediments which dip landward (Figure 20).

Seely (1979) presented age estimates on the strata of the Guatemala continental shelf based on paleontological dating of cores from the Esso Petrel well. Using these age estimates we have determined by thermal modeling that early Tertiary and Cretaceous sediments buried deeper than 3,200 m should be mature with respect to oil generation. The main phase of wet gas generation should be occurring where the sediments are buried 4,500 m or

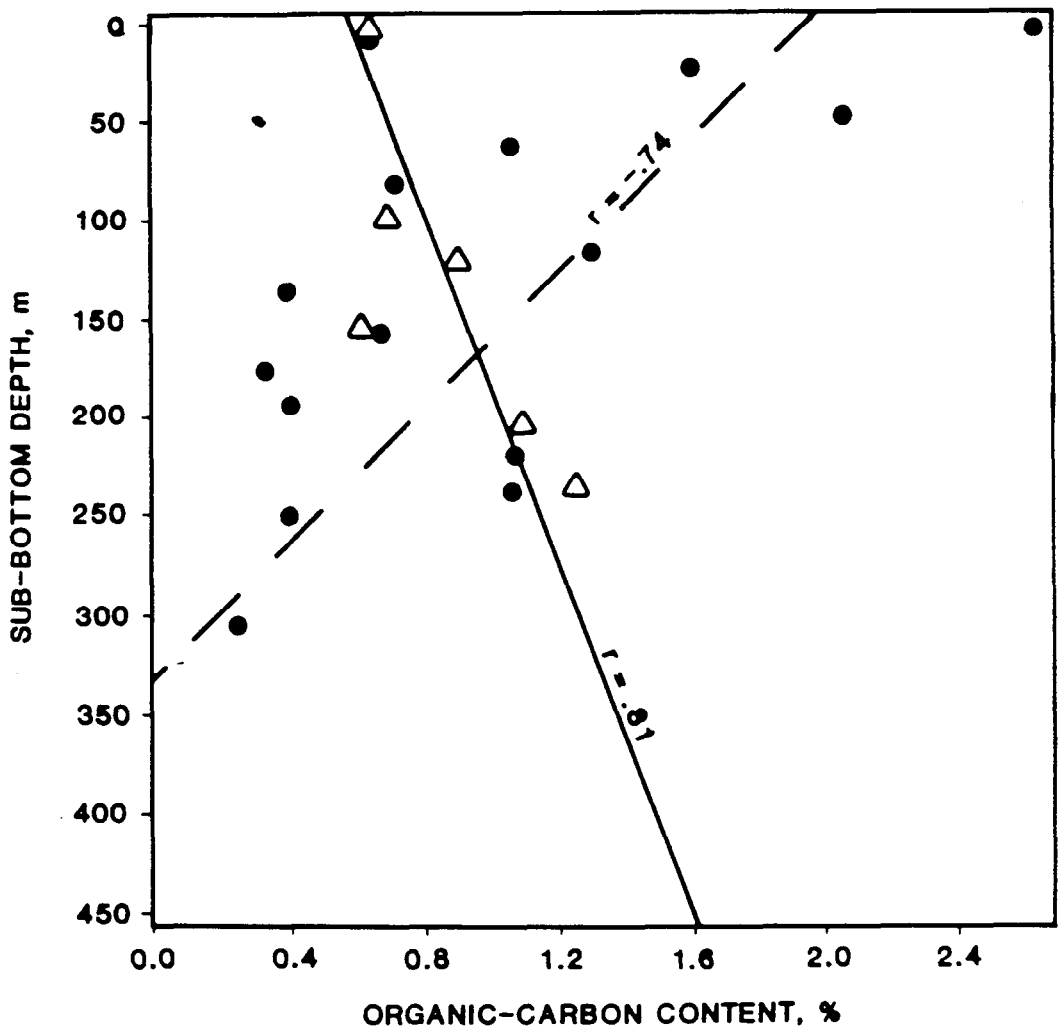

Figure 18. TOTAL ORGANIC CARBON CONTENT AT DSDP SITE 569

Data from Gilbert and Cunningham, 1985 (△,–),
and Kennicutt et al., 1985 (●,--)

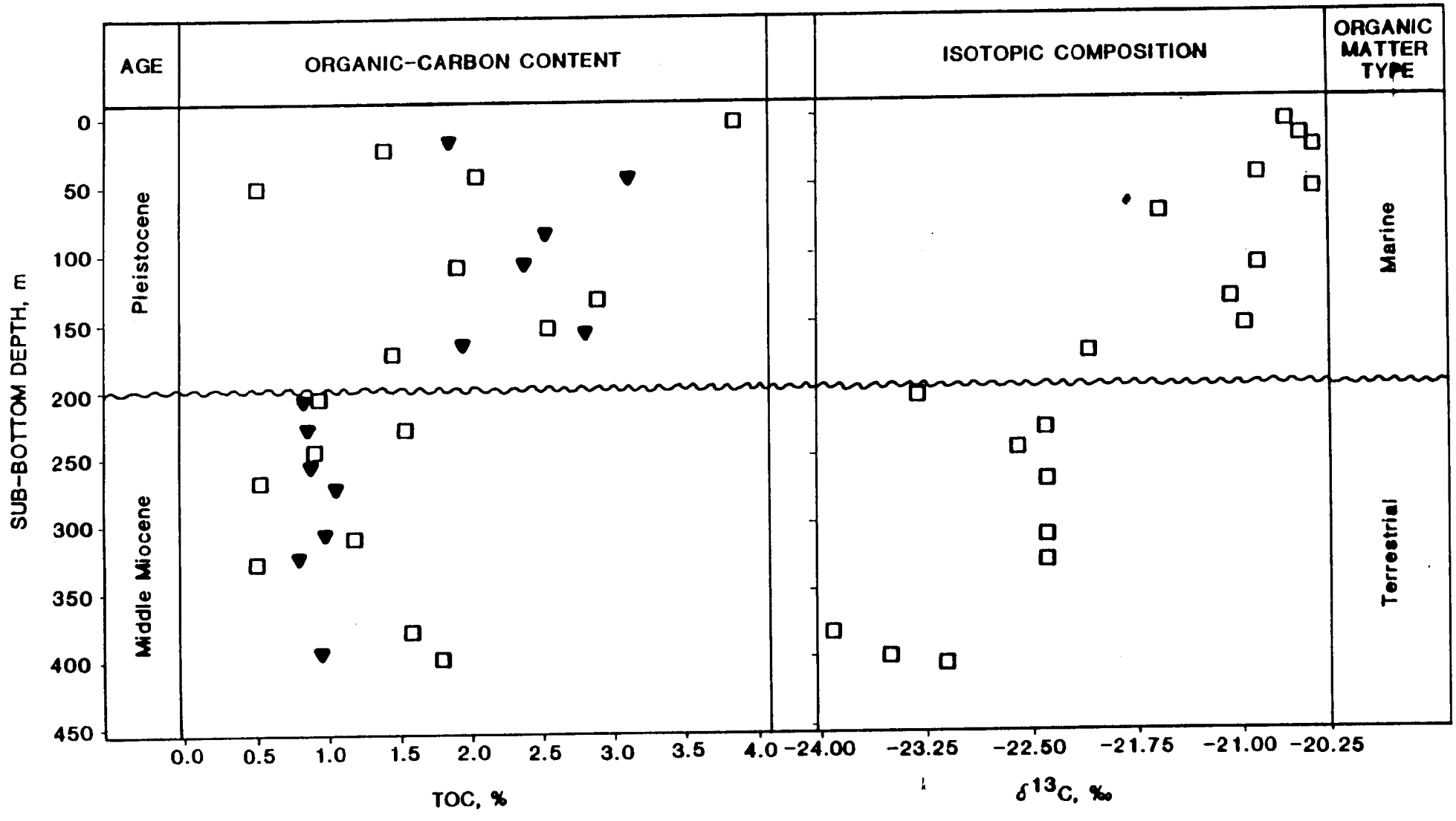

Figure 19. ORGANIC CARBON CONTENT AND CARBON ISOTOPIC COMPOSITION OF SEDIMENTS FROM DSDP SITE 568

Data from Gilbert and Cunningham, 1985 (▼), and Kennicutt et al., 1985 (□)

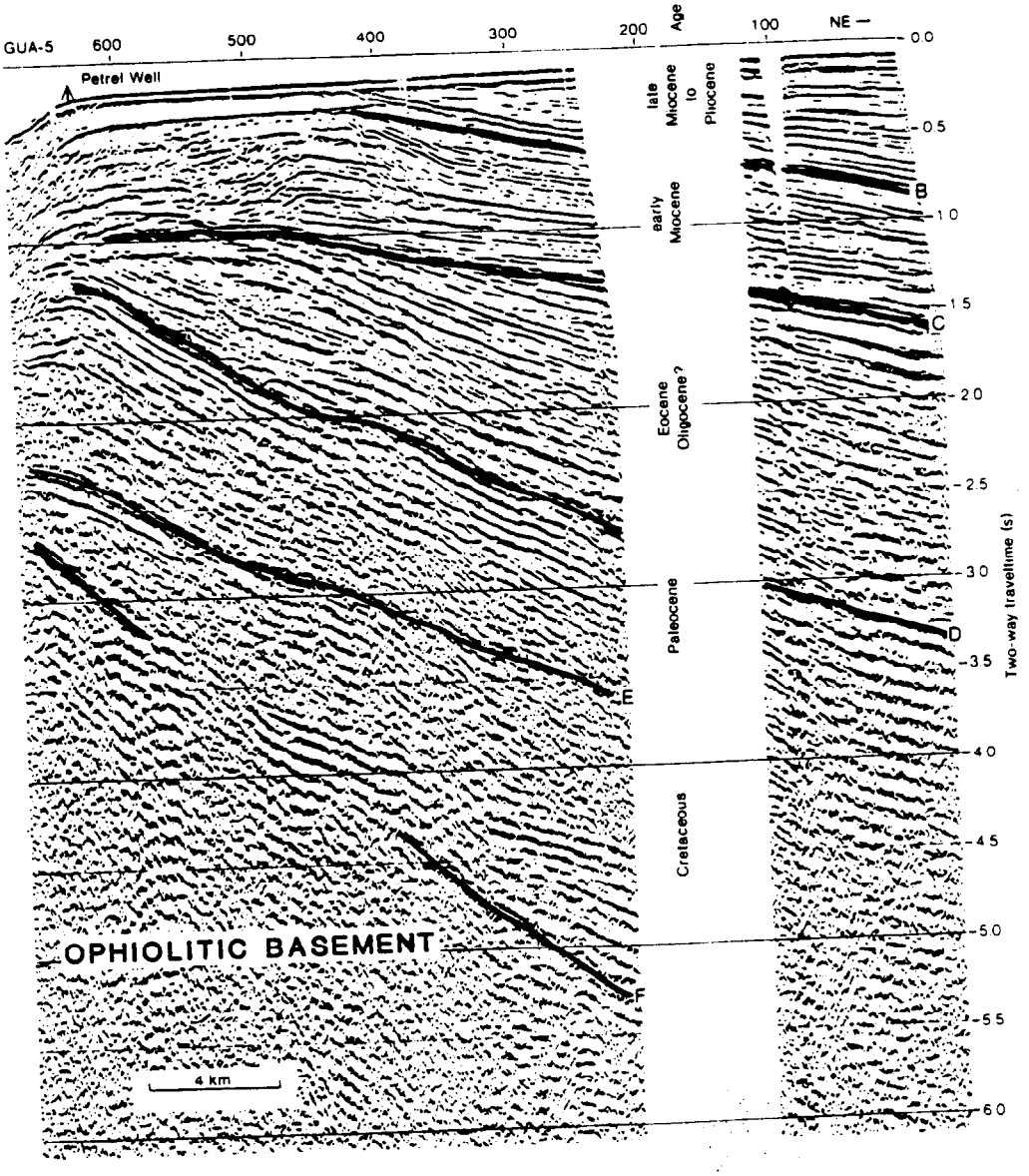

Figure 20. SEISMIC LINE GUA-5 SHOWING STRUCTURE OF FOREARC BASIN OFFSHORE GUATEMALA

After Ladd and Schroder, 1985

more. Thus, huge volumes of mature potential source rocks may exist beneath the continental shelf along Central America.

The structure of the forearc basin suggests that hydrocarbons generated in the forearc basin may not be available for gas hydrate formation. Forearc basin strata dip landward. Uplift of a wedge of ophiolitic basement has produced angular unconformities between strata, an obvious example of which is seen between Oligocene and Miocene strata on seismic line GUA-5 (Figure 20).

The uplifted ophiolite coincides with the shelf-slope break and is continuous along the Guatemala margin. The dip of the beds suggests that any hydrocarbons generated at depth in the forearc basin would migrate up dip toward the anticlinal trap formed at the shelf-slope break. Migration from the structural high down the slope would be unlikely. Thus, contribution of thermogenic hydrocarbons from the forearc basin to gas hydrates is unlikely; natural migration pathways out of the basin should concentrate thermogenic gas at the seaward edge of the continental shelf where water depths are insufficient to stabilize gas hydrates.

Erosion of the continental shelf by the San Jose canyon makes it possible for thermogenic gas from the forearc basin to migrate to the gas hydrate stability zone. The San Jose Canyon cuts deeply into the continental margin of Guatemala (Figure 13). Thus, within the trench, water depths may be sufficiently deep to stabilize hydrates. Erosion has exposed landward dipping forearc basin strata which could serve as carrier beds to deliver thermogenic hydrocarbons from the deep axial portion of the basin to the trench. Figure 21 shows a section of seismic line GUA-18 which was shot within the upper reaches of the San Jose Canyon where it breaches the continental shelf. The dashed line on Figure 21 is a projection of the topography of the continental shelf based on nearby profiles. From Figure 21 it is clear that the channel has eroded into the continental shelf, truncating the landward dipping forearc basin sediments and burying the erosional remnants with canyon-fill deposits.

The time of formation of the San Jose Canyon is not known with certainty (von Huene et al., 1985). The rate and timing of erosion may effect assessment of the thermal history of the underlying forearc basin sediments; early canyon cutting could have cooled the sediments, increasing the depth to a given level of thermal maturity. From the sharp landward canyon cut into Miocene to Pliocene sediments, a Neogene age is suggested. If rapid and relatively recent removal of the shelf sediments is assumed, then thermal maturity indices calculated from age data of Seely (1979) should be applicable. Thermal anomalies in the forearc basin sediments from the formation of the San Jose Trench should be local and diminish downward. Additionally, drainage of hydrocarbons into the canyon-fill sediments should occur from source rocks on either side of the downdip projection of the trench cut, further minimizing the canyon's effect on thermal maturity of potential source rocks in the trench.

Exact determination of the depth to thermally mature sediments in the forearc basin is difficult because of uncertainties in burial history, thermal gradients, and seismic velocities. Numerous unconformities and tectonic tilting of beds limits the accuracy of thermal modeling. Thermal gradients have been determined only for slope and shelf-slope break locations offshore of Guatemala (von Huene et al., 1985). Similar gradients can be assumed for the forearc basin (2° to 3.5°/100 m), but the resultant uncertainty is large. Uncertainty exists in the seismic velocities of deep forearc basin sediments (von Huene et al., 1985) and therefore thickness of the sediments pictured in

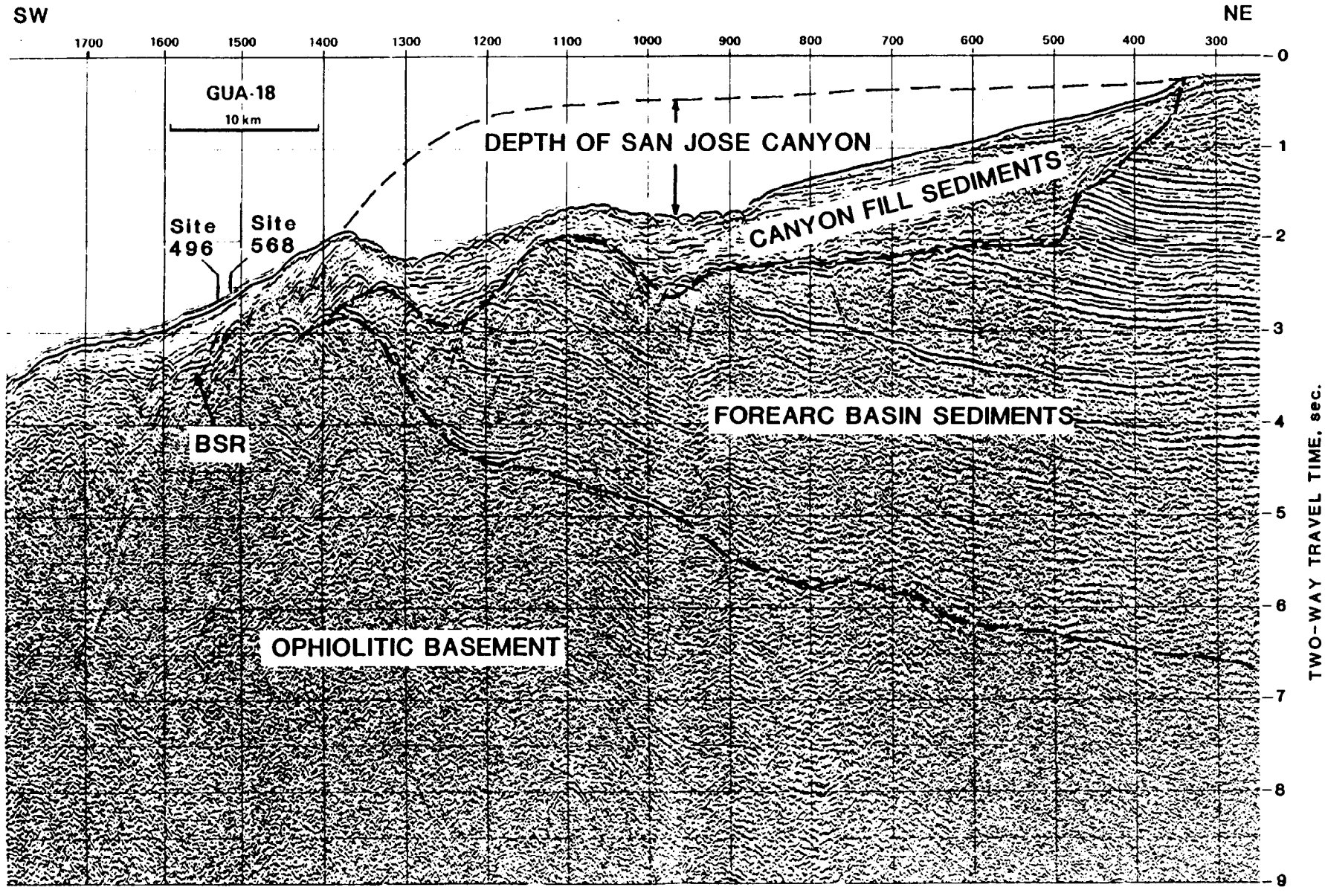

Figure 21. SEISMIC LINE GUA-18 SHOWING FOREARC BASIN SEDIMENTS EXPOSED BY SAN JOSE CANYON

After Ladd et al., 1982. Lithological boundaries after von Huene et al., 1985.

the seismic line in Figure 21. Ladd et al. (1985) determined ages for the seismic horizons of the forearc basin, based on ages reported by Seely et al. (1979). Those ages have been questioned by McDougall (1985). Due to these uncertainties only rough estimates of depths of mature potential source rocks is possible.

A rough estimate of thermal maturity in the forearc basin puts the oil generation window between 3.5 and 4.2 sec with the main phase of wet gas generation extending from 4.2 to 4.8 on Figure 21. This implies that the forearc basin sediments which are truncated by the San Jose Canyon between shot points 900 and 1,200 in Figure 21 have downdip extensions which are thermally mature with respect to hydrocarbon generation. Ladd and Schroder (1985) interpreted most of the rocks in the forearc basin to be fan deposits, which should have adequate amounts of well preserved gas-prone organic matter by analogy with fan systems of the Gulf of Mexico. Updip migration of hydrocarbons out of the forearc basin could be impeded by the apparent fault or fold at shot point 940 on Figure 21 which produces anticlinal closure in deeper strata at shot point 900. However, a migrated depth display of line GUA-18 presented by von Huene (1985) showed no reversal of dip at shot point 940; upward migration along permeable beds should not be affected.

The depth of water overlying the axis of the San Jose Canyon as shown in Figure 21 should be sufficient to stabilize gas hydrates. Gas hydrates were recovered from Site 570 under 1,718 m of water corresponding to 2.3 sec two-way travel time. Well developed BSRs are found at beneath water depths of 1,500 m (2.0 sec) on lines GUA-1 and GUA-14 on the Guatemala continental slope 20 to 40 km northwest of seismic line GUA-18 (Ladd et al., 1982; von Huene et al., 1982). The sea floor in the San Jose Canyon between shot points 1,200 and 1,350 on line GUA-18 (Figure 21) is deeper than 1,500 m. The exact minimum water depth for gas hydrate stability offshore of Guatemala is probably 800 to 1,000 m (1.1 to 1.3 sec) depending on water temperature. Thus, gas hydrates could exist anywhere seaward of shot point 850 on Figure 21, provided that sufficient gas is generated in or delivered to the gas hydrate stability zone. The gas hydrate stability zone could extend to even shallower water depths if thermogenic gas containing large amounts of heavier hydrocarbons is present.

There is potential for thermogenic gas hydrates within the San Jose Canyon, but no direct evidence of gas hydrates in the canyon exists. Direct migrational pathways from mature potential source beds empty updip to porous canyon-fill sediments within the gas hydrate stability zone. A short, indistinct BSR is seen near DSDP Site 568 and 496 on line GUA-18, but it is unlikely that hydrates causing that BSR could be formed from gas generated in the forearc basin given the geometry of the rock bodies. A possible BSR is located at 0.83 sec subbottom beneath the canyon floor between shot points 1,050 and 1,150 on Figure 21. The BSR is deeper subbottom than that near Sites 496 and 568, suggesting a lower geothermal gradient or possible thermogenic gas. No drilling has taken place in the San Jose Canyon where we project a reasonable potential for thermogenic gas hydrates, so their existence remains untested.

Source of Hydrocarbons in Metamorphic Rocks

Hydrocarbon gases were found in the ultramafic basement rocks of Sites 566 and 570 (von Huene et al., 1985; Table 2). In both cases the gases contained proportionately less methane than the gas in overlying sediments.

TABLE 2.

COMPOSITION OF HYDROCARBON GASES FROM
IGNEOUS AND METAMORPHIC ROCKS OFFSHORE GUATEMALA
After von Huene et al., 1985

DSDP Site	Depth m	Lithology	Methane %	Ethane ppm	Propane
566-C	118	Serpentinite	49	1,200	560
566-C	128	Serpentinite	45	2,800	1,400
567-A	319	Serpentinite	32	89	0.55
567-A	336	Serpentinite	44	123	0.59
567-A	346	Serpentinite	66	209	0.71
567-A	377	Gabbro	1.3	6.8	0.62
567-A	412	Diabase	1.2	4.2	0.34
567-A	421	Serpentinite	13	51	0.37
567-A	430	Basalt	0.2	2	0.30
567-A	438	Gabbro	0.16	3.3	0.36
567-A	446	Meta-gabbro	3.50	21	0.37
567-A	486	Meta-basalt	1.30	6.5	0.36
570	386	Serpentinite	69	3,600	1,400
570	394	Serpentinite	25	3,000	910

Also, the isotopic composition of the basement hosted gas was heavier than nearby sediment gas, but the isotopic change with depth across the sediment-basement boundary was progressive rather than abrupt (Jeffrey et al., 1985, Galimov et al., 1985).

Gas was also measured from meta-igneous rocks at Site 567. A 30 m thick block of serpentinite underlain by a Cretaceous limestone bed was drilled between 320 and 350 m subbottom. Three gas samples were taken from that interval. The results of the analyses (Table 2) show that hydrocarbon gases are abundant in the apparently exotic serpentinite. The basement at Site 567 is composed of a layered complex of metamorphosed gabbro, diabase, and basalt. Gas samples taken from the basement (365-501 m subbottom) show significant amounts of hydrocarbon gases (Table 2). The amounts of methane recovered from the basement cores of Site 567 are substantially less than from the serpentinite of Sites 566 or 570.

One other DSDP site was drilled to basement, Site 569. Amphibolites typical of high temperature - low pressure metamorphic conditions were intercepted at 351 m and were cored for 14 m. Gases were sampled from sediment cores to a depth of 333 m. Thus, the deepest 18 m of sediments and the metamorphic basement cores were not sampled for gas content. The deepest samples analyzed contained consistently high hydrocarbon gas levels showing no tendency toward diminishing with depth. Thus, it is also possible that hydrocarbon gases could be present in the ultramafic metamorphic basement of Site 569.

Kvenvolden and McDonald (1985) reported that the abundance of hydrocarbons larger than methane in the serpentinite cores from Sites 566 and 570 led the scientists aboard to assume that the hydrocarbons were thermogenic in origin and had migrated into fractures in the basement.

Jeffrey et al. (1985) also contended that the serpentinite hosted hydrocarbons from Sites 566 to 570 were migrated thermogenic gases. The isotopic content of the gas from Site 566 was much lighter (-60 per mil) than expected for thermogenic gas, leading Jeffrey et al. (1985) to propose that the gases from Site 566 were mixtures of migrated thermogenic and biogenic gases. The preponderance of isopentane over n-pentane, and isobutane over n-butane was interpreted to indicate gases which were immature, i.e. produced by low temperature diagenetic reactions instead of high temperature kerogen degradation. The isotopically heavy ethane and propane from the serpentinite gases suggested that the gases were of diagenetic rather than thermal origin. The $\delta^{13}C$ values measured for ethane and propane from the basement of Site 570 are among the heaviest ever reported (-21.6 and -21.4 per mil). According to the natural gas classification scheme of Stahl and Carey (1975), such isotopic signatures signify an overmature gas, from a deep, hot source. Jeffrey et al. (1985) cited more recent work on the isotopic content of ethane and propane which indicated that very early formed diagenetic gas is isotopically heavy, suggesting that the serpentinite gases may not have been formed by thermal breakdown of sedimentary organic matter.

Kvenvolden and McDonald (1985), Jeffrey et al. (1985), and Galimov and Shabaeva (1985) all stated that the hydrocarbon gases in the serpentinite basement rocks must have migrated into the serpentinite. However, none of the independent studies addressing the subject derived a source of the gas that was consistent with all of the geochemical data.

The data for Site 570 were especially enigmatic. The composition of the gas was much different from that in the overlying sediments with much higher concentrations of heavier hydrocarbons, especially propane. However, the depth trend in the isotopic composition of methane which was observed in the overlying sediments continued unabated into the serpentinite. The carbon isotope content of methane became progressively enriched in ^{13}C downhole from -83 per mil at the surface to -41 per mil in the basal sediments at 346 m subbottom (Jeffrey et al., 1985; Galimov and Shabaeva, 1985). The $\delta^{13}C$ values for serpentinite gases ranged from -41.9 per mil (Claypool et al., 1985) to -40.2 per mil (Jeffrey et al., 1985), to a very enriched value of -35.9 per mil (Galimov and Shabaeva, 1985). This interesting trend could be interpreted in various ways. It could be argued that the same depth dependent property responsible for the isotopic enrichment throughout the drilled sediment section at Site 570 continues in the serpentinite. Claypool et al. (1985) proposed that the unusually enriched methane in the deeper sediments of Site 570 are due to bacterial reduction of anomalously reduced dissolved carbonate species. Perhaps, then, the bacterial reduction is proceeding in the serpentinite basement with increasingly enriched CO_2 being present in the serpentinite. The question of the source of the anomalous CO_2 remains unaddressed, however.

Another possibility is that the progressive enrichment of methane in ^{13}C with depth reflects the mixing of typical biogenic methane with an isotope signature of -60 per mil to -90 per mil with isotopically very enriched methane which is migrating from below. The isotopic data from the serpentinite would then suggest that the isotopically heavy methane was being delivered to the sediments via fractures in the serpentinite.

Slope Sediments. It is possible that the hydrocarbons migrated into the serpentinite from overlying sediments. The isotopic content of the basement hydrocarbons would then resemble that of the deepest sediments, which is the case. However, it would be expected that the migrated hydrocarbons would be enriched in the most mobile hydrocarbon, methane. There was evidence of overpressuring sediments elsewhere on the Guatemala continental slope. Thus a reverse pressure gradient could have injected gases into the serpentinite. However, no evidence of overpressuring was found at Site 570. Additionally, it is likely that an overpressured condition in the sediments would also be expressed in the underlying serpentinite. If both the sediments and the basement were overpressured, the necessary inverse pressure gradient would not develop and downward migration of hydrocarbons from the sediments to the serpentinite would not be likely.

Subducted Sediments. The serpentinite gases may have originated from thermal maturation of subducted sediments. The hydrocarbon gas may have migrated to the level at which it was drilled at Sites 566 and 570 via fault and fracture systems in the ophiotitic basement. Such gas would be expected to be thermally mature or overmature.

The depth of the subducting slab carrying pelagic and trench sediments beneath Sites 566 and 570 is difficult to determine with precision. However, the oceanic crust can be traced seismically landward from the trench to a depth of 3 sec. beneath the projection of Site 566. Assuming the highest measured seismic velocity of Site 566 serpentinites of 4 km/sec. for the entire serpentinite section, the basal subducted sediments would be 6,000 m

beneath Site 566. Site 566 is 38 km landward from the edge of the subduction front. Using a plate convergence velocity of 7 cm/year (Drummond et al., 1985), the sediments under Site 566 were subducted approximately 540,000 years ago. If a thermal gradient of 3°C/100 m is assumed for the serpentinite beneath Site 566, a Lopatin burial history plot can be constructed for these sediments. Using the method proposed by Waples (1980), a time-temperature index (TTI) value of 12 is obtained. The value is below the quoted lower limit of active oil generation of 15. The temperatures expected at 6,000 m depth are high (~180°C) but the short time of heating results in a low value of the maturity. Ritter (1984) suggests that the method of Waples (1980) is overly simplified. Empirically derived maturity indices indicate that maturity depends on rate of heating (burial) and varies in an as yet undetermined complex manner. However, for short burial times, Ritter (1984) stated that Waples' (1980) values should be reasonably accurate. Generally accepted TTI-to-maturity relationships were derived for slow burial in typical sedimentary basins. The effects of the very high rate of heating of subducted sediments is not known.

Hydrocarbons with the molecular composition of those at Site 566 may have been generated by the subducted sediments at the calculated maturity levels. The TTI value corresponds to a vitrinite reflectance value of about 0.60% (Waples, 1980). Several instances are known where marine sediments with vitrinite reflectance values of 0.60-0.62 have generated large volumes of wet thermogenic gas (e.g. Smagala et al., 1984).

Hydrocarbon gases containing appreciable ethane and heavier hydrocarbons are known to be produced from thermally immature sediments by low to moderate temperature chemical diagenetic processes (Hunt et al., 1980). Gases from early diagenetic processes are typified by an abundance of isobutane and isopentane over their normal (straight chain) isomers (Hunt et al., 1980). Jeffrey et al. (1985) noted the same abundance of branched chain alkanes over straight chain alkanes in the serpentinite hosted gases.

The thermal maturity of subducted sediments is more difficult to estimate for Site 570 than for Site 566. Since 570 is farther from the trench axis than Site 566, the subducted plate is deeper. Site 570 is beneath 1,500 m of water as opposed to the 3,600 m water depth of Site 566 making the thickness of the section between the basement rocks drilled at Site 570 and the subducted source rocks great. Available seismic lines do not resolve subducted oceanic crust as far from the trench as Site 570; therefore, the depth of the subducted crust must be based on speculation. Projection of reflectors coincident with oceanic crust landward beneath the Guatemalan continental margin indicates that the subducted sediments should lie at 8 sec. two-way travel time. The 1600-m water depth at site 570 can be subtracted resulting in a probable rock thickness of 6 sec. over the subducted plate at Site 570. At a probable seismic velocity of 4.5 km/sec., the 6 second section corresponds to 13,000 km. A similar figure can be derived by assuming a 12° subduction angle and a 6,000 m trench depth. The thickness of rock over the subduction zone is (6,000-2,000) + (Tan 12° x 44,000). With a convergence rate of 7 cm/year, the subducted material beneath Site 570 would have required 640,000 years to have been buried 13,000 km deep. Lacking a more confident estimate of the geothermal gradient over a subduction zone, 3°C/100 m can be assumed. The conditions of high temperatures (390°) and quick heating (1,600 years/degree) at these depths are so extreme that the maturation models of Waples (1980) and Ritter (1984) do not directly apply.

The two models predict incompatibly diverse values. The values range from being well within the gas generating window to being far off the maturity scale. Ritter (1984) pointed out that his model needs to be modified to account for very high pressures, in which case a retardation of maturation was postulated. Determination of the conditions of thermal maturation of the subducted sediments below Site 570 appear to be intractable at this time. While available models cannot be directly applied they do tentatively suggest that the sediments did reach thermal maturity with respect to oil generation and may be in or beyond wet or dry gas windows.

The isotopic values of the serpentinite-hosted gas of Sites 566 and 570 are systematically different. The $\delta^{13}C$ values of the methane, ethane, and propane at Site 566 (-60.2, -30.6, and -33.3 per mil) are markedly lighter than those at the bottom of Site 570 (-41, -24.3, and -21.5 per mil; Jeffrey et al., 1985). This could be interpreted as suggestive evidence of a subduction source. According to Stahl (1977), such a shift in isotopic values between Sites 566 and 570 would correspond to an increase in maturity of the source rock from Site 566 to Site 570. This view is contradicted by Schoell (1983) who argued that maturation results in isotopically lighter ethane. The isotopic value for the Site 566 methane is, as previously stated, too light to be considered a thermogenic gas. However, the isotopic signature of the methane at Site 566 is the value expected for early diagenetic gas according to Schoell (1983). The isotopic signature of the methane in the serpentinite basement of Site 570 is exactly in the range of values expected for a mature thermogenic gas.

The isotopic values of the gases recovered from serpentinite basement cores at Sites 566 and 570 do not rule out the possibility that the gases were formed by thermal maturation of subducted sediments. The abundance of isobutane and isopentane over the normal isomers, however, argues against migration from a mature source.

Sub-Thrust Sediments. The serpentinite-hosted hydrocarbons could conceivably have migrated into the metamorphic rocks from sediments over which the serpentinite was thrusted during emplacement and uplift. The exotic block of serpentinite found resting on sedimentary rocks at Site 567 demonstrates that large blocks of serpentinite have been structurally displaced on the Guatemala margin. The serpentinites recovered at Sites 566, 567 and 570 resemble those which crop out on the Santa Elena Peninsula of Costa Rica in both mineralogy and texture (Bourgois, et al., 1985). Azema et al. (1985) have shown that the Santa Elena ophiolites overthrust radiolarites and volcaniclastics of Late Cretaceous age. The unusually shallow stratigraphic position of the serpentinites drilled on Leg 84 suggests that they may have been elevated by a Late Cretaceous to early Tertiary faulting event. If the style of faulting along the Guatemala margin was similar to that farther south in onshore Costa Rica, gas generative sediments may be trapped beneath the serpentinite "basement".

Invoking the presence of sub-serpentinite petroleum source rocks can alleviate some of the difficulties associated with subducted Quaternary sediments as sources for the serpentinite-hosted hydrocarbons. The extreme differences postulated for the maturity of subducted sediments beneath the lower slope (Site 566) and the upper slope (Site 570) could be assuaged by assuming layers of source rocks emplaced below the serpentinite by faulting. The Late Cretaceous to early Tertiary subthrust source beds could have been

under generative conditions for an extended period of time and may have injected hydrocarbons into the fractured serpentinite. Different source lithologies could be invoked to account for the differences in isotopic content of the hydrocarbons measured in serpentinite at Sites 566 and 570.

For the most part, though, the concept of migration of hydrocarbons from thermally mature source rocks beneath thrusted serpentinite allochthons still suffers from the same inconsistencies that plague the other two migratory models. The isotope data for Site 566 strongly suggest that the basement hydrocarbons are of early diagenetic origin. All basement hydrocarbons detected at Site 570 are anomalously heavy. The abundance of heavier hydrocarbons and the progressive isotopic change with depth in the serpentinite suggests that the hydrocarbons were migrating from or through the serpentinite into the overlying sediments, favoring the subduction or thrust models. However, the large proportion of branched chain isomers relative to straight chain isomers argues for an early diagenetic source rather than a deep thermogenic source, which would favor the interpretation of hydrocarbons migrating from overlying sediments. Overall, the geochemical data from the basement hydrocarbons are paradoxical; no internally consistent migratory model can accommodate all the observed properties of these unusual hydrocarbons. One common characteristic of the serpentinite gases at both holes is the large amount of propane relative to both ethane and butane. None of the migratory models contains a mechanism to produce such an enrichment in propane.

In Situ Generation. One possible source for the hydrocarbon gases discovered in serpentinite at DSDP Leg 84 which was not considered by the workers associated with the project is in situ generation. The heating, hydrothermal circulation, pressure, and shearing which accompanied the transformation of peridotite to serpentinite could have conceivably generated the hydrocarbons. Conversion of the peridotite to serpentinite involves introduction of water into the igneous rock. In the formation of ophiolite complexes, such as the basement of the Guatemala continental margin, the water introduced to produce the serpentine minerals is ocean water. The dissolved material in the seawater, including carbonates, can be incorporated into the ophiolitic complex in the hydrothermal minerals formed. Later alteration of the serpentinite may release CO_2 and H_2 which could possibly be reduced to hydrocarbons.

Recent experimental evidence suggests that this unconventional mechanism for generating hydrocarbons directly from ultramafic rocks is possible. Morency et al. (1986) heated ground samples of serpentinized perididotites and dunites from eastern Canada and analyzed the gases which were expelled from the rock. As expected, large quantities of water and hydrogen were evolved from decomposition of the hydrous phyllosilicate serpentine minerals. A most remarkable finding was the detection of significant quantities of hydrocarbons from methane to pentane. Some rocks also produced measurable quantities of aromatic hydrocarbons. The results of the work of Morency et al. (1986) are summarized in Table 3.

One feature of the data from Morency et al. (1986) that is particularly intriguing is that the molecular distribution of the gas evolved from serpentinite in the laboratory is very similar to that of the gases recovered from the serpentinite basement rocks at Site 570. In particular, the very unusual overabundance of propane relative to both ethane and butane which

characterized the Site 570 gas is duplicated in the laboratory experiments. In Table 4 the ratios of the hydrocarbons to their next heavier homolog, i.e. methane:ethane, ethane:propane, etc., are listed for the gases from samples of serpentinites from Morency et al. (1986) and the gases from serpentinites of Sites 566 and 570. The DSDP samples all have greater proportions of methane to ethane than the samples heated in the laboratory by a factor of about 10. The ratios of ethane to propane and propane to butane of the laboratory gas are almost identical to the ratios for Site 570 gas. These ratios do not match those from Site 566, but are consistent within the a factor of 2 to 4.

The data published by Morency et al. (1986) did not differentiate between the isomers of butane and pentane. No isotopic values for the hydrocarbons produced were presented. The serpentinite gases from Leg 84, particularly from Site 570, had distinctive isomeric distributions and isotopic values. Given the close match in gross molecular composition of gases derived from Site 570, more complete geochemical data on the laboratory gas may provide insights into the origin of these enigmatic basement gases from the Guatemala continental margin. A more precise understanding of the processes by which the hydrocarbon gas developed in the serpentinite may be useful in interpreting the nature of gas hydrates in the overlying sediments.

TABLE 3.

HYDROCARBON GASES EVOLVED BY HEATING SERPENTINITE
After Morency et al., 1986

Sample	Methane ppm	Ethane ppm	Propane ppm	Butane ppm	Pentane ppm
UR 80-7	2500	40	90	60	570
LC 81-1	670	150	150	60	70
RB 80-2	3180	90	120	50	30
LF 81-5	2760	125	130	20	20

TABLE 4.

HYDROCARBON RATIOS OF SERPENTINITE HOSTED GASES
After Morency et al., 1986, and von Heune et al., 1985

Sample	Methane: Ethane	Ethane: Propane	Propane: Butane	Butane: Pentane
VR 80-7	63	0.44	1.5	0.1
LC 81-7	45	1.0	2.5	0.8
RB 80-2	35	0.75	2.4	1.7
LF 81-5	22	0.96	6.5	1.0
570-41-2	191	0.75	3.1	48
570-42-1	83	0.88	3.2	52
566-6-1	408	2.1	1.0	2.5
566-7-1	160	2.0	0.9	33

PART II

FORMATION AND STABILITY OF GAS HYDRATES

Gas hydrates have been cored from at least five locations in the Middle America Trench study region. Frozen material which was probably gas hydrate was recovered from three additional locations. All gas hydrate recoveries in the study region were from continental slope sediments. Gas hydrates were hosted in permeable ash or sand strata, or in fractured mudstone. A sample of massive gas hydrate was recovered from one location.

Bottom simulating reflectors (BSRs) which probably mark the base of the gas hydrate stability zone, have been identified from high quality seismic reflection profiles in the study region. The BSRs were identified in seismic lines from the continental slope landward of trench axis beneath water 1,500 to 4,000 m deep. The available seismic coverage of the study region does not permit region-wide mapping of BSR extent.

Several mechanisms have been proposed in the literature for the formation of the massive gas hydrate recovered from the study region. The available data do not confirm a specific mode of origin for the massive gas hydrate. Formation of the massive gas hydrate in and along a fault zone is the formation mechanism most consistent with the available geological, geophysical, and geochemical data.

Changes in the chemical composition of pore water with depth have been noted at some locations in the study region. Dissociation of gas hydrates has resulted in some of the observed changes. The pore water chemistry changes cannot entirely be ascribed to gas hydrate presence.

A variety of factors influence gas hydrate formation in the study region. An abundant hydrocarbon supply and permeable host sediments are required. Structural deformation may enhance gas hydrate formation. Rate of sedimentation shows no direct influence on gas hydrate formation.

Direct Evidence of Gas Hydrates

Gas hydrate samples were recovered from sediments in the study area cored during three cruises of the Deep Sea Drilling Project (DSDP). Frozen material which released gas was cored from three drill sites offshore of Acapulco, Mexico (Watkins et al., 1982). The material from at least one hole was proven to contain gas hydrates based on the volume of gas released upon decomposition. Offshore of San Jose, Guatemala gas hydrates were recovered from four locations (Aubouin et al., 1982; von Huene et al., 1985). One location was on the lower slope near the trench floor; the remaining

recoveries were from upper slope sediments. The gas hydrates were found in interstices of permeable sediments, fractures, and in a massive form. Although all holes drilled on the continental slope offshore of Guatemala contained methane gas, hydrate recoveries were isolated to specific intervals. Gas hydrates were also recovered from the only DSDP hole drilled on the continental slope offshore of Costa Rica (von Huene et al., 1985).

DSDP Leg 66

Ice and frozen sediments were recovered from Sites 490, 491, and 492. These unusual substances released varying amounts of hydrocarbon gas and carbon dioxide upon melting, leading Shipley and Didyk (1982) to infer the presence of gas hydrates. Details of host lithology and gas composition of the nine anomalous intervals are summarized in Table 5.

The probable gas hydrate recoveries from Leg 66 took two principal forms: pieces of impure ice and frozen sediments (Shipley and Didyk, 1982). The icy material was recovered from gas expansion cracks in the sediment and from voids in the core. It is not known whether this material was gas hydrate formed in situ. Another possibility raised by Shipley and Didyk (1982) is that the material may have been ice formed from pore water during or after core recovery. They speculated that the rapid cooling caused by the phase change of hydrate to gas or the exsolution and expansion of gas dissolved in pore water may have locally frozen the pore water. There is no indication ice inclusions were preferentially formed in any particular type of sediment. The recovery of the icy material from voids and cracks raises the possibility that it may have originally been located in natural fractures in the mudstone sediment. The gas from the icy material at 139 m depth at Site 490 was anomalously rich in carbon dioxide (23.23%).

The majority of the probable hydrate recoveries on Leg 66 were in the form of interstitial material cementing porous sediment (Shipley and Didyk, 1982). The sediments were typically fine-grained sand and volcanic ash. These frozen sediments were recovered as cohesive chunks with recognizable sedimentary structures. Upon melting, however, the samples collapsed into structureless lumps of wet sediment.

It is possible that other intervals of Leg 66 cores contained gas hydrates which were not detected (Shipley and Didyk, 1982). The gas hydrates were originally detected by resistance of certain core intervals to being split during onboard core processing. Subsequently recovered cores were inspected for unusually cold sectons which may have contained gas hydrates. When located, cold intervals were opened more quickly than other cores in an effort to recover any gas hydrates present prior to dissociation. In spite of these precautions it is likely that other gas-rich intervals may have originally contained gas hydrates.

Probable gas hydrates were recovered exclusively from continental slope deposits on Leg 66. Sites 491 and 492 were characterized by ashy mud and mudstone slope deposits overlying uplifted trench deposits composed of coarse sand. Within the slope deposits, probable gas hydrates were concentrated in the more porous ash and sand beds implying that permeability of the host lithology may have facilitated gas hydrate formation. However, the trench deposits, which would be expected to be very permeable based on grain size, were apparently barren of hydrates, since none were recovered from the trench. It is likely that another gas hydrate formation requirement, such as

TABLE 5.

SUSPECTED GAS HYDRATE OCCURRENCE, DSDP LEG 66
After Shipley and Didyk, 1982

Hole	Water Depth m	Subbottom Depth m	Lithology/Comments	Gas Content CO_2 %	Methane %	Ethane %	Propane ppm	Butane ppm	Pentane ppm	$\frac{C_1}{(C_2+C_3)}$
490	1761	139.73-139.75	Ice inclusion Ice inclusions in mud near large wood fragment	23.23	76.77	na	na	na	na	na
		145.40-145.75	Frozen sediment Frozen muddy to silty laminated volcanic ash	3.00	97.00	na	na	na	na	na
		166.50-166.85	Frozen sediment Frozen sandy to silty laminated ash layer, temperature -2° to -0.8°C	1.56	98.19	0.25	11	8	3	376
		364.00-364.50	Frozen sediment Frozen bioturbated (mixed) mudstone and clayey ash, temperature 1.7°C 2 hr. after core on deck	0.47	99.21	0.26	249	217	34	348
491	2883	88.90-89.00	Ice inclusion Ice blebs in mud	1.62	98.34	0.03	55	42	22	2809
		162.70-163.15	Frozen sediment Frozen bubbling fine sand beds (10 cm and 15 cm) temperature 1 to 1.5°C	0.73	99.18	0.08	37	12	8	1180
		168.30-168.35	Ice inclusion Frozen mud and ice	0.79	98.27	0.89	478	194	110	100
492	1935	140.95-141.10	Frozen sediment Frozen muddy laminated volcanic ash layer	0.22	99.59	0.18	50	47	nd	1200
		169.50-169.57	Frozen sediment Frozen muddy laminated volcanic ash, temperature 0.8°C	0.23	99.68	0.08	34	37	nd	1200

abundant methane, was not met in the trench deposits. The site reports for Sites 491 and 492 mention that the organic carbon content varied between 0.8 and 2.9% in these holes, but the depth relationship of TOC was neither tabulated nor graphed. Methane content of the cores at Site 491 and 492 did not decrease appreciably in the trench deposit intervals.

DSDP Leg 67

Cores from DSDP Leg 67 provided both direct evidence of gas hydrate presence and evidence of widespread methane generation in the sediments of the Guatemala continental margin (Aubouin et al., 1982). Samples of gas hydrates were observed in coarse sediments in the cores from Sites 497 and 498 (Aubouin et al., 1982). Hydrocarbon gases were detected in cores from six of the DSDP sites from Leg 67. The only location where hydrocarbons were not detected was in the pelagic sediments of the Cocos Plate seaward of the Middle America Trench. The gas and gas hydrate content of each individual site are discussed below in the order of the most seaward site (495) to the most landward (Site 496).

Site 495, located on the Cocos Plate 22 km seaward of the Middle America Trench, cored 447 m of hemipelagic and pelagic chalks without encountering any evidence of hydrocarbons.

Site 499. Four holes were drilled at Site 499 on the floor of the Middle America Trench. The upward transition in sediment character from pelagic carbonates to turbidites documented the approach of the Cocos Plate to the subduction zone.

Methane with trace concentrations of ethane was detected at Site 499. The percentage of methane in the core liner gas dropped with depth from 80% at 10 m depth to about 10% at a depth of 52 m before gradually increasing to 75 - 80% again at 80 m depth. The methane maintained this concentration to 150 m, the deepest analysis reported. The ethane profile of Site 499 increased from essentially nil down to 65 m to a maximum of 21 ppm at 89 m before falling to 5 ppm at 120 m. There is no obvious lithological relationship to the gas content or makeup of the cores. The shipboard scientists claimed that the lack of ethane above 60 m in the Quaternary sediments indicates that ethane was stripped from the pore fluids during downslope mass transport. The cores show that the transition from turbidites to hemipelagites occurs at about 120 m.

Site 500. Located in the Middle America Trench 1.5 km landward of Site 499, Site 500 drilled turbidites, pelagic sediments and basalt. The drilled section was faulted such that Miocene chalk beds were in contact with Pleistocene turbidites.

Abundant methane was found in core gases. The downhole methane content is similar to that at Site 499 with a marked depletion between 60 m and 70 m depth. No relationship of gas content and lithology was apparent. Ethane content was very low at Site 500, less than 5 ppm. Pore water showed no systematic depletion of salinity or chlorinity with depth.

Site 494. Drilled on the lower continental slope 5 km from the contact of the slope and trench floor, Site 494 revealed a section of slope sediments,

hemipelagic sediments, and altered igneous basement at least as old as Late Cretaceous.

Abundant methane was found in all sediment cores sampled. The basal Cretaceous rocks were either not sampled or contained no gas. Ethane content increased with depth to a maximum of 210 ppm at a depth of 260 m. The logarithmic decrease in methane to ethane ratio of Site 494 is typical of that observed at DSDP sites worldwide (Claypool and Kvenvolden, 1983). Pore water salinity showed no evidence of gas hydrate presence at Site 494; chlorinity increased with depth.

Site 498 was offset 1.5 km along strike from Site 494. The drilled section was similar, but the rocks were more highly fractured.

Gas hydrates were recovered cementing the grains of a coarse vitric ash bed at 310 m at Site 498 (Harrison and Curiale, 1982; Table 6). Once the gas hydrates had decomposed at atmospheric temperature, the ash collapsed into an unstructured slurry of vitric shards and clay. Cores from 221 to 250 m were ejected from the liners by intense degassing which is suggestive of gas hydrates; but no gas hydrates were positively identified from the shallower depths. Also, large gas expansion cracks in the cores from depths of 278 - 288 were noted.

The holes at Site 498 were drilled rapidly with few cores down to a depth of 200 m. The shallowest gas samples analyzed were from depths of 100 and 150 m. The methane content of the core liner gases fluctuated between 5% and 80% in the 9 samples taken. Considerably more ethane was measured at Site 498 than at the nearby Site 494 or the two trench floor locations, Site 499 and Site 500. The ethane content of the cores which were ejected from the liners (228 - 250 m) was particularly high, 350 ppm. The gas collected from dissociating gas hydrates was considerably enriched in ethane (1,991 ppm).

The rapid increase in ethane content and the recovered gas hydrates led to the abandonment of drilling at 310 m.

Site 497 was located on the upper continental slope 30 km landward of Sites 494 and 498. Gray and olive hemipelagic muds and mudstones with interbedded volcanic ash were drilled to a depth of 396 m.

Violent core degassing was encountered from depths of 159 m to 380 m subbottom (Harrison and Curiale, 1982). Five cores were ejected from the plastic core liners by gas pressure. A solid piece of hydrate 2 cm in diameter was recovered in the core catcher from core 39 at 368 m (Table 6).

Hydrocarbon gases were abundant at Site 497 below 50 m. Methane remained the principal gas from the shallowest reported sample (50 m) to the bottom of the hole. Ethane concentrations increased regularly downhole reaching 380 ppm from core 41. Of all gases analyzed from this site, the gas recovered from the dissociating gas hydrate nodule in core 39 was the most enriched in ethane with a concentration of 501 ppm. This high level of ethane in hydrates agrees with analyses at Site 498.

The pore waters squeezed from Site 497 sediments displayed a regular decrease of salinity and chlorinity with depth.

Site 496 was drilled beneath 2,049 m of water, the most landward location of the Leg 67 continental margin transect. Mud and sandy mudstone of Holocene to Miocene age were drilled to a depth of 378 m.

TABLE 6.

GAS HYDRATE OCCURRENCES ON DSDP LEG 67
After Harrison and Curiale, 1982

Hole	Core	Subbottom Depth m	Observation/Comments	CO_2 %	Methane %	Ethane ppm	Propane ppm
497	39	358.5-368.0	Core ejected from liner; hydrate in core catcher	0.1	90.4	501.5	n.d.
498A	15	307.0-316.5	Hydrate in vitric sand	0.2	83.0	1991	4.2

Hydrocarbon gases were monitored in all cores from the sea floor to total depth. Methane constituted about 75% of the core gas, with a slight tendency toward an increase with depth. Only trace amounts of ethane were detected to a depth of 150 m, where a marked increase was noted. Ethane content reached 780 ppm at total depth. The rapid increase in ethane and the detection of hydrocarbons up to pentane led to abandonment of drilling for safety considerations.

No anomalous core degassing features or any other observable evidence of gas hydrates were detected.

In spite of the lack of observed gas hydrates, the pore water at Site 496 diminished drastically with depth in salinity and chlorinity.

DSDP Leg 84

Evidence of gas hydrates was encountered at all but two locations drilled on Leg 84 (Kvenvolden and McDonald, 1985; von Huene et al., 1985). Gas hydrate samples were recovered from three sites: 565, 568, and 570 (Table 7). Indirect evidence of gas hydrate presence was recorded at Site 566. No indication of gas hydrates was found at Site 567 and 569. However, substantial amounts of hydrocarbon gases were detected at all sites drilled on Leg 84.

Site 565 was drilled offshore of the Nicoya Peninsula of Costa Rica, 700 km southeast of Sites 566 - 570. Early Miocene to Holocene age muds and mudstones were drilled to a depth of 328 m.

Three samples of gas hydrates were recovered from Site 565 (Table 7). A core from 285 m degassed violently. A sample of an ice-like substance was removed from the part of the core which was degassing most vigorously. At 319 m, cold, fizzing sandstone was noted in material which had been ejected from a core liner by degassing. A piece of an icy material weighing 1.67 g was recovered in the core catcher from the same core. The piece was large enough to permit physical tests to determine its character. The material released a volume of gas upon dissociation which was 133 times that of the resulting water. The volume increase is in the range of that expected for a hydrate and greater than possible from degassing of the sediment. The dissociated gas contained much less n-butane and larger hydrocarbon gases than adjacent sediments (Table 8). This also indicated that the icy material may have been hydrates; molecules as large as n-butane are excluded from the hydrate crystal lattice limiting their presence in hydrate gas. The water obtained from dissociating the material was very fresh, 1.1 per mil salinity. Since inorganic ions are also excluded from gas hydrates, this measurement also indicated that gas hydrates had been recovered at Site 565.

Hydrocarbons were detected in all core gases analyzed from depths of 56 m to 320 m. The content of ethane and other heavier hydrocarbons increased downhole, with a methane to ethane ratio of 2,000 to 2,800 in the interval from which gas hydrates were obtained.

Interstitial water decreased in both salinity and chlorinity in a manner which was proposed to be consistent with gas hydrate presence.

The gases and pore fluids from Site 565 were analyzed for isotope distribution by four groups. Core gases were analyzed for ^{13}C content of methane by Jeffrey et al. (1985). Isotopic analyses were also performed on carbon dioxide when sufficient quantities were available for determination.

TABLE 7.

DESCRIPTION OF GAS HYDRATES RECOVERED ON DSDP LEG 84
Modified from Kvenvolden and McDonald, 1985

Site and section	Subbottom depth (m)	Comment	Gas Sample Number
565-30-6	285	White, frothing gas hydrate (~0.3 cm^3) was observed through the core liner in a region of degassing sediment.	
565-33,CC	319	Pieces of muddy, gas-releasing sandstone were expelled from the end of the core barrel. When broken open, the sandstone showed increased evolution of gas.	
565-33,CC	319	White, frothing gas hydrate (~1.5 cm^3) was recovered from stiff mud at top of core catcher.	1
568-43-4	404	White gas hydrate was recovered from fractures in a tuffaceous mudstone.	2
570-21-1	192	Ash laminated with gas hydrate at top of core.	3
570-26-5	246	White gas hydrate in fractures of mudstone.	
570-27-1	249	Massive gas hydrate 1.05 m long.	4
570-27-1	249	White gas hydrate in fractures of dolomite. This sample is at the base of the massive gas hydrate.	5
570-28	259-268	White gas hydrate in fractures of mudstone.	6
570-29-3	273	Same as above.	
570-32-4	303	Gas hydrate associated with ash.	
570-36-1	338	Gas hydrate associated with sand.	

TABLE 8.

ANALYSIS OF GAS FROM GAS HYDRATES RECOVERED ON DSDP LEG 84
Modified from Kvenvolden and McDonald, 1985

Sample Number	Section	C_1 %	C_2 ppm	C_3 ppm	i-C_4 ppm	n-C_4 ppm	neo-C_5 ppm	i-C_5 ppm	n-C_5 ppm	CO_2 %	C_1/C_2
1	565-33,CC	89	440	5	0.2	----	----	0.1	---	0.03	2000
2	568-45-4	64	1200	0.3	1.4	----	0.04	----	---	0.10	530
3	570-21-1	44	390	0.9	0.7	0.2	----	----	---	0.34	1100
4	570-27-1	74	1200	31	10	7	0.6	6	3	----	600
5	570-27-1	58	2600	79	37	45	3.5	34	12	0.30	220
5	570-27-1	69	1600	48	23	28	1.0	17	8	0.25	440
6	570-28	75	890	11	2	7	0.06	4	2	0.24	840
6	570-28	75	1200	14	3	9	0.16	6	3	0.24	620

Claypool et al. (1985) independently analyzed core gas for ^{13}C content of methane and carbon dioxide where concentrations were sufficient. Core gas methane was also analyzed for D (deuterium) content. Claypool et al. (1985) also analyzed pore water for ^{13}C content of the total dissolved carbonate fraction (ΣCO_2) and ^{18}O content. Galimov and Shabaeva (1985) reported the results of ^{13}C determinations for methane and carbon dioxide from core gas samples.

Isotopic values of methane were fairly consistent among the three groups independently analyzing the core gases. The group means for $\delta^{13}C$ values agreed within 2 per mil. The data of Jeffrey et al. (1985) are heavier (less negative) than those of Claypool et al. (1985; Figure 22). The values presented by Galimov and Shabaeva (1985) are typically situated between those of the other two groups. The general trend is for methane to become heavier with depth, varying from approximately -72 per mil at 54 m subdepth to -63 per mil at 317 m. The values are well within the range expected for bacterially generated methane (Schoell, 1984).

Since the gas from Site 565 was dominantly methane with only small concentrations of carbon dioxide, fewer $\delta^{13}C(CO_2)$ data points exist. Galimov and Shabaeva (1985) reported 10 values with a mean of - 18.3 per mil. Jeffrey et al. found only one core with sufficient carbon dioxide to make a quantitative determination; core 21 at 195 m depth had a $\delta^{13}C$ value of -7.3. From the same core, Galimov and Shabaeva reported a value of -16.5 per mil. It is not clear whether the difference in values is from a true difference in isotopic signature of gases from different sections of the core, or if it is an artifact from the different analytical methods used by the two groups. The data of Galimov and Shabaeva (1985) show a trend to lighter values at greater depths, opposite of that evident in the methane isotopic data.

Claypool et al. (1985) reported that the total carbonate fraction of the pore water at Site 565 became heavier with depth to 180 m and then became lighter to 251 m (Figure 22).

The limited number of samples and the question of the reliability of the carbon dioxide data do not permit the assignment of a distinct relationship among the isotope values. The depth trends of $\delta^{13}C$ values for methane and total carbonate are not consistent or parallel as typically expected (Claypool and Kaplan, 1974).

Site 566 was drilled on the lower continental slope of Guatemala. The location of the drill site near the floor of San Jose Canyon permitted sampling of serpentinite basement rocks at shallow depths.

Abundant hydrocarbon gas was recovered from cores of the serpentinite basement rocks of Site 566. The gases were anomalously rich in the heavier hydrocarbons (Jeffrey et al., 1984; Table 9). Carbon isotope values for the methane in the basement gas averaged -60.3 per mil, suggesting its biogenic origin. Cored sediments were apparently not sampled for gas.

Indirect evidence exists that the hydrocarbon gas in the fractured serpentinite basement may have been in hydrate form. The site report stated that "Rubble associated with the fractured serpentinite degassed vigorously." Kvenvolden and MacDonald (1985) proposed that structure II gas hydrates may have been present in the fractured serpentinite based on the high ratio of isobutane to normal butane and the relative scarcity of molecules as large as or larger than normal butane. Since structure II gas hydrates exclude hydrocarbons larger than isobutane, it was assumed that gas from dissociating hydrates should have a high isobutane:normal butane ratio. However, a check

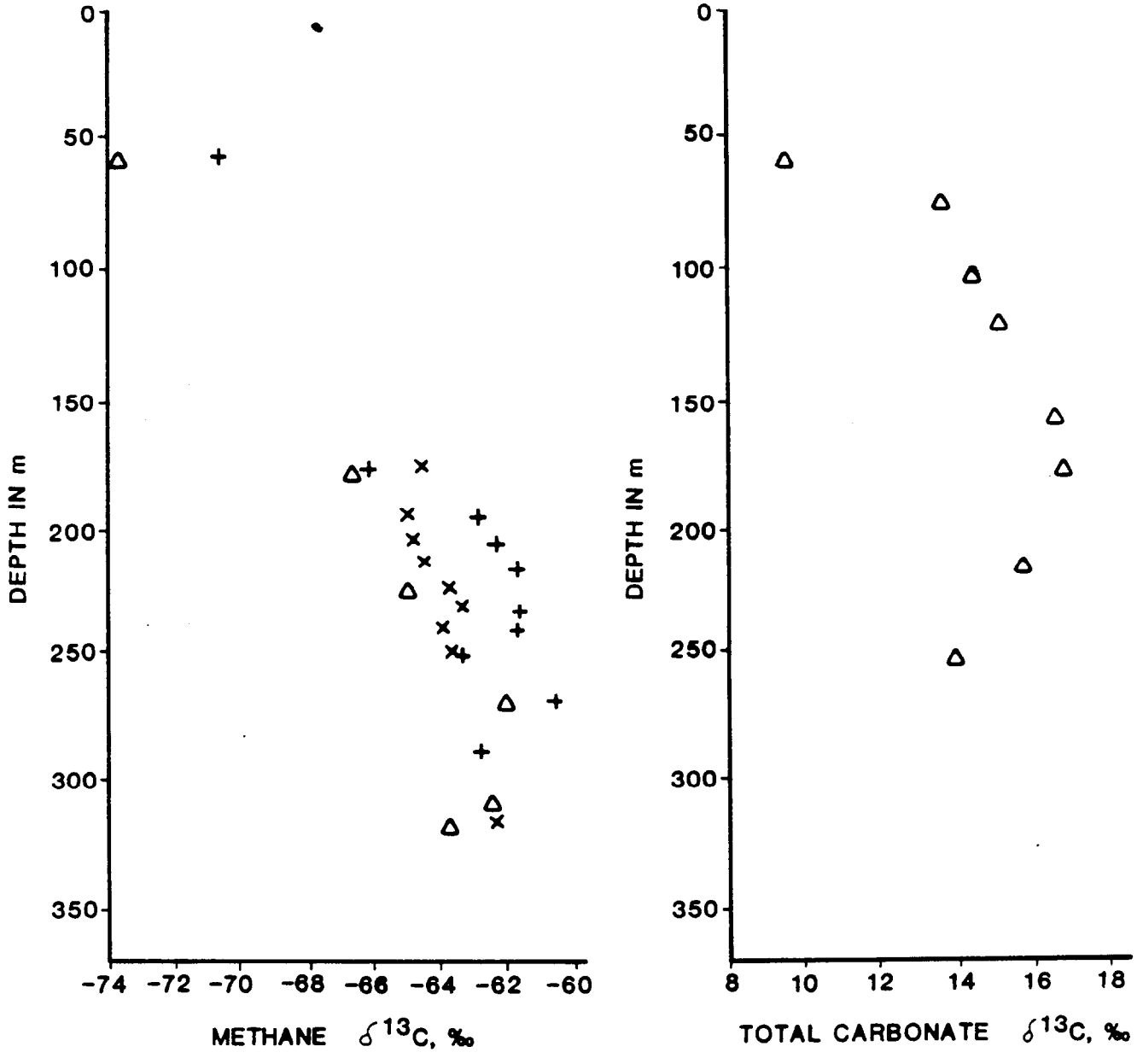

Figure 22. CARBON ISOTOPE CONTENT OF PORE WATER METHANE AND CARBONATE AT DSDP SITE 565

Data from Claypool et al., 1985 (Δ), Galimov and Shabaeva, 1985 (×), and Jeffrey et al., 1985 (+)

of butane isomer ratios for all Leg 84 sites calculated by Jeffrey et al. (1985) shows no correlation of high isobutane values with reported gas hydrate presence. Hesse et al. (1985) stated that gas was released from "chips of ice-like material from these fractures," which suggests gas hydrate presence.

TABLE 9.

DISTRIBUTION OF HYDROCARBON GASES, DSDP SITE 566.
After von Huene et al., 1985

Core-section	Subbottom depth m	C_1 %	C_2 ppm	C_3 ppm	i-C_4 ppm	n-C_4 ppm	neo-C_5 ppm	i-C_5 ppm	n-C_5 ppm
6-1	118.4	49	1200	560	540	29	2.4	5.3	3.9
7-1	127.8	45	2800	1400	1500	110	7.9	36.0	4.3

Site 567 was drilled on the lower continental slope of Guatemala 3 km upslope from the floor of the Middle America Trench. A sedimentary section from Quaternary through Upper Cretaceous and ophiolitic basement were drilled.

Hydrocarbon gases were detected in all cores from deeper than 200 m. The gas was mostly methane, with methane to ethane ratios of 2,000 to 7,000. There is no mention of violent core degassing phenomena.

The pore water from Site 567 increased in chlorinity and salinity with depth. This led the shipboard scientific party to conclude that no gas hydrates were present. Hesse et al. (1985) also noted the unusual Ca^{2+} and Mg^{2+} profiles. These were considered as evidence of diffusive exchange of pore water constituents with the ophiolitic basement. Expulsion of fluids from the basement into the overlying sediments is consistent with the steep pressure gradient, approaching geostatic which was documented for Site 567 by von Huene (1985). Pore waters would be expected to migrate from the overpressured basement upward into the normally pressured (hydrostatic) sediments and mix with the connate waters of the sediment. Thus it may be that the lack of expected decrease in pore water salinity and chlorinity does not conclusively indicate that no gas hydrates were present at Site 567; the influx of highly saline water from the overpressured basement may have overprinted any pore water freshening resulting from gas hydrate dissociation.

Site 569 is located 32 km landward from the Middle America Trench axis approximately in the middle of the Guatemala continental slope. An Eocene to Holocene sedimentary section 351 m thick and 14 m of metamorphic basement was drilled.

Abundant hydrocarbon gas was measured in all sediment cores tested. The gas was composed of methane and ethane with very small amounts of heavier hydrocarbons. Site 569 is unique among the Middle America Trench DSDP sites in that the ethane concentration in the core gas did not increase with depth. The methane to ethane ratio averaged 8,300. The isotopic

composition of the carbon in the methane indicates typical biogenic gas, from -88 per mil at 60 m depth to -65 per mil at 333 m (Jeffrey et al., 1985). No samples of core gas from basement cores were reported.

The few interstitial water samples collected for analysis from Site 569 showed a slight decrease in salinity and chlorinity with depth. The authors of the site report stated that "The decreasing values with depth of chlorinity and salinity support the conclusion that gas hydrates were present (von Huene et al., 1985). Kvenvolden and MacDonald (1985) stated that "the decreasing chlorinity of pore waters suggests that gas hydrates were also present there (Site 569)." On the other hand, Hesse et al. (1985) claimed that the salinity decreases were minor, and that the chlorinity "decrease is too small to be identified with the occurrence of hydrates."

No visual evidence of gas hydrates was noted at Site 569.

Site 568 was located on the upper Guatemala continental slope beneath 2,010 m of water. The location selected for drilling was 1 km upslope from Site 496 of Leg 67. Site 496 had been abandoned due to concern over possible gas hydrate presence. Subsequent reprocessing of seismic line GUA-13 had shown a distinct BSR beneath Site 496 (Figure 17). Site 568 was designated specifically as a gas hydrate study location based on both seismic evidence and drilling evidence for their presence. An Oligocene through Holocene sedimentary section comprising muds, mudstones, and volcanic ash layers was drilled to a depth of 417 m.

Although each core was carefully inspected for gas hydrates, none were detected above 403 m. Pieces of white gas hydrate were recovered from fractures in a tuffaceous mudstone between 403.2 and 404.7 m. Samples of the gas hydrate were allowed to dissociate in a pressure vessel producing about 30 volumes of gas per volume of water. The released water had a salinity value of about 5.5 per mil.

Abundant hydrocarbon gas was measured from all cores analyzed. Ethane content increased irregularly from 2.2 ppm near the sea floor to 1,000 ppm at 414 m. Hydrocarbons through pentane were also measured in the core gases.

The project scientists interpreted the fluctuation of hydrocarbon gas content with depth to indicate zones of hydrate and gas. According to this interpretation, stratigraphic intervals with gas hydrates can be recognized by a preponderance of methane and ethane and a depletion of propane through pentane due to the exclusion of the larger compounds from the gas hydrate lattice. If only structure I hydrates were present, propane and all heavier hydrocarbons should be depleted; structure II hydrates would be marked by depletion of only normal butane and larger alkanes. The DSDP scientists stated that the gas analyses showed that the sedimentary section of Site 568 could be divided into five zones relative to inferred gas hydrate presence (Table 10).

The proposed interpretation is of merit in that it addressed an anomalous feature of the Site 568 data relative to typical DSDP gas distributions. At Site 568 the relative and absolute amounts of hydrocarbons with three or more carbon atoms per molecule fluctuate irregularly with depth. From the sea floor to about 200 m subbottom, the proportion of these heavier molecules in the core gas is about 3 times higher than in the remainder of the hole (6.8 vs. 3.2 ppm; Figure 23). This is contrary to the trend observed in many DSDP holes where heavier hydrocarbons tend to increase regularly with depth

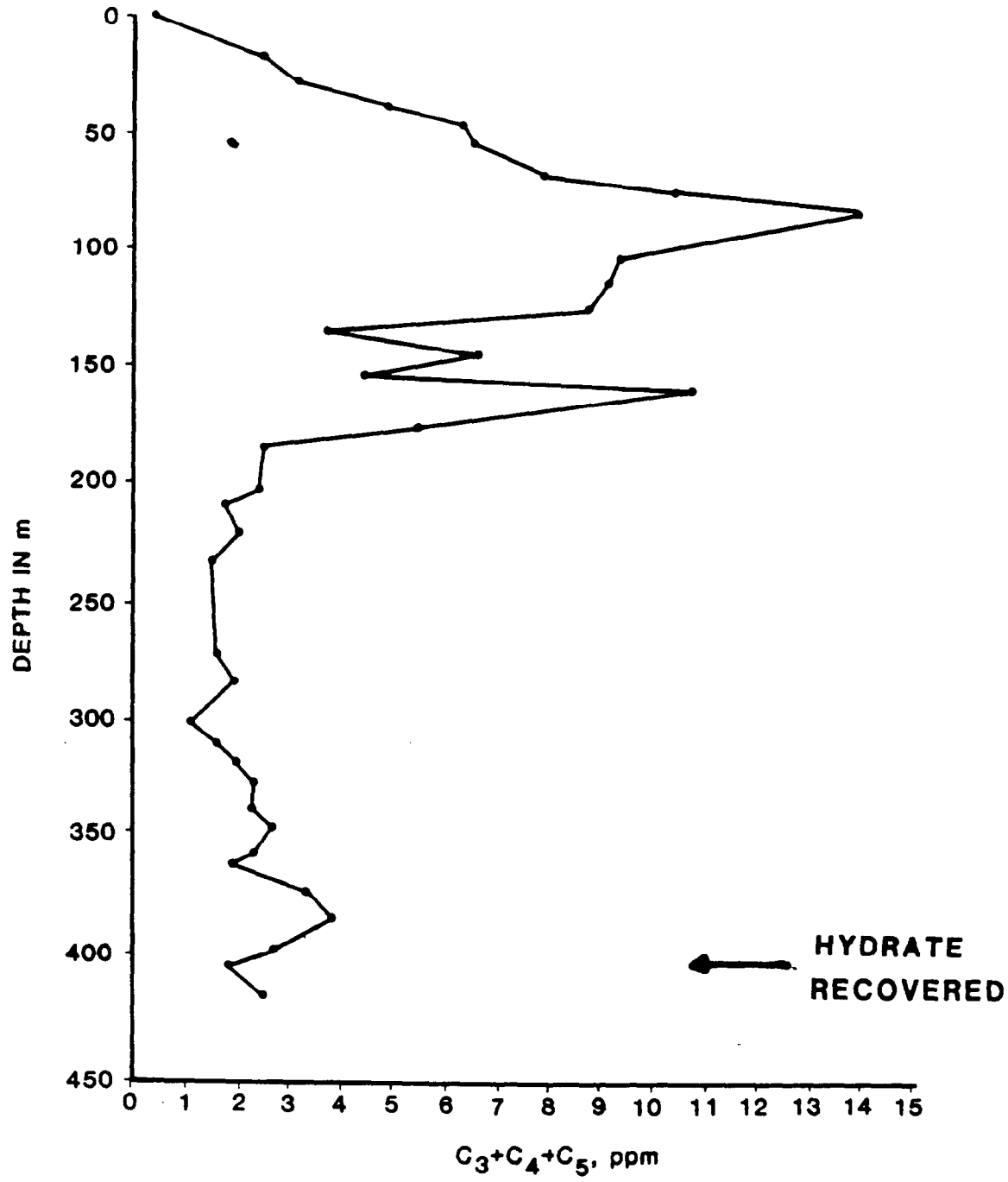

Figure 23. CONCENTRATION OF HEAVY HYDROCARBON GASES IN CORES FROM DSDP SITE 568

as would be expected in conformity with the probable diagenetic origin of these gases.

TABLE 10.

DEPTH DISTRIBUTION OF GAS HYDRATES AT DSDP SITE 568 FROM CORE GAS COMPOSITION.
After von Huene et al., 1985

Subbottom depth, m	Gas occurrence
0-190	Biogenic gas followed by gas resulting from early diagenesis
190-345	Gas hydrate dispersed in fine-grained sediment
345-391	Gas in sediments in a nonhydrated state
391-410	Dispersed and solid gas hydrate
410-417	Gas in a nonhydrated state

The differentiation of Site 568 sediments into zones of different degrees of gas hydrate concentration as proposed by Kvenvolden and McDonald (1985) actually involves two concentration trends. The very high levels of propane through pentane shallower than 190 m indicate no hydrates present. The low levels of hydrocarbons heavier than methane deeper than about 200 m indicate some degree of gas hydrate presence, with the extent of hydrate development measured by relatively minor fluctuation in gas composition.

The large change in hydrocarbon distribution at 190 to 200 m depth can be explained without invoking gas hydrates. A major unconformity exists at Site 568 near 190 to 200 m subbottom. The depth of uncomformity was not precisely located, but benthic forams indicate a depth of 195 m. The unconformity separates late Miocene and Pleistocene sediments, spanning 3 to 10 m.y. Work by Gilbert and Cunningham (1985) and Kennicutt et al. (1985) demonstrated that properties other than gas content also change abruptly at the 190 to 200 m depth. Organic carbon is on average over twice as abundant in the upper 190 m (Figure 19). Also the $\delta^{13}C$ signatures of the organic matter are much different above and below that depth (Figure 19). Optical analysis of the organic matter showed that the Miocene sediments contain principally terrestrial organic matter, whereas the Pleistocene organic matter is dominantly of marine origin (Figure 19). Since the quantity, composition, and origin of the organic matter changes so drastically at 190 to 200 m depth, it is reasonable to expect a corresponding change in composition of gases formed from that organic matter. The changes in gas concentrations proposed by Kvenvolden and McDonald (1985) to correspond to gas hydrate presence beneath 190 to 200 m are of the type that would be expected from the organic matter contrast. Marine organic matter is generally considered "oil-prone", whereas terrestrial organic matter is "gas-prone" (Tissot and

Welte, 1978; Gilbert and Cunningham, 1985). This well accepted generalization implies that for a given degree of diagenesis, hydrocarbons derived from marine organic matter should contain a higher proportion of heavier hydrocarbons than from terrestrial organic matter. Although the gas vs. oil generating tendency of organic matter types was determined from thermally mature sections, we know of no studies which would suggest a different relationship in early diagenetic gases. It is also pertinent that there was no evidence of sudden appearance of gas hydrates at 190 to 200 m to support the contention of Kvenvolden and McDonald (1985). The core descriptions indicate that gas expansion voids were probably more abundant above the unconformity than below. To attain the 50% average decrease in heavy hydrocarbons in core gas measured across the unconformity, at least 50% of the available gas would have to be in hydrate form below the unconformity. Such a high degree of gas hydrate development would suggest that some evidence of its sudden appearance between 190 and 200 m should persist in the cores.

The proposed differentiation of the lower part of the hole into 4 degrees of hydrate presence is based on much finer-scale fluctuation in gas levels. The researchers did not report which gas was used to determine the intervals of hydrate presence described above. A plot of the downhole variation of abundance of three gases which should be most sensitive to the hydrate exclusion effect is presented for depths between 170 and 420 m depth in Figure 24. A distinct enrichment in propane, isobutane and normal butane is noted between about 350 m and the bottom of the hole. This corresponds well to the assertion that gas in a nonhydrated state is present. Within this region from 350 to 415 m, a zone of hydrate was proven to exist by recovery of a sample of gas hydrate at 404 m. This hydrated layer should be marked by a drop in concentration of heavier constituents in core gases. Such a decrease is seen in Figure 24 at a depth of 404 meters in the levels of propane and isobutane, the two gases which should best show exclusion by structure I gas hydrates. A decrease in the quantity of normal butane would also be expected, especially if structure II hydrates were present, but n-butane levels actually increase somewhat at that depth. A distinct increase in propane and isobutane is noted at 414 m depth in concurrence with the lack of observed gas hydrates at this depth.

Fluctuations in isobutane levels at least as great as those noted at 404 m depth are evident at 300 and 363 m. The levels of isobutane measured at 300 m drops substantially, while the concentrations of propane and n-butane remain on the expected trend. This could be attributed to instrumental malfunction, analytical error, or a fluctuation in gas content unrelated to gas hydrate presence. In any event, the magnitude of this unexplained fluctuation at 300 m suggests that caution should be used in ascribing hydrate presence as the sole cause of a lesser fluctuation at 404 m. If the drop in quantities of heavier gases present at 404 m is truly related to a zone of hydrate development, then it is probable that the drop of larger magnitude at 363 m also indicates a gas hydrate band not noted by DSDP scientists.

Since the quantities of methane and ethane also vary downhole, a measure of the ratios between the gases which can form hydrates and those which would be excluded should better display trends proposed to be due to gas hydrate formation. A graph obtained by processing the data presented in the site report is shown in Figure 25. On the graph, two quantities are displayed. The sum of all measured alkanes larger than ethane, and the sum of all alkanes larger than isobutane represent the gases which would be

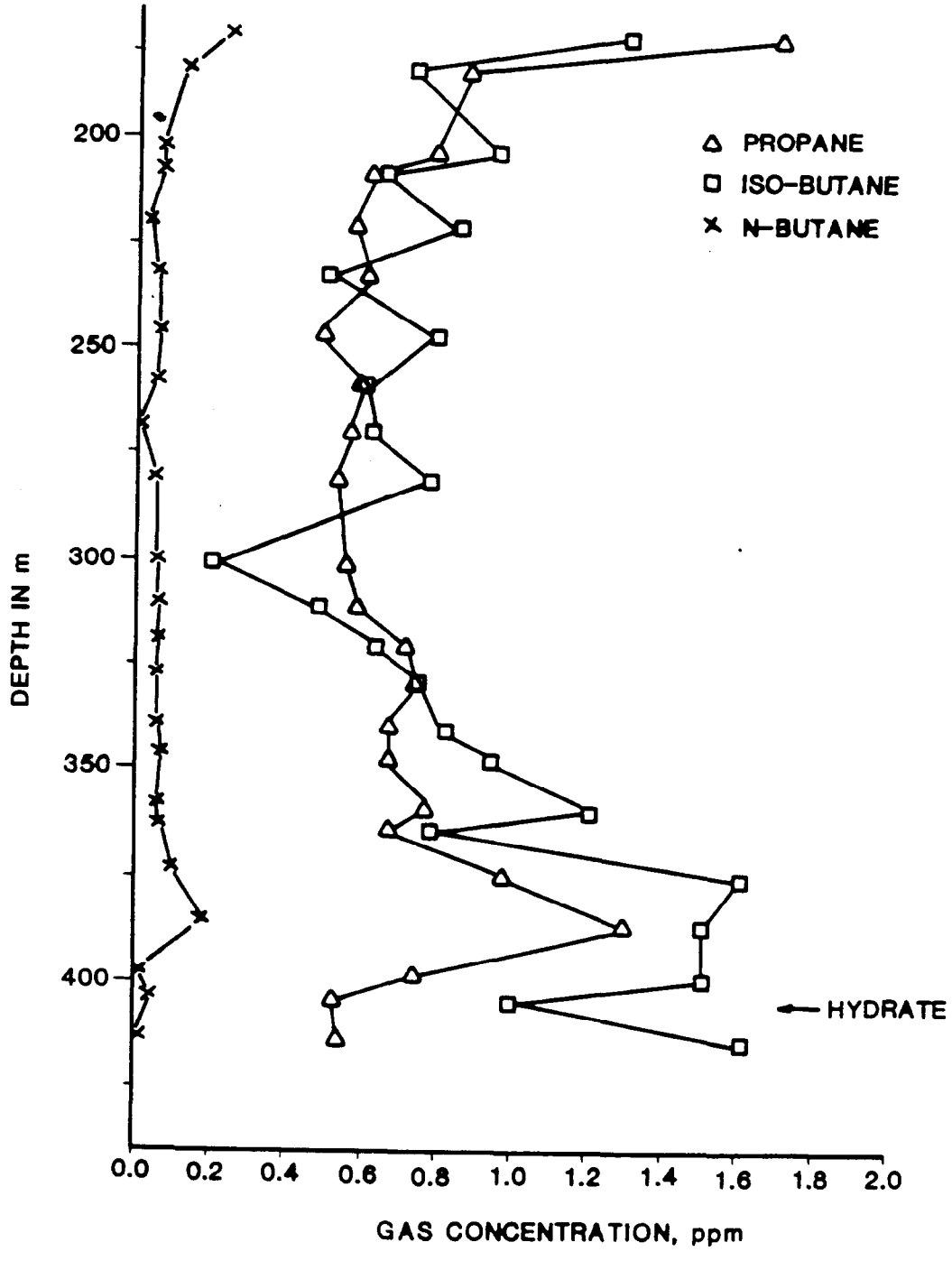

Figure 24. CONCENTRATION OF HEAVY HYDROCARBON GASES IN MIOCENE SEDIMENTS OF DSDP SITE 568

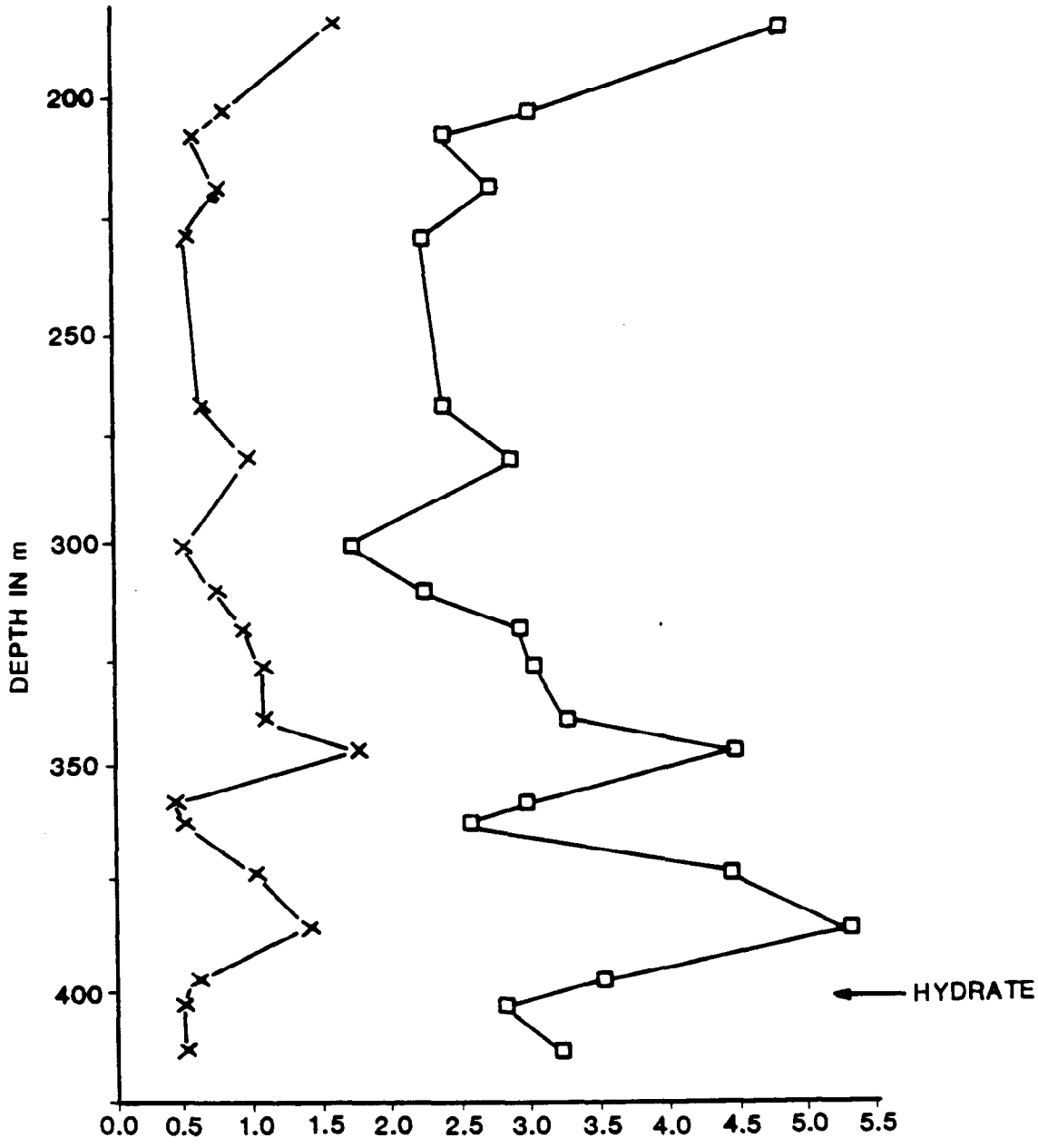

□ = $(C_3+C_4+C_5)/(C_1+C_2) \times 10^6$

× = $(n\text{-}C_4+C_5)/(C_1+C_2+C_3+C_4) \times 10^6$

Figure 25. RATIOS OF HEAVY TO LIGHT HYDROCARBONS IN CORE GASES AT DSDP SITE 568

excluded from structure I and structure II gas hydrates respectively. A parameter representing the ratio of the sum of values for all alkanes larger than ethane to the sum of abundance of methane and ethane is plotted. Similarly the ratio of alkanes larger than isobutane to the sum of the concentration of methane through isobutane is plotted to highlight exclusion by structure II hydrates.

Since the two parameters plotted on Figure 25 are ratios involving methane content, gas composition data from two cores were removed from consideration. Samples from cores 27-3 at 247 m and 28-4 at 259 m registered only 6.2% and 3.8% methane. This is in contrast to a mean methane value of 72% and values of 65% and 68% in the immediately shallower and deeper cores. The values for heavier hydrocarbon content in the two cores in question are in line with those expected based on surrounding values. This is consistent with the analytical method used; gas samples were analyzed for methane and for heavier hydrocarbons using different instruments. If the low methane values in the two questionable cores were due to excessive air dilution of the gas rather than to analytical error, the heavier fractions should be likewise depleted which they are not. The possibility that the low methane values are correct is remote; the heavy to light isomer ratios in such a case would be three times the highest values from the site and are out of line with any local trend. The deletion of the two methane values is supported by knowledge of the analytical methods employed.

The values plotted on Figure 25 suggest that the depth relationship to gas hydrate development at Site 568 proposed by von Huene et al. (1985) may be valid, but that the inconsistencies noted previously in this section still exist. The best data point to begin the analysis is the gas content at 404 m where gas hydrates were recovered. According to the proposed classification system, increases in heavier excluded components above the gas balance at this point signify decreasing gas hydrate content of the sediment. The data point from 414 m subbottom corresponds with a gas mixture which the DSDP staff contended indicated a lack of hydrates. On Figure 25 it can be seen that the change in the gas ratios is small in going from 404 to 414 m. In keeping with the proposed detection method, a value of 3.0 would thus correspond to the transition from free gas to gas hydrate in the sediment. If so, the cores at 358 and 363 m which show ratio values less than 3 should, by extension, contain hydrates. Also using this threshold value, the projected hydrated zone from 190 to 345 m would be reduced to occupying the interval between 203 to 328 m, a reduction of 60% over the proposed extent of hydrated sediments.

An alternate approach yields similar observations. If we assume the validity of all of the stated zones of hydrate development except for the barren zone at the bottom of the hole, a gas ratio of about 4 would mark the break between hydrated and nonhydrated sediments. In this case, the zone between 345 and 391 m which was claimed to be composed of gas in a nonhydrated state would be interrupted by a hydrate zone some 20 m thick between 350 and 370 m.

In summary, our analyses of the Site 568 core gas data suggests that the contentions of the DSDP staff that discrete zones of gas hydrate development can be identified by gas variations presents some inconsistencies. If the resolution of the data is sufficient to divide the hole into the 5 zones described by the staff, then a sixth zone exists, and the boundaries are different than reported. If the validity of one of their zones of gas-free sediment (410 - 417 m) is discounted, then the proposed zone boundaries can

be maintained. However, the hydrated zone between 350 and 370 m must be recognized in this case also. These inconsistencies suggest that the core gas data does not have sufficient reliability as a measure of gas hydrate presence to be routinely applied.

It is possible, indeed likely, that much of the fluctuation ascribed to gas hydrate presence may be due to normal stratal variation in diagenetic gas composition.

Pore water at Site 568 decreased in both salinity and chlorinity with depth. Both salinity and chlorinity decreased rapidly for the first 160 m at which point the chlorinity began to increase and salinity leveled out. Salinity and chlorinity reached a local maximum of 23.1 and 13.3 ppt respectively at a depth of two meters. These two indices again decreased regularly to values of 19.8 and 11.4 ppt at a depth of 337 m. A rather sharp rise in both salinity and chlorinity to 23.1 and 13.4 ppt at 374 m was followed by a drop of both values to the lowest values recorded for this core at a depth of 404 m. At this depth, which coincides with the observed gas hydrates, the salinity was measured at 17.3 ppt and the chlorinity at 9.54 ppt. The measures increased again to 18.7 and 10.6 ppt respectively at a final depth of 414 m.

The pore water data show some similar patterns to the core gas data. The common general trend to lower values of both chlorinity and content of heavy hydrocarbons with depth is displayed in Figure 26. A distinct similarity is found from 339 m to 414 m depth. The detailed graph of this zone shown in Figure 26B shows a nearly identical pattern in both the chlorinity and heavy alkane plots if intermediate data points at which no water analysis data are available are ignored. From a moderately low value at 339 m, the plots increase to a relative maximum at 374 m before dropping again at 404 m in depth corresponding with the zone of recovered gas hydrate. Both curves then increase sharply to 414 m. The water data appear to corroborate the published conclusions derived from gas analyses. The greater distance between the water samples may have obscured the possible gas hydrate horizon at 350 m which we suggested may exist, in our above discussion on core gases. The indication is that in the bottom 80 m of the hole chlorinity and heavy isomer ratios are both independently measuring the same phenomenon or process, probably gas hydrate presence.

Further up the hole, large differences in magnitude and degree of response are seen for the salinity and heavy isomer ratio plots (Figure 26A). The most profound disparity occurs at 160 m, where a local high in hydrocarbon content coincides with a local low in salinity. At 220 m depth a local high in chlorinity occurs simultaneously with a value of heavy isomers which is lower than that measured at 404 m depth where gas hydrates were recovered.

On a larger scale some other differences are seen. One substantial contrast between the two proposed geochemical indices of gas hydrate presence exists at the depth at which the gas hydrate sample was recovered at Site 568 (404 m). At this depth, the chlorinity is at its minimum for the entire hole. However, the depth of proven hydrate occurrence corresponds to only a local minimum in heavy hydrocarbon ratio (Figure 26). By extension it is apparent that the two indices suggest two different modes of gas hydrate distribution. The chlorinity profile suggests that the degree of hydrate development increases in a generally linear relationship with depth. The hydrocarbon profile suggests that the hydrate distribution is largely bimodal, with no hydrates above 200 m and varying amounts at greater depths.

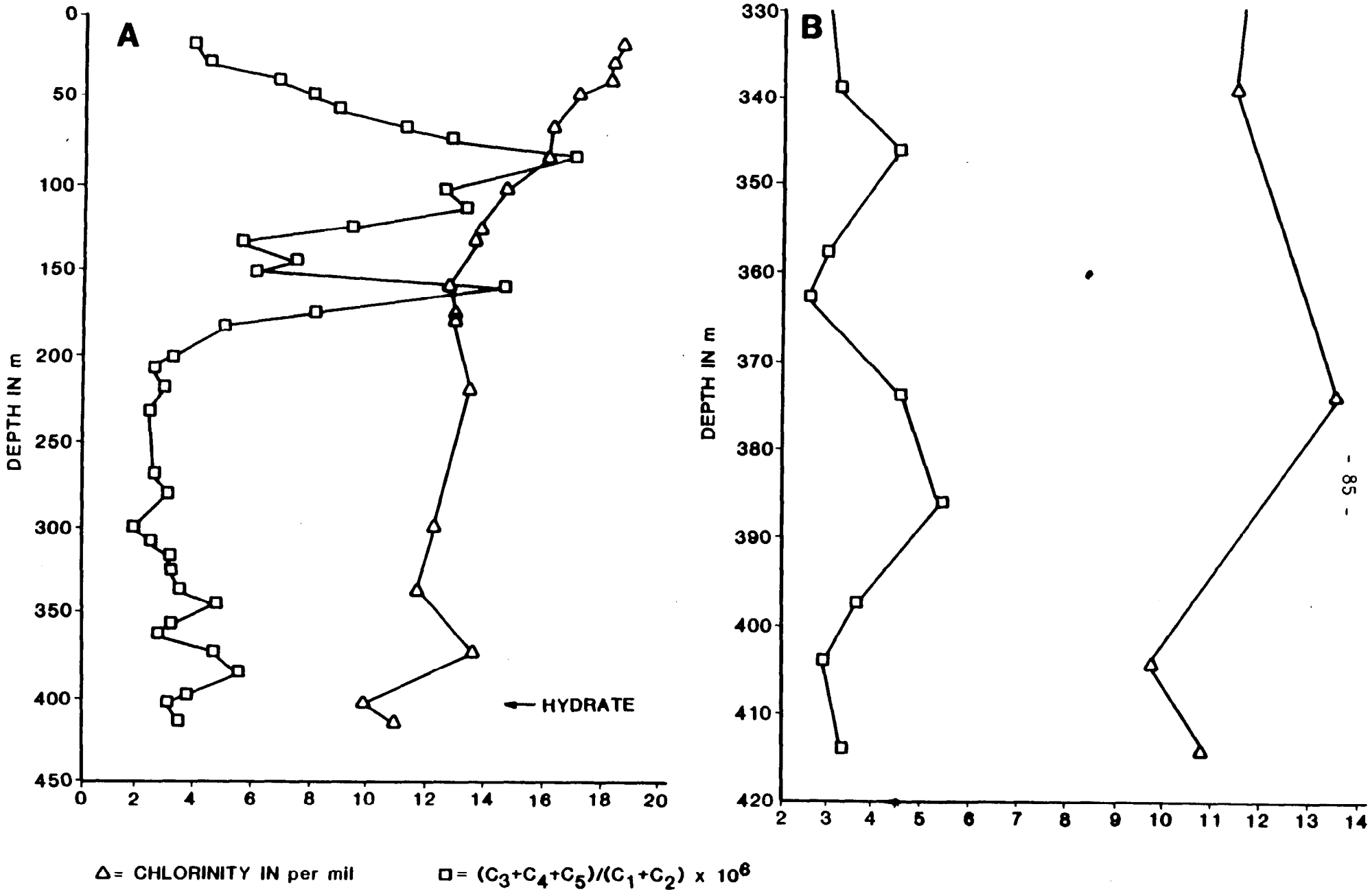

Figure 26. PORE WATER CHLORINITY AND RATIO OF HEAVY TO LIGHT HYDROCARBONS IN CORE GASES FROM DSDP SITE 568

The grossly bimodal character of the hydrocarbon index may be a manifestation of the unconformity. It is perhaps therefore indicated that the fluctuations of the Quaternary section (about 190 m to the sea floor) and the Miocene section (417 to about 190 m) should be considered separately. The small-scale fluctuations in the hydrocarbon ratio may convey much useful information on gas hydrate presence. However, the general trend of increase between 200 m and 400 m may reflect an increase in the background of the heavier hydrocarbon content as a simple result of the increasing degree of diagenesis with depth. This approach may explain the close agreement between pore water and hydrocarbon ratios over short distances near the recovered hydrate and their divergence at other depths.

The possibility that the dissimilarity of the large-scale trend of the salinity curve and the hydrocarbon ratio curves between 200 and 420 m is due to an increase in the hydrocarbon background with depth can be explored by simple modeling. The assumption upon which such a model would be based is that the changes in levels of hydrocarbons heavier than ethane that were measured in core gas from these depths is due to two processes. Gas hydrate formation excludes these molecules; thus the levels of these gases in cores containing gas hydrates are diminished by the diluting effect of dissociated hydrate gas. However, the content of heavier alkane gases in the pore water should generally increase with depth regardless of whether gas hydrates are present in situ or not. Since the measured data reflect these two independent factors, it should be possible to filter out the effects of one by numerically simulating the process and subtracting its contribution from the observed values. The values so obtained should then reflect only the effect of the remaining process. Since the effect of hydrate presence on gas content is being sought, the contribution of increasing depth will be modeled.

Two scenarios will be modeled. One is an assumption that the heavy hydrocarbons increase linearly with depth. The other assumes that the logarithm of the hydrocarbon ratio is proportional to depth, similar to the trend typically seen in methane to ethane ratios from other DSDP sites (Claypool et al., 1973; Claypool and Kvenvolden, 1983). Since gas hydrates were recovered from only one interval, both models use pore water chlorinity as an indicator of gas hydrate presence as proposed by Hesse and Harrison (1981). Although the relationship of pore water chlorinity to hydrate presence has not been proven, it is widely regarded as an accurate indicator (Kvenvolden and Claypool, 1985).

The linear model was developed by assuming that the mean increase in the hydrocarbon ratio between 200 and 420 m is due to increased background concentrations. The mean increase in the interval was approximated by constructing a line of best fit on the graph of the hydrocarbon ratio vs. depth. The line was drawn by a least-squares line fitting program and independently by manual estimation. Both methods produced a general trend of a two-unit increase in the hydrocarbon ratio per 170 m depth increase. Upon subtracting this general rise from the hydrocarbon ratio, a plot is obtained which, within the assumption of the model, should show only the fluctuation due to dilution by hydrate gases. This plot shows a much better agreement with the chlorinity plot (Figure 27). Most specifically, the data point at 404 m corresponding to the depth of recovered gas hydrate has the lowest value of the interval, completely in accordance with the chlorinity plot. The local minima in the linear model curve at 300 and 363 m are still apparent, but they are shifted to values above that at which recoverable hydrates are indicated, again in agreement with the chlorinity curve.

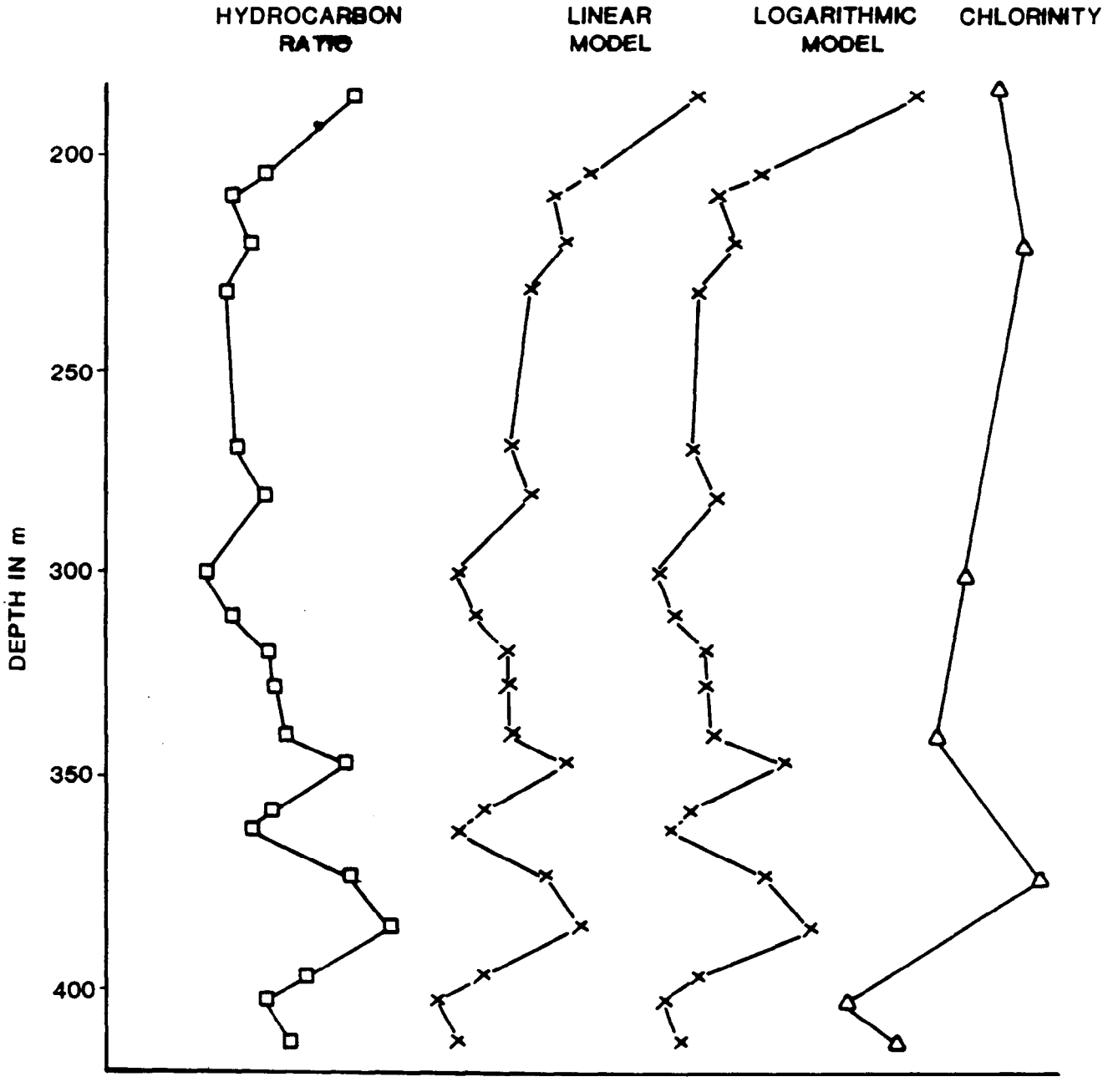

Figure 27. RESULTS OF COMPENSATION OF HEAVY HYDROCARBON RATIO OF DSDP SITE 568 FOR DOWNHOLE DIAGENETIC GAS BUILDUP

The logarithmic model operates on the assumption that the log of the hydrocarbon ratio increases with depth. The resulting plot (Figure 27) strongly resembles that from the linear model, but the calculated increase in background hydrocarbon levels is less in the logarithmic model. As a result, the general downward trend observed in the plot of the linear model is not as marked in the logarithmic example. As a result of this, the local minima on the curves at 300 and 363 m should correspond to gas hydrate intervals since the hydrocarbon ratios at these points are of the same magnitude as at 404 m depth where gas hydrates were recovered.

In summation, these modeling exercises show that core gas data can yield very similar patterns to those seen in interstitial water chlorinity data. The recovery of gas hydrates at 404 m depth at Site 568 where both the interstitial water chlorinity data and the modeled hydrocarbon ratio data achieve distinct minima suggest a consistency among indices. It is not proposed that the elementary model of hydrocarbon background developed above is a realistic approximation of subsea conditions or that it has wide applicability. The model was presented to illustrate that many factors other than gas hydrates can affect geochemical parameters. By careful analysis of data from many sources, geochemical parameters can yield useful information. The analyst must be cognizant of the effect of geological factors on the geochemical indices, eg. a major unconformity at 190 m at Site 568 where a major change in the hydrocarbon index occurs. In short, the geochemical data from DSDP holes may yield powerful indicators of hydrate presence, but changes due to factors other than hydrates must be detected and compensated for prior to routine use of these data for prediction. The proportion of methane and heavy hydrocarbon in core gas does not reliably correlate with gas hydrate presence as was proposed by von Huene et al. (1985) and Kvenvolden and McDonald (1985).

The gases and pore water from Site 568 were analyzed for isotope distribution by at least five groups. Core gases were analyzed for ^{13}C content of methane by Jeffrey et al. (1985). Isotopic analyses were also performed on carbon dioxide, when sufficient quantities were available for determination. Claypool et al. (1985) independently analyzed core gas for ^{13}C content of methane and carbon dioxide where concentrations were sufficient. Core gas methane was analyzed for D (deuterium) content. Claypool et al. (1985) also analyzed pore water for ^{13}C content of the total dissolved carbonate fraction (ΣCO_2) and ^{18}O content. Galimov and Shabaeva (1985) reported the results of ^{13}C determinations for methane and carbon dioxide from core liner gas pockets.

The isotopic values for methane obtained by the three groups agree closely. The depth profile of the methane carbon isotope values defines a smooth sigmoidal profile of increasing ^{13}C content with depth (Figure 28). The rate of increase of $\delta^{13}C$ values becomes greater in the interval of 150 to 220 m depth (cores 16 - 25) roughly corresponding to the early Pliocene to Pleistocene unconformity.

The methane in the lower 100 m of the hole (cores 35 - 45) is abnormally heavy for continental slope sediment gas. The $\delta^{13}C$ values of the gas in this interval average -44 per mil. These values are typically associated with thermogenic gas (Schoell, 1984). However, the core gas is almost entirely methane which argues against its thermal origin.

The isotopic values reported for carbon dioxide show discrepancies similar to those noted in the Site 565 data (Figure 29). The values reported by Claypool et al. (1985) and Jeffrey et al. (1985) are in fairly good agreement, but the values reported by Galimov and Shabaeva (1985) are much

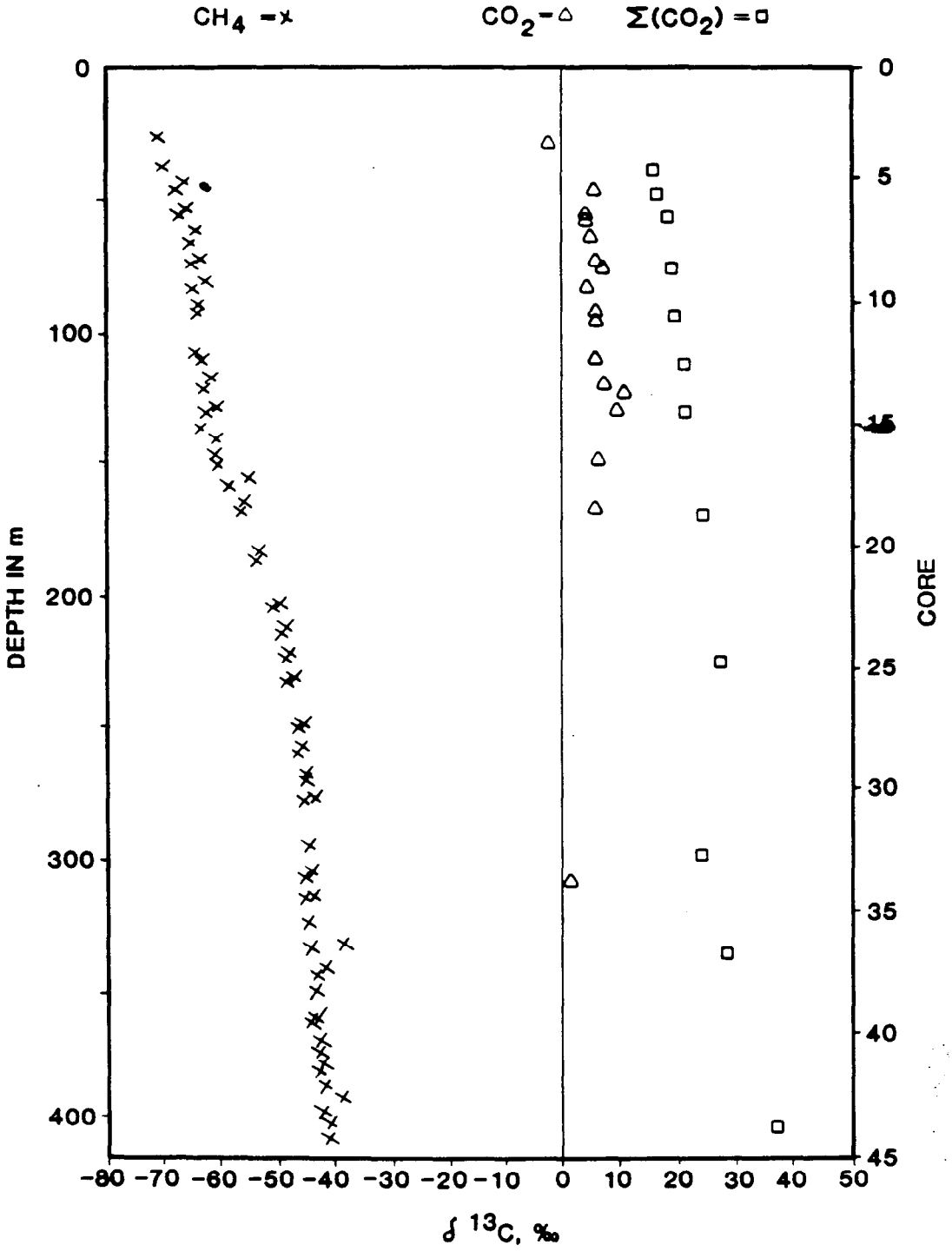

Figure 28. CARBON ISOTOPE VALUES FROM DSDP LEG 568

After Claypool et al., 1985, Galimov and Shabaeva, 1985, and Jeffrey et al., 1985

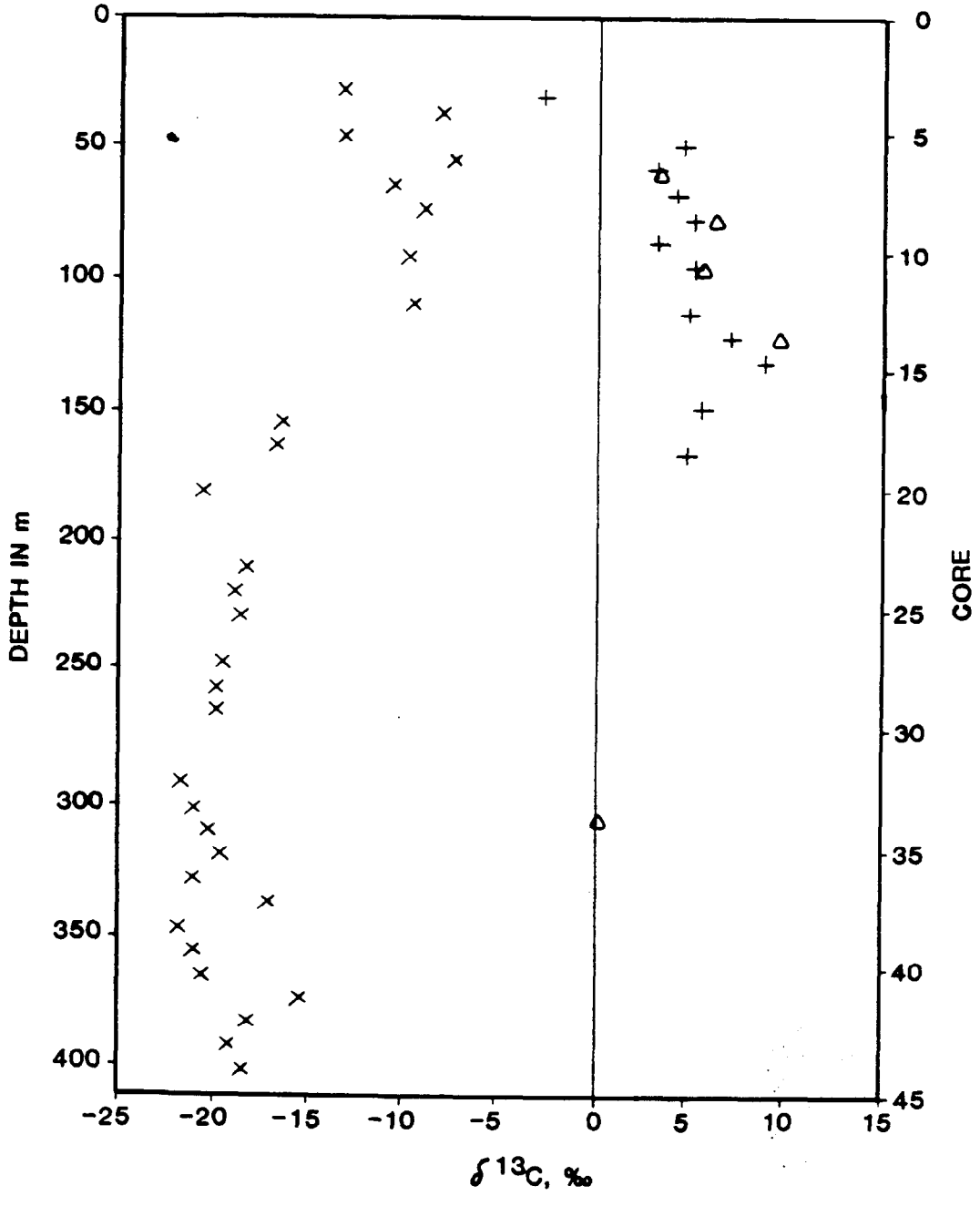

Figure 29. DISCREPANCIES IN REPORTED ISOTOPIC VALUES FOR CARBON DIOXIDE AT DSDP SITE 568

Data from Galimov and Shabaeva, 1985 (×), Jeffrey et al., 1985 (+), and Claypool et al., 1985 (△)

lighter, averaging 15 to 20 per mil more negative than measurements by the other analysts on corresponding cores. The general trend noted in all data sets is a broad maximum in the 50 to 150 m interval with a marked trend toward lighter values at greater depths.

The $\delta^{13}C$ values for the total carbonate fraction of the pore water increase with depth in a manner similar to that of the isotopic plot for methane (Figure 28). The total carbonate trend converges somewhat with the methane trend; the difference between values decreases from about 85 per mil at shallow depths to about 70 per mil near the bottom of the hole.

The trends of the carbon isotopic content of the pore water total carbonate (ΣCO_2) and the core liner gas carbon dioxide generally parallel one another to a depth of 140 m (core 15), whereupon the carbon dioxide values become lighter and the total carbonate values become heavier with depth. The mean difference between measurements from corresponding cores increases from a mean of 12 per mil from 28 m to 125 m (cores 3 to 14) to 19 per mil at 160 m (core 18), and finally 23 per mil at 299 m (core 32). This divergence of the total carbonate and carbon dioxide trends with depth from a difference of 12 per mil to a difference of 23 per mil corresponds to a decrease in total carbonate concentration in pore water from about 70 mMol/kg to 6.3 mMol/kg (Claypool et al., 1985). Thus, the degree of isotopic partitioning between coexisting carbon dioxide and dissolved carbonate (HCO_3^-) may be concentration dependent.

Site 570 was drilled on the Guatemalan continental margin beneath 1,700 m of water. The drilling location was offset 75 km northwest from the other sites of Leg 84 and Leg 67 which were tightly grouped near San Jose Canyon (Figure 13). Site 570 was located on a rise between two small canyons and 1.5 km from a large outcrop of ophiolitic basement (Volpe et al., 1985). A sedimentary section 374 m thick of Eocene to Holocene age and 28 m of serpentinite basement were drilled at Site 570.

Gas hydrates were recovered from a depth of 192 m and occurred in sediment cores from 246 m to basement (Table 7). The shallowest occurrence of hydrates was from "ash laminated with gas hydrate" (von Huene et al., 1985; Kvenvolden and McDonald, 1985). In the core descriptions the same interval was described as "Very ashy sand. Contained gas hydrate. Structureless" (von Huene et al., 1985). Hydrates were next reported from core 26 at a depth of 246 m from fractures in mudstone. In core 27, 249.1 - 258.8 m, a 1.05 m sample of massive gas hydrate was recovered. Gas hydrates were also recovered from fractures in a dolomite at the base of the massive gas hydrate interval in core 27. Cores 28 and 29 (258.8 - 268.4 m and 268.4 - 278 m) also contained pieces of gas hydrates occupying fractures in mudstone. Table 7 and the text from Kvenvolden and McDonald (1985) state that gas hydrates were also found at 303 m in core 32 and at 338 m in core 36. In the site report it was stated that all cores from 30 through 37 (278 - 354.8 m) had visible evidence of gas hydrates.

Gas concentrations. Since Site 570 had not been designated as a gas hydrate study site by the DSDP, the shipboard geochemical program was much less extensive than that at Site 568. Thus fewer data on core gas and pore water composition are available for Site 570.

Abundant hydrocarbon gases were encountered from depths of 17.5 m to 394 m. Beneath 100 m the ratio of methane to ethane diminished smoothly to a depth of 246 m. The methane to ethane ratio remained in the 400 to 450 range to a depth 274, whereupon it increased to 1,900 at 317 m. Below

this depth the methane to ethane ratio dropped rapidly to 80 in the fractured serpentinite basement at 394 m.

The zone of ethane enrichment between 246 and 284 m corresponds to depths at which the best developed gas hydrates were found. At 246 m, where the methane to ethane ratio was measured to be 400, gas hydrates were recovered from fractures in mudstone. A ratio of 431 was obtained from the massive gas hydrate at 250 m. The depth of 267 m at which a methane to ethane ratio of 410 was recorded, as well as 274 m with a ratio of 450 correspond to zones with well developed gas hydrates.

The gas hydrates which were found in this 40 m zone of ethane enrichment are different from the other hydrates found at Site 570. The hydrates between 247 and 274 m are of two types: massive, or fracture-filling. The other occurrences of gas hydrates at Site 570 were hosted in volcanic ash (192 m, 303 m) or feldspathic sand (338 m). The sand- and ash-hosted hydrates were developed in the interstitial spaces of the sediment.

With such a marked increase in ethane content corresponding to the zone of well developed gas hydrates, examination of the abundance of hydrocarbon gases heavier than ethane is warranted. Since ethane is incorporated into the gas hydrate lattice, it is possible that such an increase in ethane content of the core gas through the hydrated zone is merely a consequence of gas hydrate presence. If the high ethane values were due to selective inclusion of ethane into hydrates followed by dissociation of hydrates, then the heavier gases which are excluded from the hydrate lattice should remain at background levels or decrease in abundance due to dilution in the hydrated intervals as was proposed for Site 568.

Hydrocarbons heavier than ethane also show dramatic enrichment in the zone of extensive hydrate development (Figure 30). Propane content rises to over 40 times the mean background value for the preceeding 230 m. Similarly large increases are seen in the measured abundance of both butane isomers and pentane as well. The increase is greatest at a depth of 246 m in core 26. The enrichment in heavier hydrocarbons decreases regularly with depth, returning to the background level by 302 m in core 32.

The enrichment of heavier hydrocarbons near the massive gas hydrate zone at Site 570 does not agree with the method proposed by Leg 84 scientists for identifying gas hydrate zones based on the Site 568 data. It was proposed that cores in which propane, butane, and pentane were depleted relative to typical values could be inferred to contain gas hydrates due to the dilution effect of dissociating methane hydrate on measured gas content. The relationship between proven gas hydrate presence and heavy hydrocarbon content at Site 570 is directly opposite of that proposed for Site 568; the best developed gas hydrates at Site 570 were found in intervals with the highest proportion of heavier hydrocarbons. This indicates that direct correlation of gas hydrates with intervals of heavy hydrocarbon depletion as proposed by Kvenvolden and McDonald should not be routinely applied.

Depletion of heavier hydrocarbons in hydrated sections did occur at Site 570, but its effect was overwhelmed by core gas which was unusually enriched in heavier hydrocarbons prior to gas hydrate formation. In each case for which gas analyses of recovered gas hydrates were reported, the hydrate was depleted in propane, butane, and pentane relative to the gas in surrounding sediment. This relationship is prevalent for the three types of gas hydrates encountered at Site 570. Figure 31 illustrates the relationship between relative gas distribution of the gas hydrate hosted in a volcanic ash layer in core 21 and gas from nearby cores. The graph shows that all measured

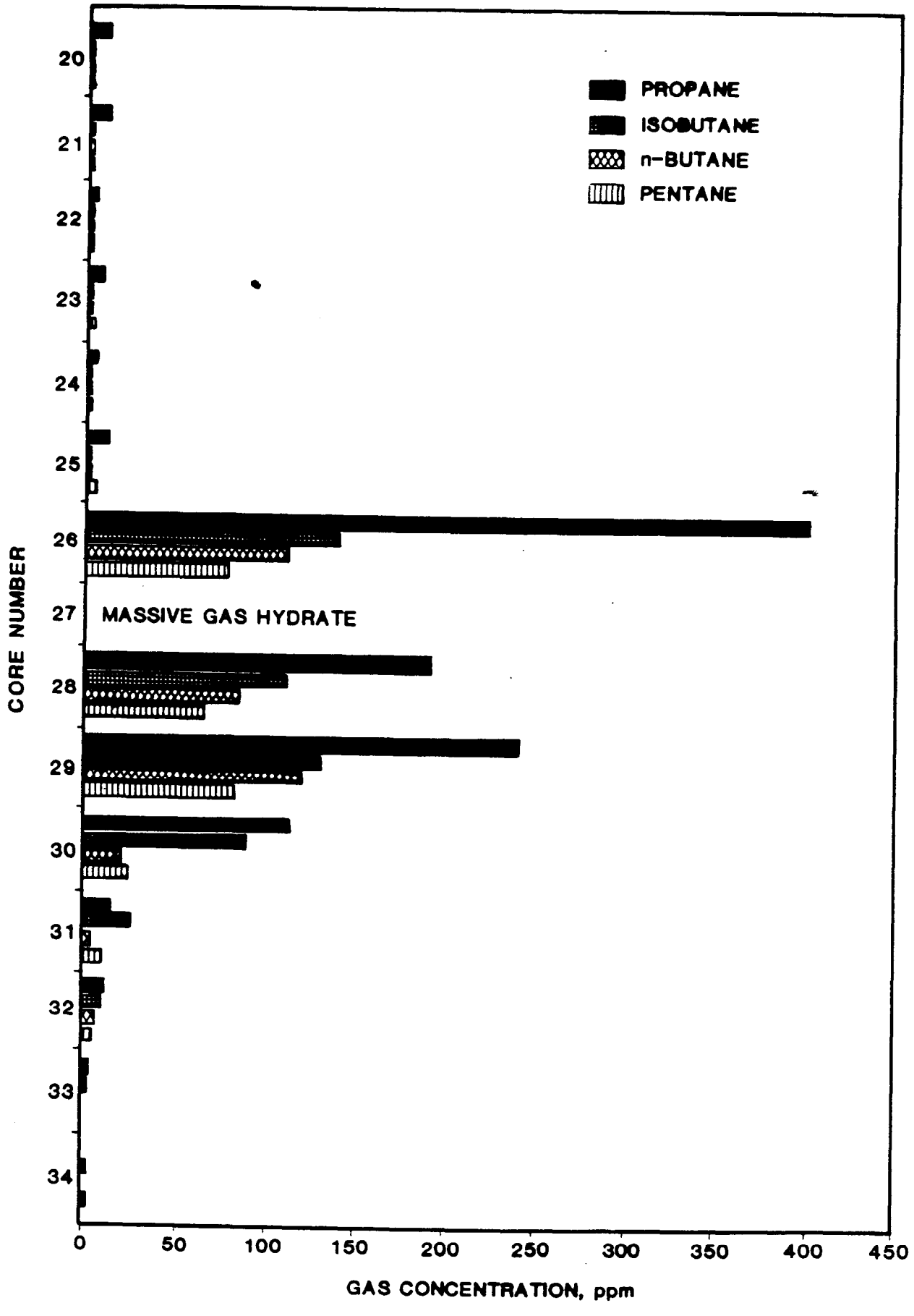

Figure 30. PROPANE, BUTANE, AND PENTANE CONTENT OF CORE GASES NEAR MASSIVE GAS HYDRATE AT DSDP SITE 570

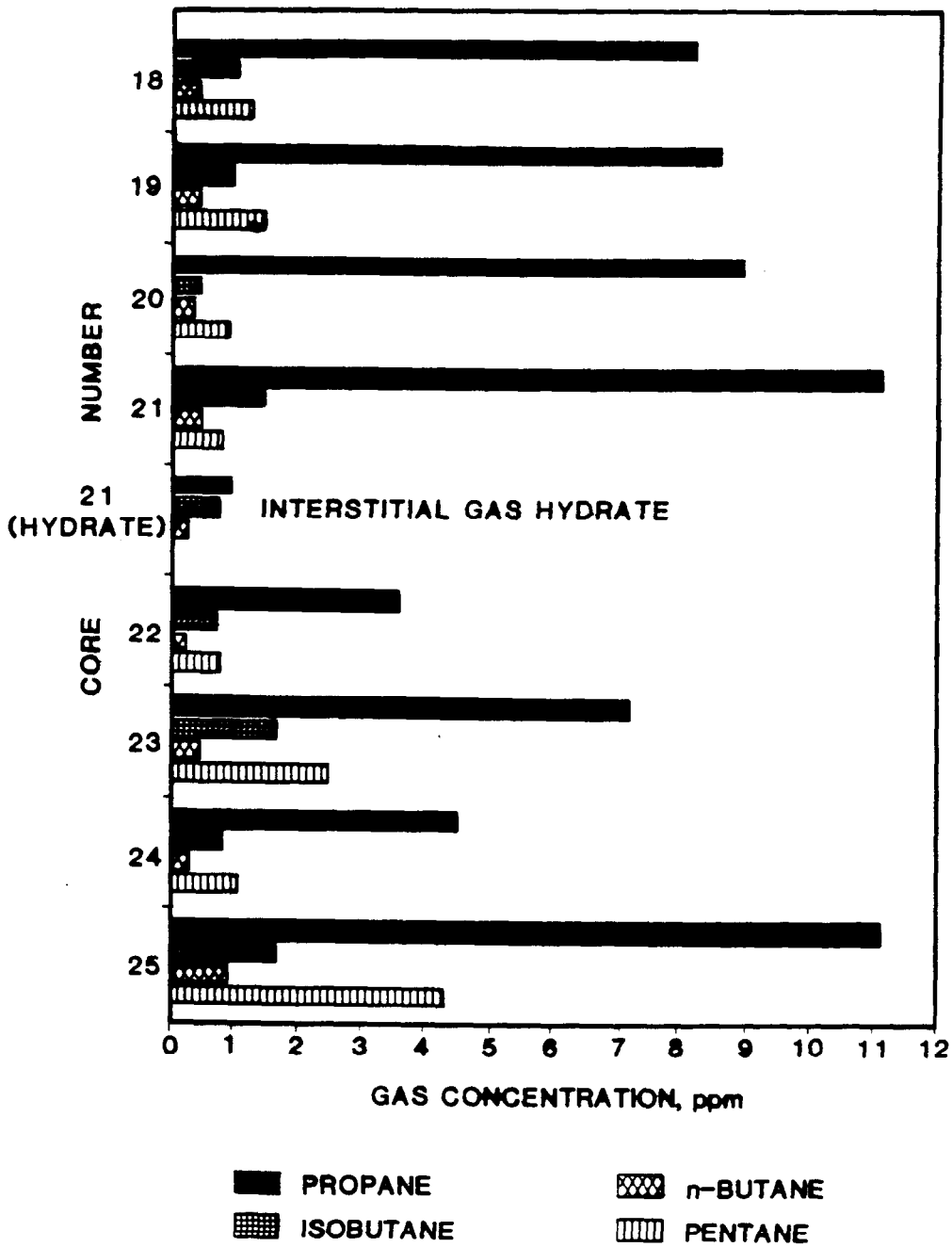

Figure 31. COMPARISON OF PROPANE, BUTANE, AND PENTANE CONTENT OF INTERSTITIAL GAS HYDRATE AND SURROUNDING SEDIMENTS AT DSDP SITE 570

hydrocarbons from propane to pentane are depleted in the hydrate. Propane and pentane are the most depleted of the gases measured. Propane is present in the gas hydrate at 10% to 30% of its abundance in nearby cores. Pentane isomers are absent in the gas hydrate, but present at levels averaging 1 ppm in the sediment cores. In contrast, the butane content of the gas hydrate is very similar to or greater than that in nearby cores. As seen in Figure 31, both butane isomers are present in the gas hydrate sample at levels which approximate the mean of the nearby sediment cores. In fact, the isobutane content of the gas hydrate is greater than in both cores 20 and 22. The n-butane content of the gas hydrate in core 21 is greater than that of core 22. However, the gas hydrate from core 21 is lower in abundance of both isomers than the core gas from the same core.

In interpreting these values for the hydrocarbon content of these cores, caution should be used when addressing the propane through pentane values. The absolute amounts of each substance are so small (0.2 to 2 ppm) that differences in reported values may reflect instrumentally or procedurally induced scatter rather than significant differences.

The abundance of the heavier hydrocarbons is one to two orders of magnitude greater in core gas and hydrate gas samples from the 246 to 289 m interval than in core 21. Thus the hydrocarbon distributions of the 246 to 289 m interval are likely to be more significant than at the shallower levels.

Propane content of both the massive gas hydrate (core 27) and the fracture-filling gas hydrate (core 28) are lower than in adjacent sediment cores. The massive gas hydrate contains 20 to 40% of the propane of nearby core gas. Propane depletion is greater for the fracture-filling gas hydrate from core 28, with the hydrate gas containing 5 to 8% of the propane found in nearby cores.

The contents of isobutane, n-butane, and pentane all show patterns similar to propane in the 246 - 289 m interval (Figure 32). Once again, the massive hydrate gas from core 27 contains 20 to 40% of the measured gases compared to subjacent and superjacent sediment core gas (cores 26 and 28). The fracture-filling hydrate gas from core 28 contains 5 to 10% of the butane and pentane found in sediment gases from surrounding cores.

The ratios of butane isomers from the 246 - 289 m interval display a trend which is opposite of that expected if structure II gas hydrates were present in the hydrate samples recovered from cores 27 and 28. As Figure 32 illustrates, isobutane is present in lesser amounts than n-butane in the gas hydrates from cores 27 and 28. However, the core gas from cores 26, 28, 29, and 30 all contain significantly more isobutane than n-butane. This gas abundance pattern is enigmatic. If the gas hydrate samples contained structure II hydrates, the hydrate gas would be expected to be enriched in isobutane relative to the core gas in surrounding sediments. Instead, the hydrate gas is depleted in both butane isomers but more so for isobutane.

The concentrations of propane, butane, and pentane in the massive gas hydrates from core 27 and the fracture-filling gas hydrates from core 28 are 10 to 100 times those found in core gases or gas hydrates from depths outside the 246 m - 289 m interval. The consistently high contents of these heavier hydrocarbons in the gas hydrates from cores 27 and 28 are particularly puzzling because the molecular sizes of these gases are too large to fit in the structure I gas hydrates, which these hydrates appear to be. Although the presence of structure II gas hydrates is not supported by the available data, invoking their existence could not completely eliminate the enigmatic enrichment in heavier hydrocarbons of the massive and fracture-filling gas

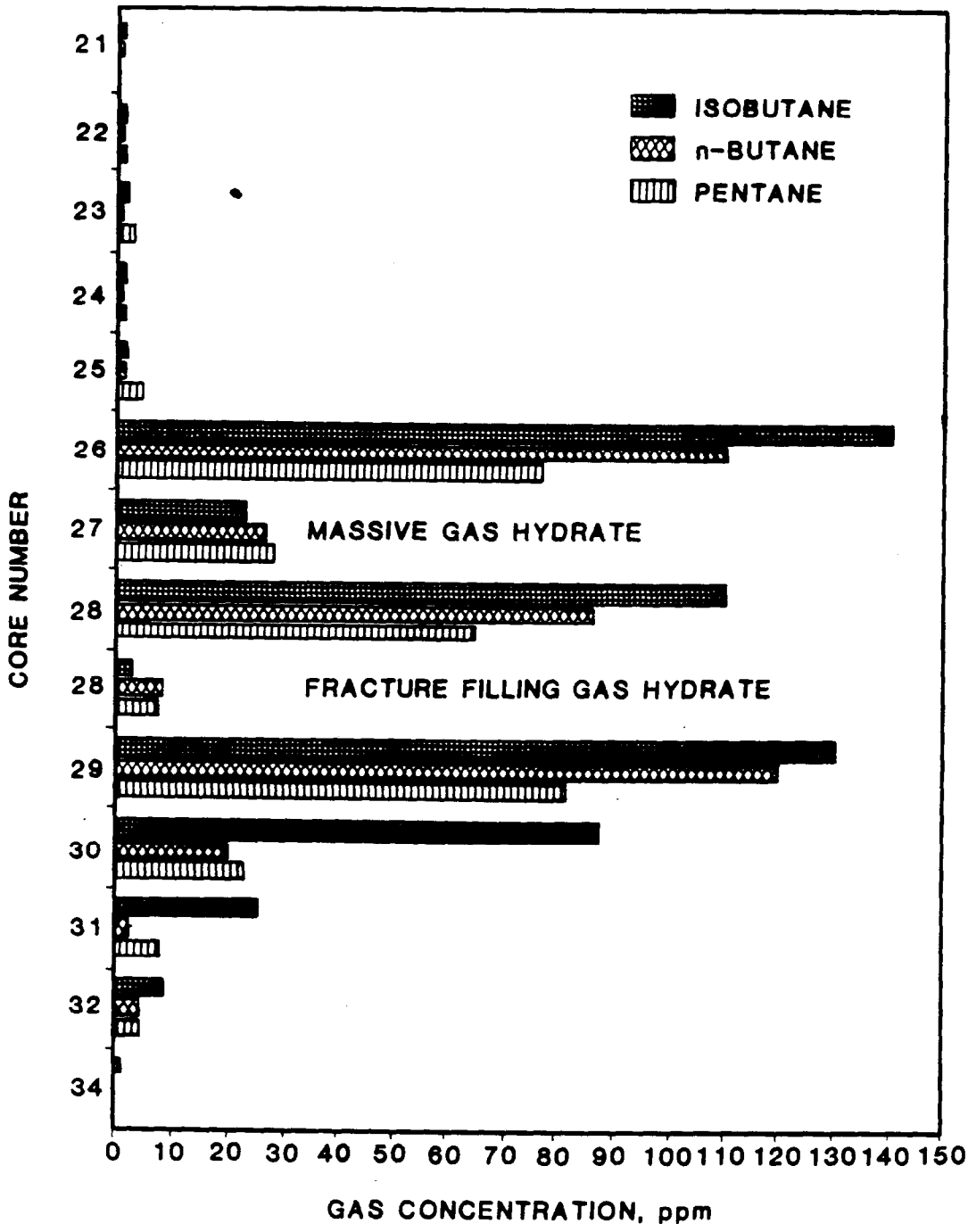

Figure 32. COMPARISON OF ISOBUTANE, n-BUTANE, AND PENTANE CONTENT OF MASSIVE GAS HYDRATE, FRACTURE FILLING GAS HYDRATE, AND SURROUNDING SEDIMENTS AT DSDP SITE 570

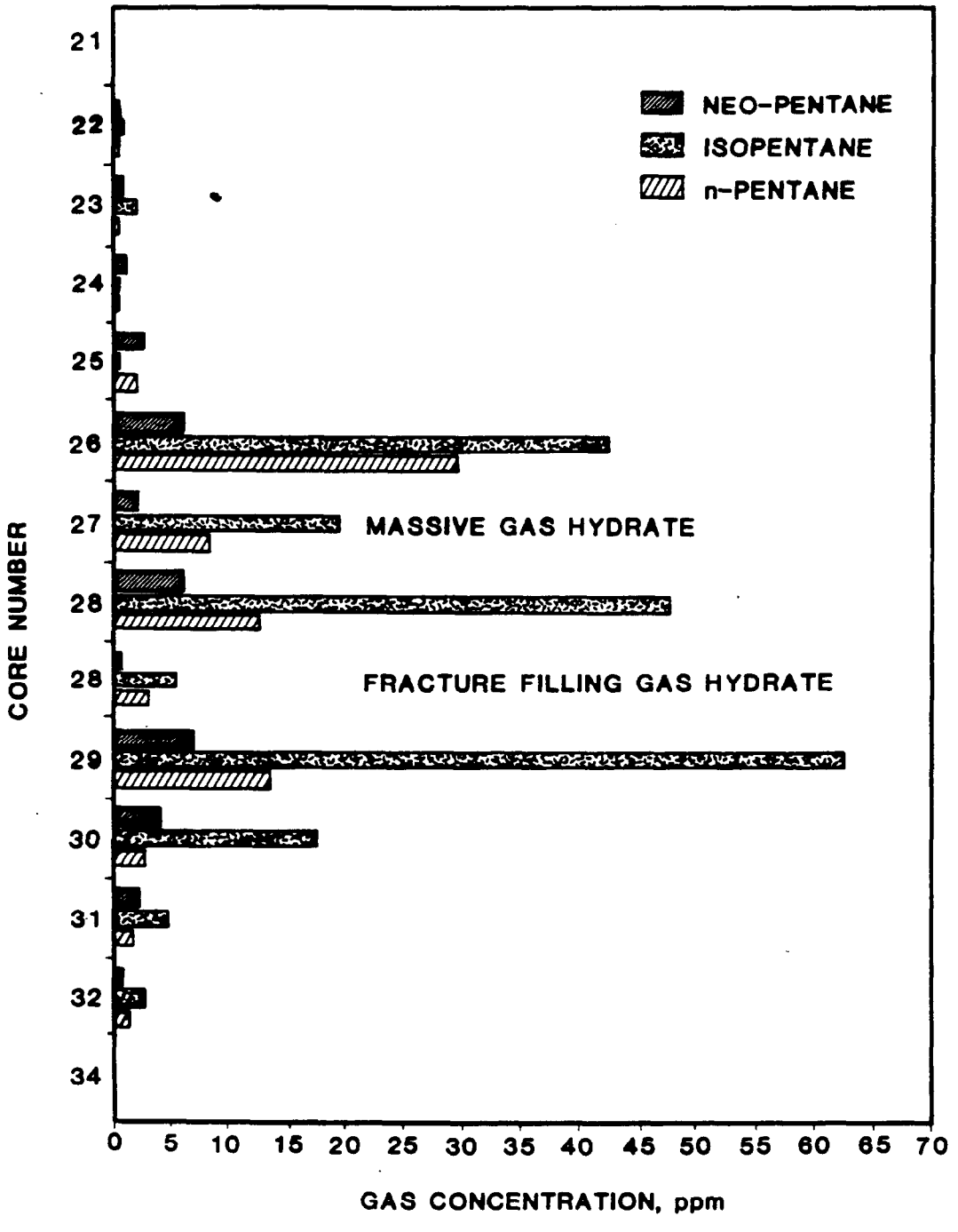

Figure 33. COMPARISON OF PENTANE ISOMER CONTENT OF GAS HYDRATES AND SURROUNDING SEDIMENTS AT DSDP SITE 570

hydrates. Neither n-butane nor any pentane isomers can form structure II hydrates, yet these hydrocarbons are present in the gas hydrates in large quantities. The bar graph in Figure 33 demonstrates not only the high concentrations of pentane in the 247 - 289 m (core 26 - 31) interval, relative to the rest of the hole, but also the close match of the pentane isomer composition of the gas hydrates to that of the nearby core gas.

These composition data suggest that the gas hydrates recovered from core 27 and 28 contain significant amounts of occluded core gas trapped within the hydrate mass, but not within the gas hydrate lattice. These gases which cannot be part of the gas hydrate lattice due to size constraints could be trapped within sediment which was present in the gas hydrate samples recovered. Another possibility is that the nonhydrated gas was present as gas pockets and/or dissolved in physically trapped pore water. Upon dissociation the gas hydrate samples from cores 27 and 28 produced only one-fifth of the gas expected from an ideal hydrate 90% occupied with gas (Kvenvolden and McDonald, 1985). This may be supportive evidence that the recovered gas hydrates were composed of gas hydrates which trapped free gas bubbles or gas-rich pore water. The much smaller expansion expected for these non-hydrated gas sources within the gas hydrate samples would lower the overall volumetric yield of gas when the mass was melted. The gas resulting from such a mix of hydrate and occluded gas and water would be expected to contain diminished, yet significant amounts of pore water hydrocarbon constituents which cannot form gas hydrates.

Davidson and Ripmeester (1978) have claimed that, contrary to generally accepted assumptions, n-butane and neo-pentane do form structure II hydrates. However, the abundance of isopentane and n-pentane in the gas hydrate samples from cores 27 and 28 (Figure 34) demonstrate that even if n-butane and neopentane are present as hydrates, the hydrates still contain appreciable amounts of nonhydrated trapped gas.

In summary, a comparison of gases from gas hydrate samples recovered at Site 570 with gases from surrounding cores shows that gases from hydrates are depleted in hydrocarbons heavier than ethane. The interval in which the massive and fracture-filling gas hydrates occur (246 - 289 m) was found to host sediment gases and hydrates which had very high concentrations of these heavier hydrocarbons. The enrichment in the heavier hydrocarbon gases of both cores and hydrates in this interval was of such magnitude that the gas from the hydrates was significantly richer in propane, butane, and pentane than core or hydrate gases from elsewhere in the hole. This relationship in conjunction with the mode of gas hydrate occurrence indicates that the gas hydrates from cores 26, 27, 28 and 29 are genetically related to the core gases from the same intervals. These core gases, and thus gas hydrates, are much different from gases and hydrates elsewhere in the hole. These observations raise the possibility that the gases from the 246 - 289 m interval have migrated to their present location.

Isotopic Data. The gases and pore fluids from Site 570 were analyzed for isotope distribution by at least five groups. Core gases were analyzed for ^{13}C content of methane by Jeffrey et al. (1985). Isotopic analyses were also performed on carbon dioxide, ethane, propane, and butane when sufficient quantities were available for determination. Claypool et al. (1985) independently analyzed core gas for ^{13}C content of methane and carbon

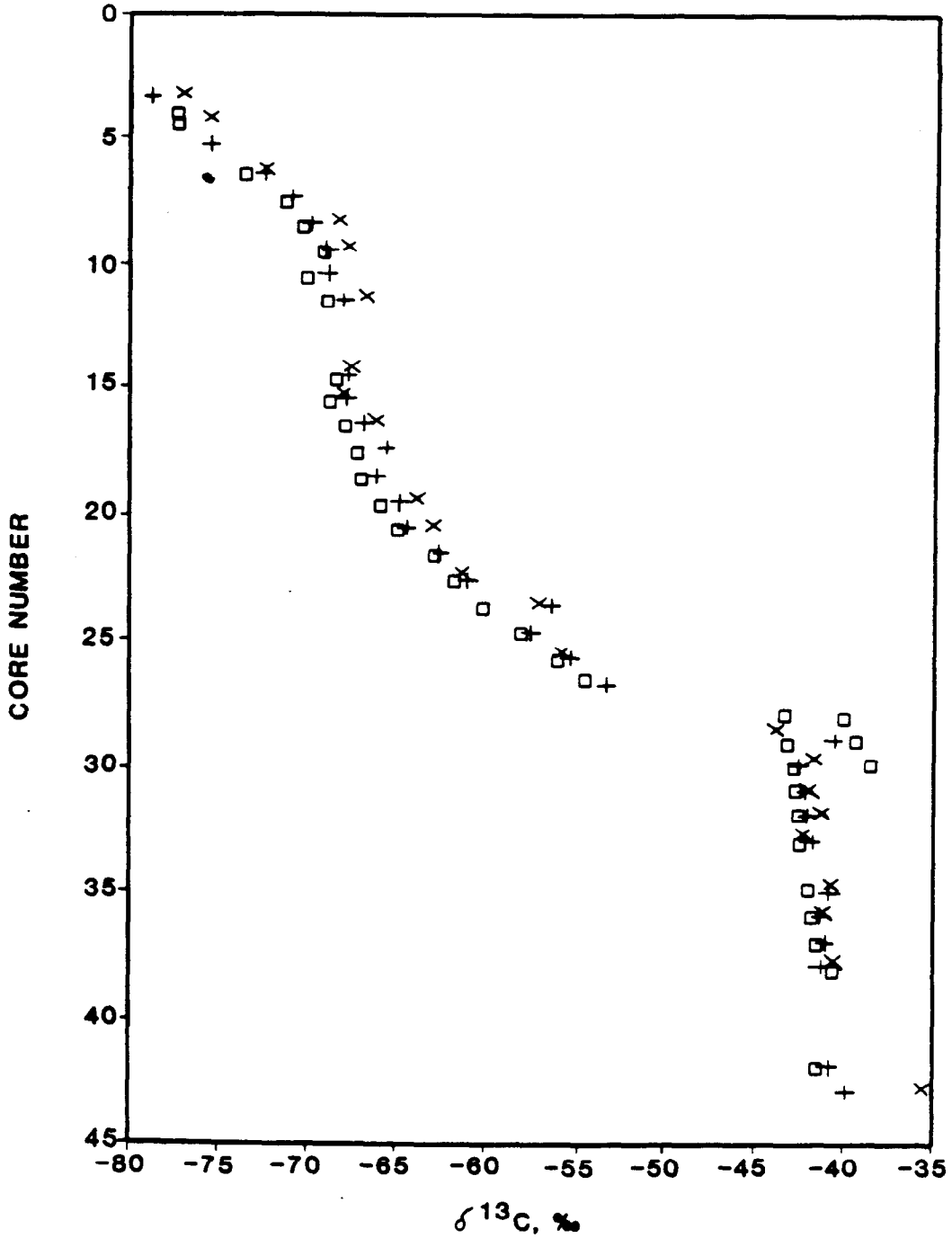

Figure 34. CARBON ISOTOPE CONTENT OF METHANE FROM DSDP SITE 570 CORES

Data from Claypool et al., 1985 (□), Galimov and Shabaeva, 1985 (×), and Jeffrey et al., 1985 (+)

dioxide where concentrations were sufficient. Core methane gas was also analyzed for D (deuterium) content. Claypool et al. (1985) also analyzed 10 samples of pore water for ^{13}C content of the total dissolved carbonate fraction (ΣCO_2) and ^{18}O content. Galimov and Shabaeva (1985) reported the results of ^{13}C determinations for methane and carbon dioxide from core gas samples. Kvenvolden et al. (1984) conducted ^{13}C analyses on methane derived from dissociation trials of the massive gas hydrate recovered in core 27. Brooks et al. (1985) reported $\delta^{13}C$ values for methane, ethane, and carbon dioxide of gas resulting from dissociation of the massive gas hydrate.

The $\delta^{13}C$ values for methane obtained by all the investigators agree well (Figure 34). The results of Jeffrey et al. (1985) and Claypool et al. (1985) are very close, usually within ±1 per mil. One exception occurs where Claypool et al. (1985) reported values for sections of cores 27, 28, and 29 which were not analyzed by Jeffrey et al. (1985). These values of -38 to -40 per mil are 4 to 5 per mil heavier (more positive) than corresponding values from other parts of the same cores. The values of Galimov and Shabaeva (1985) are similar, but average 1 to 2 per mil heavier than the values of Jeffrey et al. (1985). The methane from dissociation experiments of the massive gas hydrate from core 27 reported by Kvenvolden et al. (1984) and Brooks et al. (1985) vary between -39.7 per mil and -44.1 per mil, but are in agreement with the range of values for sediment gases of cores 27 and 28 as reported by Claypool et al. (1985), Galimov and Shabaeva (1985) and Jeffrey et al. (1985).

The $\delta^{13}C$ values for methane become heavier with depth (Figure 34), as often occurs in DSDP holes (Claypool et al., 1973). Values range from less than -80 per mil near the sea floor (Claypool et al., 1985; Jeffrey et al., 1985) to -36 per mil in the serpentinite basement (Galimov and Shabaeva, 1985).

One feature of $\delta^{13}C$ enrichment with depth which is seen at Site 570 is its bimodality. From the sea floor to 246 m (core 26) the isotopic values increase smoothly with depth from about -80 per mil to -55 per mil along a somewhat sigmoidal path (Figure 34). A sharp break in the trend is seen at core 27 (249 - 258 m) where the $\delta^{13}C$ value abruptly jumps to -40 to -44 per mil. From core 27 to the bottom of the hole, the isotopic values generally increase, but the rate of increase with depth is substantially less than in the first 246 m of the hole. The break in continuity at core 27 corresponds with both the zone of massive gas hydrates and with a Miocene to Pliocene unconformity estimated to span 0.5 m.y. (von Huene et al, 1985). It is interesting to note, however, that unconformities of 3, 3 and 27 m.y. occur in core 35 (von Huene, 1985), but no offset is noted in the $\delta^{13}C$ profile at 330 m (Figure 34).

Another unusual feature of the isotopic composition of methane at Site 570 is similar to that found at Site 568. The $\delta^{13}C$ values for the lowermost 150 m of the hole (cores 27 - 41, 249 - 402 m) are very heavy in comparison to typical biogenic gases cored by DSDP (Claypool et al, 1973). The reported values of -44.1 to -35.9 are in the range typical of overmature thermogenic gas (Scholle, 1983; Whiticar et al., 1986). However, the predominance of methane in this interval strongly suggests biogenic origin (Claypool et al., 1985; Jeffrey et al., 1985; Kvenvolden and McDonald, 1985).

Large discrepancies exist among the four sets of data for ^{13}C content of carbon dioxide reported for Site 570 (Figure 35). Once again the best

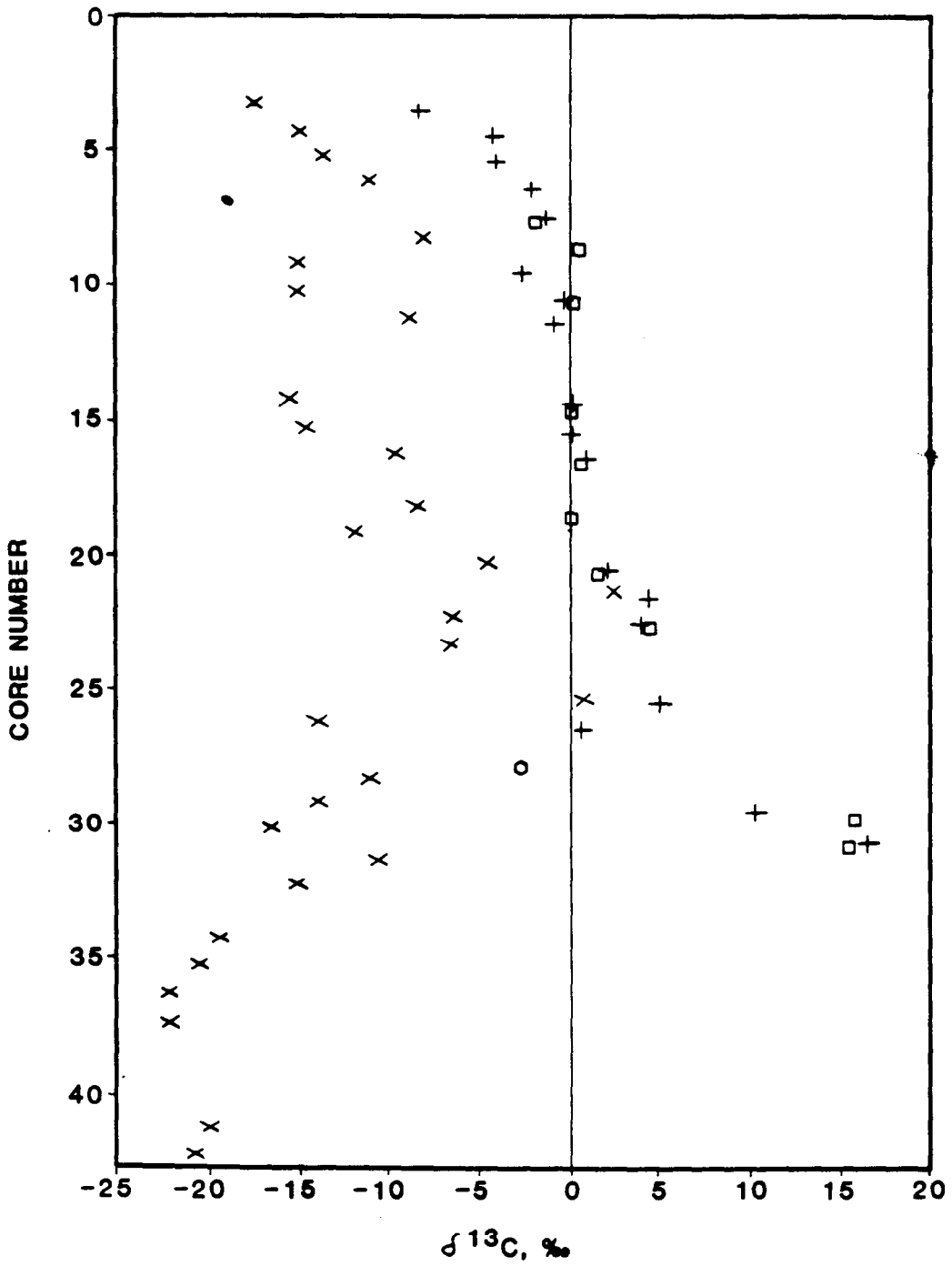

Figure 35. **CARBON ISOTOPE CONTENT OF CARBON DIOXIDE FROM DSDP SITE 570**

Data from Brooks et al., 1985 (○), Claypool et al., 1985 (□), Galimov and Shabaeva, 1985 (×), and Jeffrey et al., 1985 (+)

agreement in analytical values is among Claypool et al. (1985) and Jeffrey et al. (1985). The data of Claypool et al. (1985) average 2 per mil heavier, but the data set of Jeffrey et al. (1985) is the more extensive and includes samples from shallower than 50 m depth (cores 1 - 6) and from 246 m (core 26) which are substantially lighter than typical. Counting only the depths for which both groups analyzed samples, the mean of the values agree within 0.5 per mil.

Data on the ^{13}C content of carbon dioxide by Galimov and Shabaeva (1985) differ greatly from those reported by Claypool et al. (1985) and Jeffrey et al. (1985). Major differences are seen in the analytical values reported for each common sample and in the trend of the values with increasing depth. The mean of the $\delta^{13}C(CO_2)$ values reported by Galimov and Shabaeva (1985) is -13.2 per mil, which is 15.7 per mil lighter than the mean of the values from Jeffrey et al. (1985). Only for two cores are the values of Galimov and Shabaeva even close to those of the other two groups: with differences of 6.4 per mil at core 21 and 4.3 per mil at core 25. The trend of the data of Galimov and Shabaeva (1985) with depth roughly parallels that of Jeffrey et al. (1985) through core 25, but displays a much greater scatter between successive cores. From core 25 to core 30 (234 - 284 m) the values of Jeffrey et al. (1985) become more positive by 10 per mil. In the same interval, the data from Galimov and Shabaeva (1985) decrease by 17 per mil. Galimov and Shabaeva (1985) reported values for cores 31 - 42 which show a decreasing trend with depth (Figure 35). Jeffrey et al. (1985) stated that in these cores carbon dioxide was "not detected" or "insufficient for isotopic analysis."

Only two values were reported for $\delta^{13}C(CO_2)$ of the gas from the dissociated massive gas hydrate from core 27. Brooks et al. (1985) published values of -3.1 per mil and -2.7 per mil. Core gas analysis was not performed on the sediment recovered in core 27; the closest sediment gas analysis reported was for cores 26 and 28. For comparison, the values obtained for $\delta^{13}C(CO_2)$ of core 28 were 10.7 per mil (Jeffrey et al., 1985) and -11.48 (Galimov and Shabaeva, 1985). Core 26 yielded a value of 0.3 per mil (Jeffrey et al., 1985). Since the analyses reported by Brooks et al. (1985) were performed using methods identical to those of Jeffrey et al. (1985) and presumably the same instruments and laboratory facilities, the $\delta^{13}C$ value for the massive gas hydrate is most directly comparable to those reported by Jeffrey et al. (1985). As such, the massive gas hydrate sample contained the most isotopically depleted carbon dioxide found at Site 570 deeper than core 6 (58 m).

The sharp increase that was noted in the $\delta^{13}C$ values for methane between cores 26 and 27 is not duplicated in the carbon dioxide data. There appears to be, however a shift in the opposite sense in the carbon dioxide data sets of both Jeffrey et al. (1985) and Galimov et al. (1985)(Figure 35). In both cases a large decrease in the ^{13}C content of the carbon dioxide between core 25 and 26 is evident. The data of Galimov et al. (1985) decrease 15 per mil in this interval. The data of Jeffrey et al. (1985) show a drop of 4.8 per mil between cores 25 and 26. This interval corresponds to an increase in the abundance of propane through pentane from core 25 to core 26 of over 4,300%. In Figure 35 it can be seen that with inclusion of the carbon dioxide isotope value for the massive gas hydrate from Brooks et al. (1985) the total decrease in $\delta^{13}C(CO_2)$ values between core 25 and the hydrate is 12.1 per mil.

Only by excluding the values for cores 26 and 27, would it appear that the carbon dioxide isotopic values follow the same trend as seen in the methane data. The carbon dioxide carbon isotope value of core 28 is 6 per mil heavier than that of core 25.

Brooks et al. (1985) reported $\delta^{13}C$ values of -26.5 and -26.8 for ethane from the massive gas hydrates. Jeffrey et al. (1985) obtained $\delta^{13}C$ values of -25.7, -25.6, and -24.2 per mil for gas from cores 26, 29, and 30 respectively. These were the only sediment cores from Site 570 with sufficient ethane for confident determination. Since both groups of investigators reported an analytical precision of ±0.2 per mil, there is a significant, although small difference in the isotopic signatures of the hydrate and core gas.

This trend is analogous to that observed in carbon dioxide. The $\delta^{13}C(CO_2)$ of the massive gas hydrate represents a local minimum superimposed on a general trend of becoming isotopically heavier with depth. However, the change, although similar in direction, is much greater magnitude for carbon dioxide than for ethane.

The $\delta^{13}C$ values for the total carbonate fraction (ΣCO_2) of the pore water of Site 570 become heavier with depth, generally paralleling the carbon isotope values for carbon dioxide from the core liner gas (Figure 36). The values increase from 7.7 per mil at 31.5 m (core 4) to 37.5 per mil at 280 m (core 30) before dropping to 27.1 per mil at 337 m (core 36). It is not known whether core liner gas carbon dioxide shows a parallel shift toward lighter values between cores 30 and 36; no reliable carbon dioxide isotopic values were reported from depths greater than 280 m.

The parallel enrichment in ^{13}C with depth of methane, carbon dioxide, and total carbonate at Site 570 has been cited as evidence of a biogenic source for the methane (Claypool et al., 1985; Jeffrey et al., 1985; Kvenvolden and McDonald, 1985). Methane from both Sites 568 and 570 is unusually enriched in ^{13}C. The isotopic signature of methane from deep sediment cores and recovered gas hydrates (-39 to -45 per mil) is in the range expected for gas resulting from thermal degradation of kerogen. The high methane content in gas from these holes argues against thermogenic origin which should produce gas rich in hydrocarbons other than methane. Unusually heavy total carbonate also exists at these sites. Bacterial methane generation functions by reduction of carbon dioxide to methane. A kinetic isotope effect in the reaction produces methane which is typically about 70 per mil depleted in ^{13}C relative to its precursor carbon dioxide. The consensus among DSDP scientists is that the unusually heavy isotopic content of the total carbonate and, to a lesser extent, the carbon dioxide from these sites together with the unusually heavy coexisting methane are consistent with bacterial methanogenesis because the same 70 per mil difference is noted. This 70 per mil difference between methane and total carbonate $\delta^{13}C$ values is interpreted to indicate that the typical methanogenic processes are working on anomalously heavy substrates to produce the heavy methane.

In Figure 37 the differences among the three isotopic measurements are plotted as functions of depth. The curve farthest to the right represents the difference between total carbonate and methane isotopic values. The graph illustrates that the methane and total carbonate values tend to converge with depth, progressing from a difference of 85 per mil at 32 m (core 4) to 69 per mil at 337 m (core 36). The middle curve of the graph depicts the difference

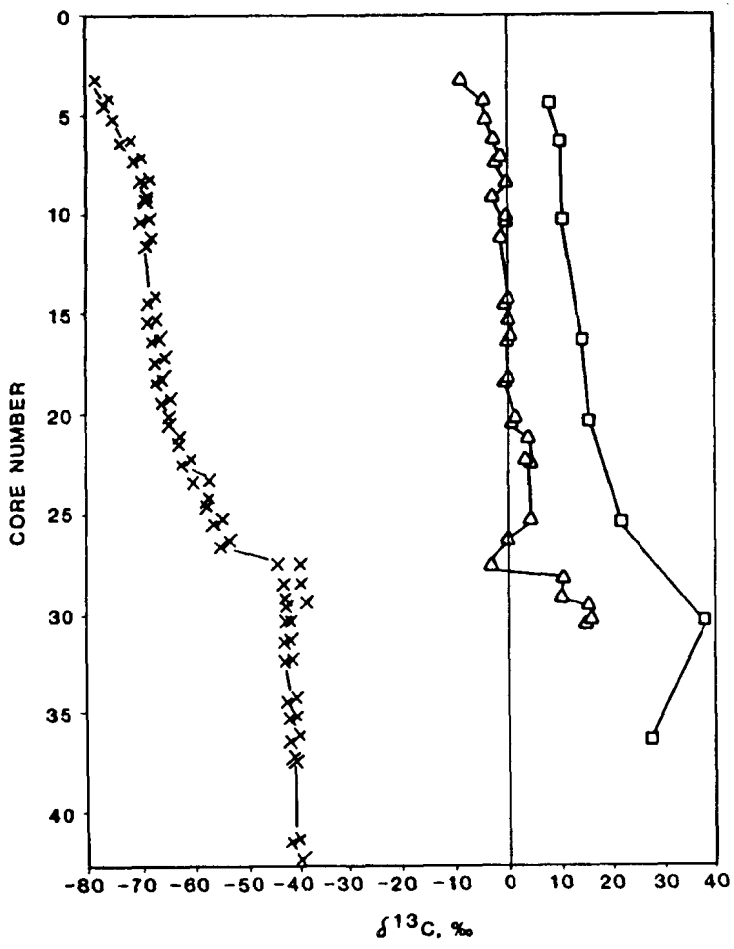

Figure 36. CARBON ISOTOPE CONTENT OF METHANE (×), CARBON DIOXIDE (△), AND TOTAL CARBONATE (□) FROM DSDP SITE 570 CORES

Data from Brooks et al., 1985, Claypool et al., 1985, Galimov and Shabaeva, 1985, and Jeffrey et al., 1985

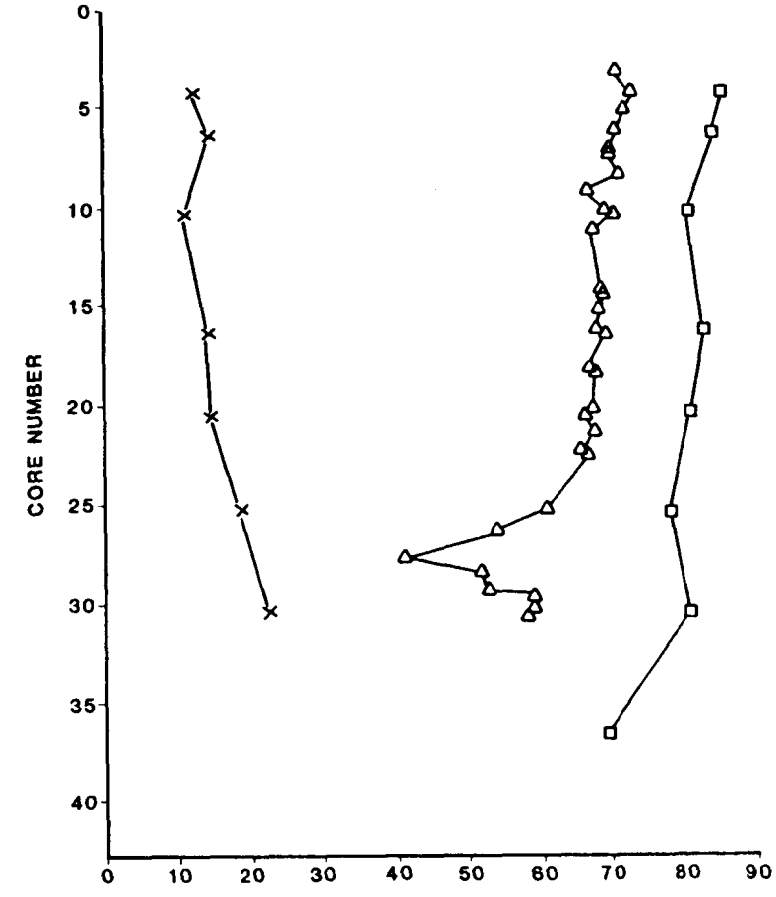

× = $\delta^{13}C(CO_2) - \delta^{13}C(\Sigma CO_2)$
△ = $\delta^{13}C(CO_2) - \delta^{13}(CH_4)$
□ = $\delta^{13}C(\Sigma CO_2) - \delta^{13}(CH_4)$

Figure 37. DIFFERENCES BETWEEN CARBON ISOTOPIC VALUES FOR METHANE, CARBON DIOXIDE, AND TOTAL CARBONATE FROM DSDP SITE 570 CORES

Data from Brooks et al., 1985, Claypool et al., 1985, Galimov and Shabaeva, 1985, and Jeffrey et al., 1985

between isotopic values for carbon dioxide from core gas and coexisting methane. The trend of this plot is nearly parallel to that of the total carbonate plot. The difference in ^{13}C content of carbon dioxide gas and methane decreases from 73 at 32 m (core 4) to 58 per mil at 280 m (core 30). The 15 per mil change in this interval corresponds to a 5 per mil change in the total carbonate-methane isotopic difference. This general correspondence of depth trends with depth of the two differences plotted on Figure 37 suggests that the two measures are consistent. The lack of exact correlation between the two measures further suggests that the magnitude of the kinetic isotope effect controlling the isotopic signature of carbon dioxide is depth dependent. The curve on the left in Figure 37 illustrates this dependence. The difference between total carbonate and carbon dioxide isotopic values nearly doubles between the shallow cores and core 30 (280 m). The concentration of total carbonate in pore water diminishes with depth from 38.7 mMol/kg at 32 m (core 4) to 2.2 mMol/kg at 337 m (core 36). Although it may be coincidental, the agreement between carbon dioxide and total carbonate isotopic data may be affected by the concentration of total carbonate in the system. At high concentrations of total carbonate in the pore water system, the difference in isotopic composition of the total carbonate and concurrently present carbon dioxide gas is small (~10 per mil). Deeper in the hole, where the concentration of total carbonate in the system is much less, the difference in the carbon isotopic values of the gaseous carbon dioxide and the total dissolved carbonate is larger (~20 per mil). Of course, many chemical and physical parameters other than total dissolved carbonate vary down hole and may also effect the observed difference.

A striking feature of the relationships presented in Figure 37 is the sharp deviation from general trends seen in the carbon dioxide trace between cores 25 and 30 (234 - 280 m). Gas from cores 26, 28, and 29 (245, 265, and 270 m), and the massive hydrate gas (core 27) have values for the difference in the carbon isotopic content of methane and carbon dioxide which are the lowest encountered in the hole (41 to 54 per mil). These values are much less than the expected values of 59 - 60 per mil derived from interpolating the general trend seen between cores 15 - 30.

This feature of the methane-carbon dioxide difference profile on Figure 37 does not appear on the total carbonate-methane difference plot. The total carbonate isotopic data were collected less frequently than were isotopic data for carbon dioxide. None of the cores which showed closer than projected agreement of carbon dioxide and methane ^{13}C content (cores 26, 27, 28, 29) were tested for total carbonate isotopic values. Thus it appears that a potentially significant deviation in the isotopic data which coincides directly with the presence of the massive and fracture-filling gas hydrates was not previously noted, possibly because the interval of interest was not analyzed for total carbonate content.

The consensus among DSDP research groups that the methane from which gas hydrates were formed at Site 570 was formed in place by bacterial reduction of anomalously heavy carbon dioxide was based on the constant 70 per mil difference in methane and total carbonate isotopic contents. The analysis above suggests that since the $\delta^{13}C$ of carbon dioxide from core liner gas pockets follows the same trends as the $\delta^{13}C$ of the total dissolved carbonate fraction of the pore water, a substantial fluctuation in the carbon dioxide data should be reflected in a parallel deflection in the total carbonate trend. A large fluctuation does exist in the carbon dioxide isotopic data in the hydrate-rich interval which was not sampled for total carbonate.

Summary. Samples of natural gas hydrates were recovered for analysis at three locations drilled during DSDP Leg 84: Sites 565, 568, and 570. Gas hydrates may have also been recovered at Site 566.

Gas hydrates were recovered from three intervals at Site 565 offshore of Costa Rica. The gas hydrate samples were composed of methane with $\delta^{13}C$ values of -62 to -63 per mil and trace amounts of carbon dioxide and heavier hydrocarbons. Methane from the sediment cores increased regularly in ^{13}C content downhole, but $\delta^{13}C$ values of the total dissolved carbonate fraction reached a maximum at 160 m and decreased downhole (Figure 22).

Gas was vigorously expelled from fractures in serpentinite cored from Site 566. The gas was composed mainly of methane, but contained substantial amounts of heavier hydrocarbons (Table 9). Gas was released from chips of ice-like material, suggesting possible gas hydrates.

Although abundant hydrocarbon gas was encountered at Site 568, only one sample of gas hydrate was recovered, from a depth of 403 m. Gas collected from the dissociating hydrate was composed of methane with traces of heavier hydrocarbons (Table 8). The $\delta^{13}C$ values of core gas increased regularly with depth at Site 568 reaching about -40 per mil at 400 m.

The vertical distribution of methane and heavier hydrocarbons at Site 568 was unlike that typically encountered in DSDP drilling. From a depth of about 190 m to the bottom of the hole the levels of hydrocarbons heavier than ethane averaged less than 30% of their concentrations in the overlying sediments (Figure 23). This unusual gas distribution was interpreted by DSDP scientists to be due to gas hydrate presence (Table 10). The upper 190 m of sediment was proposed to be free of gas hydrates. Since hydrates exclude the heavier hydrocarbons, diminished concentrations of propane, butane, and pentane beneath 190 m were thought to reflect dilution by dissociating hydrates composed of methane and ethane. Slightly higher concentrations of propane through pentane from 345 to 391 m and from 410 to 417 m were interpreted to indicate a lack of gas hydrates in those intervals.

We conclude that the unusual core gas profile at Site 568 was not due to gas hydrate presence. The major change in gas composition at 190 m depth reflects a coincident unconformity (Figure 19). Minor fluctuations in gas composition between 190 and 417 m predict hydrate presence where none was noted. Gas composition may have potential for predicting gas hydrates, but the method appears too sensitive to other factors to be widely applied.

Gas hydrates were recovered from Site 570 from depths of 191 m to 337 m (Table 7). Hydrates were found in porous ash or sand layers above 245 m and below 280 m. Between 245 and 280 m fracture-filling and massive gas hydrates were recovered. The 245 to 280 m interval is also characterized by abundant hydrocarbon gases heavier than ethane (Figure 30 and 32). The composition of both core gas and hydrate gas suggests that hydrocarbons from 245 to 280 m are genetically different from hydrocarbons elsewhere in the hole and may thus have migrated to their current position. The use of core gas composition as a gas hydrate indicator as had been proposed for Site 568 did not predict observed gas hydrate distribution at Site 570.

Hydrocarbons and pore water constituents at Site 570 are unusually enriched in ^{13}C (Figure 36). The isotopic signature of methane near the bottom of the hole is similar to that at Site 568, but the depth relationship is not regular; major discontinuities are noted in the $\delta^{13}C$ values of all measured components at the depth of the massive gas hydrate (Figure 36). A discontinuity also is seen in the differences in isotopic values of coexisting methane and carbon dioxide (Figure 37). However, sampling density is insufficient to detect a similar trend in total carbonate composition.

Seismic Evidence of Gas Hydrates

Abundant evidence of gas hydrates exists in seismic records of continental slope sediments of the Middle America Trench. Shipley et al. (1979) reported bottom simulating reflectors (BSRs) from multichannel seismic lines from at least four locations along the Middle America Trench. The distribution of BSRs offshore of Acapulco, Mexico was mapped by Shipley and Didyk (1982). Von Huene et al. (1982) mapped the distribution of BSRs offshore of Guatemala.

Multichannel Seismic Lines

The University of Texas Marine Science Institute has produced an extensive set of high quality seismic lines from the Middle America Trench study region. Numerous cruises of the R/V Ida Green were made in the study region in the late 1970s and early 1980s. The cruises were concentrated in four principal areas of the Middle America Trench. Offshore of Mexico south of Acapulco was extensively surveyed in 1977 and 1978 for preliminary DSDP site characterization studies for Leg 66. The region offshore of Guatemala was surveyed in preparation for the drilling transects of Legs 67 and 84. The trench and slope offshore of Nicaragua and the offshore of Costa Rica were the sites of closely spaced grids of seismic profiling.

Offshore Mexico. Bottom simulating reflectors were reported on 12 seismic lines from the continental slope offshore of Mexico (Figure 38) by Shipley and Didyk (1982). The occurrences were reported to occupy two widely separated areas. The larger area, approximately 750 km^2 occurs close to DSDP sites drilled on Leg 66. Sites 491 and 492 where gas hydrates were recovered are directly underlain by a BSR on line MX-16 (Figure 39). It is probable that gas hydrates were also recovered at Site 490, which is located 8 km landward from the nearest BSR on line OM-7N (Figure 40). A smaller area of about 50 km^2 was mapped by Shipley and Didyk (1982) about 100 km southeast of the principal concentration of BSRs.

After examining the UT lines upon which Shipley and Didyk (1982) based their BSR distribution map, we suggest that another small area of BSR presence exists. A BSR which is less distinct than those previously mapped, but very similar in form and subbottom depth, occurs on line OM-4N between 1505 and 1555 hr. GMT (Figure 41). The same reflector can be traced along the two intersecting strike lines, OM-1W and OM-2W. Based on these three seismic lines, we estimate the areal extent of this third BSR to be about 100 km^2.

Shipley and Didyk (1982) proposed that BSRs tended to be present on seismic lines which also showed landward dipping reflectors (LDRs; Figure 39). Landward dipping reflectors had generally been considered to be records of imbricate thrust faults caused by accreting of sediments to the continental margin by the subduction process (Seeley, 1979). Several drill holes on Leg 66 penetrated seismic LDRs. Rather than discrete fault zones, Leg 66 drilling revealed that the LDRs offshore of Mexico corresponded to sharp lithological changes from hemipelagic fine-grained slope deposits to coarse sands interpreted to have been deposited in the trench (Shipley and Didyk, 1982). It

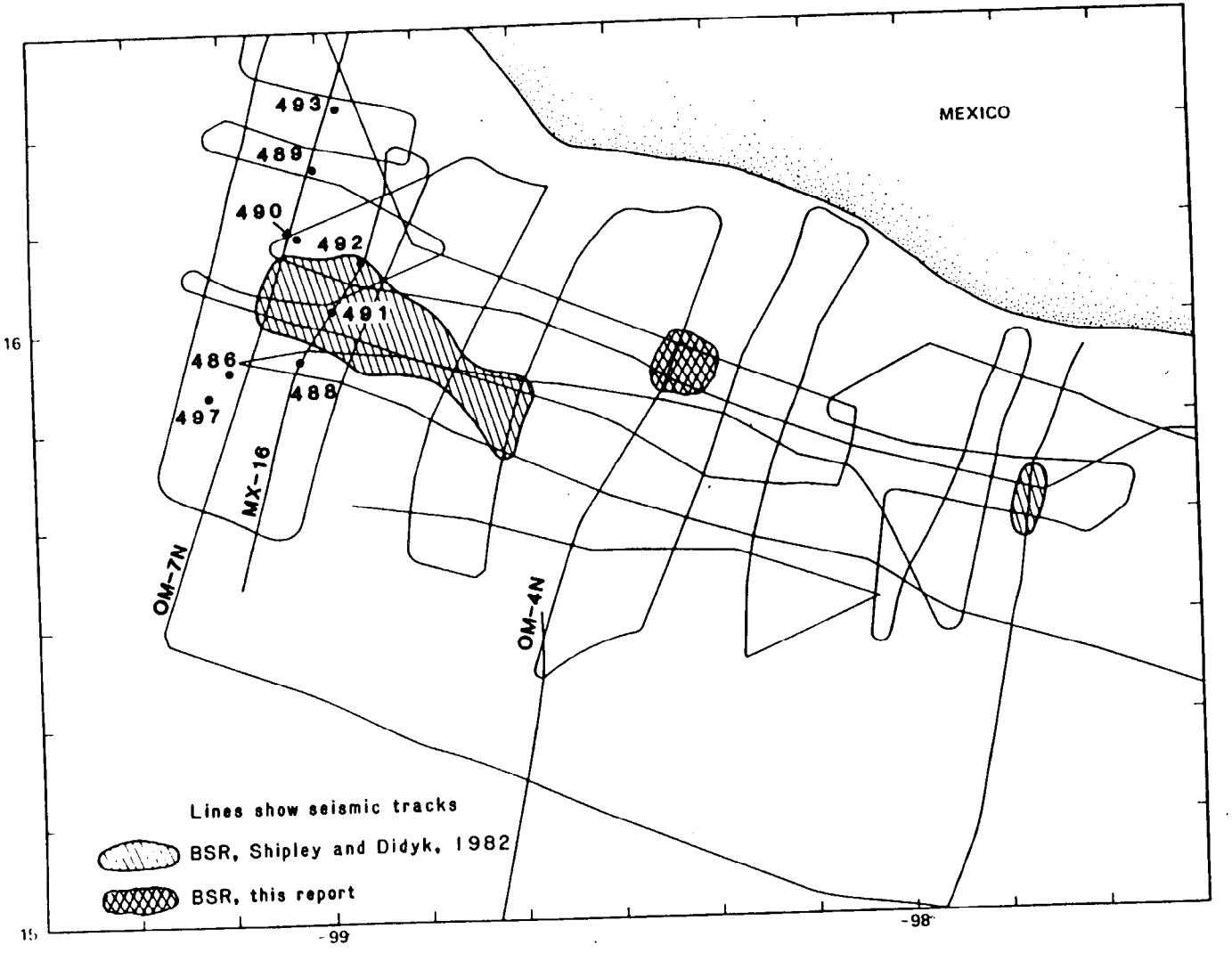

Figure 38. **DISTRIBUTION OF BOTTOM SIMULATING REFLECTORS FROM MULTICHANNEL SEISMIC LINES OFFSHORE MEXICO**

Modified from Shipley and Didyk, 1982

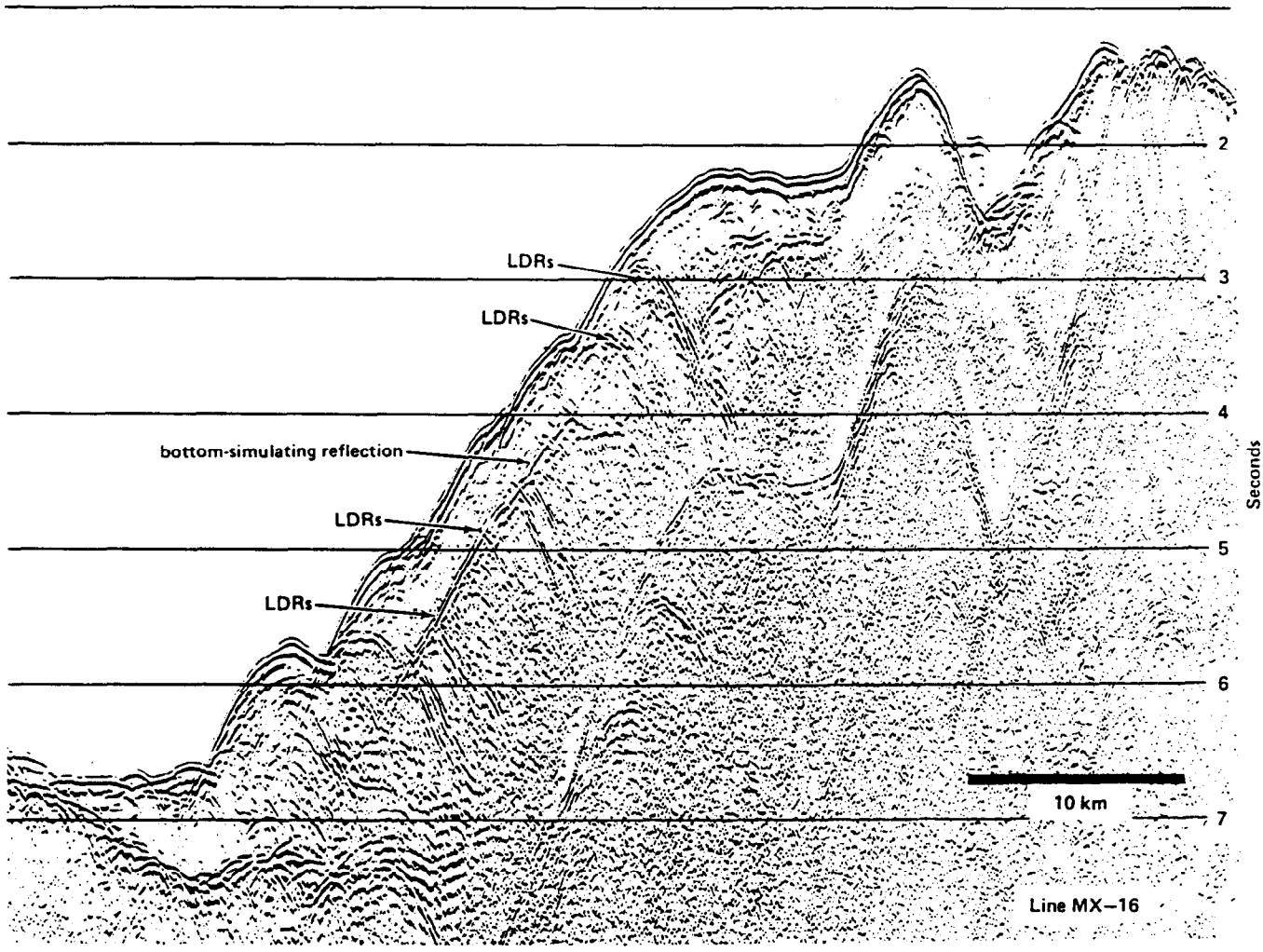

Figure 39. SEISMIC LINE MX-16, OFFSHORE MEXICO

After Shipley and Didyk, 1982

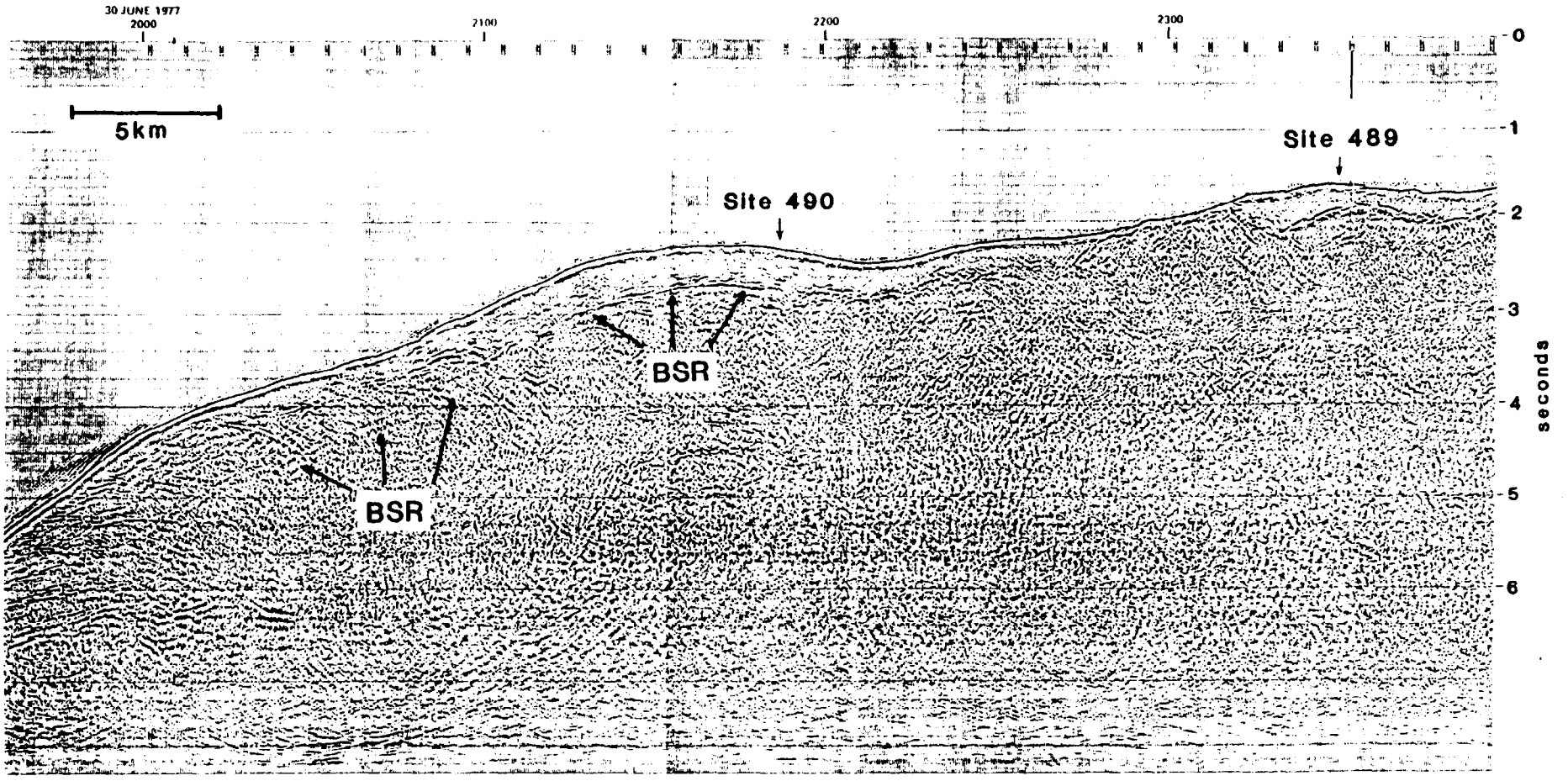

Figure 40. SEISMIC LINE OM-7N, OFFSHORE MEXICO

After Shipley, 1982

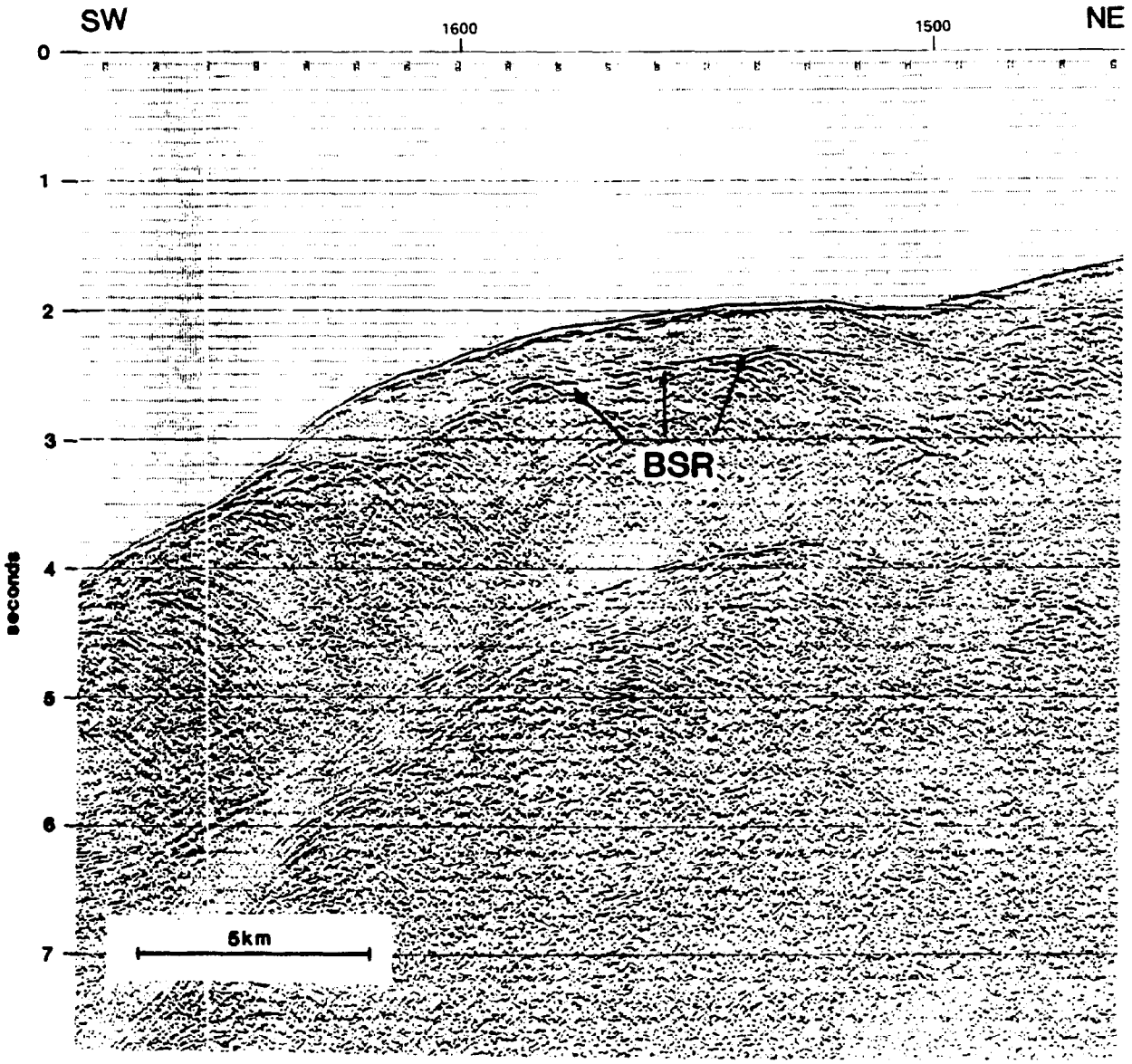

Figure 41. SEISMIC LINE OM4N OFFSHORE MEXICO

After Shipley, 1982

was proposed that these coarse accreted sand layers may have acted as migrational conduits to deliver gas to the gas hydrate stability zone. A similar but more distinct correspondence between BSRs and reflections interpreted as imbricate thrust surfaces was noted along the northern continental margin of Colombia by Finley and Krason (1986) using seismic data of Ladd et al. (1984).

The faint BSRs on lines OM-4N, OM-1W, and OM-2W follow the LDR relationship noted by Shipley and Didyk (1982). The BSR on line OM-4N (Figure 41) occurs only beneath water shallower than 2.5 sec. (1,800m). A few faint LDRs can be discerned near the BSR on line OM-4N. The lower slope segment of line OM-4N is devoid of both BSRs and LDRs.

The BSRs on the University of Texas seismic lines from offshore of Mexico show a very rapid increase in subbottom depth with increasing water depth. This feature is to be expected of a gas hydrate phase boundary since the increasing pressure beneath deep water stabilizes the hydrate allowing it to exist at the higher temperatures of the deeper sediments. Although some deepening with water depth is seen in all BSRs, the effect is much more evident on the seismic lines from offshore of Mexico. Such an effect could be due to decreasing geothermal gradient, increasing geostatic pressure gradient, decreasing seismic velocity or increased input of stabilizing gases downslope.

Modeling the change in BSR depth due to water depth suggests that the geothermal gradient decreases downslope offshore of Mexico. A previously developed model was used to calculate the thickness of the gas hydrate stability zone for a range of geothermal gradients (Krason et al., 1986). Figure 42 shows the expected relationship of BSR depth to water depth for water depths of 1,500 to 4,500 m and geothermal gradients of 2 to 5°C/100 m. Superimposed on Figure 42 are the measured depths of BSRs in lines MX-15, MX-16, and OM-7N from offshore of Mexico. The diagram indicates that the geothermal gradient beneath shallow water columns is between 3.5 and 4.0°C/100 m, whereas downslope the geothermal gradient decreases to between 2.5 and 3°C/100 m. Using our model, none of the BSRs indicate the 2.2°C/100 m gradient which Shipley and Didyk (1982) derived for the entire continental slope.

Our modeling omitted possible contributions of gas composition, pressure gradients, and seismic velocity changes. Gas from the lower slope could have more carbon dioxide, hydrogen sulfide, or heavier hydrocarbons which could stabilize gas hydrates and produce deeper BSRs. There is no apparent reason why the lower slope sediments should consistently contain more of these additional gases than the upper slope sediments. Increasing pressure gradient downslope could stabilize gas hydrates. Von Huene (1985) documented overpressure on the lower continental slope of Guatemala. A similar situation offshore of Mexico would stabilize gas hydrates and allow a geothermal gradient higher than that calculated from our model. If the lower slope is overpressured, the change in geothermal gradient downslope (Figure 42) could be eliminated, but the constant geothermal gradient would be in the range of 3 to 4°C/100 m. A decrease in seismic velocity downslope would increase the return time of the acoustic pulse and thus make the BSR deeper in a time display seismic line than its true depth. Overpressuring can result in decreased seismic velocity, as is often seen in the Gulf of Mexico (Krason et al., 1986). However, the overpressured rocks drilled offshore of Guatemala

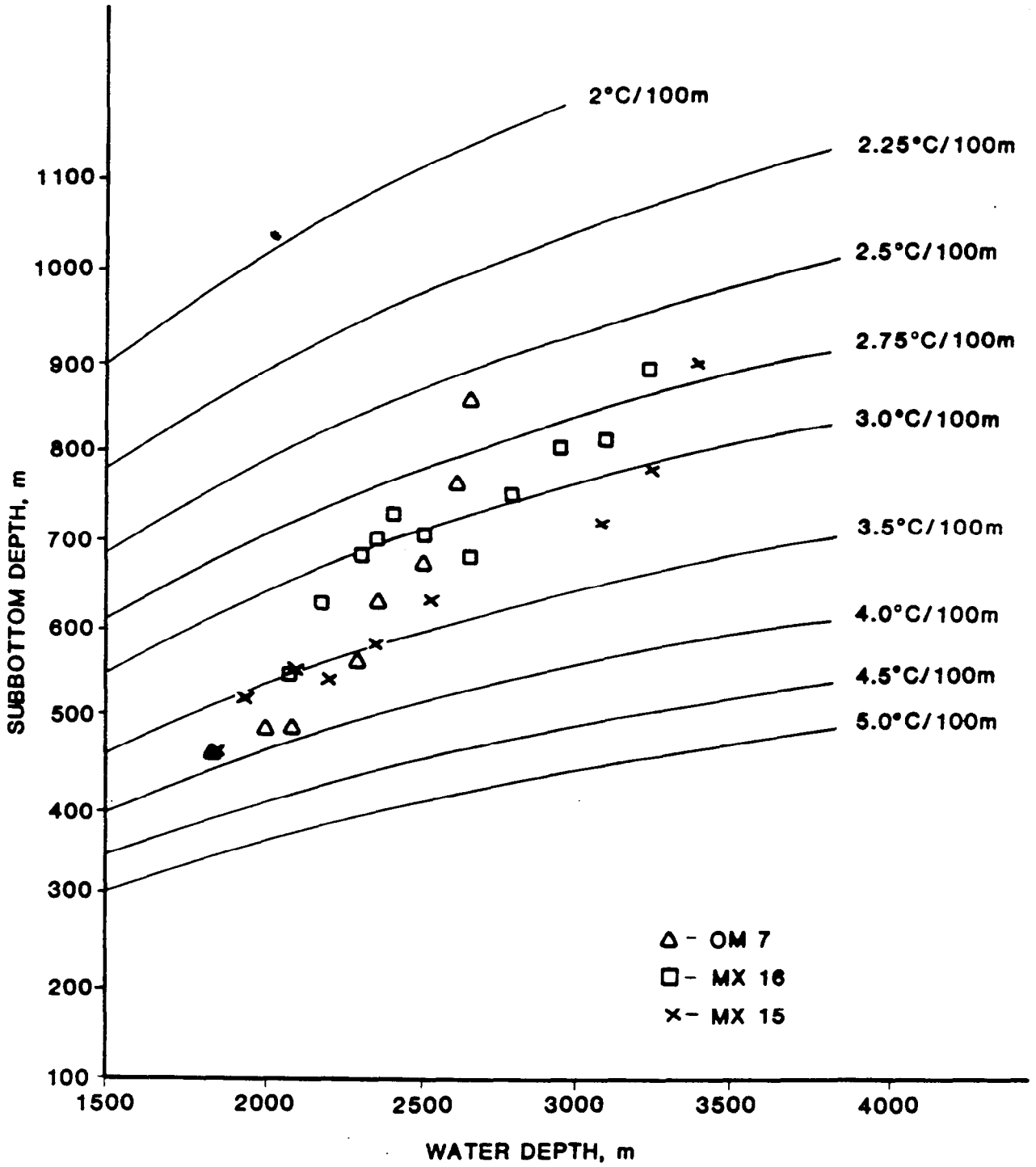

Assumes: hydrostatic pressure, bottom water temperature of 2°C.

Figure 42. DEPTH OF BOTTOM SIMULATING REFLECTORS OFFSHORE MEXICO COMPARED TO THE DEPTH OF THE BASE OF THE GAS HYDRATE STABILITY ZONE AT DIFFERENT GEOTHERMAL GRADIENTS

tended to be overcompacted and thus would have high rather than low geothermal gradients. The lower slope sediments offshore of Mexico are younger than upper slope sediments and thus may not be as compacted. Therefore the lower slope sediments may have lower seismic velocities. The typical progressive increase in seismic velocity with depth of burial should lead to a masking of the deepening effect of BSRs in deep water. The thicker gas hydrate zone beneath deep water would occur in more compact sediments with higher seismic velocities. Thus, the increase in thickness seen in a time section seismic line would be less than the true thickness change. Although these alternative explanations of the rapid increase of BSR depth with water depth offshore of Mexico could be applicable, the most straightforward explanation for the effect is a decrease in geothermal gradients downslope. If some of the above processes are active, the resulting geothermal gradient would be much higher than the 2.2°C/100 m proposed by Shipley and Didyk (1982).

A similar downslope decrease in geothermal gradients on the landward slope of a trench was noted by Claypool et al. (1973). Heat flow from the Aleutian Trench region showed low heat flow near the trench and progressively greater heat flow up the slope. The effect was readily explained by the subduction of cold oceanic crust and sediments depressing the heat flow and thus geothermal gradients near the trench.

No drill holes on DSDP Leg 66 were reported to have penetrated a BSR. Due to safety concerns, DSDP drilling is routinely stopped before reaching the depth of BSRs. Thus, the vertical distribution of gas hydrates which caused the BSRs offshore of Mexico is still unknown. Site 490 was drilled to a depth of 588 m. Site 490 was located less than 5 km landward of the termination of a BSR at 0.4 sec subbottom. At 1.8 km/sec seismic velocity the BSR would be found at 360 m subbottom. Drilling at Site 490 thus may have penetrated the base of the gas hydrate stability zone, and in fact recovered frozen tuff which released gas at 364 m subbottom. The possible correspondence of the base of gas hydrate zone and the drilled gas hydrate was not noted by project scientists, probably due to a lack of a reliable estimate of geothermal gradients in the upper slope.

A section of seismic line OM-7N near DSDP Site 490 is included as Figure 43. The prominent reflector at about 0.4 sec subbottom loses continuity at about 1 km from the drill site. The exact nature of the reflector is uncertain; drilling at Site 490 did not recover any rocks with sufficient seismic impedence contrast to produce such a high amplitude reflector. By correlating the BSR distribution map of Shipley and Didyk (1982, Figure 38) with line OM-7N (Figure 41) the landward extent of the BSR was determined. Shipley and Didyk (1982) identified the BSR on line OM-7N as extending to within 3.2 km of Site 490 (Figure 43). The only reflector on line OM-7N which parallels the sea floor and thus possibly a hydrate BSR is the prominent reflector at 0.4 sec subbottom. If this reflector from the left margin of Figure 43 to 3.2 km from Site 490 is a BSR as claimed by Shipley and Didyk (1982), then its landward continuation should also be. There is no obvious difference in the nature or amplitude of the reflection along its extent from the segment interpreted as a BSR by Shipley and Didyk (1982) to the segment identified as a "strong subbottom reflector" in the site report. Thus, it appears that the reflector which is continuous to within 1 km of DSDP Site 490 may be a hydrate BSR.

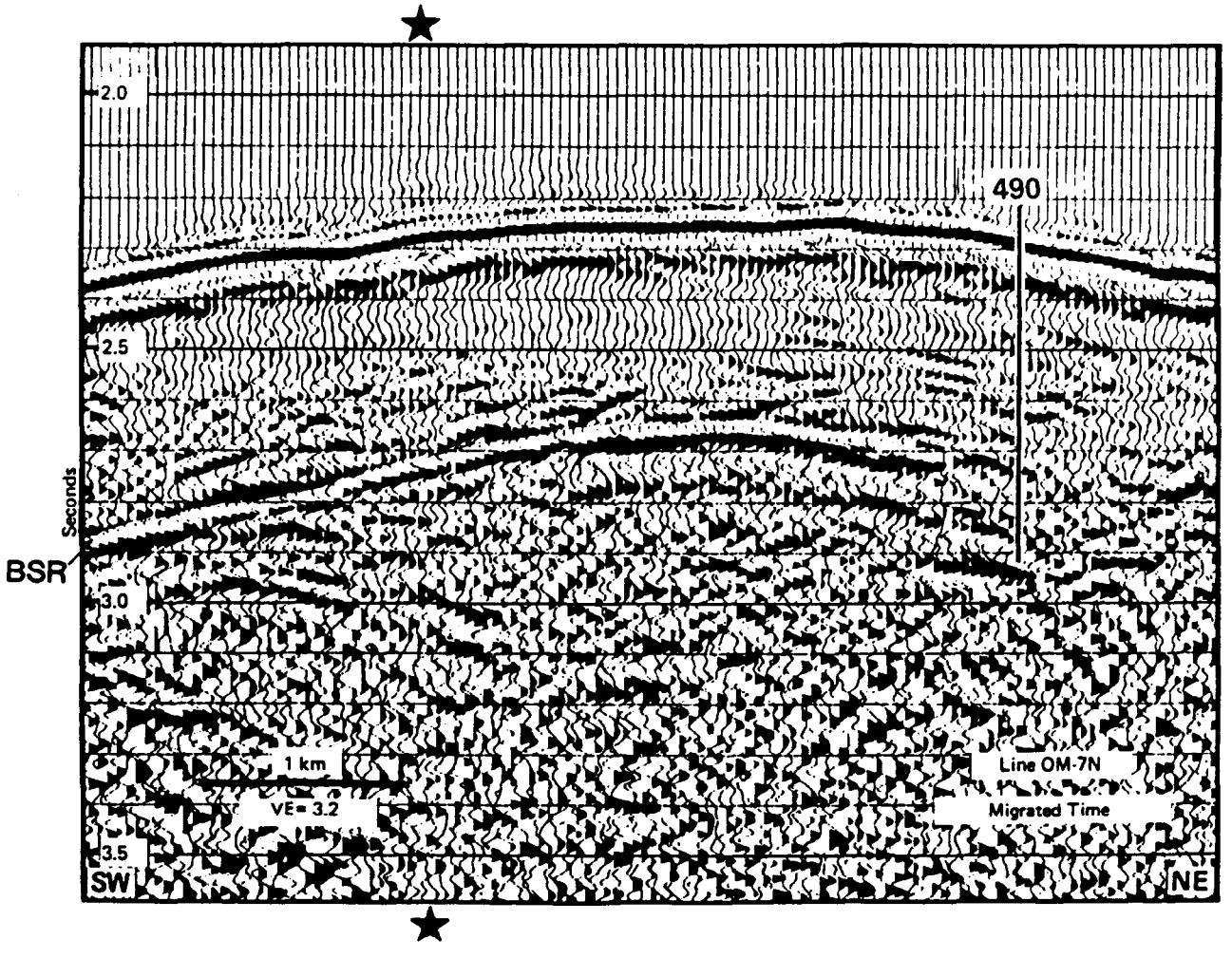

Figure 43. SEGMENT OF SEISMIC LINE OM-7N SHOWING RELATIONSHIP OF BOTTOM SIMULATING REFLECTOR AND DSDP SITE 490

After Watkins et al., 1982

Reflector to left of stars mapped as hydrate BSR by Shipley (1982), Figure 38

The shallow depth of the reflector in Figure 43 suggests a very high geothermal gradient at Site 490. Using the estimate of 2.2°C/100 m from Shipley and Didyk (1982) and a 1,250 m water depth, the base of the gas hydrate stability zone would occur at 800 m subbottom (Figure 42). Thus the entire 588 m of sediment drilled at Site 490 would be in the gas hydrate stability field and the reflector in Figure 43 could not be a hydrate BSR. However the trend to steeper geothermal gradients at shallower water depths offshore of Mexico diagrammed in Figure 42 indicates that a geothermal gradient of 3.5 to 4.5°C/km is likely for Site 490. For a base of hydrate reflector at 0.42 m subbottom, a geothermal gradient of about 4.5°C/100 m would be required. Such a high gradient may be suspect. Thus it cannot be confidently concluded that the reflector at 0.42 sec subbottom and the gas hydrate drilled at 364 m depth coincide with the base of the gas hydrate stability zone. However, based on the higher than reported gradients diagrammed in Figure 42, it is probable that drilling at DSDP Site 490 did penetrate the base of the gas hydrate stability zone.

Shipley and Didyk (1982) indicated that the BSRs from offshore of Mexico could have been produced by the acoustical contrast of disseminated gas hydrates and underlying sediments. The acoustic impedance change represented by the BSRs does not require the presence of underlying free gas. Using methods previously developed (Shipley et al., 1979), a reflection coefficient of -0.08 was obtained by Shipley and Didyk (1982) for the BSRs offshore of Mexico. Shipley and Didyk (1982) substituted -0.08 and values for seismic velocity (1.8 km/sec) and density (1.9 g/cm^3) obtained from drilling at Site 490 into the equation for seismic impedance. They obtained a value of 2.4 for the product of seismic velocity and density of sediments beneath the BSR. Since various geologically possible combinations of density and velocity could result in a product of 2.4 (eg. $\rho = 2.4$, $v = 1.0$; $\rho = 1.6$, $v = 1.5$), Shipley and Didyk (1982) indicated that combination of density and seismic velocity necessary for the observed impedance contrast at the BSR are within the range expected for normal sediments. The low seismic velocity and density of gas charged sediments is not required.

In recalculating the necessary velocity and density values for BSRs we obtained different numerical values than Shipley and Didyk (1982); however, the revised figures still agree with their conclusions. The reflection coefficient, (r) measured from seismic profiles, is related to the impedance of the sediment by the following equation (Shipley et al., 1982):

$$r = \frac{\rho_2 v_2 - \rho_1 v_1}{\rho_2 v_2 + \rho_2 v_2}$$

Where ρ and v indicate the density and velocity of the sediments, the subscript "1" refers to sediments above the reflector, and "2" refers to sediments below the reflector. Substituting the values of 1.9, 1.8, and -0.08 for ρ, v, and r respectively, we obtained an impedance value of 2.9 instead of the 2.4 reported by Shipley and Didyk (1982). Since combinations of greater velocity and/or density of the sediment below the BSR would be needed to obtain an impedance of 2.9, the conclusions of Shipley and Didyk (1982) are consistent with this new value.

Values other than those suggested by Shipley and Didyk (1982) for acoustic velocity and density of sediments above the BSR may be more appropriate. The values of 1.8 km/sec. and 1.9 g/cm were obtained from the geotechnical work by Shephard et al. (1982) on cores recovered from Site 490. The basic premise of a gas hydrate BSR is that the in situ gas hydrates within the hydrate stability zone increase the seismic velocity of the sediment above the reflector creating an impedance contrast with underlying slower velocity sediments. The values measured by Shephard et al. (1982) correspond with unhydrated sediments and thus the slower, underlying sediments. It is likely that the seismic velocity of the hydrated sediments at the depth of the BSR would have higher seismic velocities than those measured by Shephard et al. (1982). However, hydrated sediments at the base of the gas hydrate stability zone would also have slightly lower densities than corresponding sediments. If the assumption is made that the sediments beneath the BSR do not include free gas, the values of Shephard et al. (1982) of 1.8 km/sec. and 1.9 $g.cm^3$ should approximate the expected properties of the nonhydrated sediments. Substituting these values for $\rho_2 v_2$ into the above equation, an impedance value for the hydrated sediments ($\rho_2 v_2$) of 4 is obtained. Assuming that the density of both the hydrated and the nonhydrated sediment is 1.9 g/cm^3, the seismic velocity of the hydrated sediment required to produce the BSR is calculated to be 2.1 km/sec. This compares with the change in seismic velocity noted by Stoll (1974) in laboratory experiments from 1.8 to values up to 2.7 km/sec. due to the formation of interstitial hydrates in sand.

Although our analysis suggests that some of the values reported by Shipley and Didyk (1982) may require revision, their conclusion on the physical nature of the contact represented by the BSR remains valid. The impedance change measured by them does not require underlying free gas; it can be produced by the velocity contrast of interstitial gas hydrate and an underlying interstitial solution of methane and water. Indeed, if our treatment of the data outlined above is valid, then the range of permissible seismic velocities for the sub-BSR sediments is considerably higher than those suggested by Shipley and Didyk (1982), i.e. 1.8 km/sec. vs. 1.3 km/sec. at a density of 1.9 g/cm^3. Thus our preliminary values more strongly support the absence of free gas beneath the BSRs than do the original numbers of Shipley and Didyk (1982).

Available multichannel seismic coverage from offshore of Mexico consists principally of the University of Texas MX and OM lines shown in Figure 38. The remainder of the available lines comprise 3 sets, the TRM, GO, and MG series. In contrast to the MX and OM lines discussed by Shipley and Didyk (1982), the TRM, GO and MG lines are oriented parallel to the continental margin of Mexico. These lines are thus less likely to display BSRs due to the general concordance of the sea floor and sedimentary layers along strike. The majority of the surveyed area of the TRM and GO lines cover the continental shelf offshore of Mexico between Acapulco and Guatemala where water depths are too shallow to stabilize gas hydrates. The MG lines were shot over the axis of the trench, and display no discernable BSRs. This is consistent with the low gas content of trench floor sediments drilled in DSDP Legs 66 and 67.

Approximately 100 km of the GO-1 line and 250 km of the TRM-4 and TRM-5 lines cover the continental slope at depths shown by Shipley and Didyk (1982) to be conducive to BSRs. One 40 km stretch of line TRM-5 (96.1 -

96.4° W, 15.6° N) displays a reflector which may be a BSR. The lack of discordance of sea floor and bedding plane reflectors on the segment prohibits confident assessment of the nature of the reflector.

Offshore Guatemala. The University of Texas GUA series of seismic lines collected as during site surveys prior to DSDP Leg 67 display BSRs on at least 6 separate lines. Von Huene et al. (1982) mapped the BSR distribution on the GUA lines (Figure 44). The diagrammatic cross sections in Figure 44 show that the BSRs typically occur in the mid-slope region. Unlike those mapped offshore of Acapulco, Mexico by Shipley and Didyk (1982), the Guatemalan BSRs do not continue beneath the lower slope. The cross sections on Figure 44 show that sediment deposits are thin on the lower slope. Drilling on Leg 84 showed that the thin sediment of the lower continental slope of Guatemala is typically underlain by ophiolitic basement at subbottom depths less than the base of the gas hydrate stability zone (von Huene et al., 1985). The difference in the depth distribution of BSRs off Guatemala and Mexico thus seems to be due to the lack of porous sedimentary rock at the base of the gas hydrate stability zone offshore of Guatemala.

One anomalous feature is readily apparent in Figure 44; the diagrammatic seismic lines show a BSR on line GUA-4 which is markedly different from those on other lines. The BSR on line GUA-4 is much deeper subbottom than the others. Additionally, the BSR appears in sediments which are under much shallower water than those on other lines of the series. Although the reflector on line GUA-4 was mapped and diagrammed by von Huene et al. (1982; Figure 44), it is absent from an accompanying plot of BSR depth vs. water depth which von Huene et al. (1982) adapted from Shipley et al. (1979). We have modified that diagram to include water and subbottom depths of the reflector from line GUA-4 (Figure 45). The diagram shows that the reflector on line GUA-4 identified as a BSR by von Huene et al. (1982) is much deeper in the sediment than BSRs from the Middle America Trench and elsewhere. Also, the expected direct relationship of subbottom depth to water depth is not followed by the reflector on line GUA-4.

A section from line GUA-4 which illustrates the anomalous reflector shows that it is discordant with adjacent reflectors (Figure 46). Between shot points 2,270 and 2,300 at a depth of 2.4 to 2.6 seconds, a steeply dipping reflector intercepts the anomalous reflector, as would be expected of a bedding plane intercepting a BSR. Close examination reveals that the steeply dipping reflector which crosses the possible BSR is found at a two-way travel time twice that of the sea floor reflector and is thus probably a water-bottom multiple.

The anomalous reflector could be a bedding plane reflection rather than a gas hydrate zone boundary as indicated by von Huene et al. (1982). Other possible sources for the reflector are processing artifacts, an extremely low geothermal gradient, or a very high geostatic gradient. One interesting alternative is suggested by Figure 45. The plot of the depth of the reflector on line GUA-4 is subparallel with that from the Bering Sea. Hein (1978) showed that the Bering Sea reflector, which showed a water to sediment depth relationship similar to line GUA-4, was most probably caused by a diagenetic change from biogenic silica to opal-CT.

The other BSRs from the multichannel lines offshore of Guatemala follow the sediment depth to water depth expected of gas hydrate boundaries (Figure 45). The shaded range of depths of BSRs from offshore Guatemala was taken directly from von Huene et al. (1982). The subbottom depths were

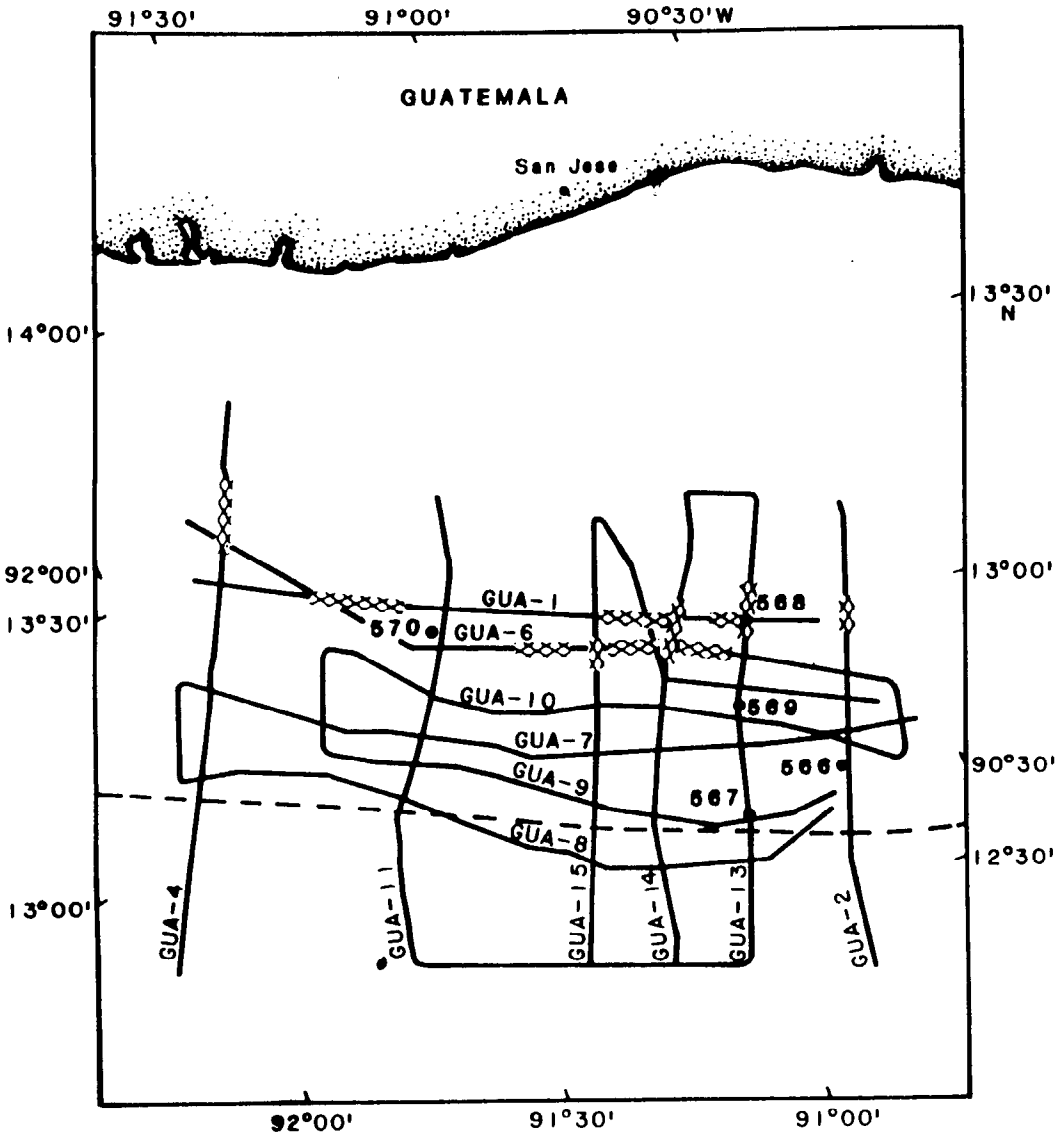

LOCATION OF SEISMIC LINES. PATTERNED AREAS ARE BSRs. DASHED LINE IS TRENCH AXIS.

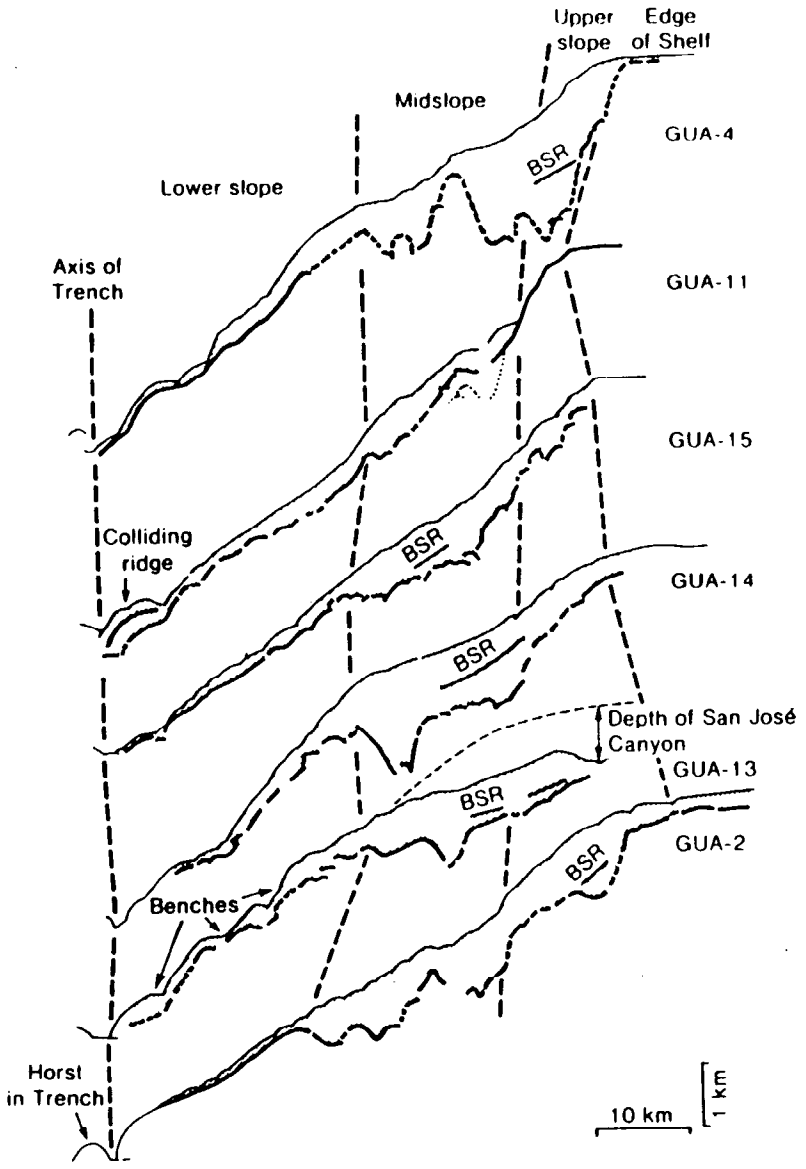

SCHEMATIC SEISMIC LINES. PATTERNED AREAS ARE SLOPE DEPOSITS.

Figure 44. LOCATION OF BOTTOM SIMULATING REFLECTORS OFFSHORE OF GUATEMALA

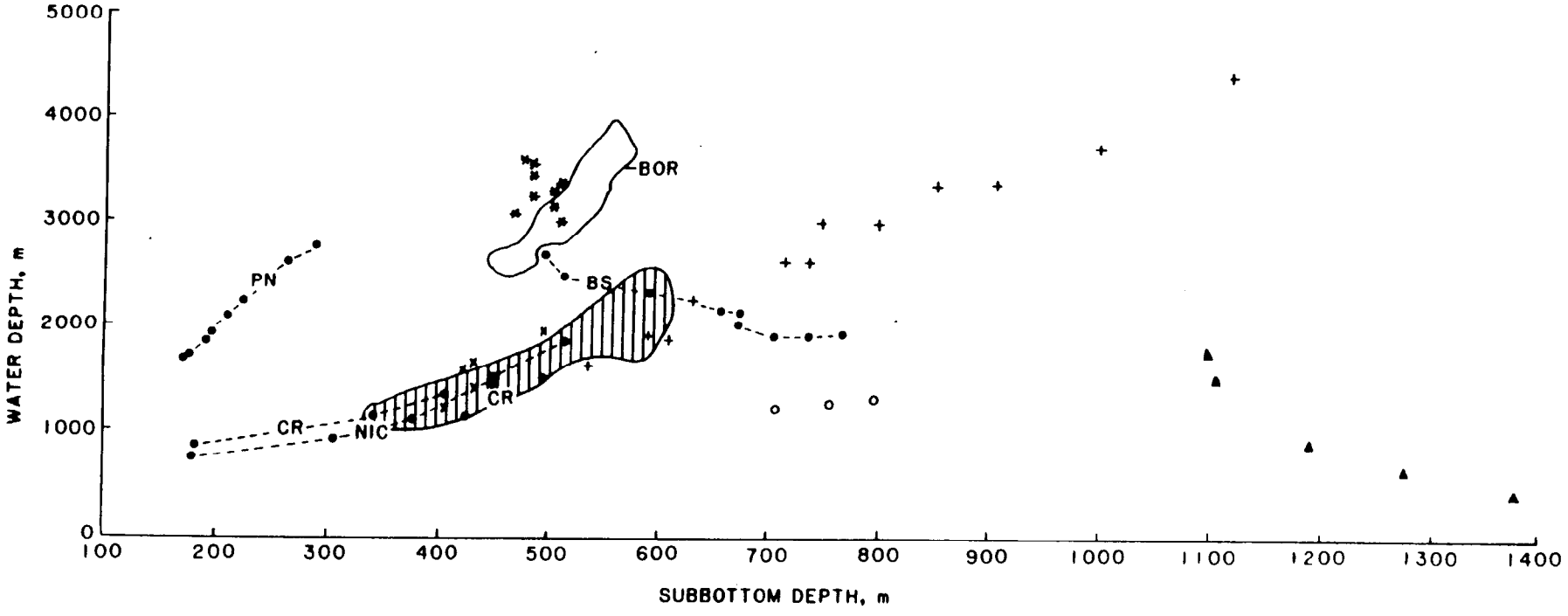

BOR BLAKE OUTER RIDGE
* BLAKE OUTER RIDGE
x WESTERN GULF OF MEXICO
PN PANAMA BASIN
CR COSTA RICA, MIDDLE AMERICA TRENCH
NIC NICARAGUA, MIDDLE AMERICA TRENCH
+ MEXICO, MIDDLE AMERICA TRENCH
BS BERING SEA
GUATEMALA, MIDDLE AMERICA TRENCH
▲ LINE GUA-4
o LINE GUA-18, SAN JOSE CANYON

Figure 45. GRAPH OF WATER DEPTH TO SUBBOTTOM DEPTH OF POSSIBLE BOTTOM SIMULATING REFLECTORS OFFSHORE GUATEMALA

Modified from Shipley et al., 1979, and von Huene et al., 1982

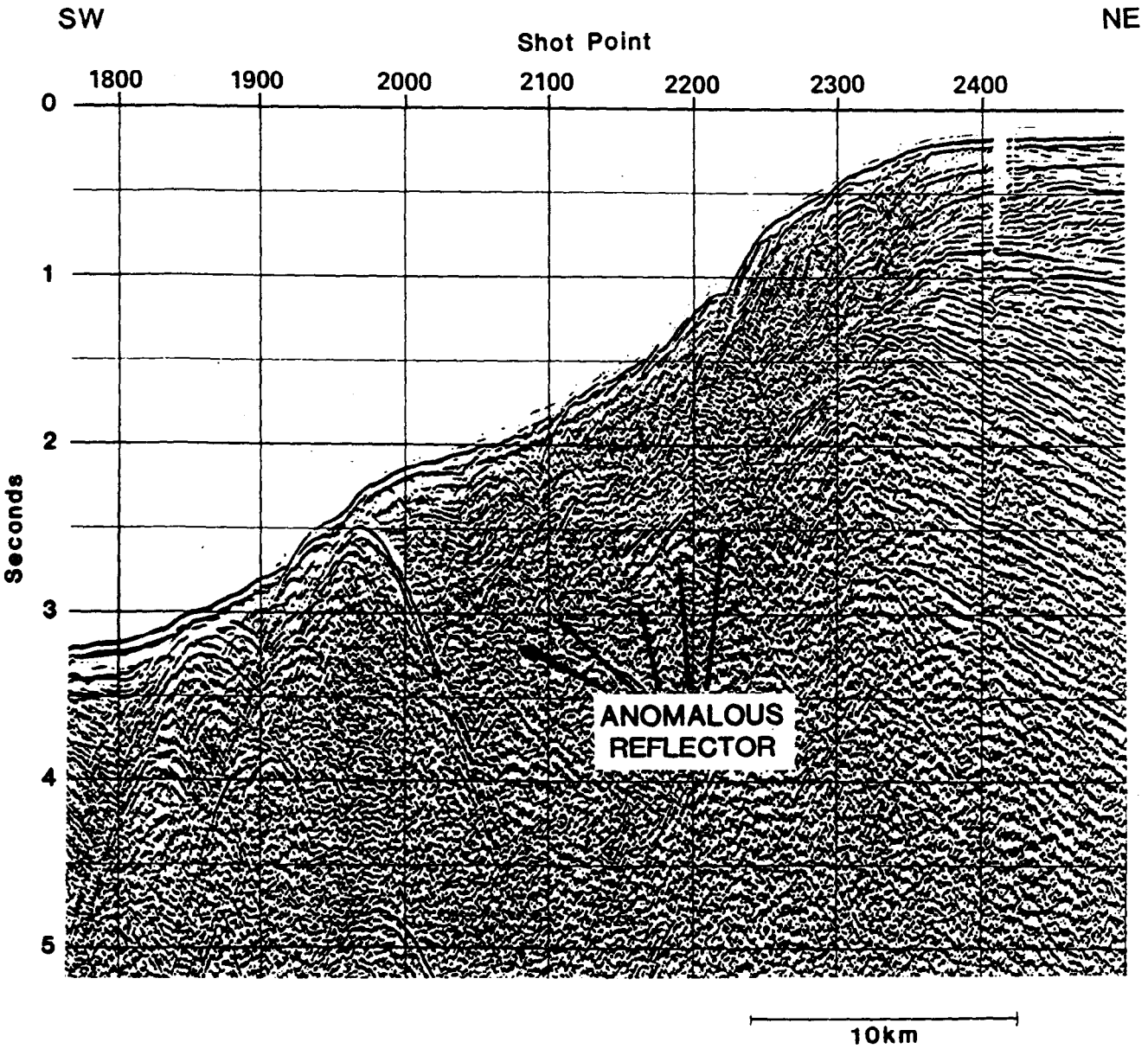

Figure 46. SEGMENT OF SEISMIC LINE GUA - 4 SHOWING ANOMALOUS REFLECTOR

After Ladd et al., 1982

reportedly calculated by assuming a seismic velocity of 1.7 km/sec. for sediments above the BSR.

Seismic lines of the GUA series display an increase in acoustic transparency within the gas hydrate stability zone. The decrease in reflection amplitude is not nearly as pronounced as that noted from the Blake Outer Ridge (Shipley et al., 1979) or the Colombia Basin (Finley and Krason, 1986). However, it was noted by Ladd et al. (1982) that the poor definition of the slope sediments on the lines may be due in part to this effect.

Ladd et al. (1982) demonstrated that the BSR on line GUA-14 has reversed polarity compared to the sea floor reflector. The BSR on line GUA-14 (Figure 47) is particularly distinct, and was recognized by Shipley et al. (1979) as a probable gas hydrate boundary prior to DSDP drilling on the Middle America Trench. An expanded display of the individual traces of the seismic reflections near shot point 620 is shown in Figure 48. It can be seen that the signal of which the BSR is composed is out of phase with the sea floor reflection; i.e., the first return from the hydrate displaces the trace to the right, whereas the sea floor wave shifts the trace to the left. This indicates that the BSR has resulted from a change from a high impedance layer to an underlying zone with lower seismic impedance.

The BSR on line GUA-14 can be analyzed to assess the possibility for underlying free gas in the sediments. The published results from DSDP 67 did not include an analysis of the actual impedance change represented by the BSRs on the GUA series of seismic lines. However, the expanded seismic traces of line GUA-14 presented by Ladd et al. (1982) contain sufficient information to estimate the impedance contrast. Work by Shipley et al. (1979) and Shipley and Didyk (1982) outlined the method for determining reflection coefficients and thus impedance contrast at the BSR using expanded single-shot traces of the seismic data.

The method of Shipley et al. (1979) and Shipley and Didyk (1982) approximates the reflection coefficient of the BSR by obtaining the ratio of the amplitude of the BSR response on a single seismic trace to the sum of the amplitudes of the water bottom reflection and the water bottom multiple reflection. This ratio is multiplied by the reflection coefficient of the water bottom reflector to obtain the absolute value of the BSR reflection coefficient.

The traces in Figure 48 lack two important factors necessary to determine the impedance contrast, the absolute value of the sea floor reflection and a recognizable water-bottom multiple reflection. The reflection coefficient of the sea floor reflection can be approximated as 0.18 based on data by Shipley and Didyk (1982) for U.T. seismic lines offshore of Panama and Mexico (Table 11).

As seen in Figure 48, the water-bottom multiple which would be expected at about 4.8 sec. subbottom cannot be differentiated from sediment reflectors. A minimum value for the hydrate reflection coefficient can be estimated by assuming that the obscured water-bottom multiple has the same amplitude as the sea floor reflector.

Using these necessary assumptions, a reflection coefficient for the BSR on line GUA-14 can be estimated. A mean value of -0.15 was obtained from 7 separate traces. The value is compared with estimates for other regions published by Shipley and Didyk (1982) in Table 11. The reflection polarity estimate for line GUA-14 is larger than any of the other estimates in Table 11. The estimate obtained for line GUA-14 is conservative; the assumption of

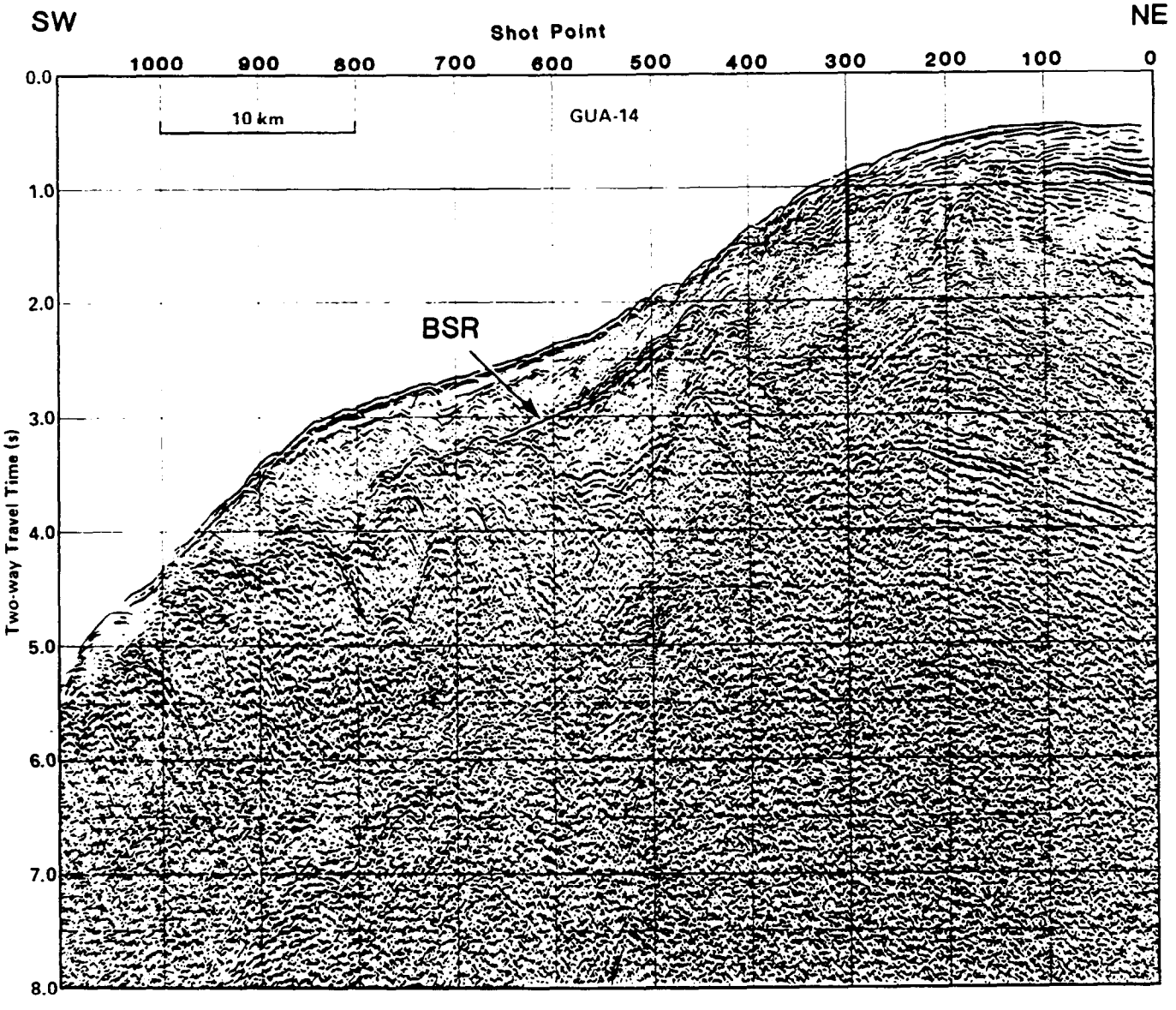

Figure 47. SEISMIC LINE GUA-14, OFFSHORE GUATEMALA

After Ladd et al., 1982

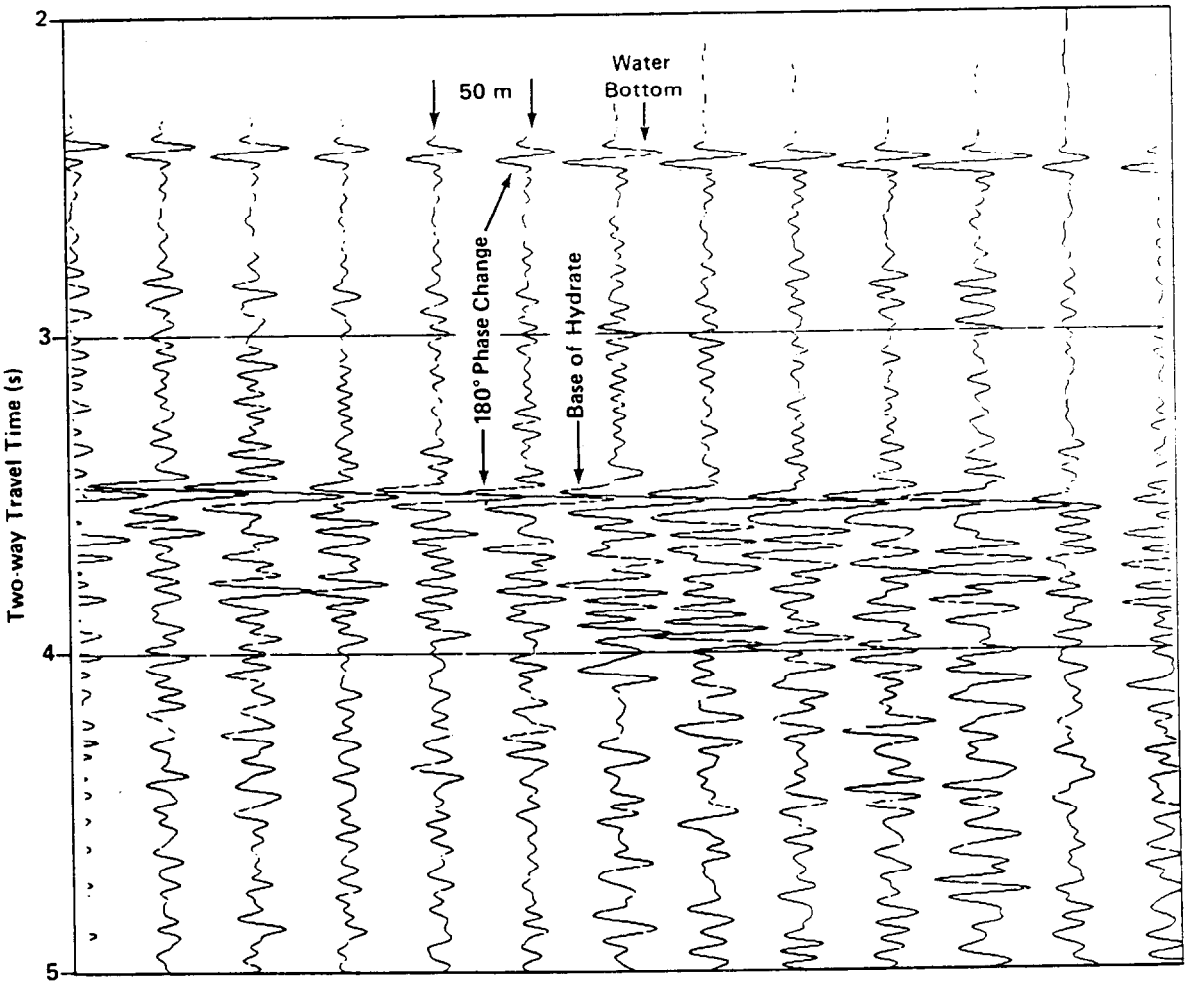

Approximate Location: Shot Points 610-630, Figure 47

Figure 48. DISPLAY OF INDIVIDUAL SEISMIC TRACES FROM SEISMIC LINE GUA-14

After Ladd et al., 1982

TABLE 11.

ESTIMATED REFLECTION COEFFICIENTS

Location	Sea Floor	BSR	n
Blake Outer Ridge	0.21 ± 0.04	-0.12 ± 0.04	13
Colombia Basin	0.19 ± 0.05	-0.10 ± 0.04	11
Panama Basin	0.18 ± 0.02	-0.05 ± 0.03	10
Middle America Trench, Mexico	0.17 ± 0.06	-0.08 ± 0.03	14
Middle America Trench, Guatemala (GUA-14)	0.18 ± 0.06	-0.15 ± 0.04	6

Modified from Shipley and Didyk (1982). Guatemala values derived from data of Ladd et al. (1982) using method of Shipley et al. (1979).

TABLE 12.

SEISMIC VELOCITY OF SEDIMENTS BENEATH
BOTTOM SIMULATING REFLECTOR ON SEISMIC LINE GUA-14

Above BSR (assumed)		Below BSR (calculated)	
Density g/cm^3	Velocity km/sec.	Density g/cm^3	Velocity km/sec.
1.9	1.8	1.9	1.3
		1.8	1.4
		1.7	1.5
1.9	2.1	1.9	1.6
		1.8	1.7
		1.7	1.8

Based on reflection coefficient of -0.15.

a low value for the water-bottom reflection coefficient and a high value for the water-bottom reflection amplitude should assure that -0.15 is on the low side of the possible range. Direct comparison with the other values on Table 11 may be suspect due to possible sampling bias. The statistical distribution of sample points from which values for the reflection coefficients from the Blake Outer Ridge, Colombia Basin, Panama Basin, and offshore of Acapulco were calculated is not clear from the work of Shipley et al. (1979) or Shipley and Didyk (1979). The sampled shots may be only from segments where the BSRs were most pronounced, or they may reflect typical rather than maximum values. The high apparent value obtained by us for line GUA-14 may therefore reflect only that all points used by us were from a segment with a particularly robust BSR, near shot point 620 on Figure 47.

From the reflection coefficient of the BSR on line GUA-14, an estimate of the accompanying impedance change can be derived. Using the equations of Shipley et al. (1979) which were previously applied to the Mexico continental margin section of this paper, the acoustic impedance of the sediment layer beneath the BSR can be calculated for any impedance assigned to the hydrated sediment layer. The seismic velocity of the two sediment zones cannot be estimated alone because the impedance obtained from calculation is the product of the seismic velocity and the density of the sediment. In Table 12, possible velocities of the sediments beneath the hydrate layer are presented for different combinations of densities and velocities of hydrated sediments.

If the density and velocity values proposed by Shipley and Didyk (1982) for the Mexican portion of the Middle America Trench, 1.9 g/cm and 1.8 km/sec, are extended to offshore Guatemala, the large reflection coefficient of line GUA-14 (-0.15) dictates very low sediment velocities (Table 12). Acoustic velocities of 1.3 and 1.5 km/sec are consistent with free gas trapped beneath the BSR. The other set of input parameters specified in Table 12 represent values expected for thoroughly hydrated sediment, 1.9 g/cm and 2.1 km/sec. Assuming these values, seismic velocities of 1.6 to 1.8 km/sec. are obtained for sub-BSR sediments.

The values listed in Table 12 indicate that the probability of free gas beneath the BSR on line GUA-14 is dependent on the model of BSR formation used. If the BSR results from the impedance contrast of hydrated sediments and underlying sediments, then the seismic velocity assigned to the overlying layer should be representative of hydrated sediments. In the two scenarios modeled in Table 12, a seismic velocity of 2.1 km/sec. would be most appropriate for a BSR caused by the seismic response of a hydrated sediment. In this case, the range of seismic velocities obtained for the underlying layer (1.6 - 1.8 km/sec.) neither precludes nor requires the presence of free gas.

Another model of BSR formation has been proposed by de Boer et al. (1985). These workers reviewed the seismic records from throughout the world which had been collected by Shell Internationale Petroleum Maatschappij. Although a large number of BSRs were detected in sections from various continental slope environments, velocity analysis of the sections with BSRs did not indicate anomalously high seismic velocity above the BSR. The BSRs were suggested to be the seismic record of the impedance change from normal velocity sediments to an underlying layer of gas-charged sediments. The gas-charged sediments producing the BSR were proposed to have been trapped by a gas hydrate layer, but the gas hydrate layer itself was claimed to be much too thin to be resolved seismically (<40 m). BSR reflectivity, therefore,

would depend on the difference in the impedance of nonhydrated sediment layers on either side of a thin impermeable gas hydrate layer rather than the impedance contrast of a thick hydrated section and underlying sediment.

Applying the BSR formation model of de Boer et al. (1985) to our reflection analysis of the BSR on line GUA-14 indicates that free gas is present beneath the BSR. Of the two seismic velocities assigned in Table 12 for the sediments above the BSR, the lesser value (1.8 km/sec.) is clearly more consistent with the assumptions of de Boer et al. (1985) of normal, nonhydrated marine sediments. The low seismic velocities of the sediments beneath the BSR (1.3 to 1.5 km/sec.) resulting from these assumptions suggest gas-charged sediments.

The strong BSR on GUA-14 is consistent with each of the prevailing models of BSR formation. This line cannot be used to indicate which model is more accurate.

A correspondence of BSRs and landward dipping reflectors (LDRs) exists on the seismic sections from offshore Guatemala. Distinct BSRs on lines GUA-13 and GUA-18 occur over or near prominent LDRs. Faint LDRs are located beneath the BSRs on lines GUA-14 and GUA-15.

The LDRs offshore of Guatemala have a different origin than those offshore of Mexico, but may promote BSR formation by a similar mechanism. Shipley and Didyk (1982) proposed that LDRs, which were shown to be composed of coarse, permeable accreted trench sediments offshore of Mexico, may function as migrational pathways delivering gas to the gas hydrate stability zone. Drilling on Leg 84 showed that the rocks which contain the LDRs offshore of Guatemala are serpentinized peridotite (von Huene et al., 1985). The LDRs offshore of Guatemala are therefore probably not wedges of uplifted trench sands as is the case offshore of Mexico. The most probable source of the LDRs offshore of Guatemala is fault surfaces or brecciated fault zones. The fault zones could serve as migration conduits in a manner similar to the sediment-derived LDRs offshore of Mexico. At Site 566 a fault was penetrated (von Huene et al., 1985). An increase in the drilling rate and hydrocarbon gas content across the fault zone indicate that such a fault zone may function as a permeable migrational pathway. The obvious question of the ultimate source of gas migrating along LDRs in the serpentinite basement is addressed in the hydrocarbon generation potential section of this report.

Offshore Nicaragua and Costa Rica. At least seven University of Texas seismic lines from the CR, NIC, and NCY series show prominent BSRs (Figure 49). The BSRs typically occur beneath 800 to 2,000 m of water. As seen on Figure 49, BSRs are found on 6 out of 8 of the seismic lines which cross the continental margin at these depths perpendicular to the strike of the trench (75%). This compares with BSRs on 4 of 6 lines (67%) offshore of Guatemala (Figure 44) and 7 of 11 lines (64%) offshore of Mexico (Figure 38).

Seismic line CR-7 did not display an obvious BSR (Figure 49). However, DSDP 565, drilled at 3,100 m water depth along line CR-7, encountered gas hydrates. The continental slope along line CR-7 dips at a constant angle. At the subbottom depths expected for a BSR, the sediment layers parallel the sea floor; a BSR may be present on line CR-7, but the concordance of the sediments and sea floor may preclude its identification.

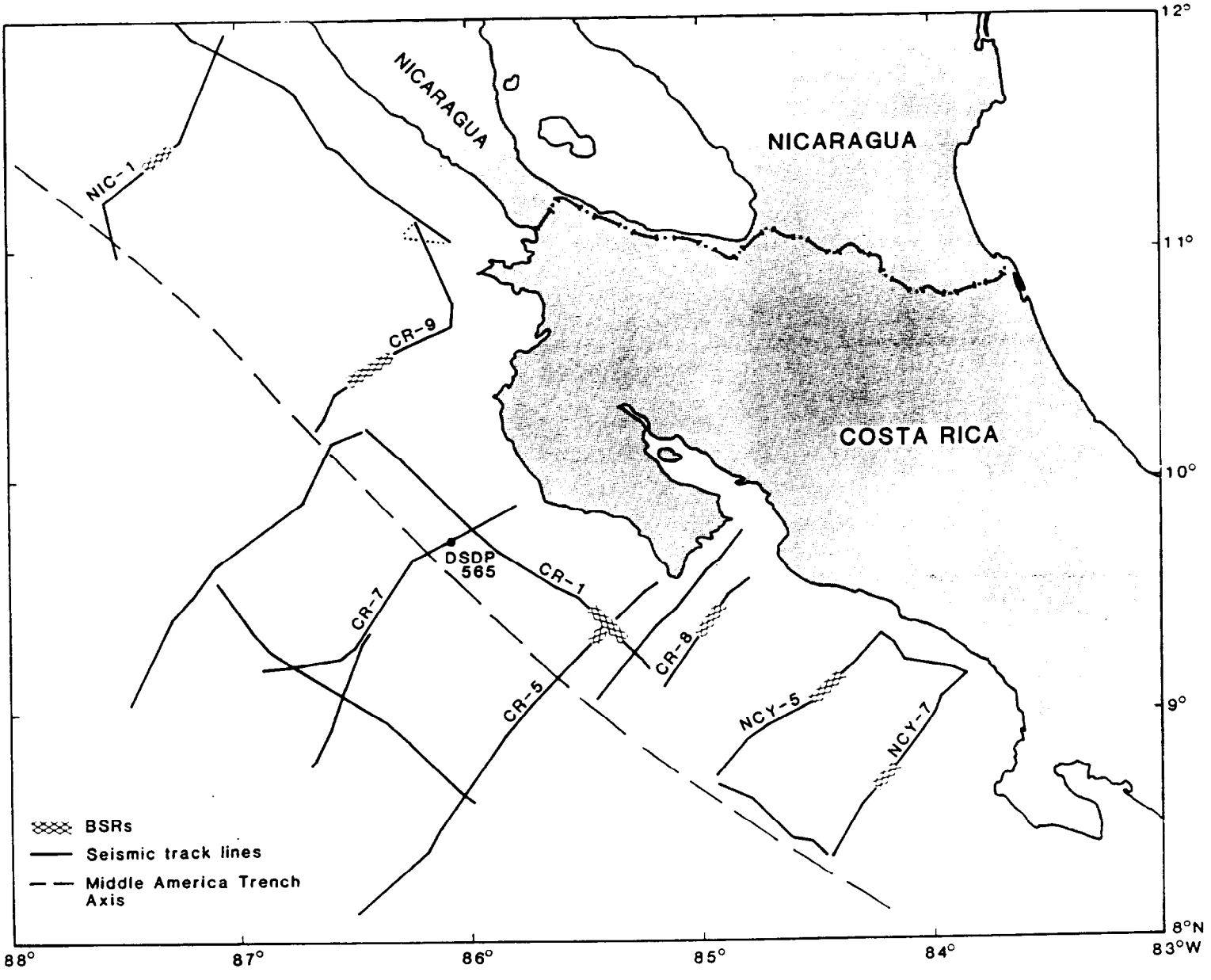

Figure 49. DISTRIBUTION OF BOTTOM SIMULATING REFLECTORS OFFSHORE OF NICARAGUA AND COSTA RICA

Single Channel Seismic Lines

In addition to the 30,000 km of multichannel seismic lines collected by the University of Texas, approximately 70,000 km of single channel seismic lines were examined in the preparation of this report. The single channel records available for the study region vary greatly in quality and coverage. The large majority of these lines have neither the penetration nor resolution for confident determination of BSRs. Additionally, most of the landward slope of the Middle America Trench where BSRs would be most likely were not surveyed; most surveys concentrated on the continental shelf or the axis of the trench. Some promising areas, such as the Gulf of Tehuantepec, were not surveyed, whereas other areas, such as the approaches to major ports, were surveyed repeatedly by many cruises.

From the seismic records of 45 cruises in the study region archived at the National Geophysical Data Center, BSRs were identified on single channel lines from 16 cruises.

Single channel records from cruises of the University of Texas research vessel Ida Green displayed BSRs at the same locations as found in the previously discussed multichannel lines. Typically, the BSRs on the single channel records were much less distinct than on the corresponding multichannel lines. Occasionally, the high quality single channel records showed slightly more detail, where diffractions on the multichannel lines obscured subtle reflectors. In these instances, the single channel lines were useful to verify questionable BSRs on the multichannel lines. However, some BSRs on multichannel lines could not be resolved in the corresponding single channel records, especially beneath deep water where the BSRs were found at subbottom depths greater than 0.8 seconds. There were no BSRs located on the single channel records which were not also represented on multichannel lines.

Single channel lines from the 1974 cruise of the University of Hawaii Institute for Geophysics research vessel Kana Keoki were of very high quality. However, that cruise was primarily concerned with investigating the Cocos Plate and the East Pacific Rise. Consequently the only lines covering the study region are a few collected offshore of Mexico in transit between ports. BSRs are well displayed in one section which crosses the Mexico continental margin parallel to the trench.

Records from the Conrad and the Vema operated by the Lamont Doherty Geological Observatory (LDGO) had fairly good areal coverage of the study region. However, the quality of the records varied markedly. Often, the LDGO surveys attained minimal penetration and were essentially bathymetric profiles. Other lines were collected with such high signal gain that details of structure and stratigraphy were obliterated. The typical presentation of the Lamont data exaggerates the vertical dimension to an extreme degree. However, a few lines offshore of Mexico were displayed with much less vertical exaggeration than typical for Lamont sections. On some of these, BSRs are well imaged.

Underway geophysical surveying from the Glomar Challenger during DSDP Legs 66, 67, and 84 showed rare BSRs. The DSDP records varied greatly in coverage and quality. Although large portions of the Middle America Trench study region were traversed during transit to, between, and from DSDP drilling sites, the deep penetration seismic gear was apparently rarely deployed. At times the quality of the few available lines is quite good; more

often it is insufficient for BSR determination. The resolution of BSRs on the few high quality records from the Challenger is less than on the single channel or multichannel lines from the Ida Green cruises. Profiling in the area of the drilling sites offshore of Mexico, Guatemala, and Costa Rica by the DSDP did not detect BSRs where they had been indicated by University of Texas lines. Although stratigraphic details were better resolved by Leg 66 and 67 profiling, BSRs were conspicuously absent. Only in-transit data from Legs 66 and 67, far from the areas surveyed by the Ida Green, displayed strong, readily identified BSRs.

The BSRs noted in the single channel data are concentrated along a section of the Mexican continental slope between Manzanillo and Acapulco with the greatest abundance offshore of Zihuatenejo (Figure 50). In this area, the track lines of the Kana Keoki, the Glomar Challenger, and the Vema are closely spaced and subparallel. The presence of the BSRs was thus confirmed independently by use of lines collected at different times and with different equipment. BSRs in this area have not been previously reported.

The BSRs plotted in Figure 50 are similar in water depth and subbottom depth to the BSRs found on multichannel lines farther to the southeast along the trench. The BSRs offshore of Zihuatenejo, Mexico occur beneath water from 900 m to 3,000 m deep. The depth of the BSRs varies regularly with water depth from 0.3 to 0.65 sec. subbottom. The BSRs display the general form to be expected of thermally controlled features; the reflectors mimic the sea floor topography, but are more subdued, with fewer small-scale undulations.

An example of BSRs visible in two parallel seismic lines is shown in Figure 51. Figure 51A is from the 1974 cruise of the Kana Keoki. The BSR can be seen crossing sedimentary strata at about 0.4 sec. subbottom. Figure 51B is a seismic line obtained during DSDP Leg 67. The DSDP line is oriented parallel to Figure 51A and offset about 3.5 km to the southwest. The BSR is very prominent on the DSDP line at the same subbottom depth as on the line from the Kana Keoki. The nonconformable relationship of the BSR and enclosing sediments is very well displayed on the DSDP line (Figure 51B) due in part to the large vertical exaggeration of the display. The enhanced resolution of the BSR in the anticlinal structure suggests trapping of free gas beneath the BSR.

Incomplete seismic coverage of the area complicates comparison of the BSRs found on single channel records with the previously published multichannel lines from farther to the southeast. The multichannel seismic lines were collected over a few small areas of the Middle America Trench study regions. Tight survey grids were established offshore of Mexico south of Acapulco, Guatemala, and Costa Rica for the University of Texas multichannel seismic surveys. No multichannel records are available for the area offshore of Mexico shown to exhibit well defined BSRs in single channel lines. The survey from which the largest number of BSRs were identified, Cruise 74-0109 of the Kana Keoki, did not cover any of the areas included in the University of Texas multichannel lines.

Single channel records from the Glomar Challenger collected during DSDP Legs 66 and 67 include both the areas covered by the Kana Keoki single channel lines and the UT multichannel lines. Although the DSDP lines showed BSRs offshore of Zihuatenejo, Mexico, the BSRs near the drilling sites reported by Shipley et al. (1979), Shipley and Didyk (1982), Ladd et al. (1982), von Huene et al. (1982), and von Huene et al. (1985) from the UT lines could

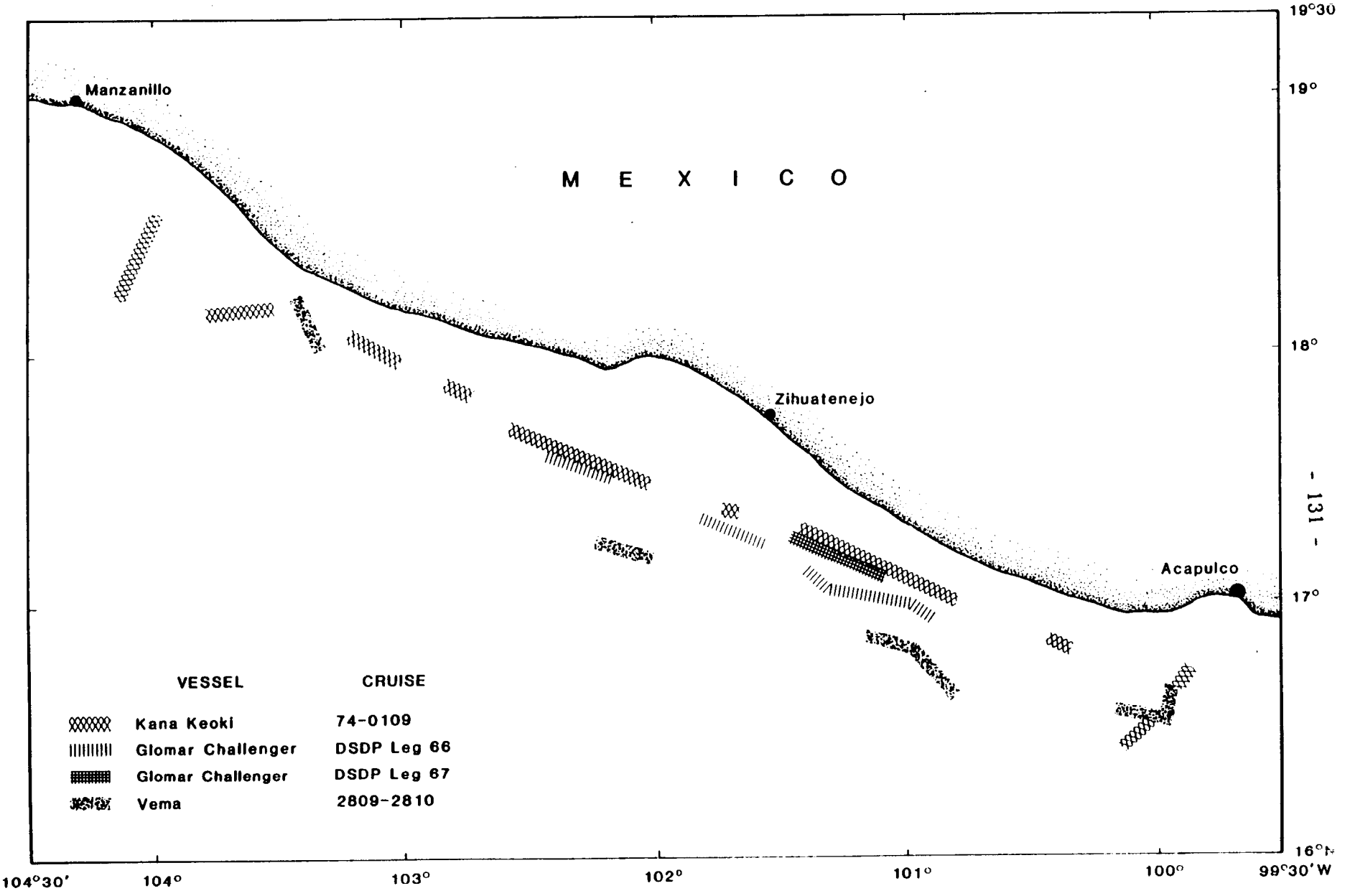

Figure 50. LOCATION OF BOTTOM SIMULATING REFLECTORS ON SINGLE CHANNEL SEISMIC LINES OFFSHORE OF MEXICO

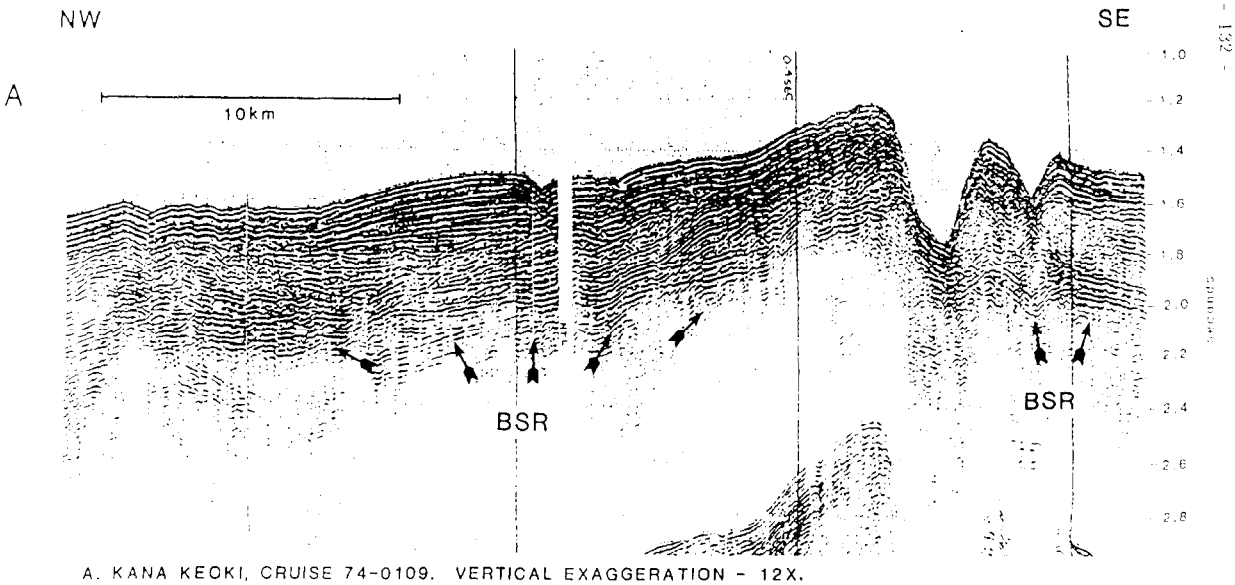

A. KANA KEOKI, CRUISE 74-0109. VERTICAL EXAGGERATION - 12X.

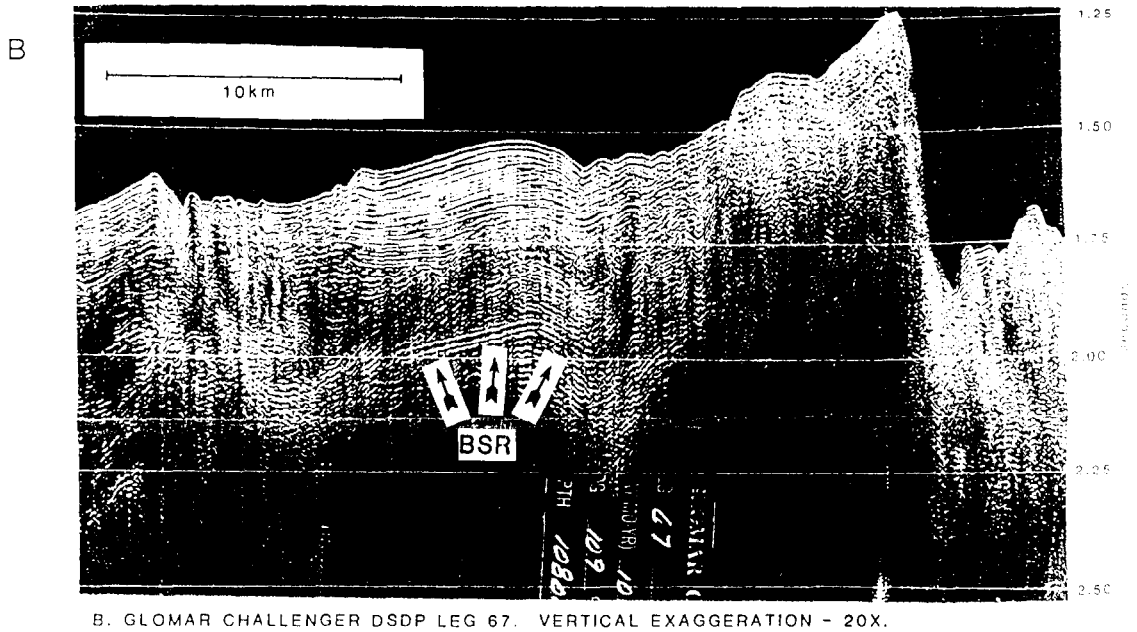

B. GLOMAR CHALLENGER DSDP LEG 67. VERTICAL EXAGGERATION - 20X.

NOTE: APPROXIMATELY 3.5km SEPARATE THE SECTIONS.

Figure 51. PARALLEL SINGLE CHANNEL SEISMIC LINES OFFSHORE OF ZIHUATENEJO, MEXICO

not be resolved. With prior knowledge of the location and depth of BSRs near the drilling sites, some faint disturbance in the response of the single channel DSDP seismic lines could be detected, but confident identification of BSRs could not be made.

One possible inference of strong BSRs on DSDP single channel records offshore of Zihuatenejo, Mexico and none over DSDP drilling sites offshore of Acapulco, Mexico and San Jose, Guatemala is that gas hydrates may be more common offshore of Zihuatenejo than at the DSDP locations. More extensive development of pore-filling hydrates above the lower boundary of the gas hydrate stability zone could increase seismic velocity to produce the better developed BSRs offshore of Zihuatenejo. Alternatively, large-scale gas migration from beneath the gas hydrate stability zone could have produced free gas accumulations, trapped by gas hydrates, possibly accounting for the very high reflectivity of the BSRs offshore of Zihuatenejo. Gas pooling beneath hydrates is supported by the general correspondence of strong BSRs beneath antiformal sections of the sea floor.

Another possible inference from the lack of correspondence of BSRs offshore of Zihuatenejo and the known BSRs near the DSDP drilling sites is that the BSRs offshore of Zihuatenejo may not be caused by gas hydrates. BSRs on UT multichannel lines near Leg 66, 67 and 84 drilling sites were shown by Shipley and Didyk (1982) and Ladd et al. (1982) to be due to gas hydrates by polarity analysis of the seismic signals. The negative polarity of the BSRs demonstrated that they resulted from a sharp decrease in acoustic impedance at the boundary. Only a gas hydrate phase boundary presents a plausible explanation of such a seismic contrast. Coincidence of the BSR depth and the pressure and temperature conditions of gas hydrate dissociation likewise strongly support a gas hydrate source for the BSRs in the University of Texas multichannel lines. Since the single channel seismic equipment aboard the Glomar Challenger could not resolve these proven gas hydrate boundaries, it could be argued that BSRs which did appear on the DSDP single channel lines must not be due to gas hydrates. Although the depths of the single channel BSRs offshore of Zihuatenejo agree closely with those expected for gas hydrates, the analog seismic records available at this time do not permit polarity analysis of the seismic signals. Thus, it is not known whether the BSRs offshore of Zihuatenejo are from gas hydrates, which would produce a negative polarity signal, or from a diagenetic boundary which would produce a positive polarity BSR signal.

Clarification of whether the BSRs offshore of Zihuatenejo, Mexico represent diagenetic boundaries or gas hydrate phase change can be obtained from seismic data from the Panama Basin. The Panama Basin is located adjacent to the Middle America Trench study region to the southeast. The Pacific margin of Panama was once an extension of the Middle America Trench, but an aseismic ridge apparently blocked subduction near the present border of Panama and Costa Rica (Krason and Ciesnik, 1986). The outlines of the inactive trench can still be discerned on seismic lines. Shipley et al. (1979) identified well defined BSRs on multichannel University of Texas seismic lines of the landward slope of the inactive trench. Shipley et al. (1979) demonstrated by polarity analysis (Table 11) and depth relationships (Figure 45) that the BSRs in the Panama Basin were most probably caused by gas hydrates. Work by Shipley and Didyk (1982) and by us has shown that the BSRs on multichannel lines offshore of Mexico and Guatemala respectively are similar to those in the Panama Basin and are thus very probably caused by gas

hydrates (Table 11, Figures 47 and 48). Single channel seismic lines were also recorded over the Panama Basin continental margin near the UT seismic lines. Lines from Cruise 74-0109 of the Kana Keoki, from DSDP Legs 67 and 84, and from the US Navy research vessel Balboa, Cruise BA-71C all display vivid BSRs in the same area as those identified by Shipley et al. (1979). Comparison of the single channel BSRs from the Panama Basin and those from offshore of Zihuatenejo, Mexico show a very strong resemblance. The records from the Kana Keoki show very similar response patterns on BSRs from both areas. The BSRs on the Kana Keoki records from the Panama Basin are at shallower subbottom depths than those offshore of Mexico. This is consistent with results from multichannel lines in the Panama Basin (Figure 45; Shipley et al., 1979; Shipley and Didyk, 1982), and is a result of the anomalously high geothermal gradients of the Panama Basin (Krason and Ciesnik, 1986). The records from the Glomar Challenger from DSDP Legs 67 and 84 are particularly interesting. The BSRs from the Panama Basin from both cruises show strong BSRs on single channel lines coincident with the multichannel lines of Shipley et al. (1979). These are the only BSRs on the DSDP seismic records from Leg 84. None exist in records which cross BSR-bearing multichannel lines offshore of Costa Rica or Guatemala. Unfortunately, no seismic record exists of the Glomar Challenger's transit from offshore Guatemala to Manzanillo, Mexico subsequent to drilling on Leg 84. The records from Leg 67 are also informative. The only BSRs on the seismic records from Leg 67 are from the Panama Basin and from offshore of Zihuatenejo, Mexico (Figure 50).

The correspondence of BSRs in single channel lines from offshore of Zihuatenejo, Mexico with those from the Panama Basin argues strongly that the BSRs offshore of Mexico are caused by gas hydrates. Careful analysis of Panama Basin BSRs by Shipley et al. (1979) strongly supported a gas hydrate origin. By analogy, it is reasonable to conclude that the abundant BSRs offshore of Mexico between Manzanillo and Acapulco indicate widespread gas hydrates throughout this largely unexplored stretch of the Middle America Trench study region.

The very high-amplitude BSRs offshore of Zihuatenejo, Mexico directly overlie the subducted Orozoco Fracture Zone. The only other locality along the western margin of southern North America to consistently display easily resolved BSRs in single channel seismic lines is on the northeast flank of the Panama Basin. Those BSRs are also located directly over a major subducted transform fracture zone, the Coiba Fracture Zone (Krason and Ciesnik, 1986). Indeed, there are no other fracture zones along the western margin of North America between the Orozoco and Coiba Fracture zones; neither are there areas which display a similar density of BSRs on single channel seismic records between these fracture zones (Figure 52). The possible connection of the structure of the subducting plate and gas hydrate presence in the overriding plate is explored in this report in the section of structural controls on gas hydrate formation.

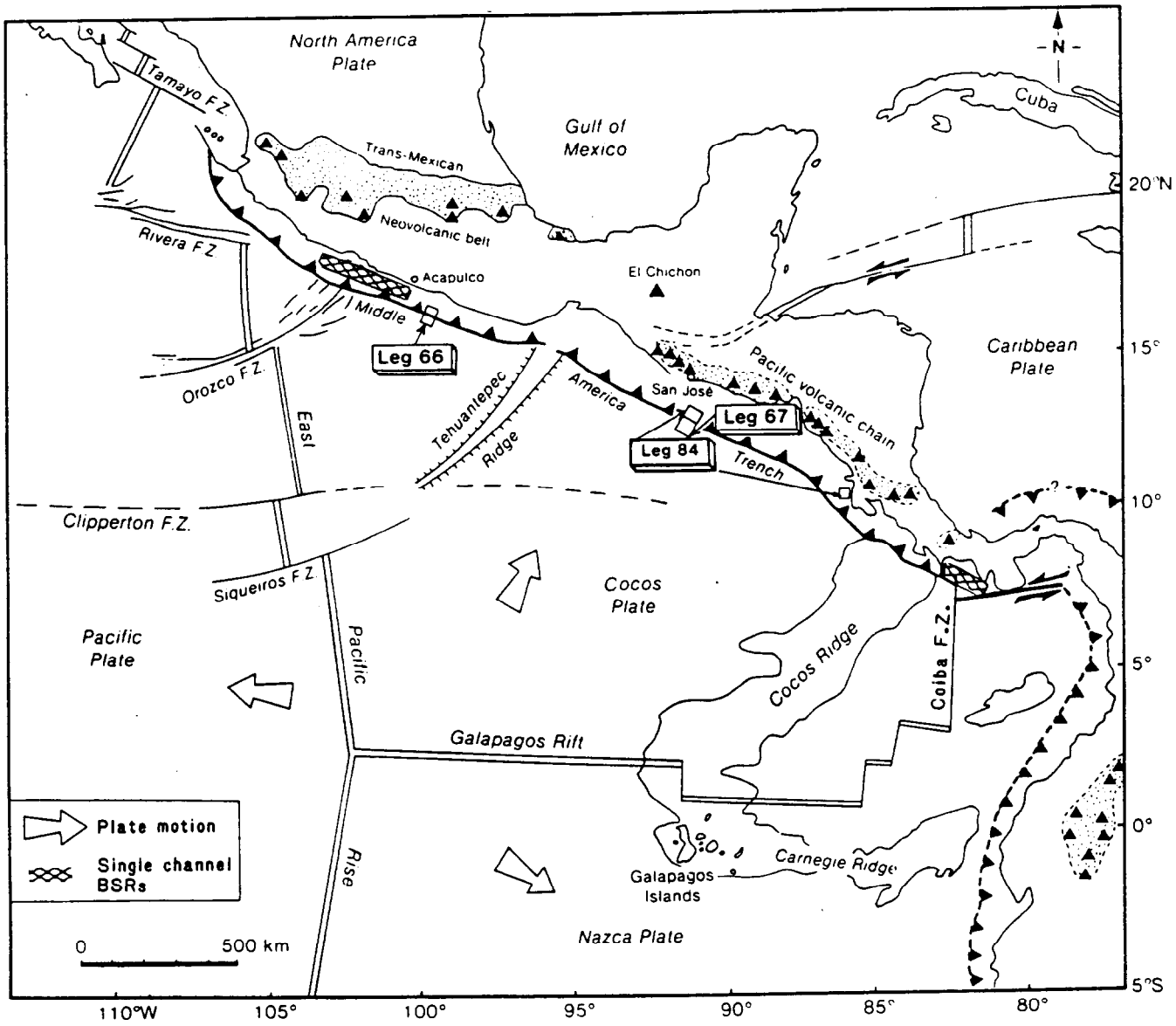

Figure 52. TECTONIC SETTING OF BOTTOM SIMULATING REFLECTORS IN SINGLE CHANNEL SEISMIC RECORDS

Base map modified from Baltuck et al., 1985

Pore Water Chemistry

Pore water at some DSDP sites along the Middle America Trench showed distinctive trends. At locations where gas hydrates were detected or inferred, the salinity and chlorinity of the interstitial water generally decreased with depth. Also, $\delta^{18}O$ values for pore water showed an increase which generally corresponded with the salinity and chlorinity decrease.

DSDP Leg 66

Data on pore water chemistry were not included in the Leg 66 Initial Reports volume (Watkins et al., 1982). Possible relationships of pore water chemistry and gas hydrate presence noted on Legs 67, 76, and 84 led to the later analysis of stored samples of Leg 66 pore water by Gieskes et al. (1985).

Analysis showed an irregular relationship of chlorinity depletion and gas hydrate presence (Figure 53). At Site 490, gas hydrate recoveries at 139 m, 145 m, and 165 m subbottom correspond with depletion of chloride to 94% of its original content. However, the hydrate recovered at 364 m does not effect the pore water chlorinity of the closest analyzed samples. Chlorinity is increased to 105% and 100.3% of its near sea-floor value at 305 and 368 m respectively. At Site 491, the hydrate recovered at 163 m corresponds to a chlorinity value 78% of the sea-bottom sample. The gas hydrate found at 89 m is not reflected in the chlorinity of nearby water samples. A minimum in chlorinity of 76% of sea-floor values occurs at 367 m. No hydrate was recovered from this interval. Likewise, no gas expansion cracks or violent degassing associated with hydrates was noted near the deeper chlorinity minimum at Site 491.

Chlorinity decreased smoothly with depth at Site 492. The gas hydrate samples recovered at 140 and 170 m depth correspond with chlorinity values 88% and 87% of the shallowest analyzed sample. The profile implies continual enrichment in interstitial gas hydrates with depth with hydrates occupying 15% of the pore volume at 210 m, the deepest sampled interval.

The chlorinity of pore water recovered from gas hydrate intervals is thought to be depleted due to dilution of pore water by fresh water from decomposition of gas hydrate crystals (Hesse and Harrison, 1982). The dilution factor should affect other dissolved species as well as chloride. In Figure 53, few depletion trends parallel to the chlorine profile can be discerned. The alkalinity profile of Site 490 has a response similar to that of chlorinity near the depths of hydrate recoveries between 139 m and 165 m.

DSDP Leg 67

Harrison et al. (1982) measured chemical concentrations in pore water from Leg 67 cores. They noted alkalinity profiles indicating active bacterial methanogenesis at all locations except Site 495 on the Cocos Plate seaward of the trench.

The pore water data from two sites at which gas hydrates were indicated were distinct from the general trends. Gas hydrate samples were

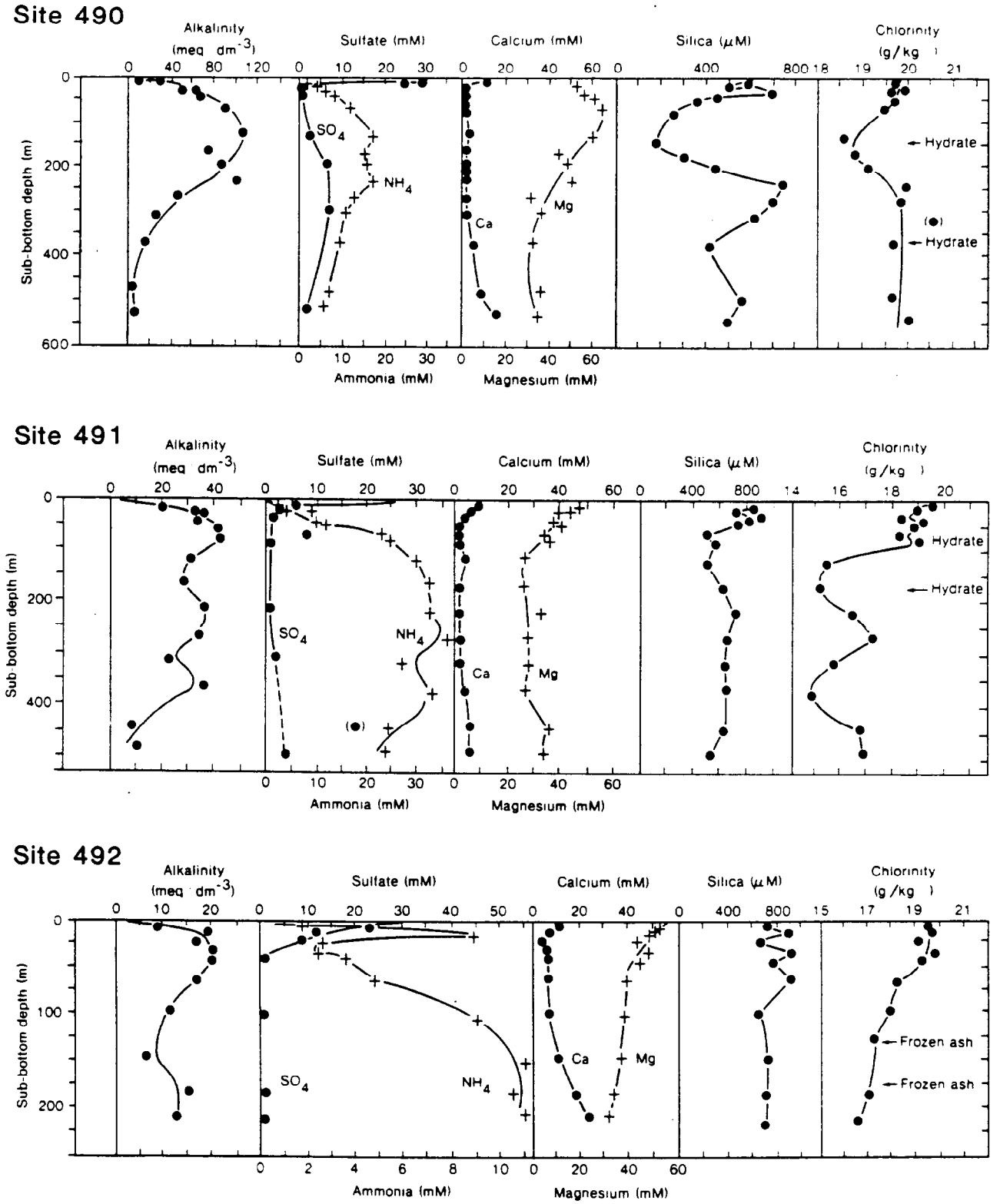

Figure 53. **PORE WATER CHEMISTRY OF GAS HYDRATE BEARING SITES OFFSHORE MEXICO**

After Gieskes et al., 1985

recovered from Site 498 (Harrison and Curale, 1982). Unfortunately only three water samples were collected from Site 498, and they were apparently contaminated with sea water (Harrison et al., 1982). Cores from Site 497 showed abundant gas expansion cracks and occasionally active degassing between 160 and 370 m. A chunk of solid gas hydrate was recovered from 368 m at Site 497. Pore water from Site 497 showed smooth trends of salinity and chlorinity decreasing with depth and ^{18}O increasing with depth (Figure 54). At 367 m, the pore water contained only 9.1 per mil chloride, 48% of sea water concentration, implying that 54% of the available pore water was occupied with hydrates. No mention of evidence for gas hydrates below 368 m was made by Harrison and Curale (1982) but the pore water is even more depleted in chloride at 394 m (9.0 per mil). A downhole increase to 2.52 per mil SMOW was measured for the ^{18}O composition of the pore water.

No gas hydrates were recovered at Site 496, but a BSR is evident beneath the drill site on reprocessed seismic lines (Figure 17). The pore water profiles of Site 496 resemble Site 497. The chlorinity values decrease from 19.1 to 9.6 per mil while ^{18}O values increase to 2.59 per mil SMOW (Figure 54).

The other drill sites tested by Harrison et al. (1982), Sites 494, 495, 499, and 500, all were characterized by relatively constant chlorinity values and $\delta^{18}O$ increases of less than 0.51 per mil.

DSDP Leg 84

Interstitial water squeezed from Leg 84 sediment cores was analyzed by Hesse et al. (1985). Characteristic decreases in chloride content were measured for the three holes from which gas hydrates were recovered, Sites 565, 568, and 570 (Figure 55). The downhole increase in $\delta^{18}O$ values recorded from Leg 67 pore water (Harrison et al., 1982) was apparent only at Site 568.

Site 565 data showed a decrease in chlorinity to 13.9 per mil at 276 m (Figure 55). No analyses were reported for the depths from which gas hydrates were recovered, 285 and 319 m. The decrease in chlorinity occurred continuously from near the sea floor; however, abundant gas was not observed in cores from depths of less than 170 m. Oxygen isotopic data from Site 565 showed no consistent increase with depth, fluctuating between -1.26 and 0.76 per mil. Hesse et al. (1985) attribute the lack of a trend suggesting hydrates in the Site 565 ^{18}O data to diagenetic alteration of volcanic ash which would presumably produce large quantities of ^{18}O depleted water. However, core descriptions from Site 565 indicate less volcanic ash than other holes cored on Legs 67 and 84 where increasing ^{18}O content was observed with depth.

Site 568 exhibited a consistent decrease in chlorinity along with an increase in ^{18}O with depth (Figure 55). Chlorinity decreased to 9.54 per mil at 401 m and 10.58 per mil at 414 m, 50% and 55% respectively of near-sea-floor values. A very high value of 3.31 per mil was obtained for $\delta^{18}O$ at 401 m. Thus, chlorinity and $\delta^{18}O$ values reach their respective minimum and maximum at 401 m, which is 2 m above the depth of the only sample of gas hydrate recovered at Site 568. The continuous change in pore water chemistry indicates that gas hydrates occur at shallow subbottom depths and increase in abundance regularly downhole. This contradicts assertions by

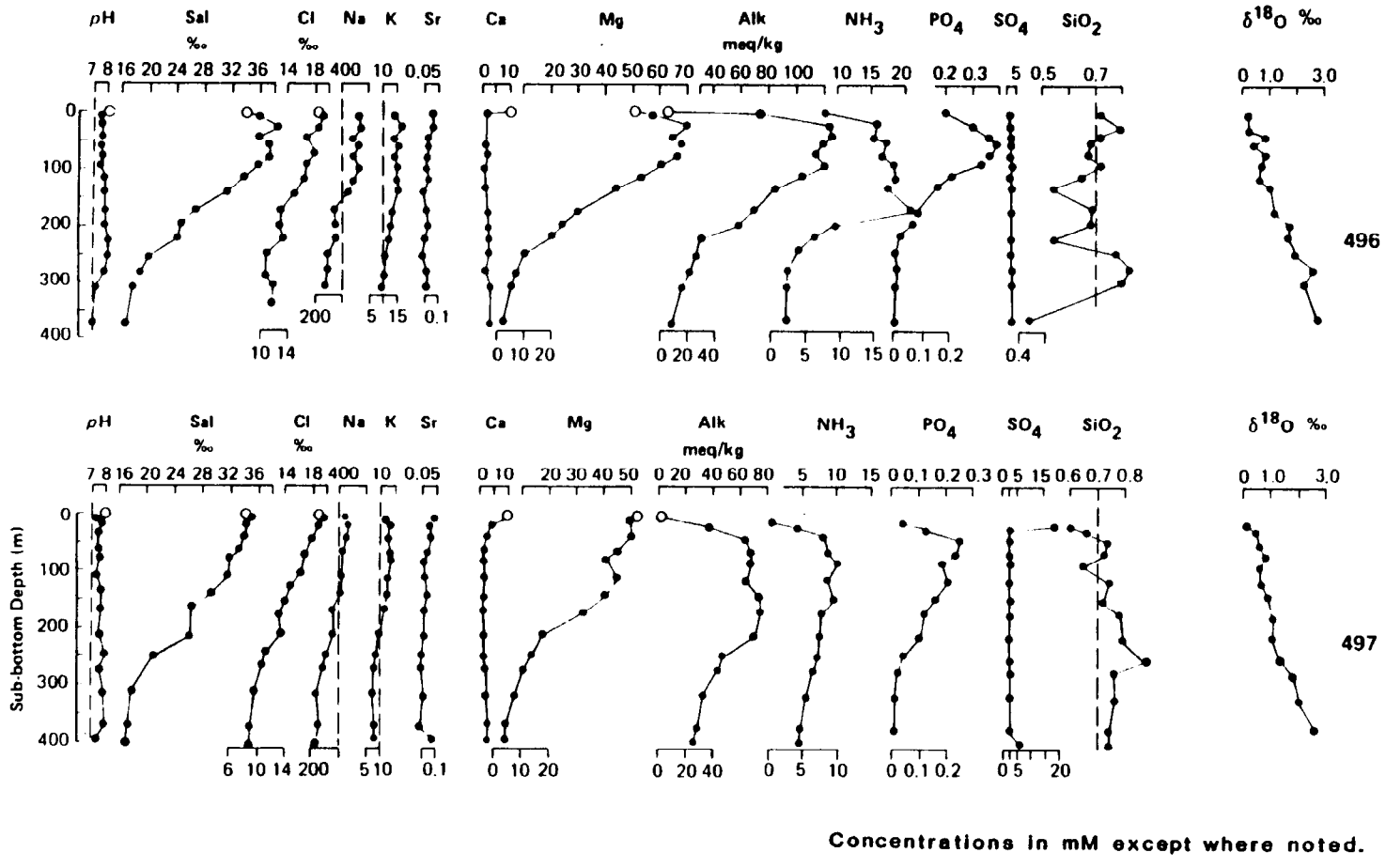

Figure 54. PORE WATER CHEMISTRY OF POSSIBLE GAS HYDRATE BEARING SITES, DSDP LEG 67, OFFSHORE GUATEMALA

After Harrison et al., 1982

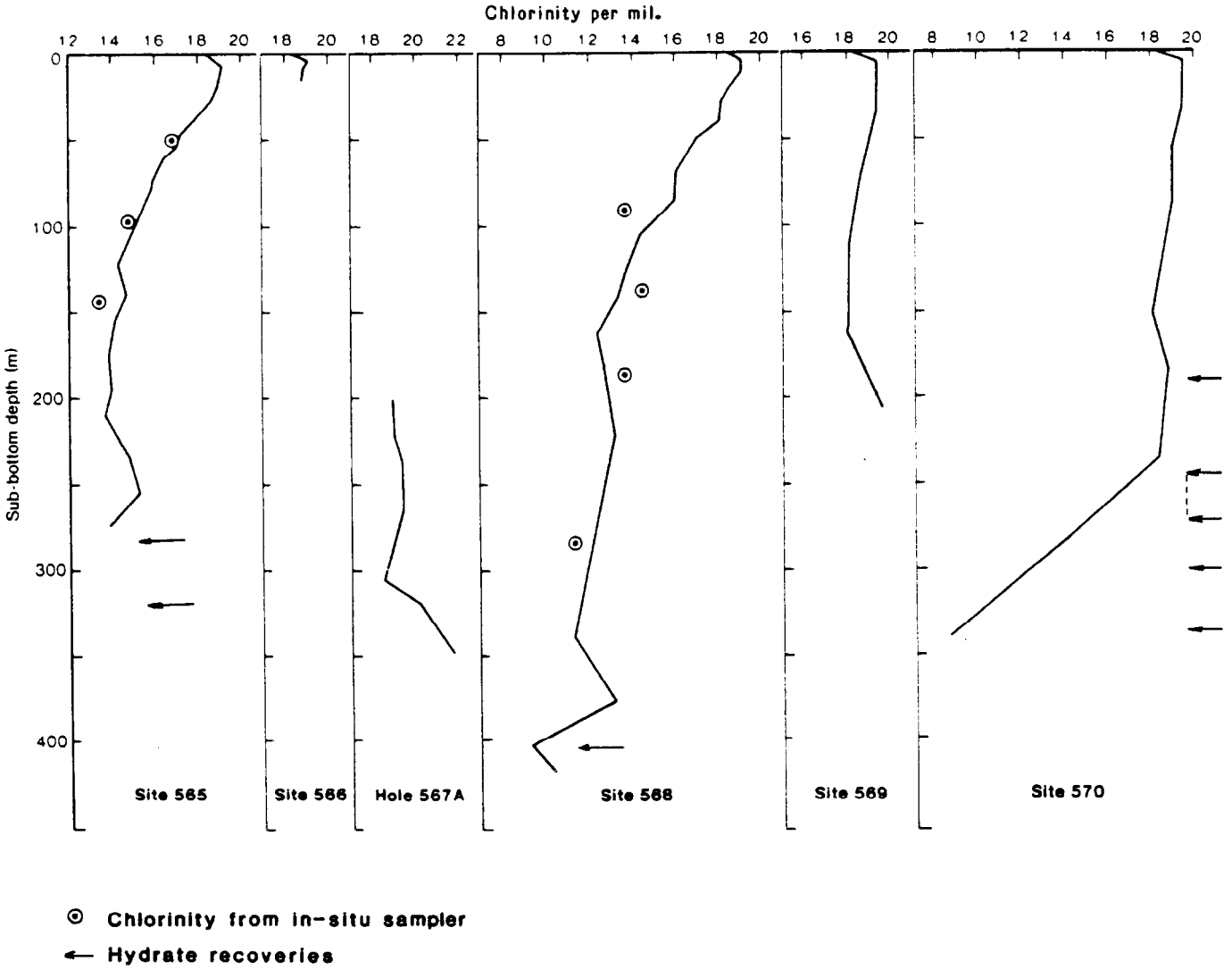

Figure 55. CHLORINITY PROFILES OF DSDP LEG 84 SITES

Modified from Kvenvolden and McDonald, 1985, using data from Hesse et al., 1985

Kvenvolden and McDonald (1985) that hydrates first occur at 190 - 200 m at 568 based on molecular distributions of core gas.

At Site 569, no consistent downhole changes are seen in pore water chlorinity (Figure 55) or ^{18}O values (Hesse et al., 1985). However, Hesse et al. (1985) asserted that gas hydrates were probably present at Site 569 based on relative transparency of seismic returns at the site. Conversely, Kvenvolden and McDonald (1985) contended that gas hydrates were present at Site 569 based on decreasing chlorinity with depth. The chlorinity profile presented by Kvenvolden and McDonald (1985) to support gas hydrate presence at Site 569 may have been incorrectly drafted. A chlorinity value of about 17 per mil was plotted for 207 m depth, implying downhole freshening of pore water, whereas Hesse et al. (1985) reported and plotted a value of 19.63 per mil, slightly above sea water chlorinity (Figure 55). Hesse et al. (1985) performed the analyses reported by Kvenvolden and McDonald (1985) and thus are probably more reliable.

Fewer pore water samples were collected for analysis at Site 570 than at Sites 565 and 568, resulting in less detailed information on downhole chlorinity trends. Also, no water samples from depths greater than 183 m were analyzed for ^{18}O content.

A slight decrease in chlorinity (0.65 per mil) is seen at Site 570 down to a depth of 234 m (Figure 55). The two deeper samples show rapidly decreasing chlorinity with depth: 18.75 per mil at 234 m, to 14.30 per mil at 280 m, to 8.95 per mil at 337 m. The sample from 280 m is from a silty mud 1 to 4 m beneath a recovered sample of fracture-filling gas hydrate. The water sample from 337 m is from a loose feldspathic sand, 20 cm below a recovered gas hydrate. Most other gas hydrate recoveries at Site 570 occur in between the widely spaced water samples. The water sample from 183 m depth is less than 8 m above the shallowest occurrence of gas hydrates at Site 570. However, that water sample corresponds to a local maximum in chlorinity and a local minimum in $\delta^{18}O$ values; proximity to gas hydrate was not indicated by these data. The zone of abundant gas hydrates including the massive gas hydrate and very common fracture-filling gas hydrates occurs between the 234 m water sample and the 279 m water sample. The only information available on the water composition from that important interval is the results of analysis of water dissociated from the massive gas hydrate recovered at 249 m. Brooks et al. (1985) reported a salinity of 2.6 per mil and a mean $\delta^{18}O$ value of 2.3 per mil for the gas hydrate water. Hesse et al. (1985) reported a chlorinity value of 0.65 per mil for the massive gas hydrate water.

Discussion

The relationship of gas hydrate presence, chloride ion depletion, and ^{18}O enrichment was derived from Leg 67 pore water data. As proposed by Hesse and Harrison (1981) and Harrison et al. (1982), when gas hydrates form in sediments, chloride and other ions are excluded from the crystal lattice similar to salt exclusion due to simple freezing. Also analogous with freezing, $H_2{}^{18}O$ is concentrated in the hydrate lattice due to the kinetic isotope effect of slower vibrational frequencies of $H_2{}^{18}O$. Subsequent to gas hydrate formation, the remaining pore water is enriched in salts and depleted in ^{18}O. According to Hesse and Harrison (1982), these local concentration gradients are eventually eliminated by diffusion of ionic substances upward toward the sea floor and diffusion of $H_2{}^{18}O$ downward to the depth at which gas hydrate

formation has depleted $H_2{}^{18}O$. By the diffusive equilibration process as envisioned by Hesse and Harrison (1982), a hydrated sediment section is eventually composed of gas hydrates and coexisting pore water with chloride and $\delta^{18}O$ values near those of sea water (~19.6 per mil and 0.0 per mil respectively). When this hydrated section is cored, the decreased pressures and increased temperatures result in dissociation of hydrates mixing hydrate water having very low salinity and high ^{18}O content with the existing pore water resulting in the observed pore water with intermediate concentrations of the indicator species.

To test whether the pore water coexisting with the hydrate is of normal chlorinity at in situ conditions as predicted by Hesse and Harrison (1981), an in situ pore water sampler was deployed at Sites 565 and 568. Two in situ samples were contaminated by sea water. The chlorinities measured by the in situ sampler on the remaining runs were very close to those measured on board ship by squeezing pore water from recovered cores (Figure 55) and were significantly depleted in chloride ion relative to sea water. These results tend to contradict the contentions of Hesse and Harrison (1981) that pore water chloride depletion results only from dilution due to dissociation of hydrates during core recovery. The presence of chloride-depleted water at in situ conditions implies that the effect may be unrelated to gas hydrate presence. Hesse et al. (1985) explained the discrepancy by asserting that the in situ water sampler extracts pore water from the formation by creating a pressure differential which dissociates any hydrates present. Thus, the in situ sampler duplicates the conditions present during shipboard sampling; since gas hydrates are dissociated during the in situ sampling process as well, the chlorinity values obtained are similar. It seems curious, however, that the low pressure drops and the relatively short time available for hydrate dissociation while deploying the in situ water sampler should result in sufficient hydrate dissociation to so closely duplicate pore water values obtained on board ship after long exposure to very low (1 atm) pressure.

Several difficulties exist in applying the pore water freshening model of Hesse and Harrison (1981), Harrison et al. (1982), and Hesse et al. (1985) to the coring results from the Middle America Trench. Holes with progressive decreases in chlorinity (eg. 496, 568) would indicate gas hydrate occurrences at shallow subbottom depths increasing regularly with depth. The magnitude of the pore water freshening implies that gas hydrates occupy a very large proportion of the available pore space (over 50%). The enrichment in ^{18}O which occurs concurrently with the decrease in chlorinity is larger than could be accounted for if the changes were caused by the dissociation of the same amount of gas hydrate.

Agreements with geological data. The previously noted lack of gas in cores from the sea floor to 170 m at Site 565 presents a difficulty because the chlorinity profile showed a continuous decrease in salinity in that interval. Although no gas hydrates were recovered from Sites 496 and 568 at the depth where chlorinity was regularly decreasing, the abundance of gas expansion voids and core liner gas at these sites suggests that the gas hydrates indicated by the pore water chemistry dissociated during drilling and core retrieval (Hesse et al., 1985). However, the lack of gas or degassing features at Site 565 where predicted by chlorinity conflicts with the proposed mechanism for chlorinity decrease. Pore water salinity decreased continuously with depth at Sites 492, 496, 497, 565, and 568, but gas hydrate recoveries at these sites were isolated. Gas hydrates were recovered at these sites only

from permeable lithologies. Fractures or interstitial pores in volcanic ash or terrigenous sand hosted the gas hydrates identified in the cores at these locations. No gas hydrates were found in nearby muds and mudstones which had low chlorinity values indicative of gas hydrates. Hesse et al. (1985) explained this disparity by once again invoking the presence of very fine crystals of gas hydrates dispersed throughout the muds and mudstone. These very fine dispersed gas hydrate crystals dissociate before being brought on deck, resulting in gas and gas expansion features, but no gas hydrates. Abundant gas and expansion cracks at these sites was cited as suggestive evidence of such a process.

Pore water chemistry results from Site 570 have been used as an example of the accuracy with which gas hydrate occurrences can be predicted by chlorinity values (Hesse et al., 1985; Kvenvolden and McDonald, 1985). At Site 570 the chlorinity decreases only very slightly to a depth of 234 m. Below 234 m chlorinity decreases very rapidly reaching a value of 8.9 per mil at 337 m. This agrees well with gas hydrate recoveries. Abundant fracture-filling, massive, and interstitial gas hydrates were recovered between 240 m and 340 m at Site 570. Above the distinct decrease in chlorinity below 234 m, only one isolated gas hydrate occurrence was recorded at 192 m.

A contradiction exists in the interpretations put forth by Hesse et al. (1985) for the relationship between gas hydrate presence and pore water chemistry at Sites 492, 496, 497, 565, and 568 on one hand and Site 570 on the other. The chemical data from Sites 492, 496, 497, 565, and 568 indicate continuous distribution of gas hydrates in sediments in which no gas hydrates were found upon recovery. Abundant gas in these sediments was interpreted to indicate that the gas hydrates responsible for the chlorinity dilution had dissociated during core recovery. At Site 570, a fairly close match of chlorinity and recovered gas hydrates showed that very little gas hydrate formation occurred in sediments shallower than 234 m subbottom. As noted above, this ignores a documented gas hydrate occurrence at 192 m. More importantly it ignores that the sediments shallower than 234 m at Site 570 were very gassy and exhibited the same degassing features as Sites 492, 496, 497,and 568. While sediment degassing was taken to indicate dispersed gas hydrates at sites where pore water chlorinity predicted hydrate presence, degassing at Site 570 where no gas hydrates were predicted by chlorinity was not taken into account. Thus, the observed gas hydrate to pore water chemistry relationship may reflect either continuous distribution of dispersed, nonrecoverable gas hydrates as exemplified by Site 568, or the discrete recoverable gas hydrate zones as seen at Site 570. It is difficult to understand how the data can consistently support both cases.

Gas volumes. Resource implications of pore water chlorinity change being due solely to gas hydrate composition are significant. Very low chloride concentrations at Sites 496, 497, 568, and 570 of 9.6, 9.0, 9.5, and 8.9 respectively were recorded in the deepest sampled intervals. These values are all less than 50% of sea water chloride concentrations. Assuming that gas hydrates exclude all chloride ions, over 50% of the porosity of the sediment is occupied by gas hydrates. Since the amount of chloride in the pore water decreases approximately linearly from the sea floor to the bottom of the hole, the median proportion of pore space occupied by gas hydrates should be about one-half of the volume calculated for the bottom of the hole, or 25%. Assuming 50% sediment porosity, 12.5% of the volume of the sediment above the deepest sampled interval is composed of gas hydrate. For Site 568, where the lowest chlorinity value was drilled at about 400 m, the sediment column

would contain 50 m^3 of gas hydrate per m^2 of sea floor area. Thus the 1 km^2 area around Site 568 would contain 5 x 10^7 m^3 of gas hydrate. At 160 m of gas per m of hydrate, 8 x 10^9 m^3 of gas at standard temperature and pressure (STP) would exist in one km^2 around Site 568 between the sea floor and 400 m depth. Converting to conventional gas volume units used by U.S. industry, 2.8 x 10^{11} ft^3 or 0.3 TCF of gas exists in each 1 km^2 area near Site 568 between the sea floor and 400 m depth.

The low chlorinity values at depth (9.0 - 9.6 per mil) exist in three nearby holes, 496, 497, and 568. These holes all occur within 20 km of each other. The minimum area over which these very low chlorinity values exist can therefore be conservatively estimated at 400 km^2. Thus a probable gas volume of 120 TCF exists in gas hydrates in just one small portion of the Guatemala continental margin is obtained if the pore water freshening mechanism of Hesse et al. (1985) are logically extended. Although these potential gas resource estimates are indeed intriguing, we contend that they are unreasonably large, given the lack of any other supporting evidence of such extensive gas hydrate presence. It is more likely that other factors in addition to dilution of pore water by dissociating gas hydrates are responsible for the low chlorinity values obtained from deep sediments at DSDP Sites 496, 497, and 568.

Differences in chemical parameters. Another complication in direct application of the pore water freshening model of Hesse and Harrison (1981), Harrison et al. (1982), and Hesse et al. (1985) is the lack of agreement of ^{18}O and chlorinity data. Chloride is excluded from forming gas hydrate crystals, while $H_2{}^{18}O$ is preferentially included. The amount of gas hydrate present can be independently estimated from either the chloride or ^{18}O content. If changes in both of these pore water constituents are caused by the same process, i.e. hydrate formation, then independent estimates of gas hydrate content based on each should be consistent.

Determining the amount of gas hydrate in sediments based on the ^{18}O content of recovered pore water is complicated by the large number of uncertain factors preventing straightforward solution of an equation. The fundamental relationship representing the isotopic content measured from the pore water is:

$$\delta^{18}O(m) = X \cdot \delta^{18}O(h) + (1-X) \cdot \delta^{18}O(w),$$

where X represents the decimal fraction of the pore space occupied by hydrates at in situ conditions, and the subscripts m, h, and w represent measured (shipboard), hydrate, and in situ pore water values respectively. The most certain value is $\delta^{18}O(m)$, which is the value measured from pore water squeezed from cores after recovery. Claypool et al. (1985) and Hesse et al. (1985) independently determined pore water ^{18}O content from three Leg 84 sites. Their results are listed in Table 13. Although the trends in $\delta^{18}O$ values reported by each group are similar, the values are not identical, with results reported by Hesse et al. (1985) being about 0.3 per mil heavier than corresponding values from Claypool et al. (1985).

The isotopic enrichment of pure hydrate, $\delta^{18}O(h)$ was measured by Brooks et al. (1985) and Claypool et al. (1985). Brooks et al. (1985) reported that water from decomposition of a sample of massive gas hydrate from Site 570 had a mean $\delta^{18}O$ value of 2.3 per mil. Claypool reported a value of 3.72 per mil for a similar water sample. Sloan (1985) reported that B. Barraclough had measured a $\delta^{18}O$ value of 2.0 ± 0.2 per mil for the hydrate water.

TABLE 13.

OXYGEN ISOTOPE CONTENT OF PORE WATER FROM DSDP LEG 84

Site-core-section	Subbottom depth m	$\delta^{18}O$, per mil SMOW		Chlorinity per mil
		Claypool et al., 1985	Hesse et al., 1985	
568-1-1	1.4	2.85	----	----
568-1-2	3.0	0.28	.69	19.1
568-2-3	7.9	0.34	----	----
568-3-4	19.0	0.37	----	18.6
568-4-3	27.2	0.37	.61	18.2
568-5-4	38.3	0.61	.60	18.1
568-6-4	48.0	1.05	.67	17.1
568-8-5	68.1	---	1.72	16.1
568-10-3	84.6	0.71	.73	16.0
568-12-3	103.3	---	1.31	14.5
568-14-4	123.8	1.18	1.60	13.6
568-18-4	162.5	1.64	2.07	12.5
568-24-4	220.7	---	2.29	13.3
568-32-5	299.4	2.20	2.56	12.0
568-36-4	336.9	2.48	2.81	11.4
568-43-2	401.7	3.02	3.31	9.5
570-1-3	4.5	0.26	.61	19.5
570-4-3	31.7	---	.91	19.5
570-6-5	53.9	0.51	.66	19.0
570-10-1	86.6	---	.55	19.0
570-16-5	150.5	0.08	.41	18.2
570-20-1	183.3	0.13	.33	18.8
570-25-3	234.2	---	----	18.5
570-30-3	279.5	---	----	14.3
570-36-1	337.1	1.74	----	8.9

The greatest source of uncertainty in calculating in-place gas hydrate volumes is the isotopic content of pore water at in situ conditions, $\delta^{18}O(w)$, which was not directly measured. Isotopic determinations were made only for the gas-hydrate-bearing locations of Leg 84, Sites 565, 568, and 570. Values for holes with no evidence of gas hydrate presence, Sites 567 and 569, could be used to estimate $\delta^{18}O(w)$ had they been obtained. On Leg 67, $\delta^{18}O$ values were measured for Sites 496 and 497 on the continental slope, Sites 499 and 500 on the trench floor, and Site 495 on the Cocos plate. Sites 496 and 497, located near Site 568, were assumed to have gas hydrates present by Harrison et al. (1982) and thus are of no value in estimating $\delta^{18}O(w)$. The remaining measured locations are not in sedimentological regimes similar to upper slope sites and thus are not directly comparable, but may be useful for approximations. Sites 499 and 500 vary irregularly in ^{18}O downhole. Site 499 values range from -0.1 per mil to 0.42 per mil, averaging 0.2 per mil, with the deepest tested sample measuring 0.0. Site 500 values range from -0.38 per mil to 0.51 per mil in the upper 62 m of sediment with an average of about 0.2 per mil. Site 495 has an upper hemipelagic member which may be correlative with slope deposits; $\delta^{18}O$ values peak at 0.73 per mil at 50 m and steadily decrease to -0.1 per mil at 170 m depth. These values suggest that the background $\delta^{18}O$ values for pore water in the absence of gas hydrates is probably positive but may fluctuate greatly between slightly negative values and positive values as high as 1 per mil. This variation also suggests that sediment ^{18}O content is dependent on many processes; it may not be justified to attribute downhole increases in $\delta^{18}O$ solely to gas hydrate formation and dissociation.

The relationship between the isotopic content of coexisting water and gas hydrates is expressed as the isotopic fractionation factor, α , defined as:

$$\alpha = \frac{(^{18}O/^{16}O)\ \text{hydrate}}{(^{18}O/^{16}O)\ \text{water}}$$

The isotopic fractionation factor is more conveniently expressed as:

$$\alpha = \frac{^{18}O(h) + 1{,}000}{^{18}O(w) + 1{,}000}$$

The isotopic fractionation factor is not known exactly for methane hydrate. Davidson et al. (1983) measured a value of 1.0027 for THF hydrate. They suggested that the value for methane hydrate may be close to that of ice, measured by O'Neil (1968) at 1.003.

The probable value of α can be used to constrain the unknown or uncertain values in our equation for pore water ^{18}O content dependence on gas hydrate content. Replacing $\delta^{18}O(h)$ with values reported by Brooks et al. (1985), Claypool et al. (1985), and Sloan (1985) and using 1.003 for α, the probable $\delta^{18}O$ value of in situ pore water ($\delta^{18}O(w)$) is obtained. Values of 0.7, - 0.7, and -1.0 per mil assuming $\delta^{18}O(h)$ of 3.74, 2.3, and 2.0 per mil respectively are thus derived.

With these provisional isotopic values, the calculation of the amount of gas hydrate in the pore spaces of DSDP sites offshore of Guatemala can be made using pore water values reported by Claypool et al. (1985), Harrison et al. (1982) and Hesse et al. (1985).

$$\delta^{18}O(m) = X \quad \delta^{18}O(h) + (1-X) \quad \delta^{18}O(w)$$

can be readily rearranged to solve directly for x:

$$X = \frac{\delta^{18}O(m) - \delta^{18}O(w)}{\delta^{18}O(h) - \delta^{18}O(w)}$$

The isotopic values to be used in this equation, assuming the measured $\delta^{18}O(h)$ values from Site 570 are representative of Middle America Trench gas hydrates, vary with which source is used for the $\delta^{18}O(h)$ values (Table 14).

TABLE 14.

OXYGEN ISOTOPE CONTENT OF IN SITU PORE WATER BASED ON ISOTOPE CONTENT OF GAS HYDRATE AND ISOTOPIC FRACTIONATION FACTOR

Source	$^{18}O(h)$	$^{18}O(w)$
Barraclough (in Sloan, 1985)	2.0 per mil	-1.0 per mil
Brooks et al. (1985)	2.3 per mil	-0.7 per mil
Claypool et al. (1985)	3.74 per mil	0.8 per mil

The results of calculations for the deepest analyzed samples at Sites 496, 497, 568, and 570 are listed in Table 15. The three columns of percentage figures in Table 15 under the oxygen isotope category represent gas hydrate volumes expected based on α = 1.003 and the $\delta^{18}O$ values for natural gas hydrates as reported by Sloan (1985), Brooks et al. (1985), and Claypool (1985) respectively. On the right half of Table 15, the pore occupancies of gas hydrates calculated from chlorinity values reported by Hesse et al. (1985) are reported. Two cases are modeled for chlorinity based estimates: one where the chlorinity of the water from the dissociated gas hydrate has a value of 0.6 per mil as reported for Site 570, and the second with a chlorinity of 3.2 per mil as reported for the gas hydrate recovered from Site 568 (Kvenvolden and McDonald, 1985).

From Table 15 it is apparent that if the $\delta^{18}O$ values for gas hydrates reported by Barraclough (in Sloan, 1985) and Brooks et al. (1985) are typical for interstitial gas hydrates, the $\delta^{18}O$ values for pore water reported by Hesse et al. (1985) are too high to be attributed only to in situ gas hydrates. Values calculated for hydrate pore occupancy at Sites 496, 497, and 568 range from 107% to 143%. Since these values exceed the available pore space, they are clearly unrealistic. These high values could indicate that isotopic fractionation is much greater in gas hydrate formation than indicated by the accepted value of 1.003 for α. Alternatively, the isotopic fractionation occurs

TABLE 15.

GAS HYDRATE PORE OCCUPANCY CALCULATED FROM OXYGEN ISOTOPES AND CHLORINITY

DSDP Site	Depth m	OXYGEN ISOTOPES				CHLORINITY		
		$\delta^{18}O$ of Pore Water, per mil	Pore Space Filled With Gas Hydrates			Chlorinity per mil	Pore Space Filled With Gas Hydrates	
			$\delta^{18}O(h)=2.0$	$\delta^{18}O(h)=2.3$	$\delta^{18}O(h)=3.7$		$[Cl^-](h)=0.6$	$[Cl^-](h)=3.2$
496	380.5	2.59	119%	110%	62%	9.6	52%	60%
497	369.7	2.52	117%	107%	60%	9.1	55%	64%
568	401.7	3.31	143%	134%	86%	9.5	53%	61%
568	401.7	3.02*	134%	124%	77%	9.5	53%	61%
570	337.1	1.74*	91%	81%	34%	8.9	56%	65%

* Data from Claypool et al. (1985); other values in column from Hesse et al. (1985)

(h) indicates values for in situ gas hydrate.

to the extent predicted by Davidson et al. (1983), but is operating on pore water which was previously enriched in ^{18}O.

If the ^{18}O content is typically much closer to the value measured by Claypool et al. (1985), 3.72 per mil, then the calculated degree of gas hydrate pore occupancy is within reasonable limits for Sites 496, 497, and 568. Values ranging from 60% to 77%, while greater than indicated by drilling, are at least within the realm of possibility.

Oxygen isotope data from 337 m at Site 570 shows isotopic enrichment which is consistent with observed gas hydrate presence. The water sample was taken from a core composed of structureless feldspathic sand, less than 20 cm from a recovered piece of gas hydrate. The core description indicates that the entire core (1.8 m) "was full of gas hydrate that has melted" (von Huene et al., 1985). The structureless quality of the sediment recalls descriptions by Shipley and Didyk (1982) that hydrate cemented vitric sands from offshore of Mexico rapidly collapsed into a structureless slurry upon hydrate dissociation. Thus, at Site 570, the geologic evidence suggests that the oxygen isotope values from the recovered pore water probably reflect dissociation of gas hydrates. At other sites at which isotopically heavy pore waters were recovered at depth (496, 497, 568), the sediment samples were at least 3 to 10 meters away from confirmed gas hydrate occurrences. The sediments from which the water samples were obtained at Sites 496, 497, and 568 retained their bedding and structures, rather than being disaggregated by degassing as occurred at Site 570. The sedimentological evidence suggests that far lower proportions of the sampled intervals at Sites 496, 497, and 568 were composed of gas hydrates than at Site 570. An extension of this observation is that the degree of ^{18}O enrichment at Site 570 is consistent with the model of pore water alteration by gas hydrates, while the extremely heavy pore water at Sites 496, 497, and 568 suggest that an additional process is affecting the ^{18}O content of the pore water.

The chlorinity-derived estimates of gas hydrate concentration in Table 15 are consistent at all four sampled locations. Calculated values range from 52% to 65% of available porosity occupied by gas hydrates. Once again the range of values obtained for Site 570, 56% to 65%, agree with the degree of degassing indicated in core descriptions. However the chlorinity-derived gas hydrate pore occupancy estimates 52% to 64% for Sites 496, 497, and 568 are not consistent with the well preserved state of the cores near the sampled intervals.

Another interesting aspect of the calculated amounts of gas hydrate present is the lack of consistency between values obtained from $\delta^{18}O$ values and those from chlorinity data (Table 15). Each set of chlorinity-derived values agrees closely with the maximum and minimum values separated by 5%. However, each set of estimates calculated from ^{18}O data varies widely between holes showing a range of values between the maximum and minimum of 52%. This observation also suggests that the ^{18}O and chloride ion contents of at least some holes are controlled by processes other than gas hydrate formation and dissociation.

Hesse et al. (1985) addressed the question of whether processes other than gas hydrate formation may be producing the observed changes in pore water chemistry. The alternative which Hesse et al. (1985) considered is a pool of fresher water deeper than any sampled interval. Based on work on previous DSDP legs, they modeled the chlorinity change expected from diffusion of chlorine into the deep pool and plotted the expected trend on a diagram of chlorinity vs. depth. They plotted the chlorinity data from Sites

496 and 568 on the same axes. They rejected the possibility of any mechanism other than dilution due to gas hydrates as a cause for observed chloride ion concentration based on a lack of agreement between the trends of Sites 496 and 568 with the model curve. We have plotted data from Site 570 on the diagram of Hesse et al. (1986); Figure 56 shows a very close agreement with the expected trends above 234 m. The two deeper Site 570 data points occur in very close proximity to documented gas hydrate occurrences; their chlorinity values are shifted to the left as expected for hydrate dilution of pore water. Figure 56 demonstrates that Sites 496, 568, and 497 (not pictured) which are all located close together have chlorinity profiles different from that at Site 570. The data at Site 570 clearly agree with reported recoveries of gas hydrates. This suggests that the chlorinity profile of Site 570 may be more representative than those of Sites 496 or 568 of the relationship of gas hydrate and pore water chlorinity, i.e. depletion of chloride only where recoverable, well developed gas hydrate intervals exist.

Multiple fractionation. Hesse et al. (1985) proposed a mechanism by which the very high $\delta^{18}O$ values could be attained in the pore waters of Sites 496, 497, and 568. As previously discussed, the accepted value for the isotopic fractionation factor, 1.003, limits the enrichment of ^{18}O in gas hydrate to about 3 per mil. Pore water analyzed by Hesse et al. (1985) was proposed to be a mixture of melted hydrates and coexisting pore water of normal composition. Thus, for example, if the pore water from Site 568 with a $\delta^{18}O$ value of 3.31 per mil came from an interval composed of 50% hydrates and 50% pore water with sea water composition (0 per mil), the gas hydrate had a $\delta^{18}O$ value of 6.62 per mil. This clearly disagrees with the possible isotopic enrichment consistent with accepted values for α. Hesse et al. (1985) proposed that the high level of ^{18}O enrichment seen at Sites 496, 497, and 568 might result from multiple fractionation. In their proposed mechanism, the base of the gas hydrate zone would fluctuate vertically over time with ^{18}O becoming more concentrated with each dissociation-formation cycle. Gas hydrates, enriched by 3 per mil over coexisting pore water would melt in response to high heat flow or rapid uplift resulting in pore water which would be enriched by, for example, 1.5 per mil. Subsequent cooling or pressure increase would again cause gas hydrate formation, resulting in gas hydrate $\delta^{18}O$ values of 4.5 per mil. Another dissociation episode could produce pore water with a $\delta^{18}O$ value of 2.25 per mil. Subsequently formed gas hydrates would have the expected 3 per mil ^{18}O enrichment over the pore water, giving $\delta^{18}O$ value of 5.25 per mil. If this sediment section composed of 50% hydrate at $\delta^{18}O$ = 5.25 per mil and 50% pore water at 2.25 per mil was then cored, the pore water sampled aboard the drilling vessel would have a $\delta^{18}O$ value of 3.75, which is the range of the pore water sampled at Site 568.

By invoking a cyclical enrichment scheme, Hesse et al. (1985) sought to accommodate both chloride depletion and ^{18}O enrichment. Since chloride ions are excluded from the gas hydrate lattice, repeated formation cycles would not effect the concentration of chloride ion in the gas hydrate. However, ^{18}O is enriched in gas hydrate relative to its coexisting pore water and thus could be concentrated by each cycle of the proposed model. The multiple episodes of formation and dissociation could then account for chlorinity values corresponding to roughly 50% gas hydrate pore occupancy while concurrent $\delta^{18}O$ values suggested unreasonably high levels of gas hydrate pore occupancy, 91% to 143% (Table 15).

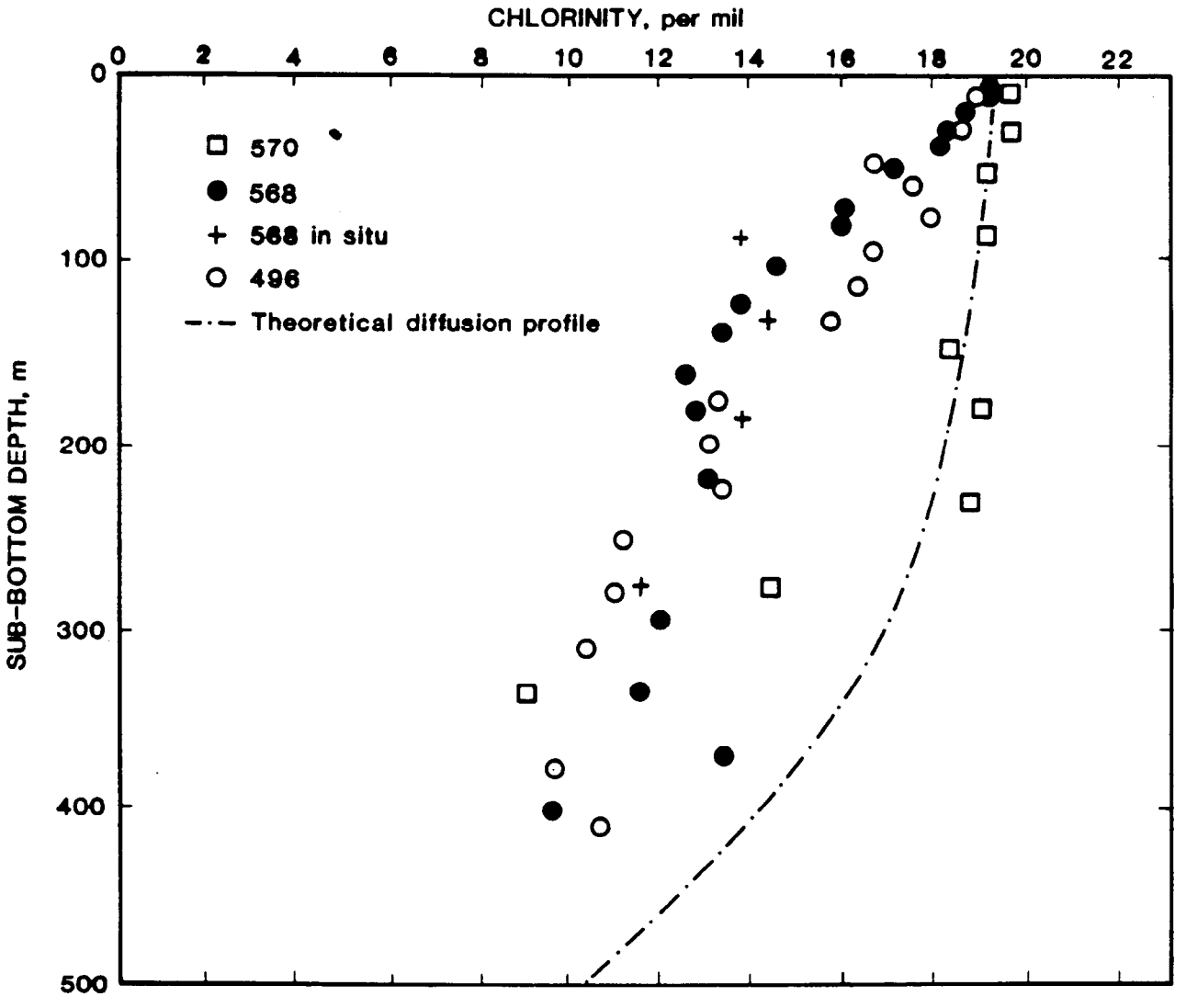

Figure 56. COMPOSITE CHLORINITY PROFILE FOR DSDP SITES 496, 568, AND 570

Modified from Hesse et al., 1985

Although the multiple fractionation model of Hesse et al. (1985) is attractive in its potential to reconcile the pore water chemistry data, its application to the geological environments of the Middle America Trench is problematical. The assumptions implicit in the multiple fractionational model are of debatable validity and in part conflict with the assumptions which form the basis of the original concept of pore water chemistry change due to gas hydrate presence.

The theory originally proposed by Hesse and Harrison (1982) and Harrison et al. (1982) to explain downhole changes in chloride ion and ^{18}O concentration assumes that the interstitial water is an open system. After gas hydrates are formed, the remaining pore water will be concentrated in chloride and depleted in ^{18}O. If the hydrate were to dissociate immediately after formation, the resultant pore water would have the same composition it had prior to gas hydrate formation. Gas hydrate formation can affect the chemistry of the pore water, as measured following core recovery, only if the pore water which coexists with the gas hydrate can reestablish approximately normal chloride ion and ^{18}O concentration by diffusion or by mass transport of the pore waters. If the pore water in contact with the interstitial gas hydrates can attain chloride and $\delta^{18}O$ values close to sea water, then dilution by dissociating gas hydrates after recovery could ideally account for anomalously low chloride concentrations and high ^{18}O concentrations measured.

In contrast, a closed pore water system seems to be required for the multiple fractionation mechanism proposed by Hesse et al. (1985) to be effective in increasing ^{18}O enrichment above the level suggested by concurrent chloride depletion. In the proposed formation-dissociation cycles, the water from the dissociated hydrate must remain available for inclusion into the next generation of gas hydrates formed. If the system were open, the $\delta^{18}O$ values in the pore water could reattain sea water values; subsequently formed gas hydrates would not be continually enriched in ^{18}O as the model requires. Only by cyclically reworking the same pore water can successive gas hydrate formation processes give the very enriched ^{18}O contents observed by Hesse et al. (1985).

The requirement of an open pore water system for the initial gas hydrate formation episode and closed conditions for the subsequent dissociation-formation cycles implies that a time constraint may exist in the process. A long period of diffusion would be necessary for the establishment of normal chemical composition following the initial formation of gas hydrates. The closed system required for the multiple fractionation process could result from a very short cycle time. If the dissociation and formation sequence occurred quickly, the pore water system would remain essentially closed; finite diffusion coefficients of ^{18}O and chloride ion through the matrix indicate that rapid formation after dissociation would affect much the same situation as limitation of diffusion by a nearly complete lack of permeability.

The requirement of a closed pore water system for the effective functioning of the multiple fractionation model of Hesse et al. (1985) suggests that the model's effect on ^{18}O content would be minimal. To be continually enriched in ^{18}O the gas hydrate formed at each cycle of the model must be formed from the pre-enriched pore water from the previous dissociation. However, by repeatedly forming gas hydrates from a finite volume of pore water, no cyclical enrichment in ^{18}O is possible. Thus, a logical paradox is developed; a closed pore water system is required for the enrichment process to operate, but the closed system itself prevents enrichment from occurring.

To illustrate the paradox, the example scenario which was presented previously to explain the model of Hesse et al. (1985) will be reexamined. In that example, a sediment interval with 50% of the pore space filled with gas hydrates and 50% filled with pore water with sea water chlorinity (19.4 per mil) and ^{18}O content (0.0 per mil SMOW). Upon in situ dissociation due to higher temperature or lower pressure, the pore water would mix with water from the hydrate with a chlorinity of 0.0 and $\delta^{18}O$ of 3 per mil. To make the fractionation mechanism work, the gas hydrate that forms in the next cycles must form from this pore water which is already enriched in ^{18}O, i.e. a closed system. In our original scenario, subsequent hydrate formation occurred with a 3 per mil fractionation of 1.5 per mil enriched pore water to produce gas hydrate with a $\delta^{18}O$ value of 4.5 per mil. Here the paradox comes into play. The initially formed gas hydrate would have a $\delta^{18}O$ value of 4.5 per mil. However, since the pore water system is closed, there is only a fixed amount of ^{18}O available. Thus, the enrichment in ^{18}O in the initially formed gas hydrate occurs at the expense of ^{18}O in the pore water, depleting the residual pool of pore water in ^{18}O. Further gas hydrate formation will still occur with 3 per mil enrichment over coexisting pore water, but the $\delta^{18}O$ value of the pore water is continually declining. Although the first-formed gas hydrate will have a $\delta^{18}O$ value of 4.5 per mil, the $\delta^{18}O$ value of later forming gas hydrates will steadily decline. Once 50% of the pore space is occupied by hydrates and then drilled or dissociated in situ, the resulting pore water will have the same chloride and ^{18}O concentrations as after the first dissociation (9.7 per mil and 1.5 per mil respectively). No net enrichment in ^{18}O would occur.

This paradox of requiring an open pore water system for any pore water chemistry change due to gas hydrates, and also requiring a closed system for the multiple isotopic model to function, could be resolved by invoking a sequence of alternating open and closed systems. The measured pore water levels for ^{18}O could be elevated to the levels measured by Hesse et al. (1985) only by invoking strict controls on the timing of the cyclical formation and dissociation. The period of time during which the gas hydrates are stable must be relatively long to satisfy the requirement imposed by Harrison and Hesse (1981) and Harrison et al. (1982) that the pore water in contact with the gas hydrate reestablish normal (sea water) ^{18}O and chloride ion concentrations. The next step, dissociation of gas hydrates and subsequent formation must occur relatively quickly so that the newly formed gas hydrate recycles the previously enriched pore water before the ^{18}O can reequilibrate by diffusion. By having a sequence of long intervals when the hydrate is solid and short intervals when it is dissociated, ^{18}O content could eventually increase in pore water in the manner envisioned by Hesse et al. (1985).

It is difficult to envision the geological conditions under which such pulsed formation-dissociation cycles could exist; but the possibility of a few such cycles occurring near DSDP Sites 496, 497, and 568 cannot be summarily excluded. However, if a large number of these cycles are necessary to produce the measured values, the likelihood that the multiple fractionation as proposed by Hesse et al. (1985) is the cause of the unusual water chemistry offshore of Guatemala is diminished.

The number of cycles needed to attain the reported $\delta^{18}O$ values can be estimated using a computer model. A simple program was developed which

calculated the isotopic content of recovered pore water after each formation-dissociation cycle. The general purpose model allows the isotopic fractionation factor, initial ^{18}O concentration, and gas hydrate pore occupancy to be specified.

Figure 57 shows the number of concentration cycles necessary to attain a given enrichment in ^{18}O. It is apparent from Figure 57 that a high degree of gas hydrate pore occupancy is necessary for any appreciable progressive enrichment in ^{18}O due to gas hydrate formation. A minimum of 50% pore occupancy is required to enrich pore water to the level measured from 337 m at Site 570. At lower in situ concentrations of gas hydrates, the possible enrichment asymptotically approaches a $\delta^{18}O$ value of less than the 1.74 per mil measured from Site 570. The same level of ^{18}O enrichment could be attained with three formation-dissociation cycles of 50% hydrates or 2 cycles of 60% gas hydrates. The minimum hydrate concentration required to reproduce the values measured at the bottom of Sites 496 and 497 is about 60%. At 60% pore occupancy, five formation-dissociation cycles are needed to attain 2.55 per mil. The same $\delta^{18}O$ values could also be obtained with four cycles if 70% gas hydrate pore occupancy is obtained in each cycle. Higher levels of gas hydrate pore occupancy do not reduce the number of cycles required.

The extreme enrichment recorded at 401 m depth at Site 568 would require many enrichment cycles, each with a very high concentration of gas hydrates in the interstices. From Figure 57, the model predicts that seven repetitions of gas hydrate formation each with 70% gas hydrates and 30% water in the sediment pores would be required. Alternatively, the same degree of enrichment could be achieved by repeating the formation process five times at 80% gas hydrate pore occupancy.

It should be stressed that the computer model used to derive Figure 57 was optimized to produce the maximum possible ^{18}O enrichment per cycle. The procedure simulates the pulsed sequence of very short dissociation-formation events followed by long periods of gas hydrate stability during which pore water can reequilibrate with surrounding interstitial water by diffusion. Thus it follows that the number of enrichment cycles necessary to achieve these $\delta^{18}O$ values would be greater in actual subsurface conditions. The modeling shows that the level of ^{18}O enrichment measured at DSDP Sites 496, 497, and 568 would require large numbers of enrichment cycles under the most favorable of circumstances. Thus we suggest that the ^{18}O enrichment measured at these sites was more likely caused by processes other than simple repetition of gas hydrate formation as proposed by Hesse et al. (1985).

If the pore water was previously enriched in ^{18}O due to some other diagenetic process, hydrate formation could further elevate the ^{18}O content to the levels recorded offshore of Guatemala. Fewer enrichment cycles would be required to attain a given $\delta^{18}O$ value with some prior enrichment of ^{18}O. The results of computer modeling of the enrichment process for various initial ^{18}O concentrations is summarized in Figure 58. Modeling of different levels of gas hydrate pore occupancy shows that high concentrations of gas hydrates in the sediment interstices are necessary to achieve substantial ^{18}O enrichment, even when the pore water is initially rich in ^{18}O. With a high degree of gas hydrate pore occupancy (e.g. 70%), pre-enriched starting material can substantially reduce the number of enrichment cycles needed to duplicate observed ^{18}O values. The $\delta^{18}O$ value measured for Site 570, 1.74 per mil, can be achieved by melting the initially formed hydrate if the original pore water was enriched 1 per mil before gas hydrate formation

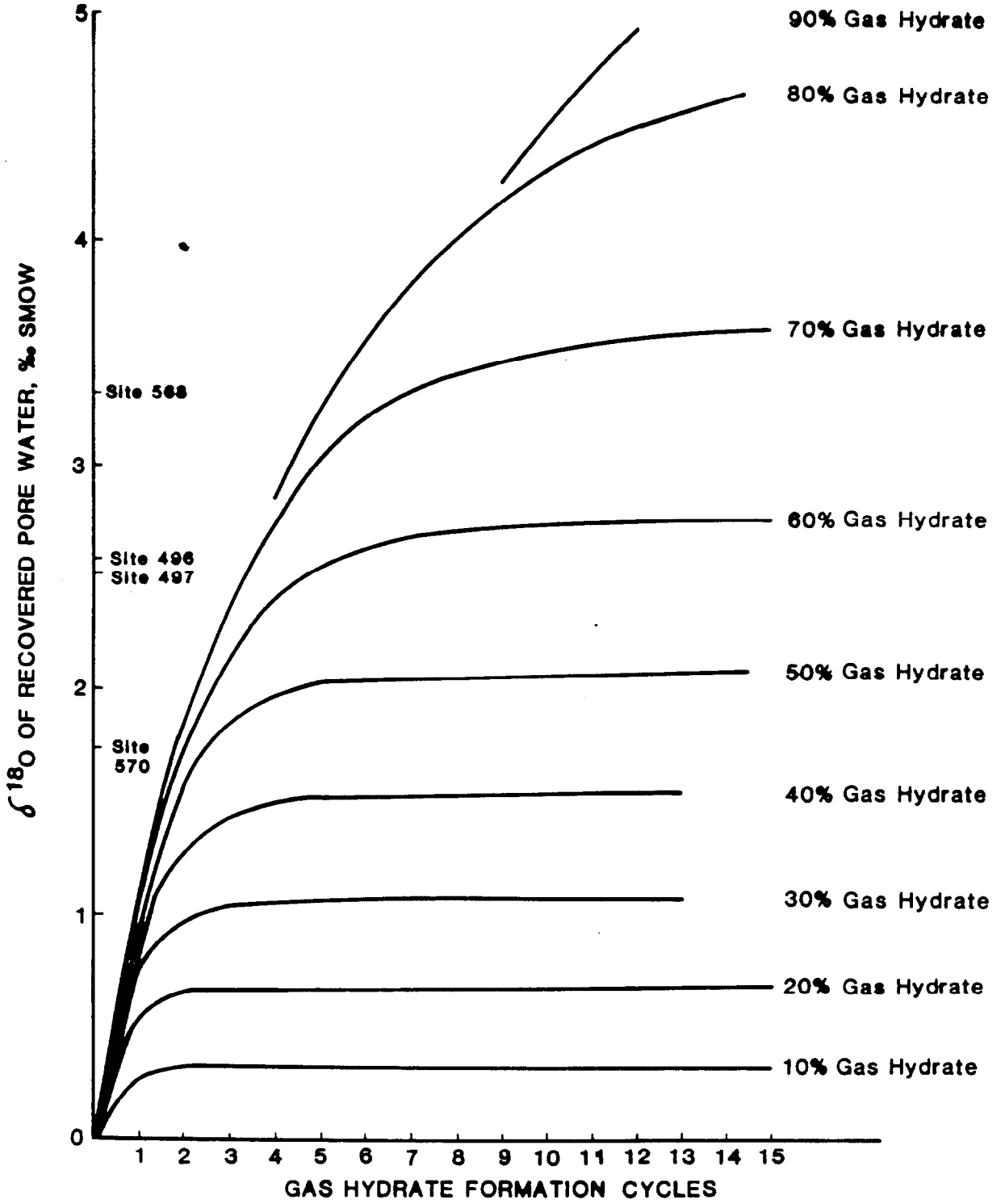

Assumes: α=1.003, pore water returns to 0.0‰ SMOW by diffusion after hydrate is formed, and no diffusion of ^{18}O from hydrate melt water

Figure 57. EFFECT OF MULTIPLE FRACTIONATION ON ISOTOPIC COMPOSITION OF PORE WATER AT DIFFERENT LEVELS OF PORE OCCUPANCY BY HYDRATES

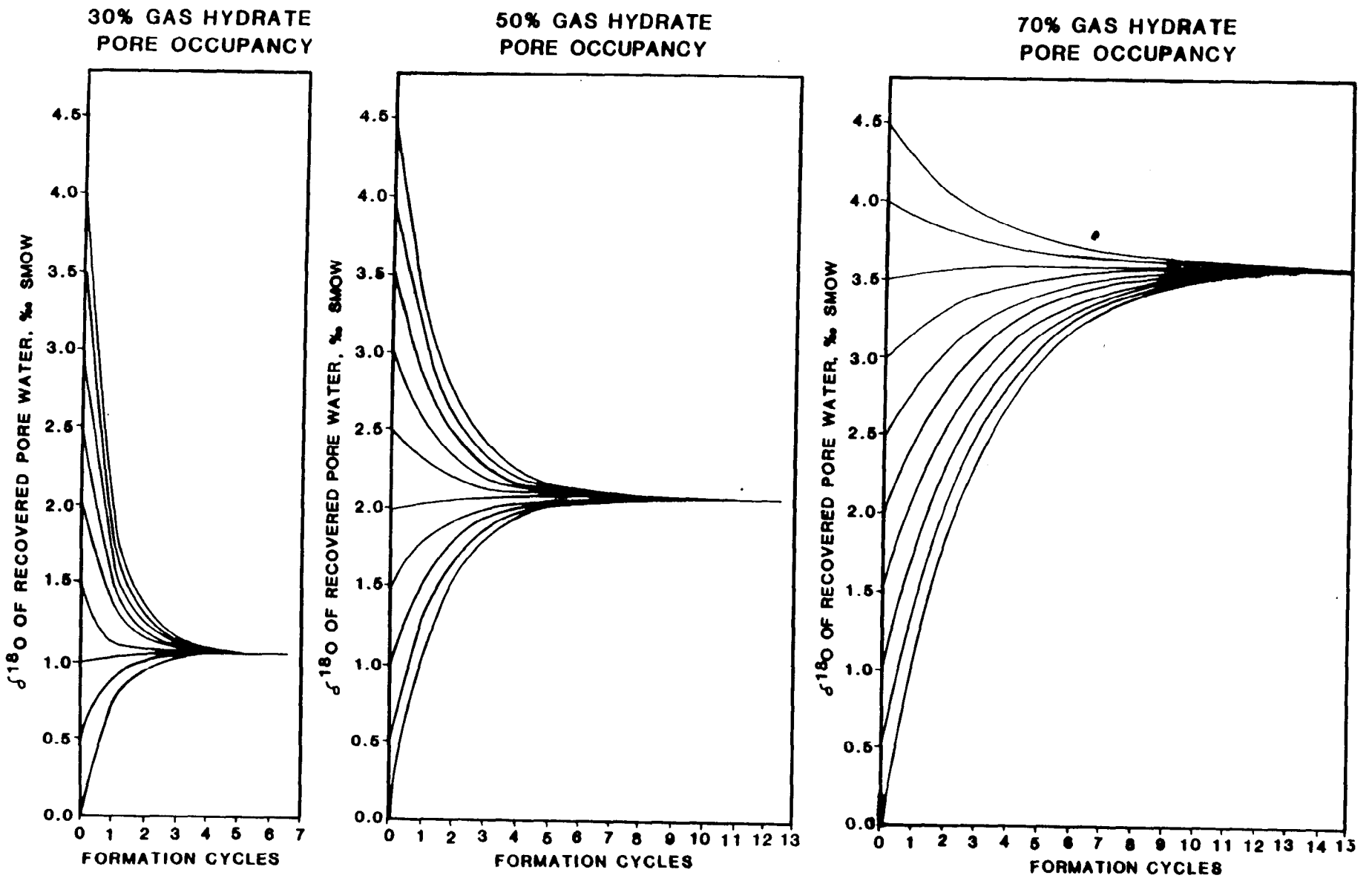

Assumes: α=1.003, pore water returns to 0.0‰ SMOW by diffusion after hydrate is formed, and no diffusion of ^{18}O from hydrate melt water

Figure 58. EFFECT OF PRIOR ISOTOPIC ENRICHMENT OF PORE WATER ON MULTIPLE FRACTION BY GAS HYDRATES

began. According to the model, no dissociation-formation cycling would be necessary to achieve the ^{18}O enrichment seen at Site 570.

Even with prior enrichment, some multiple fractionation cycles are needed to achieve the ^{18}O levels measured in cores from Sites 496, 497, and 568. Site 496 and 497 values could be duplicated by dissociating hydrate formed from pore water with a $\delta^{18}O$ value of 2 per mil. One additional cycle of enrichment would be necessary if the pore water was initially at 1.5 per mil. A total of two enrichment cycles would be needed if the initial pore water had an initial ^{18}O concentration of 0.5 per mil. The ^{18}O value measured at Site 568 would still require many enrichment cycles unless the initial pore water was already highly enriched in ^{18}O (e.g. 3.0 per mil).

The models described above adhere strictly to the assumptions of Hesse et al. (1985). One modification can be made to the model which improves its geological realism. One principal assumption in the theories of Harrison and Hesse (1981), Harrison et al. (1985), and Hesse et al. (1985) is that during the period of time when gas hydrates have formed and are stable, the coexisting pore water reequilibrates with sea water by replenishing ^{18}O and ejecting excess chloride by diffusion to acquire a chlorinity of 19.4 per mil and a $\delta^{18}O$ value of 0 per mil. This condition was simulated in the computer model, even in instances where the pore water was enriched in ^{18}O prior to hydrate formation. It is also possible that pore water in contact with stable gas hydrates would equilibrate to an ^{18}O content other than sea water. If some prior concentration of ^{18}O in pore water occurred before gas hydrate formation, it is reasonable that the pore water would equilibrate to an ^{18}O content greater than sea water. One possibility is that the pore water would assume a $\delta^{18}O$ value similar to the pore water from which the gas hydrate formed.

Figure 59 shows the results of modeling the situation in which the pore water returns to its original level of ^{18}O enrichment before the dissociation process begins. The results are plotted in eight graphs representing interstitial gas hydrate concentrations of 20% to 80%. At each level of gas hydrate pore occupancy, concentrations of ^{18}O in the pore water prior to the formation of gas hydrate between 0.5 and 2 per mil are diagrammed. From Figure 59 it is clear that efficient enrichment of the pore water is possible by this mechanism. The concentration occurs principally because when the gas hydrate dissociates, whether in situ or in a recovered core, the pore water with which the gas hydrate melt water is mixed has an elevated level of ^{18}O. Thus, the dilution of ^{18}O due to mixing with pore water is much diminished.

The plots for 50% and 60% gas hydrate occupancy in Figure 59 are of particular interest. Chlorinity measurements suggested that DSDP Sites 496, 497, 568, and 570 had between 52% and 65% of the interstitial water in the form of gas hydrates (Table 15). The observed $\delta^{18}O$ value for 337 m depth at Site 570, 1.74 per mil, could be achieved without multiple fractionation by maintaining an in situ pore water $\delta^{18}O$ value of 0.5 per mil. The values measured from Site 496 and 497 cores, 2.52 and 2.59 per mil, could be duplicated if pore water ^{18}O content of 1 per mil was established prior to gas hydrate formation and was reestablished prior to hydrate dissociation. The very high $\delta^{18}O$ values of 3.31 per mil from Site 568 would require a prior concentration of at least 1.5 per mil or multiple fractionation at lower pore water ^{18}O concentrations.

Summary

The computer modeling exercise shows that gas hydrates can cause chlorinity decrease and ^{18}O enrichment to the degree measured in DSDP cores from the Middle America Trench. To produce the very high $\delta^{18}O$ levels measured at Site 496, 497, and 568 requires a significant enrichment of ^{18}O in the pore water prior to gas hydrate formation.

Geological interpretation indicates that the pore water chemical changes recorded at Site 570 are closely related to gas hydrate presence. No pore water chemical anomalies are noted for intervals where gas hydrates were absent from cores. Gas hydrates were confirmed to exist in the two sampled interals where substantial pore water chemistry aberrations were noted. The physical conditions of the recovered cores in the sampled intervals agree with the level of gas hydrate dissociation needed to produce the pore water chemistry changes.

The geological observations conflict with the pore water chemistry at Sites 496, 497, and 568. Optimizing parameters and invoking substantial prior concentration of ^{18}O in pore water, the measured chemical values can be duplicated by computer modeling. However, gas hydrates were not recovered in intervals showing extreme pore water anomalies. The possibility that abundant disseminated gas hydrates causing the pore water anomalies were dissociated prior to core examination is not supported by the physical condition of the recovered cores. The chlorinity and $\delta^{18}O$ values of these three sites are much more extreme than values recorded at other gas hydrate-bearing sites along the Middle America Trench. The high $\delta^{18}O$ and low chlorinity are also much different from Site 533 on the Blake Outer Ridge where gas hydrates were recovered (Jenden and Gieskes, 1983). Similarly, only slight pore water chemistry changes were noted at DSDP Sites 88, 89, 90, and 91 in the Gulf of Mexico (Manheim et al., 1973) where gas hydrates were probably cored (Krason et al., 1986). Additionally, Sites 496, 497, and 568 are all located in close proximity over a very small area of the continental slope. The lack of evidence for gas hydrates or degassing features where predicted by pore water chemistry, the lack of such extreme values at other proven gas hydrate locations, the contradictory results of the in situ pore water samples, and the local nature of the phenomenon leads us to conclude that the very high ^{18}O levels and low chloride levels at Sites 496, 497, and 568 are not due entirely to dissociation of interstitial gas hydrates upon core recovery as proposed by Hesse et al. (1985).

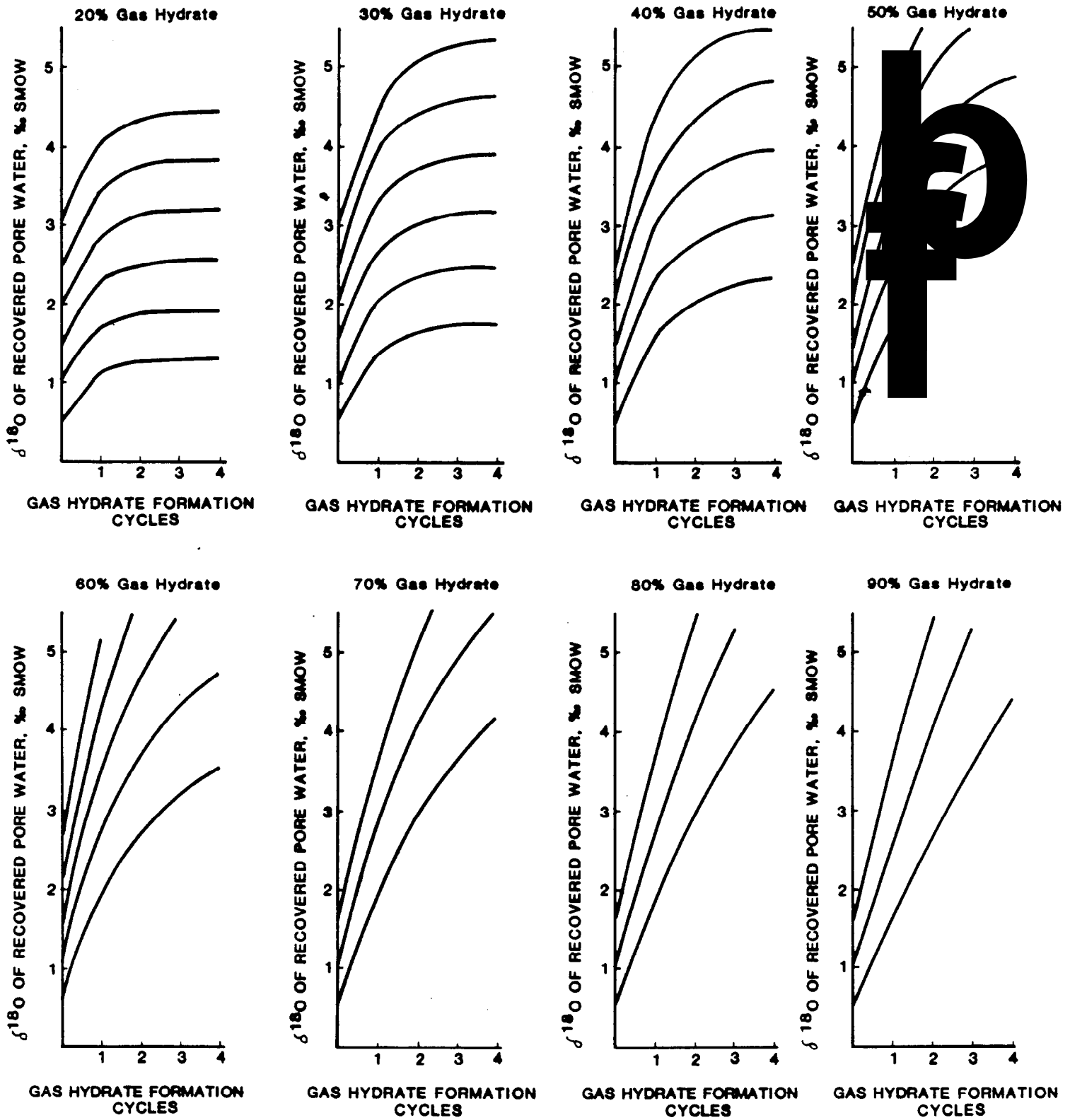

Assumes: α=1.003, pore water returns to original enrichment after hydrate formation, and no diffusion of ^{18}O from hydrate melt water

Figure 59. EFFECT OF ISOTOPE REPLENISHMENT ON MULTIPLE FRACTIONATION BY GAS HYDRATE

Massive Gas Hydrate Formation

The 3- to 4-m thick massive gas hydrate layer drilled at Site 570 requires invoking special geological circumstances to explain its formation. The gas hydrate must have either formed in a void space, or made space for itself as it formed (Kvenvolden and McDonald, 1985). The massive nature of the gas hydrate dictates that the constituent gas must have migrated from surrounding sediments to the gas hydrate (Kvenvolden and McDonald, 1985).

Massive Gas Hydrate Formation Model

A model of the formation of the massive gas hydrate has been proposed by Kvenvolden et al. (1984) and Kvenvolden and Claypool (1985). The model integrates findings from DSDP drilling and oceanographic data to explain how the very large quantities of gas required for formation of the hydrate came to be localized at Site 570.

The model of Kvenvolden et al. (1984) and Kvenvolden and Claypool (1985) consists of three main components:

1. Very efficient microbial methane generation
2. An indurated cap rock to trap generated hydrocarbons
3. Tectonic uplift to make more methane available for hydrate formation

Site 570 is claimed to have been the site of very efficient bacterial methane generation. The abundance of gas in core liner pockets, even at shallow subbottom depths where gas hydrates are not expected shows that methane generation is pervasive throughout the section. Site 570 is thought to have experienced more intense methane generation than other Leg 84 sites, based on the large amounts of organic carbon available for methanogenesis. Indeed, Site 570 has the highest average total organic carbon content (TOC) of all Leg 84 sites (Figure 60). The interval between 230 m and 280 m, which includes the massive gas hydrate zone, has very high TOC values with a mean of 2.6%. Kvenvolden and Claypool (1985) stated that the coastal upwelling currents and a shallow oxygen minimum zone along the Middle America Trench combine to deposit and effectively preserve large quantities of methane for subsequent methanogenesis.

It is claimed that a thin layer of dolomite immediately above the massive gas hydrate at Site 570 acted as a seal to trap and concentrate gas in sufficient quantities for gas hydrate formation (Figure 61). A sample of the dolomite was recovered in core 27 along with the massive gas hydrate. At or near this same depth, paleontologists identified a brief unconformity between upper Miocene and lower Pliocene sediments. The ^{13}C value of the dolomite (-13 per mil) was interpreted by Kvenvolden et al. (1984) to indicate that the dolomite was precipitated at a depth of less than 10 m subbottom. Methane gas concentration is usually relatively low in sediments near the sea floor, but a lithological cap would prevent loss of methane to sea water by diffusion and therefore permit methane to accumulate to concentrations necessary for gas hydrate formation. The shallow sediments beneath the dolomite cap would presumably not be indurated, which would enhance the

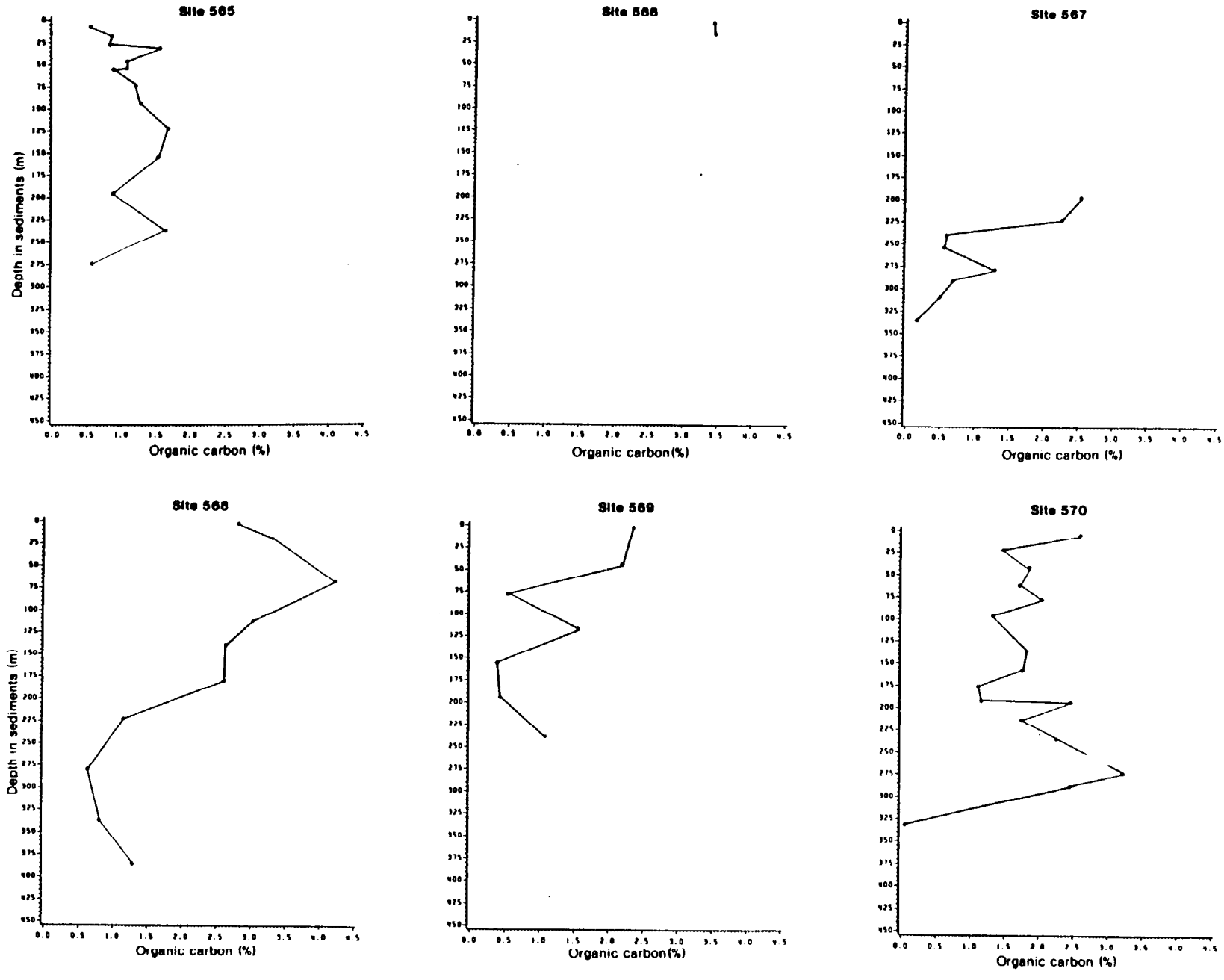

Figure 60. ORGANIC CARBON CONTENT AT DSDP LEG 84 SITES
After Kvenvolden and McDonald, 1985

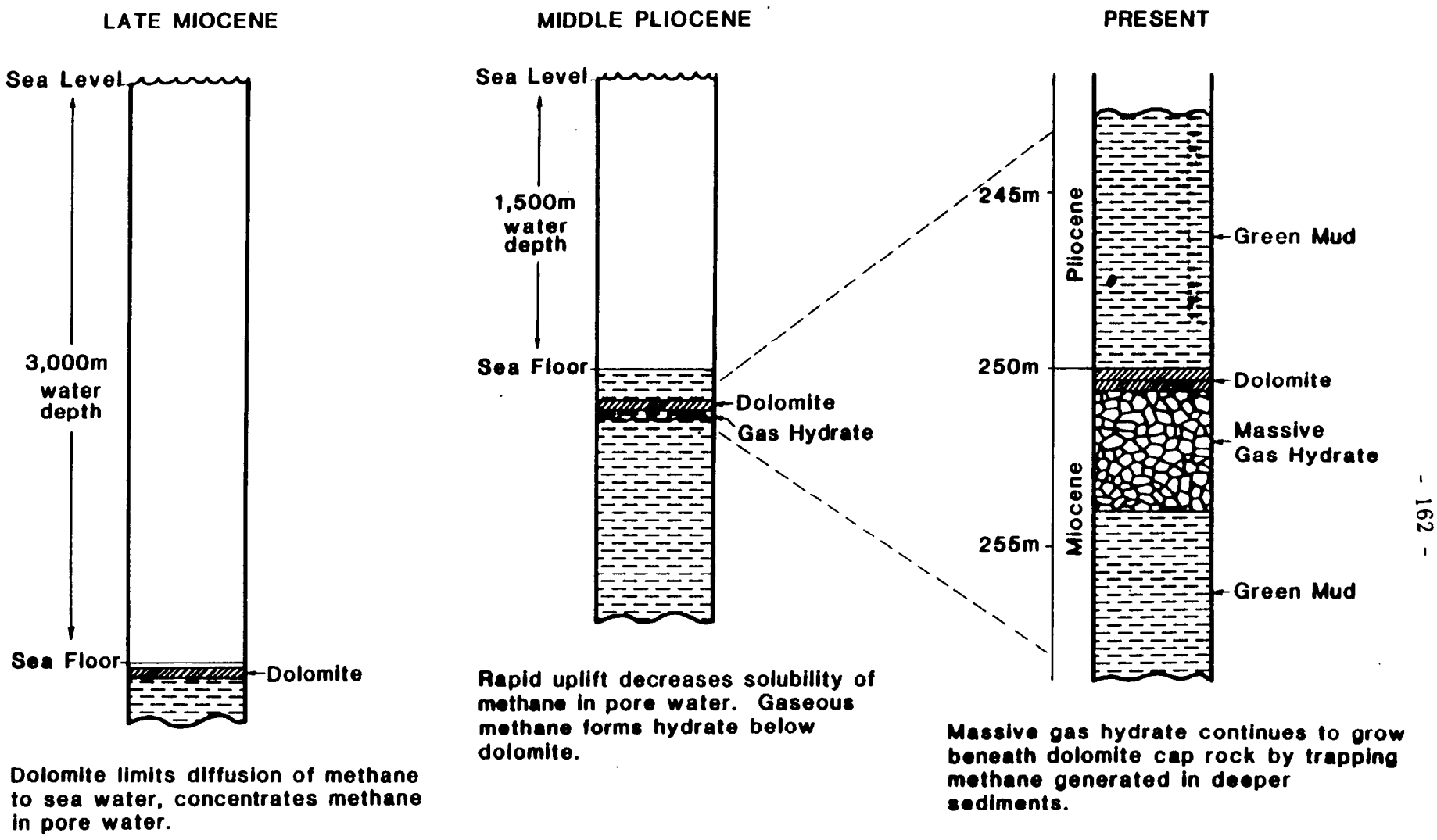

Figure 61. PROPOSED MODEL OF MASSIVE GAS HYDRATE FORMATION AT DSDP SITE 570

Redrafted from Kvenvolden and Claypool, 1985

possibilities for growing disseminated gas hydrates to displace enough sediment to form massive hydrates.

Tectonic uplift of the Guatemalan continental margin was proposed to have made more gas available for gas hydrate formation at Site 570 (Figure 61). Kvenvolden and Claypool (1985) stated that the continental slope at Site 570 was uplifted up to 2 km during late Miocene and early Pliocene time. Kvenvolden et al. (1985) reported that water depth at Site 570 became shallower than present during late Miocene to middle Pliocene time. The concomitant decrease in confining pressure reduced the solubility of methane in pore water. The methane in excess of that soluble in pore water was thus made available for gas hydrate formation. The net result of this fortuitous combination of geological factors is best summarized by Kvenvolden et al. (1984):

> A large amount of gas hydrate formed preferentially in the pore space of the dolomite-capped, organically rich late Miocene sediments.
>
> Subsequent subsidence and continued C_1 generation in the sediments above and below the late Miocene gas hydrate layer caused it to grow in such a way as to exclude the enclosed sediment and to assume its present massive aspect.

The model of massive gas hydrate formation at Site 570 which was proposed by Kvenvolden et al. (1984) and Kvenvolden and Claypool (1985) represents the first published attempt to synthesize the voluminous findings of the DSDP drilling offshore of Guatemala into a credible formation mechanism consistent with the data. The model is contingent on intense bacterial methanogenesis, presence of an impermeable dolomite layer, and rapid, large-scale uplift of the continental slope in late Miocene to middle Pliocene time. The proposed model does not require structural deformation of the host sediments, long distance gas migration, or thermogenic hydrocarbon generation. To determine the accuracy of the proposed model and to evaluate its potential for future application as an exploration tool, each of the assumptions will be examined in detail. Other data from the DSDP Middle America Trench cruises which may further elucidate the formation mechanisms at Site 570 will also be presented.

Dolomite Cap Rock

The dolomite layer which is proposed to have acted as a barrier to the diffusive escape of methane to the sea floor was sampled in core 27 along with the 1.05 m core of massive gas hydrate. The dolomite was the subject of many different analytical procedures by investigators from Leg 84, including biostratigraphic, physical property, petrographic, and well log analyses.

Investigators from DSDP Leg 84 disagree on the stratigraphic position of the fractured dolomite relative to the massive gas hydrate at Site 570. All agree that dolomite, dolomitic sandstone, or dolomitic sandstone with calcite veining was recovered in core 27. They also are all in accordance that a 1.05 m core of massive gas hydrate was recovered in core 27. Some researchers place the distinctive dolomite stratigraphically higher than the

massive gas hydrate as in the model of Kvenvolden et al. (1984) and Kvenvolden and Claypool (1985). Conversely, a surprisingly large group of investigators described the dolomite as being under the massive gas hydrate zone. Since Kvenvolden et al. (1984) and Kvenvolden and Claypool (1985) assigned critical importance to the impermeable dolomite cap rock in the formation of the massive gas hydrate, determination of the relative position of the dolomite and gas hydrate is crucial in evaluating their proposed model.

Description. Three sources from the DSDP Leg 84 staff agreed that the dolomite was indeed located above the massive gas hydrate zone.

Baltuck et al. (1985) presented a most convincing description of the relative position:

> The occurrence of dolomite at this site (Core 27) was unexpected. About 15 cm of highly fractured, well-indurated micritic dolomite containing grains of quartz and feldspar is veined by calcite. Gas hydrate filled fractures in the dolomite. Immediately below this layer, a spectacular 1.3-m-long core (Core 27) of massive hydrate was recovered at about 250 m sub-bottom.

In a general introduction to their paper on well logs from Site 570, Mathews and von Huene (1985) presented a similar account:

> The first visual observations of gas hydrate were made near and at the bottom of this unit (at sub-bottom depths of about 192 and 240 m, respectively). Below this, the core containing about 1.5 m of massive hydrate, capped by about 20 cm of sandstone and fractured dolomite with veins filled by calcite (249-259 m), was recovered. Immediately below and separated by a hiatus is an upper Miocene mudstone unit that is more lithified and fractured (259-326 m).

The lithostratigraphic column included in the Site Report also placed dolomitic sandstone above the massive hydrate, between 249 and 259 m depth in core 27 (Figure 62).

The core description on the standard DSDP forms for Site 570 (von Huene et al., 1985) suggests that the dolomite was located above the gas hydrate without specifying so outright:

> core 27:
>
> Dominant lithology: sandstone. Color: light olive gray (5Y 3/2).
>
> Very hard siliceous rock. Composed of quartz and dolomite. Medium grained. Highly fractured with calcite filling the veins.
>
> The rest of the core is composed of gas hydrate ice.

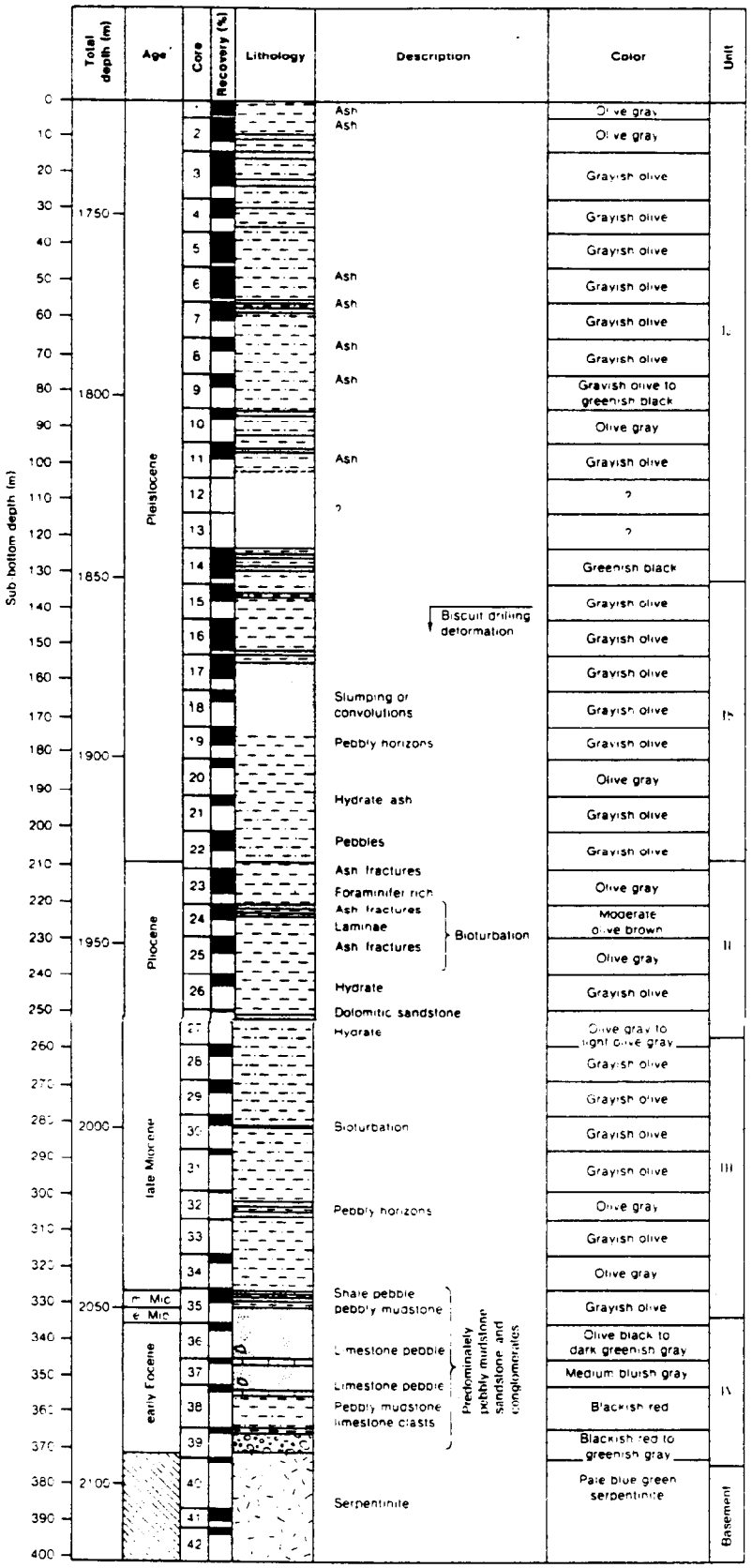

Figure 62. **LITHOSTRATIGRAPHIC SUMMARY OF DSDP SITE 570**
After von Huene et al., 1985

> Minor lithology: sandy mud. Color: olive gray (5Y 3/2). Very soupy - so it is structureless.

Two citations present equivocal descriptions of the relative position. In the gas hydrate chapter of the Leg 84 Initial Reports, Kvenvolden and McDonald stated that:

> The most spectacular occurrence of gas hydrate was found at 249 m sub-bottom where a 1.05-m core of massive gas hydrate was recovered (Fig. 8C). This gas hydrate was associated with fractured dolomite at its bottom and was apparently located at the contact between upper Miocene and Pliocene sediments.

In the organic geochemistry section of the Site 570 Site Report, which according to Baltuck et al. (1985) was also authored by Kvenvolden and McDonald, a similarly worded passage described the dolomite:

> The next lower core (Core 27) encountered a massive gas hydrate between about 250 and 255 m sub-bottom. This almost pure gas hydrate was associated with fractured dolomite at its base and was located at the unconformity between late Miocene and Pliocene.

Interpretation of these passages is difficult due to the imprecise wording used. In the common passage, "This gas hydrate was associated with fractured dolomite at its base (bottom) and was located at the contact (unconformity) between late Miocene and Pliocene," it is unclear whether "its" refers to the dolomite or the gas hydrate. To us, it appears that "its" refers to the gas hydrate. That would place the dolomite below the massive gas hydrate. However, the intended meaning of the phrase in question could be different from our interpretation.

In their paper on gas hydrates from Leg 84, Kvenvolden and McDonald (1985) indicated that the dolomite was beneath the gas hydrate. In a tabulation of gas hydrate recoveries, they described two different gas hydrate occurrences in core 27 (Table 7). One was a "Massive gas hydrate ~ 1.05 m long." The other hydrate occurrence located the dolomite relative to the massive gas hydrate: "White gas hydrate in fractures of dolomite; ~18 cm^3 used for analysis. This sample is at the base of the massive gas hydrate."

The description of core 27 in the Lithologic Summary section of the DSDP Site Report stated that the gas hydrates were above the dolomite.

> The base of Unit II is marked by a highly fractured and indurated dolomite. Some fractures in the dolomite were filled with solid gas hydrate (Core 27). The rock contains up to 5% quartz and feldspar grains of volcanic origin that float in a dolomite matrix. Solid gas hydrate was recovered in Cores 26 and 27 immediately above the dolomite. In Core 27 at least 1.05 m of solid gas hydrate were present.

In the geophysics section of the Site Report, the well logs from Site 570 were briefly described:

> The Pleistocene, Pliocene, and Miocene mud sections are of uniform velocity, density, porosity, and resistivity, thus providing a clear background for thin limestone and sandstone beds. The massive hydrate is clearly defined and can be separated from the underlying thin dolomite bed.

The dolomite and clastic sediments which were either within the massive gas hydrate as matrix or very near to the gas hydrate were dated paleontologically by Filewicz (1985):

> Section 570-27-1 contains silty mud interbedded with gas hydrate. The silty mud matrix is assigned to the lower Pliocene Ceratolithus acutus Zone. Fractured siliceous dolomite interbedded with gas hydrate in 570-27,CC (258.8 m) is barren of nannofossils.

From this information the ages of the two units in question cannot be determined. However, the sample nomenclature suggests that the dolomite is beneath the hydrate. The silty mud matrix material was from section 570-27-1. In the standard DSDP core identification, the final digit identifies the section of the core numbered from the top of the core downward. The "1" signifies that the mud tested came from the highest 1.5 meter of recovered material, that is, from 249.1 to 250.6 m subbottom assuming complete recovery. The massive gas hydrate was also recovered from section 570-27-1. The core recovery at Site 570 was only 15%, so the original in situ depth of both the mud matrix and the massive gas hydrate is unknown. The fractured siliceous dolomite which was also examined by Filewicz (1985) had an identifying code of 570-27-CC. The "CC" designates that the sample was recovered from the core catcher, the bottommost part of the core. The depth cited by Filewicz (1985) for the dolomite sample (258.8) is the lowest possible position on core 27 which penetrated from 249.1 to 258.8 m. This implies that the dolomite was stratigraphically lower than the hydrate.

Physical properties of the Site 570 cores were described in a paper by Taylor and Bryant (1985) and in the Physical Properties section of the Site Report which was authored by Taylor according to Baltuck et al. (1985). Samples were analyzed for bulk density, porosity, p-wave sonic velocity, and water content. Acoustic impedance was calculated from measured density and velocity data.

Results of bulk density, water content, and porosity determinations at Site 570 are plotted in Figure 63. Two samples from core 27 were analyzed, one massive gas hydrate and one "dolomite or marl". Taylor placed the hydrate above the dolomite in the physical property log published in the Site Report, on which Figure 63 is based.

The absolute depths of the two samples from core 27 were not provided in the Site Report. However, Taylor and Bryant (1985) presented some depth data on the dolomite. In the tabulation of physical property data in the Appendix of their report, the dolomite was listed as coming from the core catcher at a depth of 250.70 m. The designation is apparently contradictory

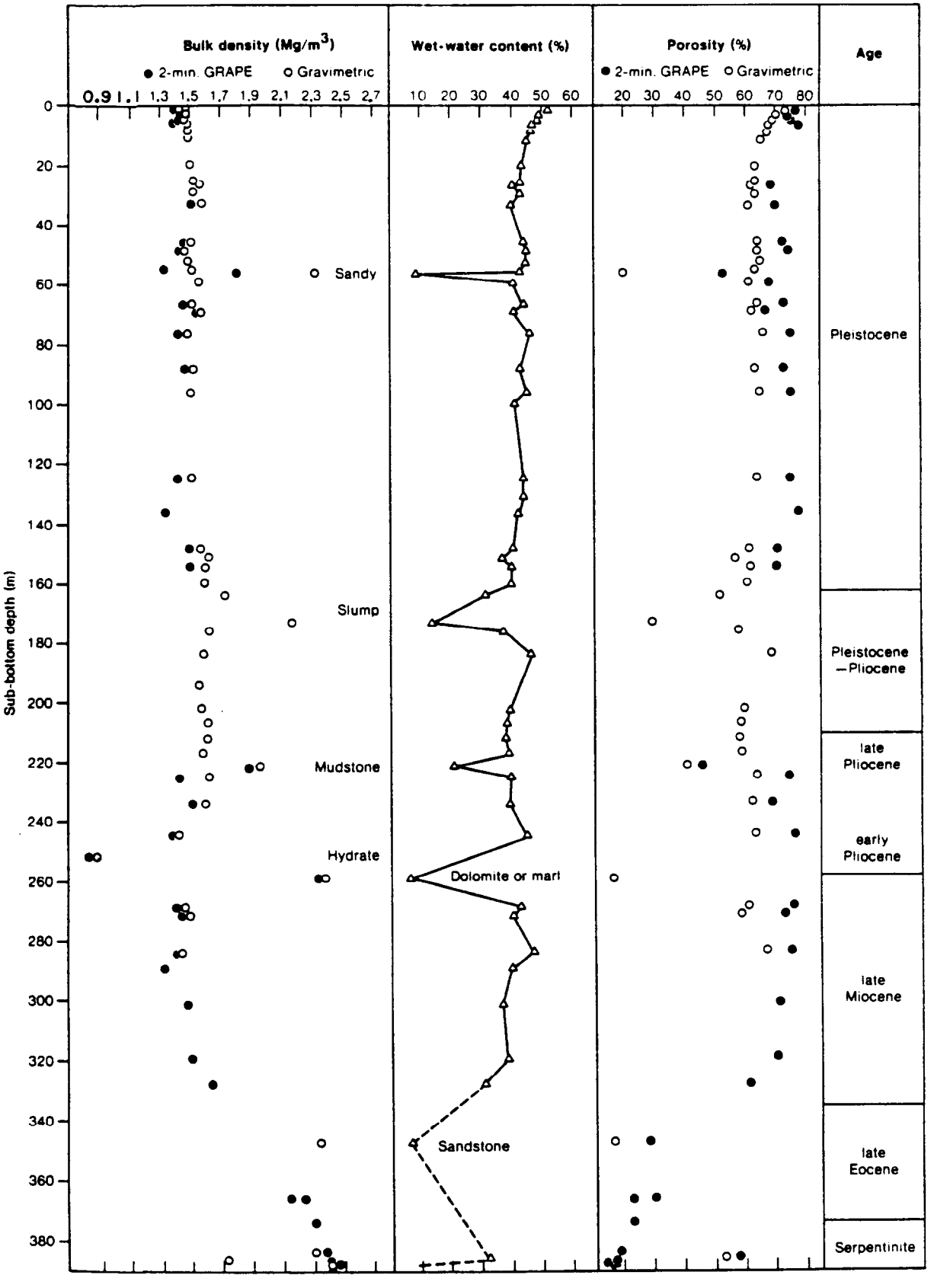

Figure 63. **PHYSICAL PROPERTIES OF SEDIMENTS AND ROCKS RECOVERED FROM DSDP SITE 570**

After Taylor in von Huene et al., 1985, Taylor and von Huene, 1985, and Taylor and Bryant, 1985

with the sample being from core catcher which is the bottom 0.2 m of the 9.7 m core, but at a depth of 250.70 m which is only 1.6 m below the top of the core at 249.1 m. The seeming paradox is a result of the unusual application of core identification conventions used by Taylor and Bryant (1985). The core recovery for core 27 was approximately 15% (von Huene et al., 1985). That corresponds to about 1.5 m of recovered material from the 9.7 m core. The cores are subdivided into 1.5 m sections which are numbered sequentially from the top of the core. If core recovery is incomplete, often void space exists above the highest occurrence of sediment in the core liner. Regardless of how far below the top of the core barrel it occurs, the first sediment recovery defines the top of section 1 of the core. Thus, in the case of partial recovery as for core 27, the exact depth of the recovered interval is not known; the core material could have come from any depth in the 249 - 258.8 m interval. Thus when only one 1.5 m sediment section was recovered above the core catcher, Taylor and Bryant (1985) arbitrarily assigned the depth of the top of Section 1 to the top of core 27, 249.1 m. Thus the depth of 250.7 assigned to the dolomite sample found in the core catcher indicates that 1.6 m of sediment and gas hydrate existed above the dolomite. Since section 2 of core 27 was not described anywhere in the Leg 84 volume, and the gas hydrate occupied at least 1.05 m of Section 1, the depth of 250.8 is consistent with the core catcher sample. The dolomite was the deepest recovered material from core 27; the gas hydrate was therefore above it.

The physical properties of the hydrate and the dolomite are very distinct from each other and from the typical mud and mudstone of Site 570. Figure 63 shows that the massive gas hydrate has a bulk density of 0.873 to 0.898 g/cm^3, the least dense material recovered from Site 570. The 2.40 g/cm^3 density of the dolomite is exceeded only by the 2.41 g/cm^3 density of a sandstone from 347 m (core 37). The density values for both the hydrate and the dolomite are far away from the typical values for mudstone in nearby cores 1.4±0.2 g/cm^3.

The porosity and water content of the dolomite are much lower than typical Site 570 sediments. The water content of 7% and porosity of 18% contrasted with typical mudstone values of 40% and 60% respectively. This indicates the anomalous induration of the dolomite. Porosity and water content values for the massive gas hydrate were not reported.

Acoustic properties of Site 570 material are diagrammed in Figure 64. The compressional velocity and acoustic impedance of the hydrate sample are presented as bars showing the range of values obtained from 13 repetitions of the analyses. The dots on the bars correspond to the mean values obtained. Few mud or mudstone acoustic measurements were published for comparison with the hydrate and dolomite values. The entire section from 260 to 345 m depth is without acoustic values. Two samples from core 24 (221 and 225 m) have acoustic values which may be typical of the mud and mudstone which make up most of the sediments above and below core 27. These samples have acoustic velocities of about 1.5 km/sec and calculated impedance values of 2 to 3 x 10^{-5} $g/cm^2/sec$. The gas hydrate samples have much higher acoustic velocity values than typical sediment, ranging from 2.2 to 5.2 km/sec compared to 1.5 to 1.9 km/sec for the mudstone and mud. The acoustic impedance of the massive gas hydrate ranges from 1.9 to 4.7 x 10^{-5} $g/cm^2/sec$ which is somewhat higher than the 2.1 to 3.0 x 10^{-5} $g/cm^2/sec$ of the mudstone, but the ranges overlap substantially.

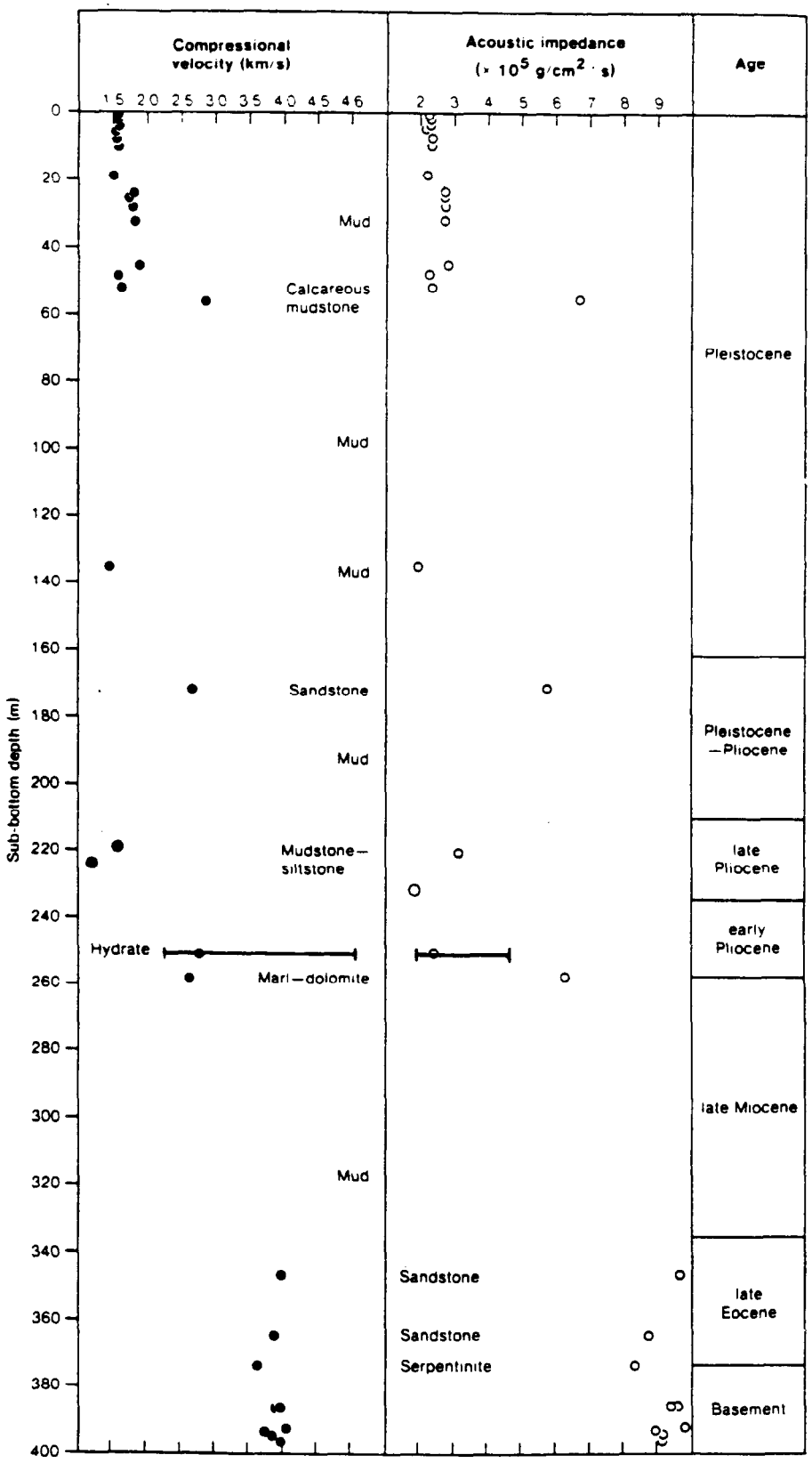

Figure 64. **ACOUSTIC PROPERTIES OF SEDIMENTS AND ROCKS RECOVERED FROM DSDP SITE 570**

After Taylor in von Huene et al., 1985 and Taylor and von Huene, 1985, and Taylor and Bryant, 1985

The marl or dolomite from core 27 has a slightly lower acoustic velocity than the mean velocity of the massive gas hydrate. However, the dolomite still has greater acoustic velocity than the typical mudstone (2.6 vs. 1.7 km/sec). The impedance calculated for the dolomite is much higher than that derived for either the massive gas hydrate or typical mudstone. Acoustic impedance is the product of bulk density and seismic velocity. The impedance of the dolomite is very high because it has fairly high acoustic velocity (2.6 km/sec.) and is very dense (2.4 g/cm^3). Although the gas hydrate has a higher overall acoustic velocity (2.2 to 5.2 km/sec) its very low density (0.89 g/cm^3) results in acoustic impedance values which are significantly less than that of the dolomite.

Physical property work by Taylor in von Huene et al. (1985) and Taylor and Bryant (1985) clearly demonstrated that a dolomite layer existed below the gas hydrate in core 27. Additionally the work showed that both the massive gas hydrate and the dolomite layer have distinctive physical properties which distinguish each from the other, and which also distinguish the massive gas hydrate and dolomite from the surrounding mudstone as summarized in Table 16.

TABLE 16.

PHYSICAL PROPERTIES, DSDP SITE 570

Lithology	Bulk density g/cm^3	Porosity %	Sonic velocity km/sec	Acoustic Impedance 10^{-5} g/cm /sec
Mud	1.331-1.962	41.5-81.2	1.504-1.895	2.164-3.018
Hydrate	0.873-0.898	--	2.224-5.272	1.942-4.734
Dolomite	2.398	17.5	2.625	6.295

Note: -- indicates not determined
After Taylor in von Huene et al. (1985)

Well Logs. An extensive suite of well logs were run at Site 570 (Mathews and von Huene, 1985). These logs define both the 4-m massive gas hydrate zone and the thin (<59 cm) dolomite layer beneath it.

The massive gas hydrate is best defined by the acoustic velocity and bulk density logs (Figure 65). The log responses reproduced in Figure 65 are plotted in meters from the Kelly bushing of the Glomar Challenger. The log depth can be converted to subbottom depths by subtracting 1,718.5. The depth range of core 27 (249.1-258.8 m) is plotted on these and subsequent logs. The acoustic velocity log shows a high velocity zone between 1,965 and 1,969 m, and a thin high velocity zone at 1,975 m. The bulk density plot shows that the high velocity zone between 1,965 and 1,970 is characterized by very low density values, while the high velocity band at 1,975 is very dense. These data suggest that the zone between 1,965 and 1,970 corresponds to

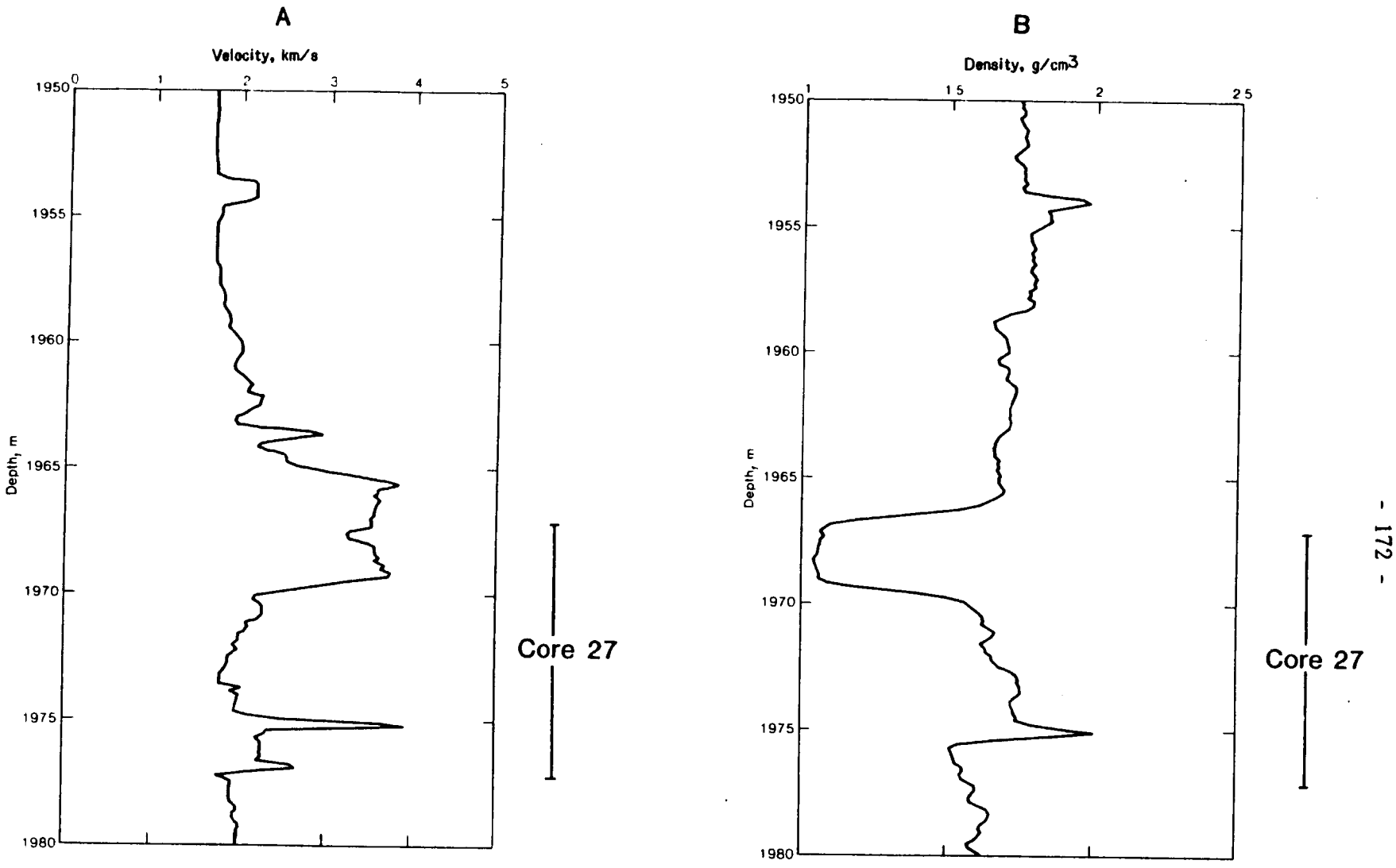

Figure 65. ACOUSTIC VELOCITY (A) AND BULK DENSITY (B) LOGS FROM DSDP SITE 570

After Mathews and von Huene, 1985

massive gas hydrate, in agreement with the physical property test results of high acoustic velocity and low density for the hydrate. The values for velocity and density are in agreement with physical property measurement values of Taylor. The 3.8 km/sec and 1.1 g/cm^3 are both close to the 2.3-5.2 km/sec and 0.9 g/cm^3 measured on the recovered cores.

The log response at 1,975 m closely matches that expected for the dolomite analyzed by Taylor and Bryant (1985). The velocity and density peaks of 4 km/sec and 2.1 g/cm^3 are in near agreement with the measured values of 2.6 km/sec and 2.4 g/cm^3 from recovered dolomite. The difference in the log values and the measured values of the dolomite could be a result of the gas hydrate content of the dolomite in situ. If the physical property measurements were made subsequent to the dissociation of the fracture-filling gas hydrates, lower seismic velocity and higher density values compared to in situ values would result. The sharp increase of the 1,975 m values above the baseline values of the surrounding mudstone also agrees with physical property measurements. Mathews and von Huene (1985) identified the high velocity, high density layer at 1,975 m as a "limestone stringer" based on sonic logs.

A concurrent plot of sonic velocity, bulk density, and calculated acoustic impedance (Figure 66) shows the relative contributions of acoustic velocity and density to impedance. The large spike at 1,975 m duplicates the observations by Taylor and Bryant (1985) that the dolomite of core 27 has a very high acoustic impedance resulting from concurrently high density and velocity values (Table 16). According to Mathews and von Huene (1985), "A thin (less than 0.5-m) impedance layer, where the maximum impedance is 7.3 Mg x km/s x m^3, is also seen to correlate with the limestone or dolomite stringer at 1975 m." The impedance value from well logs is greater than the 6.3 obtained from laboratory measurements of core 27, as would be expected based on the greater sonic velocity value obtained from the well log.

A large impedance peak with a value comparable to the dolomite layer at 1,975 m occurs at the top of the massive gas hydrate zone at 1,966 m. Such a large impedance value at the stratigraphic position in which Kvenvolden et al. (1984) and Kvenvolden and Claypool (1985) claimed a dolomite layer exists bears careful examination. It can be seen in Figure 65 that the negative deflection of the density log which indicates the gas hydrate zone occurs at 1,966.7 to 1,969.5 m. The positive deflection of the sonic velocity log occurs at a shallower depth, 1,965.4 to 1,969 m. Also, the thickness of the massive gas hydrate layer as defined by the density log is 1.3 m less than the zone indicated by the sonic velocity log. These differences were addressed by Mathews and von Huene (1985):

> These differences in depth and thickness probably result from the differences in the two logging tools. The density tool is a volume statistical measurement with a small depth of investigation. The sonic tool has a somewhat deeper depth of investigation and is basically a mechanical properties or molecular measurement.

Since the impedance as plotted on Figure 66 is the product of the density and acoustic velocity, the offset leads to an apparent impedance anomaly at 1,965.4 - 1,966 m. In this interval, the increase in sonic velocity is not compensated for by a simultaneous decrease in density. Therefore, the derived impedance value is greatly amplified over its probable true value.

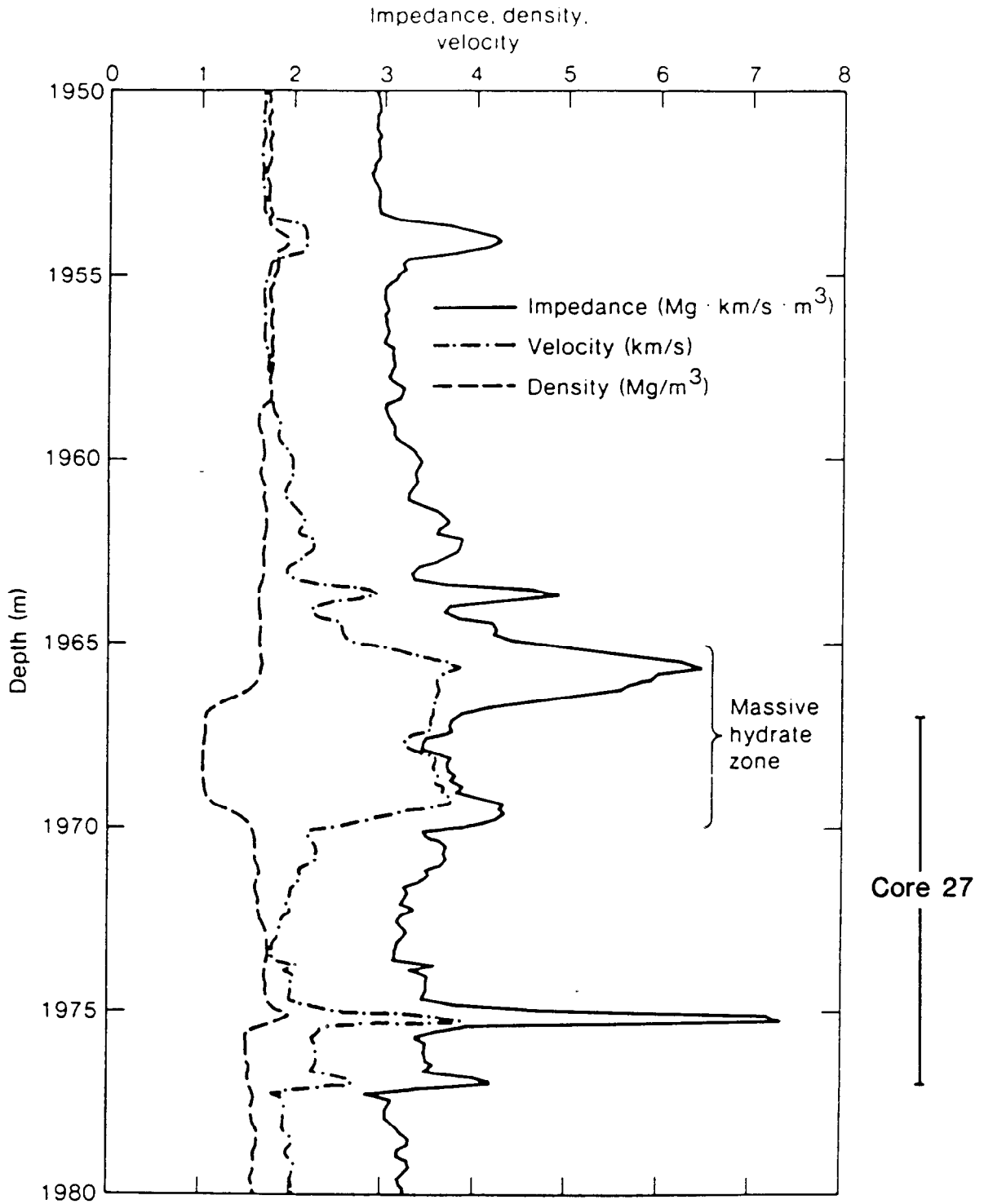

Figure 66. **COMPARISON OF IMPEDANCE, DENSITY, AND VELOCITY DATA FROM 1950 TO 1980 m, DSDP SITE 570**

After Mathews and von Huene, 1985

It could also certainly be argued that the misalignment of the density and sonic velocity curves is not due to different response characteristics of the logging tools, but is a result of the presence of the proposed dolomite cap rock. The seismic velocity curve on Figures 65A and 66 has a local peak at 1,965.4 concurrent with the impedance peak which could conceivably correlate with a dolomite cap rock. The value of the sonic velocity log at 1,965.4 m is very close to the value recorded at 1,975. It is possible that the density log is accurately depicting the lithologies rather than exhibiting delayed instrument response. Note that the velocity and density log responses are perfectly aligned at 1,975 m and at a sandstone layer at 1,955 m. Since the fractured dolomite cap rock would have a similarly positive density response, the negative effect of the fracture-filling gas hydrate reported to be in the dolomite may cancel, giving no deflection.

The peak at 1,965.4 m on the sonic velocity log and another at 1,969 m were addressed by Mathews and von Huene (1985):

> Also, two small peaks or ears are noted on the sonic log at each edge of the 4-m interval of the massive methane hydrate zone (solid gas hydrate was recovered in Core 27 from this interval). This characteristic is seen in other massive hydrate zones (Scott et al., 1980; Mathews, 1982, 1983) and is a feature of the sonic tool and an abrupt velocity change (edge effect).

The resistivity and neutron porosity logs (Figure 67) agree with the interpretation of the dolomite from core 27 being located at 1,975 m rather than the slight possibility of its actually being located at 1,965.5 m. The resistivity log shows a typical dolomite kick at 1,975-1,975.5 m depth. No such kick is seen at 1,965.5 which would be the expected depth of the projected dolomite cap rock. Although masking of tool response by gas hydrates could possibly be invoked to explain the lack of a dolomite deflection in the density log, such an explanation would not apply to resistivity. As shown by the resistivity peak at 1,968 m, where massive gas hydrate development is greatest, the resistivity response of both limestone (dolomite) and gas hydrate are similar.

The neutron porosity log (Figure 67B) shows the distinct drop in porosity at the 1,975 m dolomite zone which was predicted from laboratory physical property measurements. No such low porosity zone exists immediately above the massive gas hydrate zone.

Another argument for the dolomite being located beneath, rather than above, the massive gas hydrate zone is that, as correlated by Mathews and von Huene (1985), a dolomite layer over the massive gas hydrate would have been found in core 26 rather than 27. It is possible that the correlation is offset by the 2 m necessary to include a cap rock, however, other log responses correlate to drilled horizons using the 1,718.5 m offset proposed by Mathews and von Huene (1985). No dolomite was reported from core 26.

Summary. Two interpretations of the relative positions of the dolomite and massive gas hydrate in core 27 from Site 570 exist. The scenario proposed by Baltuck et al. (1985), Kvenvolden et al. (1984), and Kvenvolden and Claypool (1985) is that the gas hydrate is capped by a fractured dolomite layer 20 cm thick. The physical property tests from core 27 by Taylor and

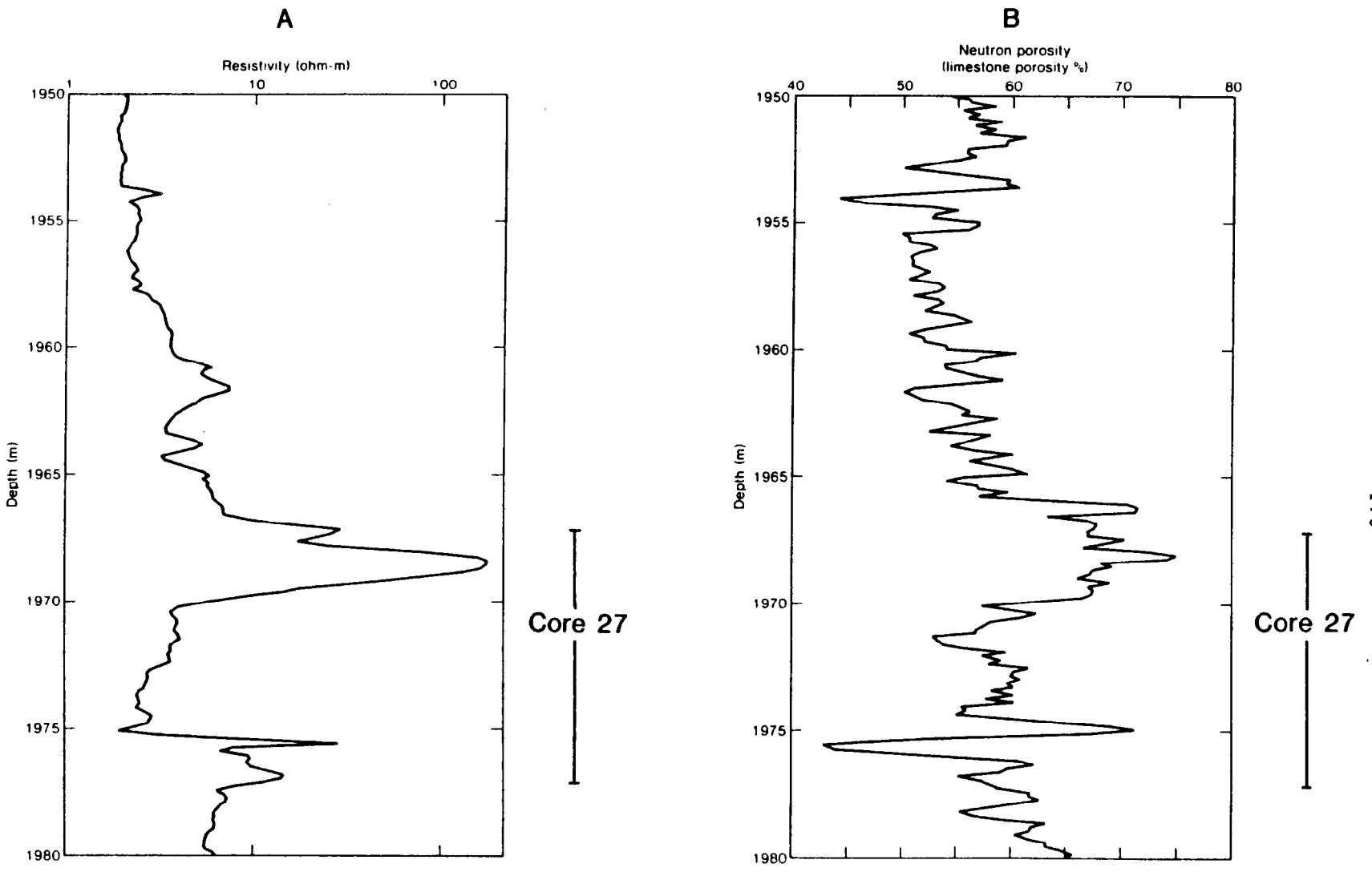

Figure 67. DEEP RESISTIVITY (A) AND NEUTRON POROSITY (B) LOGS FROM DSDP SITE 570

After Mathews and von Huene, 1985

Bryant (1985) and the geophysical logs from Site 570 presented by Mathews and von Huene (1985) and core descriptions by Kvenvolden and McDonald (1985) place the dolomite layer below the gas hydrate layer.

We have concluded that the evidence presented by Taylor and Bryant (1985) and Mathews and von Huene (1985) is the most convincing. We have also concluded that the dolomite cap rock, proposed by Kvenvolden et al. (1984) and Kvenvolden and Claypool (1985) to be a principal factor in the formation of the massive gas hydrate, had little if any influence on massive gas hydrate formation. The geophysical logs show no evidence of massive gas hydrates below the dolomite layer at 1,975 m (256.5 m subbottom), nor do they show a dolomite cap over the massive gas hydrate at 1,966-1,970 m (247.5-251 m).

The presence of two dolomite layers, one capping the gas hydrate at 1,965 m (247 m subbottom) and one beneath the gas hydrate at 1,975 m (256.5 m subbottom) cannot be conclusively ruled out. However, the geophysical logs presented by Mathews and von Huene (1985) make such a possibility remote. Moreover, the documented existence of a dolomite layer at 1,975 m (256.5 m subbottom) makes the possible existence of an additional dolomite layer immediately above the gas hydrate zone a moot point. The relatively impermeable, well indurated dolomite at 1,975 m (256 m subbottom), which is located beneath the massive gas hydrate layer, indicates that trapping of gas by a tight cap rock is not a factor in massive gas hydrate formation at Site 570; if it were, the gas hydrate would have formed at 1,975-1,979 m (256.5 to 270.5 m subbottom) rather than at 1,966-1,970 m (247.5-251.1 m subbottom) regardless of whether another dolomite layer may have existed at 1,965 m (246.5 m subbottom).

Tectonic Uplift

Another critical factor in the model of massive gas hydrate formation proposed by Kvenvolden et al. (1984) and Kvenvolden and Claypool (1985) is rapid uplift of the Guatemala continental margin in late Miocene to early Pliocene time by an estimated 2,000 m. These authors proposed that the decreased hydrostatic pressure from such an uplift diminished solubility of methane in pore water and "made available" much methane for gas hydrate formation in sediment pores beneath the purported dolomite cap rock.

In the proposed model, three properties of the uplift were stressed. The timing of the uplift is important. Whatever uplift may have occurred must have taken place after the gas hydrate-bearing sediments were deposited, and methanogenic processes had begun to be effective. The rate of the uplift must also be "geologically rapid" (Kvenvolden et al., 1984). Thirdly, the uplift was claimed to have been of great magnitude, as much as 2,000 m vertically (Kvenvolden and Claypool, 1985).

Timing. The uplift was alternately claimed to have occurred in the late Miocene and early Pliocene (Kvenvolden and Claypool, 1985) or late Miocene to middle Pliocene time (Kvenvolden et al., 1984). Since any uplift must have taken place subsequent to deposition of the sediments recovered in core 27, Kvenvolden et al. (1984) and Kvenvolden and Claypool (1985) claimed that the sediments which host the massive gas hydrate are of late Miocene age. Paleontologic studies on the sediments differ on that age assignment (Figure

68). Filewicz (1985) claimed an early Pliocene age for the silty mud matrix of core 27 based on calcareous nannofossils. A sand sample from between 2 and 3 cm from the top of section 570-27-1 was reported by Baltuck et al. (1985) to be of early Pliocene age. The lithostratigraphy section of the Site Report places the massive gas hydrate and the nearby thin dolomite layer in the early Pliocene section. The detailed description of core 27 also assigned it an early Pliocene age. McDougall (1985) determined an early Pliocene age for core 27, and for the upper part of core 28 based on planktonic foraminifers. Glacon and Bourgois (1985) did not date core 27 directly, but assigned a lower Pliocene age to core 26 and a late Miocene age to core 28 based on planktonic foraminifera. Diatoms analyzed by Winsborough and Abbott (1985) did not resolve the Miocene to Pliocene boundary; cores 31 through 24 are all in a single late Miocene to early Pliocene diatom zone. An exception to the early Pliocene age given to core 27 by Leg 84 workers is the late Miocene age assigned to cores 27, 26, and 25 by Stone and Geller (1985) based on planktonic foraminifera.

One equivocal statement of the age of the massive gas hydrate host sediment is that of Kvenvolden and McDonald (1985) who claimed that the hydrate was "located at the contact between upper Miocene and Pliocene sediments."

The disagreement on age of the core 27 sediments restricts the timing of the proposed uplift. If the work of Baltuck et al. (1985), Filewicz (1985), Glacon and Bourgois (1985), McDougall (1985) and the lithologic descriptions of Baltuck et al. in the Site Report (von Huene et al., 1985), all of which assign an early Pliocene age, are more accurate than that of Stone and Geller (1985), then only uplifts in the Pliocene to Pleistocene could have had any effect on methane solubility of the sediments of core 27.

Rate. Kvenvolden et al. (1984) stated that "water depths became shallower than at present during late Miocene to mid Pliocene time" and that the uplift occurred "over a relatively short period of time." The source of their information was listed as McDougall (1985). Similarly Kvenvolden and Claypool (1985) stated that the "continental slope was uplifted by as much as 2 km by accretionary tectonic processes during the late Miocene and early Pliocene", but they listed no source for their information.

McDougall (1985) used benthic foraminifer abundance to infer the dominant biofacies of deposition of Leg 84 sediments. In so doing, she was also able to infer the development and distribution of various distinct oceanic water masses through time. The present biofacies distribution of the Guatemala continental slope is diagrammed in Figure 69. Site 570 is presently located in the lower middle bathyal biofacies. Precise determinations of depths were not possible because biofacies vary not only with depth but also with water temperature changes due to altering currents and climates.

McDougall (1985) concluded that the Guatemala continental margin has undergone gradual uplift since Miocene time. Apparently the majority of the uplift occurred in early Miocene and Pleistocene time. McDougall stated that "Water depths did not change during the late Miocene, and may have been slightly deeper during the Pliocene." According to the biostratigraphic interpretation used in McDougall's (1985) article (Stone and Geller, 1985), the only late Miocene sediments recovered on Leg 84 were from Site 570. Thus, Site 570 remained at a constant depth during the deposition of cores 28 through 25. Cores 28-25 were deposited under the Pacific Intermediate water

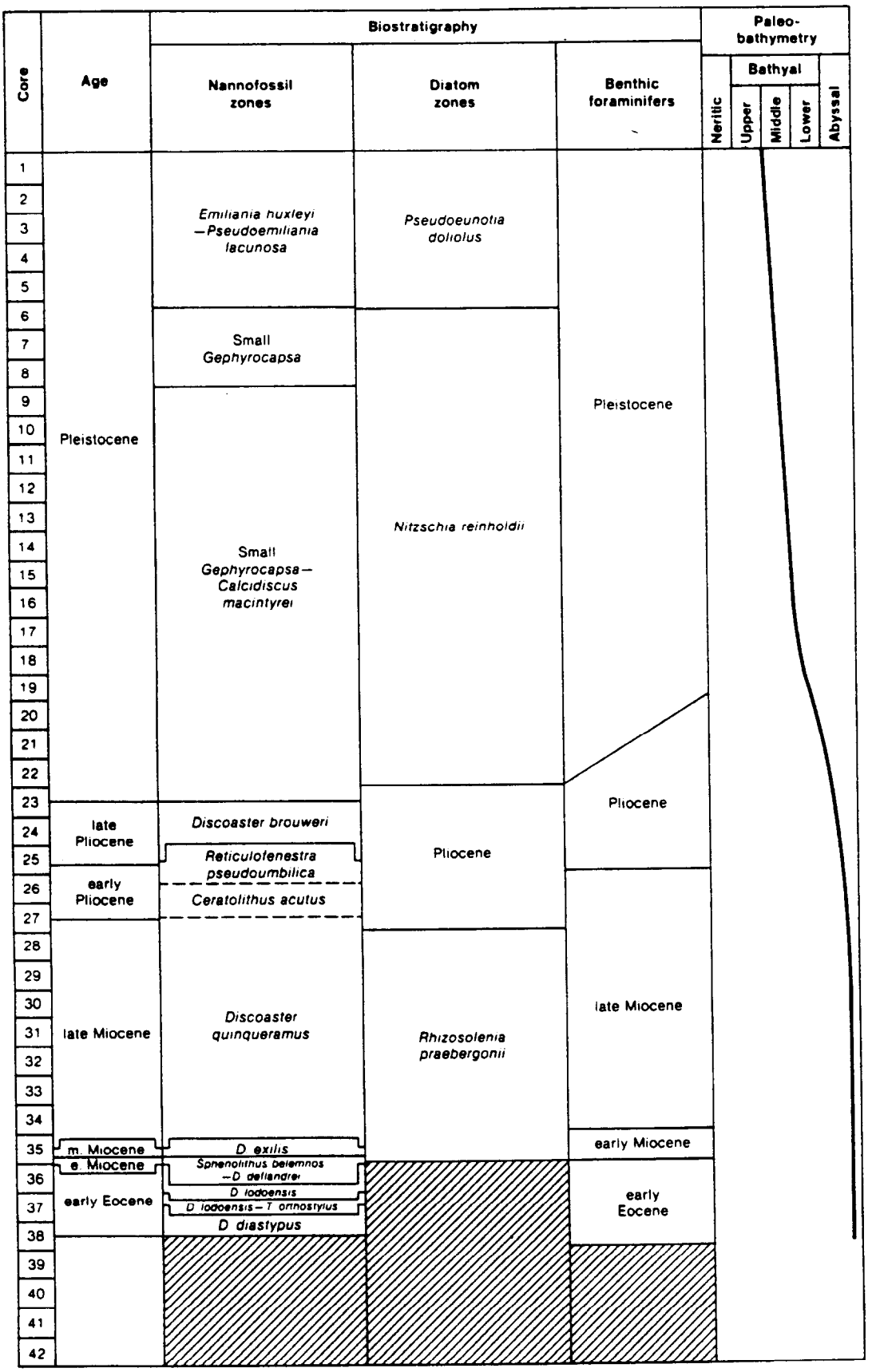

Figure 68. **BIOSTRATIGRAPHIC AND PALEOBATHYMETRIC SUMMARY, DSDP SITE 570**

After von Huene et al., 1985

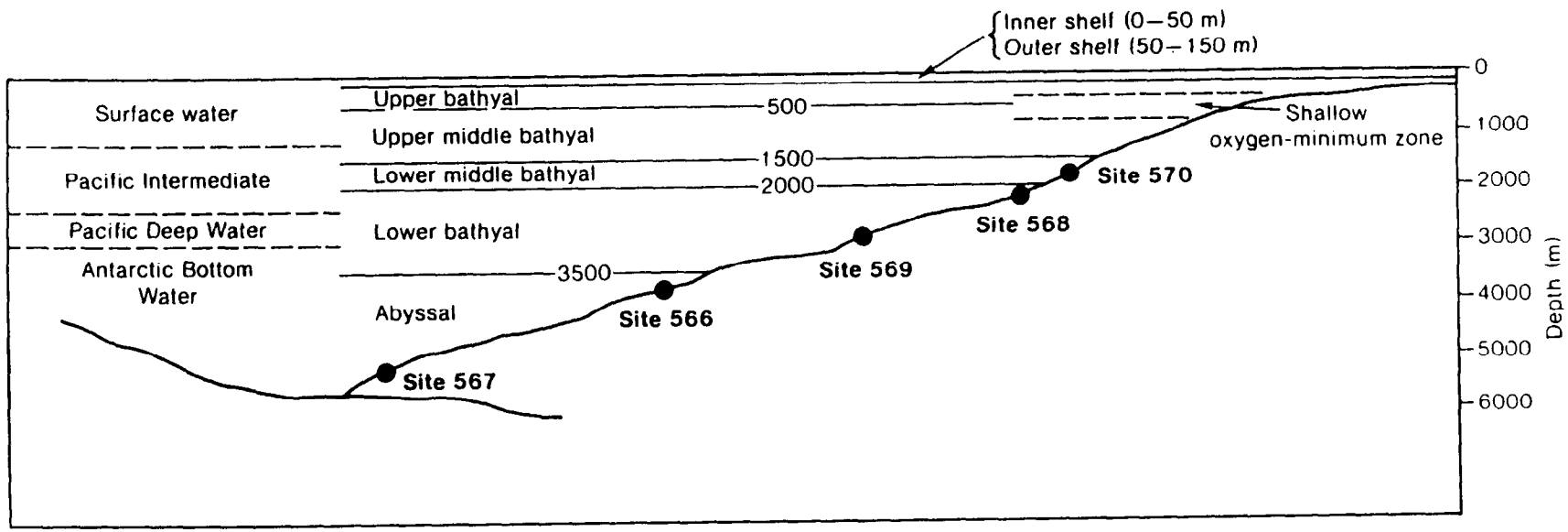

Figure 69. **DISTRIBUTION OF WATER MASSES AND BENTHIC FORAMINIFERAL BIOFACIES NEAR DSDP LEG 84 SITES**

Modified from McDougall, 1985

mass (Figure 69). Deepening in the Pliocene (McDougall, 1985) is attested to by the presence of forams deposited in the Pacific Deep water mass in core 24. Gradual uplift to present depth during the Pleistocene is demonstrated by fauna indicating a change from Pacific Deep water to Pacific Intermediate water.

Although McDougall (1985) indicated that a foundering occurred in Pliocene time (core 24), it must have been minor. She stated cores 28 through the lower part of core 24 were deposited in the Lower Middle Bathyal biofacies. The thickness of the Lower Middle Bathyal biofacies is presently about 500 m, from 2,000 m to 1,500 m water depth. If the same biofacies had a similar thickness in Pliocene time, the foundering would have been limited to <500 m.

The work of McDougall (1985) does not support the claims of tectonic uplift by Kvenvolden et al. (1984), although her work is cited as the source of the claim. McDougall (1985) presents no evidence or speculation that "water depth became shallower than at present during late Miocene to middle Pliocene time" (Kvenvolden et al., 1984). McDougall's (1985) interpretation of graduate shoaling throughout the Pleistocene coupled with the possible foundering in the Pliocene suggests that the present depth of Site 570 (1,700 m) is the least it has experienced since the deposition of the sediments found in core 27.

Nor are the claims of Kvenvolden and Claypool (1985) that "The continental slope was uplifted as much as 2 km by accretionary tectonic processes in the late Miocene and early Pliocene" supported by McDougall (1985). The previously discussed conclusions by McDougall (1985) that the slope remained at a constant depth during the Miocene and may have become deeper during the Pliocene clearly do not allow for 2 km of uplift during that same interval.

Eustatic sea level change. Kvenvolden et al. (1984) suggested that their proposed uplift may have been supplemented by a concurrent drop in sea level. They cite the work of Vail et al. (1977) showing that a global lowstand of sea level of 200 m below present sea level occurred in the late Miocene. The work of Vail and Michum (1979) demonstrates that this brief lowstand was followed by a high stand in the early to middle Pliocene of 132 m above present sea level. Thus any lowering of hydrostatic pressure due to the Miocene lowstand would have been more than compensated for by the rise in sea level during the Pliocene.

Effect of Uplift

The mechanism by which the uplift proposed by Kvenvolden et al. (1984) and Kvenvolden and Claypool (1985) was to have enhanced gas hydrate formation at Site 570 has been contested in the literature. The decrease in hydrostatic pressure from uplift and/or sea level drop were proposed to have reduced the solubility of methane in the pore water and have allowed large quantities of methane to come out of solution. This free gas was then to have rapidly hydrated. Work by Miller (1974) indicates that the free gas would not have existed under such conditions and that no additional hydrate would be expected to form upon an uplift of as much as 2 km.

The proposed mechanism of increased gas hydrate formation subsequent to a rapid uplift is a direct outgrowth of the statement by Kvenvolden et al. (1984) that: "Of the methane present, only the amount in excess of that soluble in water is available for gas hydrate formation." Thus supersaturation of pore water in methane is necessary for gas hydrate formation.

Miller (1974) investigated the thermodynamics of gas hydrate formation in sediments. He adapted the methods developed by Glew (1960) in his pioneering work on bromochlorodifluoromethane hydrate. The approach of Miller (1974) involved determination of the equilibrium value of fugacity of methane in water under pressure and temperature conditions in which gas hydrates are stable. His work indicated that pore water need not be saturated with methane for gas hydrates to form. Thus, the prerequisite of free gas bubbles for gas hydrate formation imposed by Kvenvolden et al. (1984) may be unnecessary.

Miller (1974) calculated the methane concentration of pore water in contact with a hydrate phase at 0°C and 400 atm pressure. Assuming nonsaline pore water, Miller (1974) derived an equilibrium value for methane concentration of 0.0571 M (moles/liter). The solubility limit of methane in water at 400 atm and 0°C was calculated by Miller (1974) as 0.352 M. The calculated concentration of methane in equilibrium with methane hydrate is 16% of the maximum solubility of methane in water under the same conditions. Saturated pore water at 400 atm and 0°C would thus precipitate gas hydrates, depleting the methane concentration of the pore water until a methane concentration of 0.0571 M was established. By this mechanism, 0.295 moles of methane per liter of pore water would be converted to hydrate.

The work of Miller (1974) indicates that free gas cannot coexist with gas hydrate for any substantial period of time except at the base of the gas hydrate stability zone. Within the gas hydrate stability zone, any free gas would go into solution in response to methane hydrate formation to maintain methane concentration in the water at the gas saturation point. As long as free gas is present in the system, the methane concentration in the water would remain at saturation point. Since the gas saturation limit is six times greater than the pore water methane concentration necessary for gas hydrate formation, methane would be quantitatively converted from free gas to dissolved methane to methane hydrate until only methane hydrate and dissolved methane at equilibrium concentrations were present. The thermodynamic treatment of Miller (1974) did not address kinetic factors. The rate at which the equilibrium concentration of methane in water is attained by hydrate precipitation may be slow, permitting methane concentrations as high as the gas saturation point to exist temporarily. However, given geological time in which to react, it is probable that the pore fluid system would eventually requilibrate, with all free gas being converted to hydrate and dissolved methane. The findings of Miller (1974) that equilibrium mixtures of water and methane will consist of methane hydrate and dissolved methane directly contradict the contentions of Kvenvolden et al. (1985) and Kvenvolden and Claypool (1985) that the equilibrium mixture consists only of free gas and dissolved methane or of free gas, dissolved methane, and methane hydrate.

Using the methods of Miller (1974), the equilibrium fugacity and concentration of methane in pore water at 0°C and 200 atm pressure were calculated. The 200 atm pressure corresponds to the pressure expected at Site 570 subsequent to the 2 km Pliocene uplift of the continental slope

proposed by Kvenvolden and Claypool (1985). The equilibrium methane content at 0°C and 200 atm so derived is 0.0576 M, essentially the same as for 400 atm. The implication of this modeling is that methane hydrate formation requires roughly the same minimum pore water methane content before or after an uplift from 4,000 m depth (400 atm) to 2,000 m depth (200 atm).

The above exercise does not adequately duplicate the physical conditions in sediment before and after the proposed uplift. The sediments presently hosting the massive gas hydrates would have been shallower than at present during the Miocene to Pliocene uplift, perhaps 10 to 60 m subbottom. However, even this close to the sea floor, the temperature of the hydrate-forming pore water would have been greater than the 0°C used by Miller (1974). The use of fresh water by Miller (1974) made his calculations much more straightforward. However, the pore water at the shallow subbottom depths of the massive gas hydrate host sediments in the late Miocene to middle Pliocene was certainly saline, probably close to sea water in total ion activity. Thus, the calculations of Miller (1974) should be repeated using input parameters which more closely approximate the actual physical and chemical environment of the sediment interstices at Site 570 to determine the applicability of Miller's (1974) conclusions to massive gas hydrate.

One problem encountered in extending the work of Miller (1974) to more realistic physical conditions is in obtaining methane solubility data for different physical conditions. Miller used a simple formula for methane solubility in fresh water 0° C derived from the work of Claussen and Polgase (1952) and Wetlaufer et al. (1964) of 2.55 x 10^{-3} M per atm fugacity. Correction of the derived value by applying Henry's Law permitted fairly accurate extrapolation to high pressures. For an independent test of the accuracy of the simple saturation relationship, we recalculated the work on methane stability at 25°C of Culberson and McKetta (1951) for different temperatures and salinities. The experimental solubility values of Culberson and McKetta (1951) were corrected to 0°C and 10°C using the temperature to solubility relationships of Weiss (1970). Methane solubilities at different salinities were also calculated using the results of Weiss (1970).

Equilibrium concentrations of methane in contact with hydrates were markedly different from Miller's (1974) values when calculated using the data derived from Culberson and McKetta (1951). Calculations at 0°C for fresh water resulted in 30% to 70% higher equilibrium methane concentrations using the solubility data of Culberson and McKetta (1951) than using the solubility formula proposed by Miller (1974). Interestingly, the results of lowering the pressure on the system under these conditions is different when using the solubility data of Culberson and McKetta (1951). The equilibrium methane concentrations at 0°C in fresh water are 0.0726 M at 200 atm hydrostatic pressure and 0.0975 M at 400 atm using the data of Culberson and McKetta (1951), whereas Miller (1974) calculated 0.0576 M at 200 atm and 0.5712 M at 400 atm. Thus, thermodynamic calculations using the equations of Miller (1974) but the solubility relationships of Culberson and McKetta (1951) show that the equilibrium methane concentration for pore water in contact with gas hydrates would decrease following an uplift from 4,000 m ocean depth to 2,000 m. Thus, a pore water system at equilibrium at a hydrostatic pressure of 400 m would form additional gas hydrates with no input of methane upon uplift to an ocean depth equivalent to 200 atm pressure. The additional gas hydrate formed would be slight; 0.27% of the available pore water would be

transformed into hydrate due to such an uplift. Thus it would appear that when Culberson and McKetta's (1951) solubility relations are used to calculate equilibrium methane concentrations, the results partially agree with the contentions of Kvenvolden et al. (1984) and Kvenvolden and Claypool (1985) that more hydrates can form subsequent to a major rapid uplift. However the additional hydrate content would appear to be very small, and the effect appears to be unrelated to the changes of solubility of methane gas in pore water due to such an uplift.

Additional thermodynamic calculations using the methods of Miller (1974) have been performed for more realistic pore water conditions. Four combinations of temperature and salinity were used to model an uplift resulting in a change at confining pressure from 400 atm to 200 atm. The results of the calculations are presented in Table 17. As expected, increasing temperature or salinity increases the pore water methane concentration necessary to stabilize gas hydrates. As discussed above, the concentrations calculated directly from Miller's (1974) method show no change in equilibrium methane concentrations with a pressure reduction, while the concentrations calculated using Miller's (1974) methods, but the solubility data of Culberson and McKetta (1951), show a 20% decrease in equilibrium concentration of methane going from 400 atm to 200 atm. The implication is that uplift of 2,000 km would result in the formation of no new hydrates if the solubility relationships used by Miller (1974) are the more accurate. If the solubility data of Culberson and McKetta (1951) is a closer approximation of reality, then small amounts of additional methane hydrate formation would be expected due to the hydrostatic pressure reduction accompanying uplift. Regardless of which view is more correct, the work of Miller (1974) indicates that any increase in hydrate formation due to uplift would be minor and is unrelated to diminished solubility of gaseous methane at lower hydrostatic pressures.

A more general implication of the different interpretations of gas hydrate formation processes proposed by Miller (1974) on the one hand and Kvenvolden et al. (1984) and Kvenvolden and Claypool (1985) on the other is evident. According to Miller (1974) free gas can only exist for a short time in the gas hydrate stability zone. Since the equilibrium methane content of pore water in the gas hydrate stability zone is less than the solubility of gaseous methane in the water, all free gas will eventually be converted to hydrates. Thus, except for transient events, the simultaneous presence of gas hydrates and free gas is not to be expected. This view is directly contradicted by the massive gas hydrate model of Kvenvolden et al. (1984) and Kvenvolden and Claypool (1985). In that scenario, gas hydrates would only be expected in the presence of free gas accumulation. If the concentration of methane in the pore water diminished below the solubility limit, the work of Kvenvolden et al. (1984) and Kvenvolden and Claypool (1985) suggests that hydrates would decompose to reestablish the maximum possible aqueous concentration of methane. At the solubility limit of methane the partial pressure of aqueous and gaseous methane are equal, and free gas pockets would be expected.

Neither of these two contrasting views on gas hydrate formation and stability are directly backed by experimental data. The equilibrium relationships proposed by Miller (1974) were based on empirical evidence of Glew (1962) on bromochlorodifluoromethane hydrate. However, the direct applicability of the conclusions to methane hydrate was apparently not

TABLE 17.

EQUILIBRIUM CONCENTRATIONS OF METHANE IN PORE WATER
Calculated Using the Method of Miller (1974)

Temp	Salinity per mil	Pressure atm	Equil. Concn. M	Saturation	Equil. Concn. (data of Culberson and McKetta) M	Saturation
0	0	200	.0576	21%	.0726	26%
		400	.0571	15%	.0975	25%
10	0	200	.136	64%	.118	56%
		400	.127	43%	.145	49%
0	35	200	.069	31%	.073	33%
		400	.068	22%	.090	29%
10	35	200	.166	96%	.114	60%
		400	.169	40%	.142	60%

confirmed experimentally by Miller (1974). Neither Kvenvolden et al. (1984) nor Kvenvolden and Claypool (1985) referenced previous experimental studies or reported on their own experimental work which would confirm that the presence of free gas is a precondition for gas hydrate formation.

Experimental data from more general gas hydrate research may have a bearing on the discrepancy of general conclusions of Miller (1974) and the massive gas hydrate model of Kvenvolden et al. (1984) and Kvenvolden and Claypool (1985). Work reported by Makogon et al. (1972), Makogon and Koblova (1972) and Makogon (1974) indicated that the solubility of methane in water decreases dramatically when pressure and temperature conditions of gas hydrate stability are met. The process by which the solubility drop was measured is not clear from the cited reports. However, as seen in Figure 70, methane solubility reaches a peak of 0.086 M at about 75 atm pressure and 10°C. Further increase in pressure, the solubility of methane in water drops sharply to 0.01 M. Subsequent increases in applied pressure result in a slow increase in solubility to about 0.018 M at 100 atm.

This work by Soviet researchers can be interpreted as experimental evidence supporting Miller's (1974) theoretical derivations. Miller (1974) contended that when pressure was increased on a system of water saturated with methane to the point where gas hydrates are stable, gas hydrates will crystallize from the solution. Continued depletion of methane from the water by hydrate growth results in the solution of any available gaseous methane. When the gas phase is consumed, continued hydrate growth results in depletion of the pore water methane concentration from the solubility limit of gaseous methane to the equilibrium concentration of methane in water in contact with hydrates. This theoretical equilibrium methane concentration for pore water in contact with hydrates is lower than the solubility limit of gaseous methane according to the calculations of Miller (1974). The methane concentration rises with increasing pressure as documented by Culberson and McKetta (1951) until the methane hydrate formation pressure is reached, 72 atm at 10°C. The drastic drop documented by the Soviets in what has been translated as methane solubility which occurs at this point could be a reflection of the change from gaseous methane solubility to methane hydrate equilibrium concentration as the dominant control on observed methane concentration. Once the system reaches pressure and temperature conditions of methane hydrate stability, the rapid formation of hydrate depletes the water of methane. If the Soviet scientists determined solubility by measuring aqueous gas concentrations, then a drop in measured values which they reported would be consistent with the predictions of Miller (1974). That is, if the quantity graphed in Figure 70 is analytical methane concentration in water, then the values obtained correspond to gaseous methane solubility values only at pressures lower than that at which hydrates are stable. Within gas hydrate stability conditions, the analytically determined methane concentration is governed not by gaseous methane solubility, but by factors related to the gas hydrate formation process. These possible controlling factors would include rate of methane solution, rate of hydrate crystallization, rate of diffusion, and eventually, the equilibrium content of methane in contact with hydrates.

A similar, but less marked change in analytically measured methane solubility was noted by Culberson and McKetta (1951). In their work the solubility of methane in water at 25°C and various pressures showed lower than expected values for pressures at which gas hydrates are stable (Figure

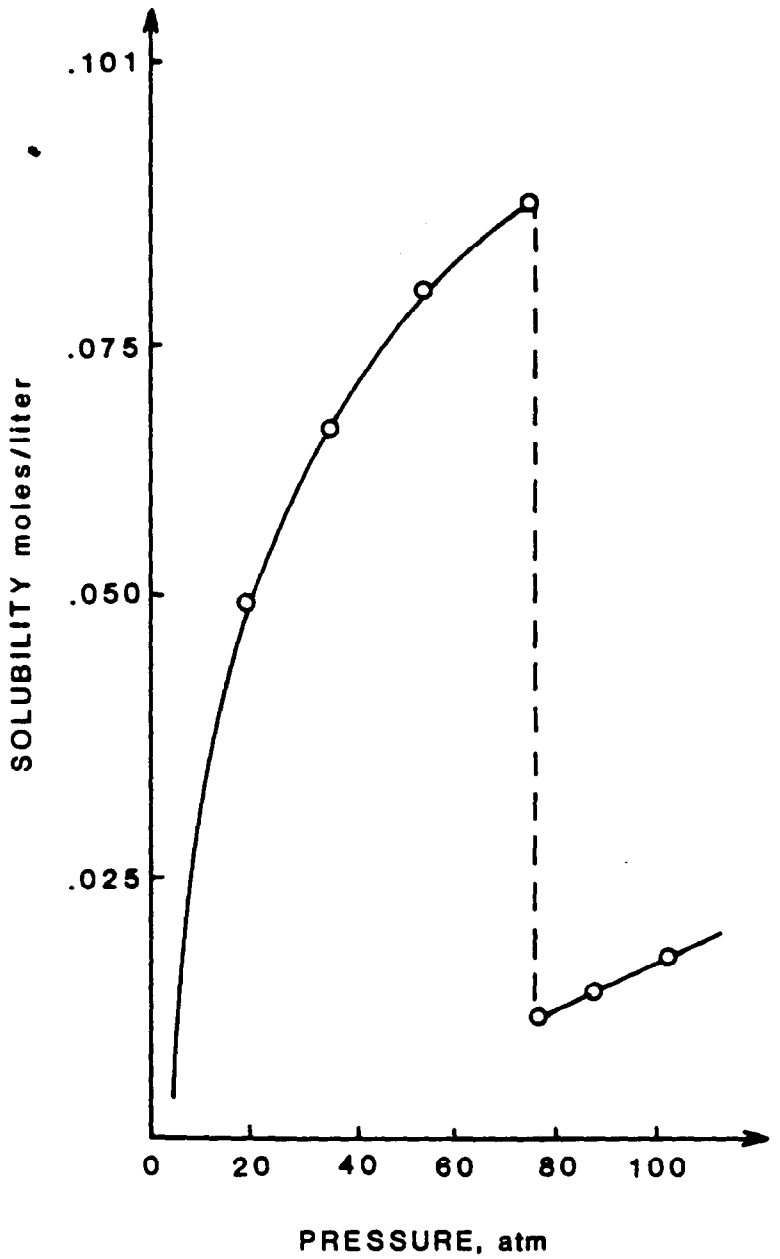

Figure 70. SOLUBILITY OF METHANE IN WATER AT 10°C

After Makogon et al., 1972

71). Culberson and McKetta (1951) reported the values, but cautioned that solubility values under conditions of gas hydrate stability reflect factors other than methane solubility in water:

> These parenthetical values are non-equilibrium solubilities determined when the liquid phase co-existed with vapor and hydrate phases. The original purpose of this investigation was the study of vapor-liquid equilibrium. For those pressures at which the hydrate formed, samples of the liquid phase nevertheless were taken. However, the attainment of equilibrium in hydrate systems is a slow tedious process, and the parenthetical values are therefore the solubilities measured before the hydrocarbon in the vapor phase had been completely transposed to the hydrate phase.

Claypool and Kaplan (1974) presented a phase diagram for methane hydrate which supports the conclusions of Miller (1974) that hydrates can form directly from a methane-water solution at concentrations less than the solubility limit of methane in water. The phase diagram (Figure 72) differs from those typically presented in that it illustrates relationships at a fixed temperature and varying pressure and composition, whereas the typical diagram displays pressure and temperature at a fixed composition. Typical gas hydrate stability diagrams are constructed for fairly high values of methane content in the system, 0.4 to 14.8 mole percent (Claypool and Kaplan, 1974). In this composition range, methane is present as a free gas. Data on gas hydrate formation and stability has typically been obtained under conditions of excess methane. The lower left corner of the phase diagram in Figure 72 shows the phase relationships at composition which is more typical of that existent naturally, where gas is present in solution at concentrations less than that of maximum solubility. The line between the liquid and the gas + liquid fields represents the solubility limit of methane gas in water. Incorporating the findings of Makogon et al. (1972), the phase diagram of Claypool and Kaplan (1974) shows that methane solubility reaches a peak at 462 atm, the minimum pressure necessary to stabilize methane hydrate at 25°C. The horizontal line at 462 atm separating the liquid field from the liquid and gas field suggests that gas hydrates should be formed directly from aqueous methane at concentrations less than the maximum solubility limit (0.4 mole percent).

Claypool and Kaplan (1974) presented an interpretation of Figure 72 which also agrees with the concept that methane hydrates can form from a methane-water solution which is less than saturated with methane.

> At this temperature, 25°C, the requirements for methane hydrate ($CH_4 \cdot 5\text{-}3/4H_2O$) stability are: pressure in excess of 462 atm, and a methane concentration that exceeds about 0.13 mole %, or about 72 mmol/kg. For methane in sea water, the critical concentration for hydrate stability would be about 20% less, or around 58 mmol/kg, assuming that the decrease in methane solubility caused by 35 per mil salinity is comparable to that for nitrogen and argon, as discussed by Weiss (1970).

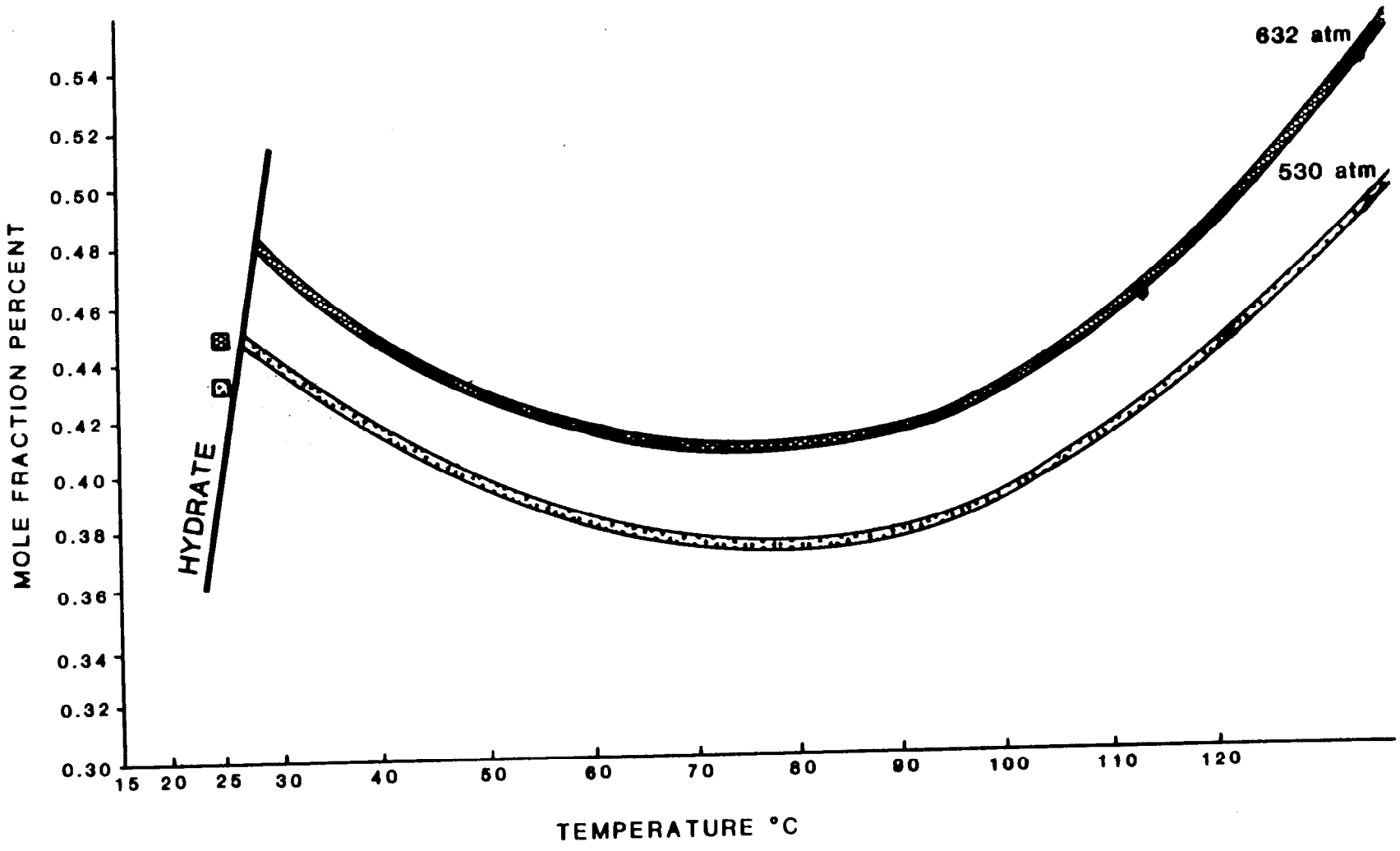

CURVES FOR TEMPERATURES GREATER THAN 25°C ARE INTERPOLATED FROM PUBLISHED CURVES.

Figure 71. **SOLUBILITY OF METHANE IN WATER AT 530 AND 632 atm.**

Data from Culberson and McKetta, 1951

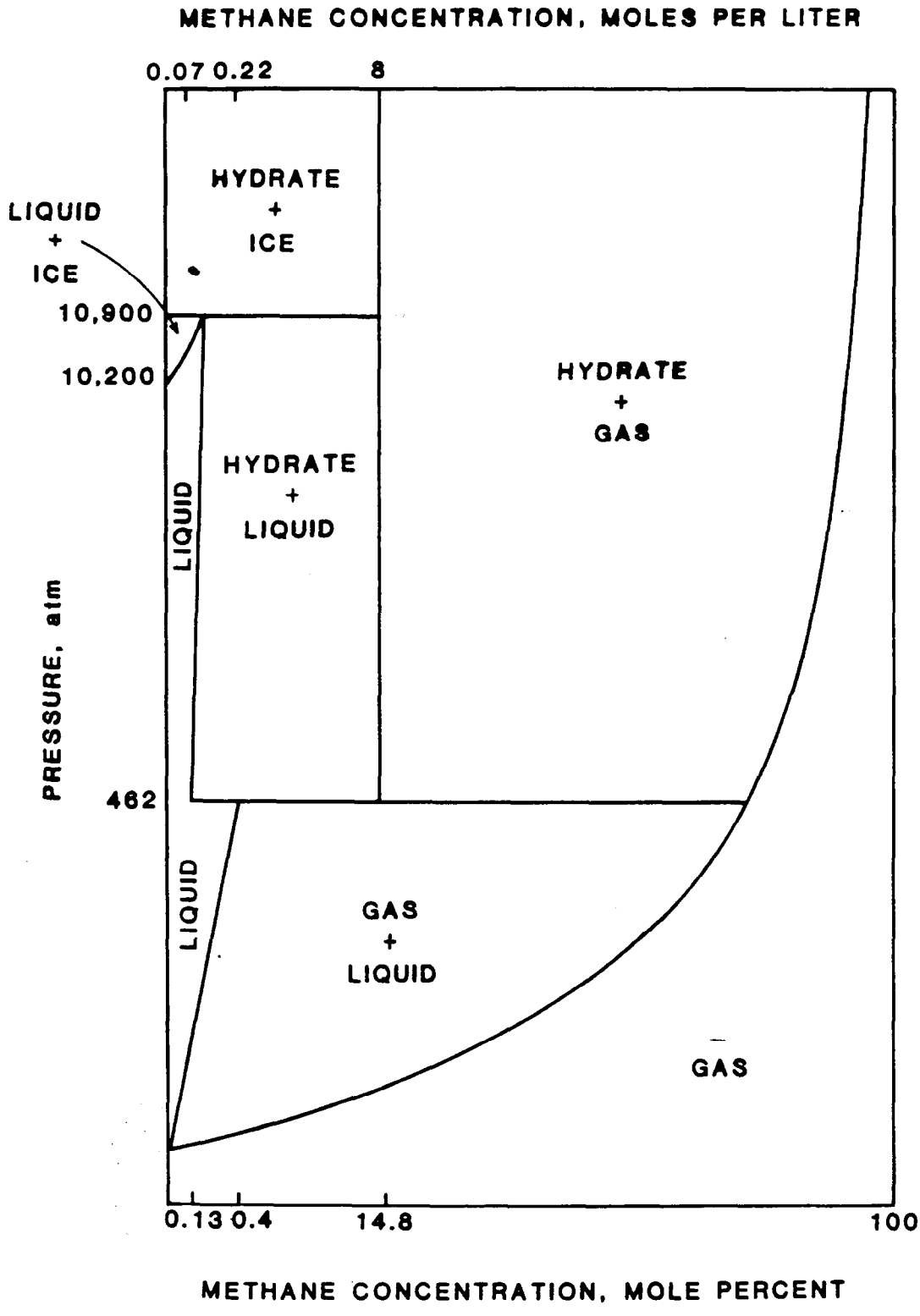

Figure 72. METHANE HYDRATE PHASE DIAGRAM AT 25°C

After Claypool and Kaplan, 1974

By this interpretation, methane hydrate can form when methane concentration is only 32% of the solubility limit of methane under these conditions as measured by Culberson and McKetta (1951).

The work of Makogon et al. (1972), Miller (1974) and Claypool and Kaplan (1974) was strongly opposed by Milton (1976). Milton (1976) agreed with Kvenvolden et al. (1984) and Kvenvolden and Claypool (1985) that only water supersaturated with respect to gaseous methane can form gas hydrates. He stated that the sudden decrease in aqueous methane concentrations at the gas hydrate stability pressure is untenable on thermodynamic grounds. Milton claimed that the liquid, hydrate + liquid and gas + liquid fields in Figure 72 must meet at a single nonvariation point.

The objections of Milton (1976) to the work of Claypool and Kaplan (1974) and Makogon et al. (1972) do not preclude the formation of gas hydrates at aqueous methane concentrations less than the saturation limit of gaseous methane. Milton (1976) showed that increasing pressure favors gas hydrate formation from methane dissolved in water. One driving force in gas hydrate formation is the volume of a gas hydrate relative to the combined volumes in methane and water. Since a pressure increase should increase the methane occupancy of the hydrate cages, the volume decrease due to hydrate formation would be greater at higher pressures. Miller (1976) thus had two objections to the gas hydrate phase diagram of Claypool and Kaplan (1974), reproduced in this report as Figure 72. (1) The liquid, hydrate + liquid, and gas + liquid lines must meet at a single point. (2) The line between the liquid and hydrate + liquid fields must have a negative slope above the triple point to accommodate the increasing stability of gas hydrate with pressure. We have altered the phase diagram of Claypool and Kaplan (1974) according to the objections of Milton (1976). In Figure 73, the curvature of the line separating the liquid and hydrate + liquid fields is interpretive; Miller (1976) did not specify the slope of the line. He did claim that the pressure effect on gas hydrate stability should be greatest between the triple point (462 atm) and 1,000 atm whereupon the gas hydrate cage would be 100% occupied. For a smooth transition at 1,000 atm, we have interpreted that the line decreases regularly in slope with rising pressure (Figure 73). If our interpretations of the shape of the line between the liquid and hydrate + liquid fields is legitimate, then it is possible for a solution of methane at concentrations less than the gaseous saturation point to form hydrates. In the example in Figure 73, a methane solution of 0.3 mole percent subjected to increasing pressure would form a hydrate as predicted by Claypool and Kaplan (1974), but at a higher pressure than they projected (about 500 atm vs. 462 atm). The work of Milton (1976) demonstrates that higher pressure is necessary for gas hydrate formation from an undersaturated solution of methane and water than where a free gas phase exists in contact with water. However, Milton's work does not preclude the formation of gas hydrate directly from undersaturated pore water.

The work of Claypool and Kaplan (1974) and Milton (1976) as summarized in Figure 73 does not support the concept of a rapid increase in gas hydrate formation due to an uplift. From within the hydrate + liquid field in Figure 73 a decrease in pressure would result only in the dissociation of existing gas hydrates upon passing into the liquid or gas +liquid fields. Although it is possible for an uplift to lead to exsolution of gas from pore water, Figure 73 suggests that this only occurs at pressures lower than the minimum necessary for hydrate stability at a given temperature. Although Figures 72 and 73 are diagrammatic and not confirmed by detailed laboratory simulations, the

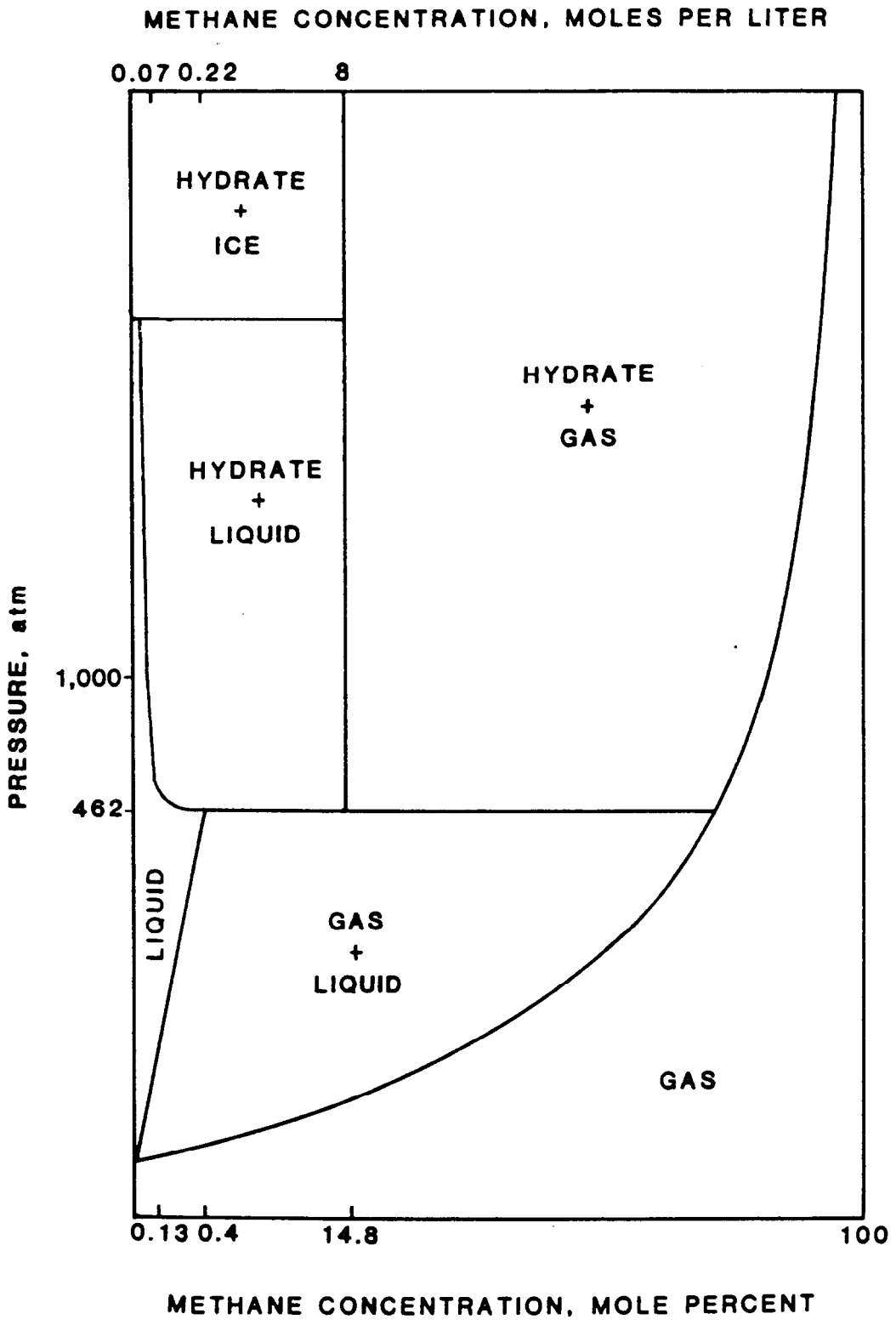

Figure 73. METHANE HYDRATE PHASE DIAGRAM AT 25°C

Modified from Claypool and Kaplan, 1974,
based on conclusions of Milton, 1976

general relationships illustrated agree with the observations of Culberson and McKetta (1951), Makogon et al. (1972), Claypool and Kaplan (1974), Milton (1976), and Dominic and Barlow (1985) that dissolved methane need not attain concentrations of saturation relative to the gas phase for gas hydrates to form.

From the foregoing review of relevant articles, it is apparent that the requirement that gas hydrates can only form from a solution supersaturated with respect to methane gas may not be valid. Thus, it is possible that the proposed rapid increase in gas hydrate formation brought about by supersaturation due to uplift may not be applicable to formation of the massive gas hydrate at Site 570. If the rapid uplift in late Miocene to middle Pliocene proposed by Kvenvolden et al. (1984) and Kvenvolden and Claypool (1985) did occur, it is not likely that significantly more gas hydrates would form, as they had proposed.

Source of Gas

In-situ microbial methanogenesis is the most likely source for the hydrocarbons in the massive gas hydrate according to the formation model of Kvenvolden et al. (1984) and Kvenvolden and Claypool (1985). The high organic carbon content of the host sediments at Site 570 is thought to have allowed intense bacterial methane generation. Unusual isotopic signatures of the gases at both Sites 568 and 570 are proposed to be a direct result of microbial methanogenesis in such organic-rich sediments. Many of the salient points on the source of the hydrate gas were previously dealt with in the gas hydrate occurrences section of this report.

The carbon isotopic contents of pore fluid gases and gas from dissociated hydrates from Sites 568 and 570 are anomalously heavy. Methane $\delta^{13}C$ values from depths greater than 200 m at Site 568 and 250 m at Site 570 range from -36 per mil to -50 per mil (Brooks et al., 1985; Claypool et al., 1985; Galimov and Shabaeva, 1985; Jeffrey et al., 1985). Isotopic values of these gases become heavier with depth, with the heaviest measured values occurring in the fractured serpentinite basement of Site 570 (Galimov and Shabaeva, 1985).

The $\delta^{13}C$ values obtained from gases from the pore fluids and hydrates are heavier (more positive) than those typical of biogenic methane (Schoell, 1983). Galimov and Shabaeva (1985) concluded that the isotopically heavy methane at Sites 568 and 570 were generated from thermal degradation of organic matter. The sediments drilled on DSDP Leg 84 from the Guatemalan continental margin were found to be thermally immature with respect to hydrocarbon generation (Gilbert and Cunningham, 1985; Kennicutt et al., 1985). Therefore, the conclusion of Galimov and Shabaeva (1985) of a thermogenic source for methane requires migration from unidentified mature source beds.

The majority of Leg 84 scientists contended that the methane from which recovered gas hydrates were formed had a biogenic origin regardless of its isotopic signature (Brooks et al., 1985; Claypool et al., 1985; Kvenvolden and McDonald, 1985; Jeffrey et al., 1985). The basis of this conclusion was the anomalously heavy carbon dioxide (CO_2) and total carbonate (ΣCO_2) which coexisted with the methane at Sites 568 and 570. Microbial reduction of CO_2 to methane exhibits a large kinetic isotope effect; the product methane is typically 60 to 70 per mil lighter than the CO_2 substrate and about 80 per mil lighter than the dissolved carbonate (Claypool and Threlkeld, 1983). Since

the isotopic signatures of carbon dioxide and total carbonate maintained the expected difference from the methane values, most Leg 84 DSDP scientists concluded that the methane resulted from biogenic processes. The unusual enrichment in ^{13}C of the methane resulted from reduction of anomalously enriched CO_2.

The heavy CO_2 was proposed to have been produced by continuous methanogenic depletion of ^{12}C in the CO_2 pool of the pore water. As methane is produced from CO_2, the ^{13}C content of the residual CO_2 increases due to the 70 per mil isotopic fractionation which accompanies the reduction. Subsequent methanogenesis results in increasing ^{13}C enrichment of the remaining CO_2. Since methane produced in latter stages of the biogenic processes is derived from the ^{13}C-enriched CO_2 pool, the isotopic content of the product methane also becomes progressively heavier while retaining its 70 per mil difference from the CO_2.

In most instances the isotopic fractionation, which results in heavier isotopic values of methane with depth, does not continue to the extent that it apparently did at Sites 568 and 570. The $\delta^{13}C$ value of the residual CO_2 typically levels off at about 10 to 15 per mil (Claypool et al., 1985). With an 80 per mil depletion of ^{13}C upon methanogenesis, the $\delta^{13}C$ values of biogenic methane would also typically level out at -70 to -65 per mil. Claypool et al. (1985) attributed this approach to a constant $\delta^{13}CO_2$ value with burial to a continual influx of CO_2 from organic material decomposition with a $\delta^{13}C$ value of about -25 per mil. The 10 to 15 per mil maximum $\delta^{13}C$ of the total carbonate fraction, which is typically seen, apparently results from equal rates of introduction of CO_2 by organic matter decomposition and removal of CO_2 from the pore water by methanogenesis.

Claypool et al. (1985) reported the preliminary results of kinetic modeling of methane forming processes at Site 570 using the methods of Wigley et al. (1978). Various combinations of possible CO_2 sources, CO_2 outputs, and methane outputs were tested to find a combination of factors which would duplicate the observed trends of increasing $\delta^{13}C$ and decreasing total carbonate content with depth. The best agreement with measured values for the gas hydrate-bearing section was obtained by assuming that (1) oxidation of organic matter to CO_2 was the sole source of CO_2, (2) dissolved CO_2 was converted to methane and also precipitated as authigenic carbonate minerals, and (3) input of CO_2 to the system equals only 80% of the total output as methane and carbonates. It was also determined that the carbonate would precipitate in amounts 1.5 times that of the methane produced. By applying this model to Site 570 data, Claypool et al. (1985) sought to demonstrate that the unusual isotopic characteristics of methane, carbon dioxide, and bicarbonates in the pore fluids could be explained by reasonable combinations of known bacterial diagenetic processes.

The amount of authigenic carbonate which the kinetic model suggests would have formed at Site 570 can be calculated. Experimental dissociation of the recovered massive gas hydrate by Kvenvolden et al. (1985) indicated a stoichiometry of $CH_4 \cdot 20(H_2O)$. Massive gas hydrate composed of 1 mole of molecules would thus contain about 0.05 moles of methane. During the generation of that amount of methane, the kinetic model detailed by Claypool et al. (1985) predicts that 0.075 moles of carbonate would be precipitated. Assuming the carbonate is calcite with a gram-formula weight of 100, 7.5 g or about 3 cm^3 would precipitate. The massive gas hydrate containing 0.05 moles of methane would occupy 16 cm^3 assuming a hydrate density of 0.9 g/cm^3. Thus, the formation of the massive gas hydrate at Site 570 requires

that carbonates amounting to 19% of the volume of the massive gas hydrate be precipitated. The 4 m thick massive gas hydrate interval drilled at Site 570 (Mathews and von Huene, 1985) is equivalent to 75 cm of dense limestone. The generation of this amount of methane could thus provide sufficient carbonate to have precipitated the 10 to 20 cm thick dolomite layer found in core 27 near the massive gas hydrate. Helm (1985) found that the deeper sections of Site 570 contained abundant calcite in the form of micritic cement. Also, iron carbonate cementation was noted. From the work of Helm (1985), calcite cementation seems to be much more prevalent at Site 570 than at other Leg 84 locations. This may be some indication that the kinetic diagenetic model of Claypool et al. (1985) is indeed relevant to Site 570 conditions.

Claypool et al. (1985) also analyzed equilibrium isotopic effects of pore water constituents at Site 570. It was claimed that the isotopic differences among methane, carbon dioxide, and total dissovled carbonate are consistent with other DSDP holes from which biogenic methane was recovered. Site 570 pore fluids and gases are anomalously enriched in ^{13}C, and thus possibly of thermal origin. To examine this possibility, and to further test their kinetic diagenetic model, Claypool et al. (1985) compared the isotopic differences among carbon species with those predicted from laboratory studies.

Mook et al. (1974) determined that the equilibrium difference in isotopic content of coexisting CO_2 and dissolved bicarbonate measured as $\delta^{13}C$ values was well approximated by a temperature function. Claypool et al. (1985) reevaluated the data of Mook et al. (1974) and proposed a slightly modified relationship: $\delta^{13}C(HCO_3^-) - \delta^{13}C(CO_2) = 9.55 \times 1000/K - 24.10$, where K = solution temperature in Kelvin. This expected relationship and the data from Site 570 are plotted on Figure 74. The match of the site data and the proposed equilibrium fractionation of Mook (1974) is not good. Claypool et al. (1985) claimed that most of the data points fall near a line parallel to the line of Mook et al. (1974), also diagrammed in Figure 74. A regression line of best fit which we obtained by the least squares method is also plotted on Figure 74. The trend of the data from Site 570 is clearly different than that predicted by Mook et al. (1974) from controlled laboratory studies. The difference between isotopic values of dissolved bicarbonate and CO_2 increases sharply with depth rather than decreasing as expected.

Claypool et al. (1985) stated that the disparity between the measured data and Mook et al.'s (1974) expected trend of isotopic content has a straightforward explanation:

> It can be assumed that the dissolved CO_2-species are in isotopic equilibrium under in situ conditions in the Guatemala slope sediments. Therefore, the disagreement shown in [Figure 74] must be due to various imperfections in the sampling and analytical procedures.

Their rationalization of the geochemical results is particularly disturbing. The conclusions of Claypool et al. (1985) that the gas at Site 570 is probably of biogenic origin is the basis for the massive gas hydrate formation models of Kvenvolden et al. (1984) and Kvenvolden and Claypool (1985). Biogenic origin was principally based on the difference between $\delta^{13}C$ values of coexisting methane and total dissolved carbonate (bicarbonate). The 77 to 80 per mil difference down the hole to a depth of 280 m was compared with a similar difference in methane and bicarbonate values noted at Site 533, where

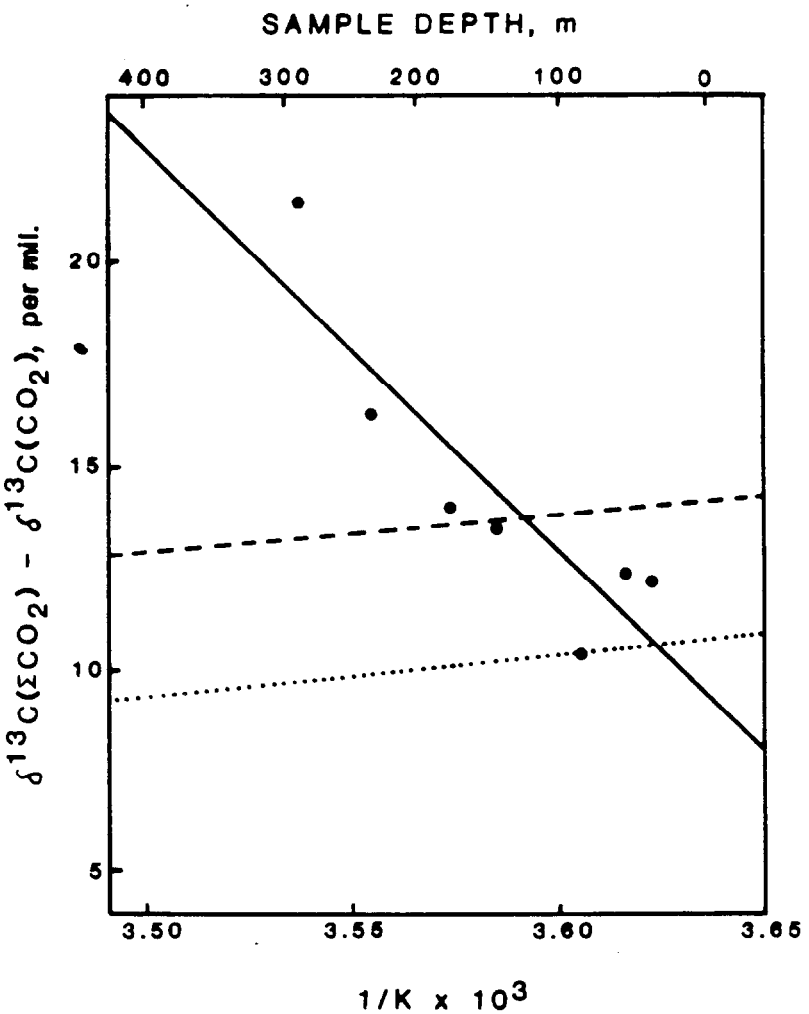

• DATA POINT

····· $CO_2 \rightarrow HCO_3$ EQUILIBRIUM (Mook et al., 1974)

--- LINE OF BEST FIT AS SUGGESTED BY Claypool et al., 1985

—— LINE OF BEST FIT BY LEAST SQUARES METHOD

K - FORMATION TEMPERATURE IN KELVIN, ASSUMING 2.6°C/100m GRADIENT AND 2°C SEA FLOOR TEMPERATURE

Figure 74. **DIFFERENCES IN ^{13}C CONTENT OF CO_2 AND ΣCO_2 AT DSDP SITE 570 AS FUNCTION OF FORMATION TEMPERATURE**

Data from Claypool et al., 1985, and Jeffrey et al., 1985

biogenic origin is a certainty. The close agreement with Site 533 was taken as a strong indication that methane at Site 570 was produced by in situ microbial reduction of CO_2 in spite of anomalously heavy methane typically associated with a thermal origin. If it is true that discrepancies seen in Figure 74 are due to analytical error, then the data upon which the proposed biogenic origin is based are necessarily suspect. Analytical or sampling errors of sufficient magnitude to produce the discrepancies seen in Figure 74 (2 to 20 per mil) are large enough to render the carbon isotope data and interpretations based thereon questionable.

It is perhaps more prudent to provisionally accept the validity of the Site 570 data, and instead address the apparent isotopic disequilibrium displayed between carbon dioxide and total dissolved carbonate. As shown in Figure 74, the difference in $\delta^{13}C$ values for the two species increases rapidly with depth, approximately doubling between 50 m and 300 m subbottom depth. The work of Mook et al. (1974) indicates that the difference in $\delta^{13}C$ values should decrease slightly with depth. Explanations for this discrepancy include the possibility that the pore water system in the deeper sections of Site 570 are not at equilibrium, or that the work of Mook et al. (1974) does not closely approximate conditions in the natural environment.

Claypool et al. (1985) also investigated equilibrium isotopic fractionation of the reduction of CO_2 to methane. They presented a plot similar to Figure 74 of $\delta^{13}C$ difference vs. 1/K for the Leg 84 data. A general trend of a decreasing difference between $\delta^{13}C(CH_4)$ and $\delta^{13}C(CO_2)$ with depth is seen. Although the general nature of the trend for Site 570 agrees with that predicted by equilibrium equations, Claypool et al. (1985) claimed that the data do not support the existence of a $CO_2 \rightleftharpoons CH_4$ equilibrium. It should be noted that the agreement of measured isotopic values and those predicted by theory is much closer for the $CO_2 \rightleftharpoons CH_4$ data, for which equilibrium was rejected, than for the $CO_2 \rightleftharpoons HCO_3^-$ system, for which equilibrium was explicitly endorsed.

Deuterium content of Site 570 methane also supports its microbial origin. Deuterium content (δD) of core gas methane was measured at -163 to -208 per mil with most readings centered around -185 per mil SMOW (Claypool et al., 1985). Hydrogen isotope values of -200 to -150 are typically associated with biogenic methane produced from marine sediments (Schoell, 1983). Of 69 samples of biogenic methane from marine sediments, Whiticar et al. (1986) obtained a mean δD value of -187 per mil, nearly identical to the mean from Site 570. Methane with such an isotopic signature alternatively could have a thermal origin (Schoell, 1983). Wet gases associated with oil or condensate have isotopic signatures which closely match Site 570 methane ($\delta^{13}C$ = -42 per mil, δD = - 185 per mil). However, the methane from Site 570 had very low concentrations of heavier hydrocarbons which would be expected to be present in an associated natural gas. Only by extensive migrational separation could an associated gas be denuded of the expected quantities of ethane, propane, and butane. Dry natural gas from thermal cracking of petroleum and/or overmature kerogen could fulfill the requirement of being nearly pure methane, but dry thermal gases typically have δD values of -150 to -120 per mil (Schoell, 1983). Thus, the consideration of hydrogen isotope data indicate that the only reasonable alternative to biogenic origin of Site 570 methane is migration of associated wet natural gas from a source bed with a vitrinite reflectance value of less than 1.2% with concomitant chromatographic stripping of all higher hydrocarbons.

In summary, we find the supposition of biogenic origin of the methane in the massive gas hydrate to be the most consistent with the available data.

Summary

The model of massive gas hydrate formation proposed by Kvenvolden et al. (1984) and Kvenvolden and Claypool (1985) has been examined in the preceding sections. Data from DSDP Leg 84 suggest that two of the three processes proposed to be major factors in massive gas hydrate did not occur at Site 570.

1. Dolomite Cap Rock was proposed to have formed at about 10 m subbottom and to have prevented diffusive loss of methane to the ocean. Methane trapped below the dolomite was then to have formed the massive gas hydrate. We have concluded that a thin dolomite layer with properties matching the dolomite recovered in core 27 was located **below** the massive gas hydrate layer. Although a second dolomite layer--above the massive gas hydrate--cannot be conclusively ruled out, evidence for it is weak. The documented existence of an impermeable dolomite layer **beneath** the massive gas hydrate layer strongly suggests that lithological trapping of methane had little influence on massive gas hydrate formation at Site 570.

2. Rapid uplift in the late Pliocene to middle Miocene was proposed to have released great quantities of gas from solution which was converted to massive methane hydrate. Paleontological evidence contradicts the proposed sudden uplift. Benthic foraminifera indicate that water depth was static during that time or may have deepened slightly. Uplift which did occur was gradual and was concentrated in the middle to late Pleistocene. Additionally, theoretical arguments and experimental evidence exists that questions whether an uplift such as that proposed would enhance gas hydrate formation significantly.

3. Biogenic Source was proposed for the methane composing the massive gas hydrate. We find no evidence to contradict biogenic methane produced from anomalously heavy CO_2. Inconsistencies exist in some isotopic measures; these data may be of use in further refining the gas generation processes operative at Site 570. The possibility of thermogenic methane at Site 570 cannot be excluded based on available evidence.

Alternative Massive Gas Hydrate Formation Model

The massive gas hydrate formation model proposed by Kvenvolden et al. (1984) and Kvenvolden and Claypool (1985) was a pioneering effort to explain the unexpected presence of the 4 m thick gas hydrate layer drilled at DSDP Site 570. The foregoing discussion of the model indicates that some of its principal assumptions have been contradicted by more recently published data. In this section, an alternative model of massive gas hydrate formation is presented and discussed.

Mathews and von Huene (1985) speculated that "drilling at Site 570 may have penetrated through a fault zone that provided the space for accumulation

of massive gas hydrate." They based their interpretation on well log analysis and a high resolution seismic study of the Site 570 area by Volpe et al. (1985). Mathews and von Huene (1985) contended that at least one of the transverse canyons on either side of Site 570 is actually the surface trace of a major fault.

Site 570 was drilled at a location 80 km to the northwest of San Jose Canyon, where DSDP Sites 566 - 569 were drilled. The location of Site 570 was selected to investigate the basement complex of the Guatemala continental margin. The area near the final drilling site showed anomalous magnetic features with a prominent magnetic high adjacent to a deep gravity low. Bathymetric surveys performed prior to DSDP Leg 67 showed that the magnetic high corresponded with a conical bathymetric high 700 m above the surrounding sea floor (Figure 75). It was postulated that the rock underlying the high would have to be a piece of uplifted igneous basement to exhibit the extreme magnetism noted. By drilling adjacent to the high, it was hoped that igneous basement could be reached at a depth shallower than the base of the gas hydrate stability zone. Finding abundant gas hydrates was unexpected, and not the main objective of Site 570 drilling. Site 570 was drilled in what appeared to be a structurally complex portion of the continental margin; extensive faulting should be expected at such a location.

Subsequent to drilling Site 570, a detailed bathymetric, seismic, and magnetic survey of the area was made by Volpe et al. (1985) aboard the R/V Thomas Washington. The survey indicated that the bathymetric high was most likely to be ophiolitic basement; it could be easily correlated seismically with the basement drilled at Site 570. Several canyons traversed the margin near the drill site. Site 570 was situated near the crest of a divide between two canyons 70 - 100 m deep (Figure 75). A larger canyon cuts the continental slope 3.5 km southeast of Site 570.

No definitive evidence of faulted sediments can be seen in the seismic sections presented by Volpe et al. (1985). In the area of Site 570, reflectors crossing sedimentary layers, and varying dips of sediment reflectors could be interpreted as evidence of faulting (Figures 75, 76, 77). However, Volpe et al. (1985) attribute these features to prograding sediment cover.

The elevated basement outcrop and the irregularity of the basement surface beneath slope sediments obviously reflect faulting. Volpe et al. (1985) indicated that the major faulting occurred before deposition of the Neogene sedimentary cover. They inferred that the deformation predated deposition based on the orientation of the sediment-basement contacts. Sediments were interpreted to lap on the irregular ophiolitic basement fault blocks; intrusive relationships were not evident. Volpe et al. (1985) concluded that movement probably occurred in Oligocene to Miocene time. It is likely, however, that faults have been subsequently reactivated; faulting at insufficient scale to be resolved seismically would be expected to cut sediments deposited subsequent to the major phase of faulting considering the location of the site landward of an active trench.

Mathews and von Huene (1985) interpreted the work of Volpe et al. (1985) to indicate a major transverse fault coincident with one of the canyons in the area. However, it is unclear which of the three canyons near Site 570 are interpreted to be faults. The abundant diffraction features on the single channel seismic lines of Volpe et al. (1985; Figure 75) conceal stratal reflectors near the canyons, hindering confirmation of fault location.

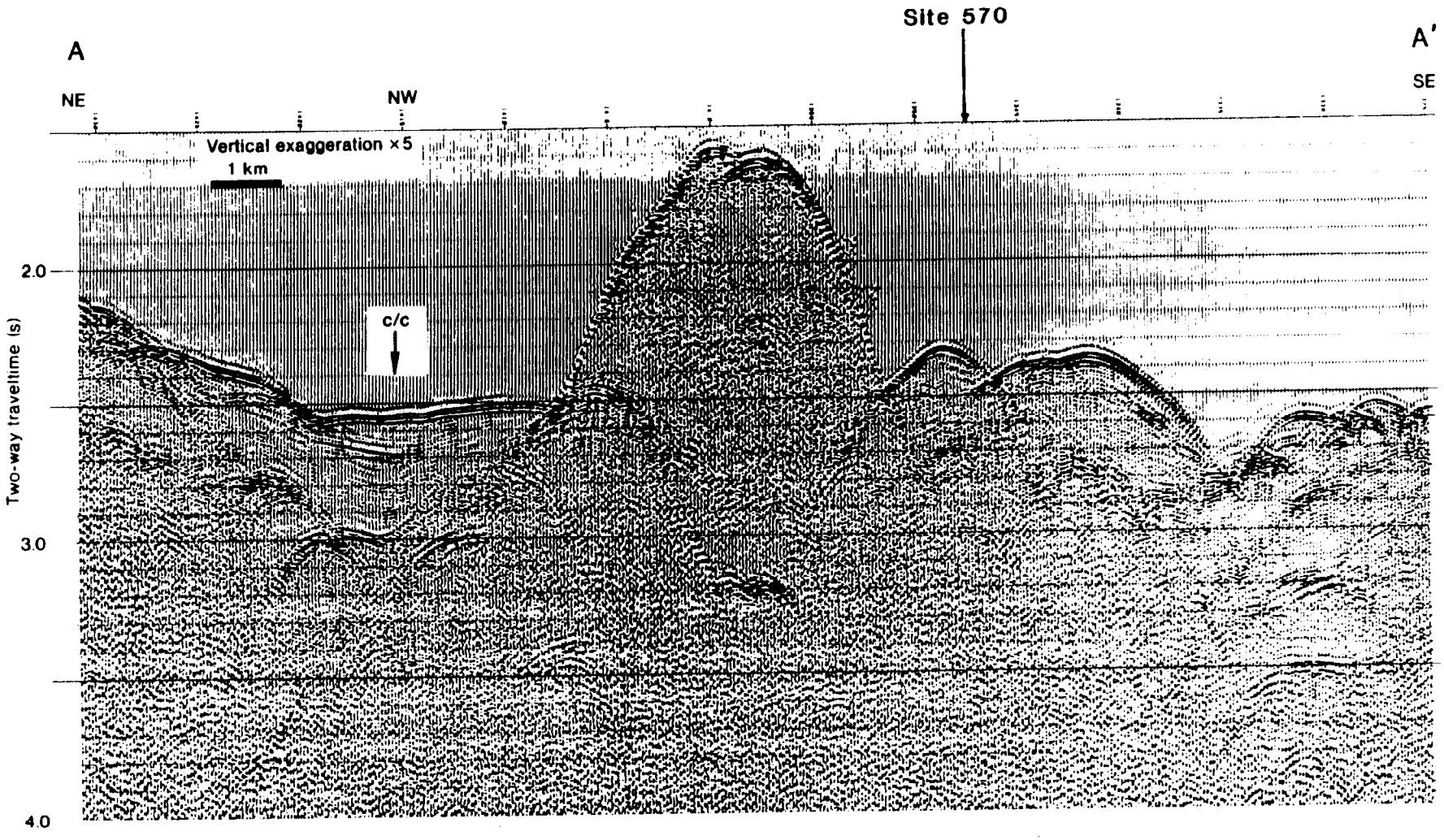

Note large topographic high composed of serpentinite adjacent to Site 570

Figure 75. DETAILED SEISMIC RECORD OF CONTINENTAL SLOPE NEAR DSDP SITE 570

After Volpe et al., 1985

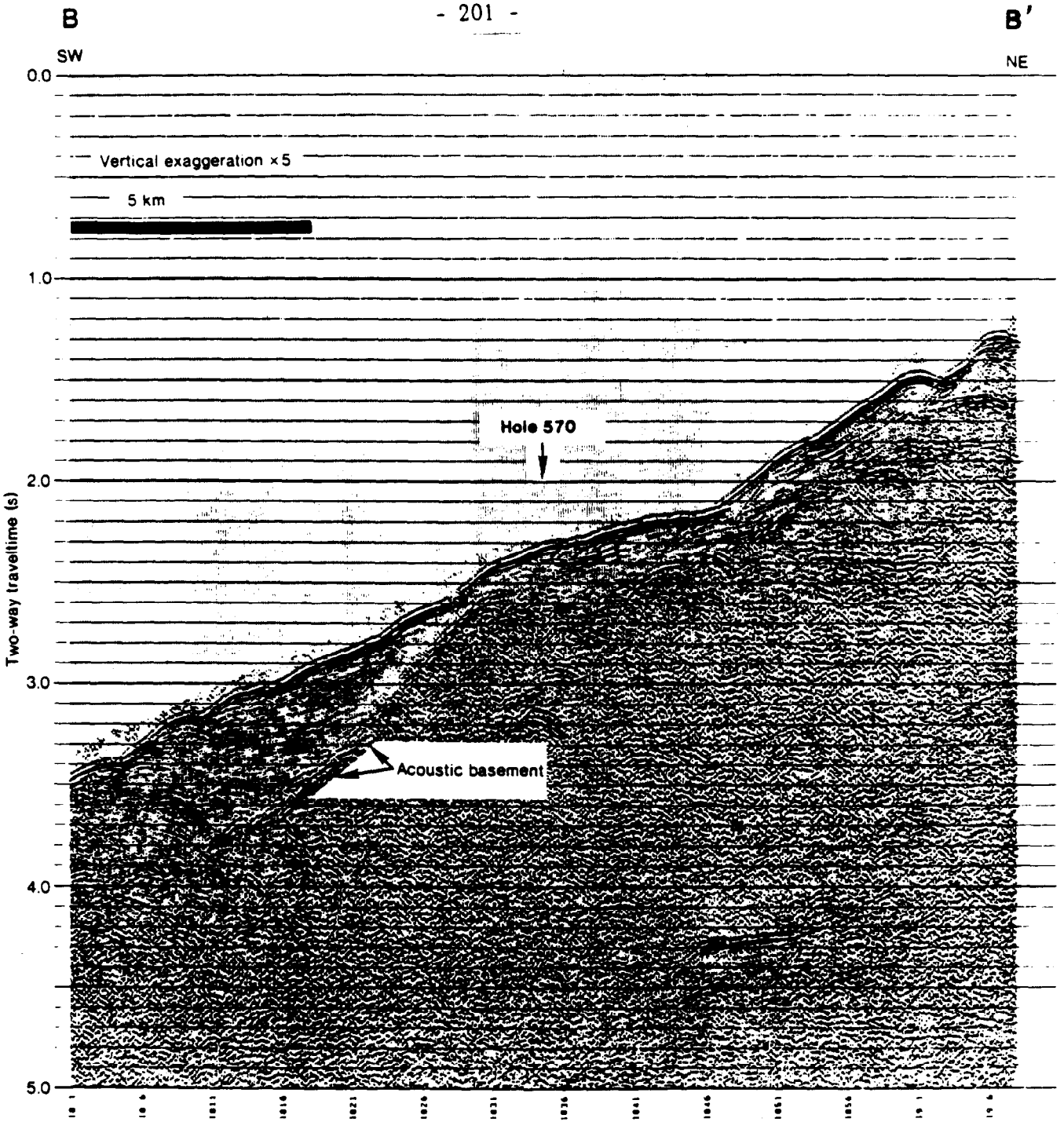

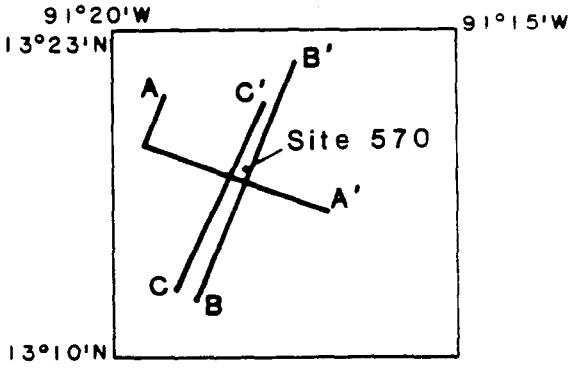

Figure 76. SEISMIC SECTION AT DSDP SITE 570

After Volpe et al., 1985

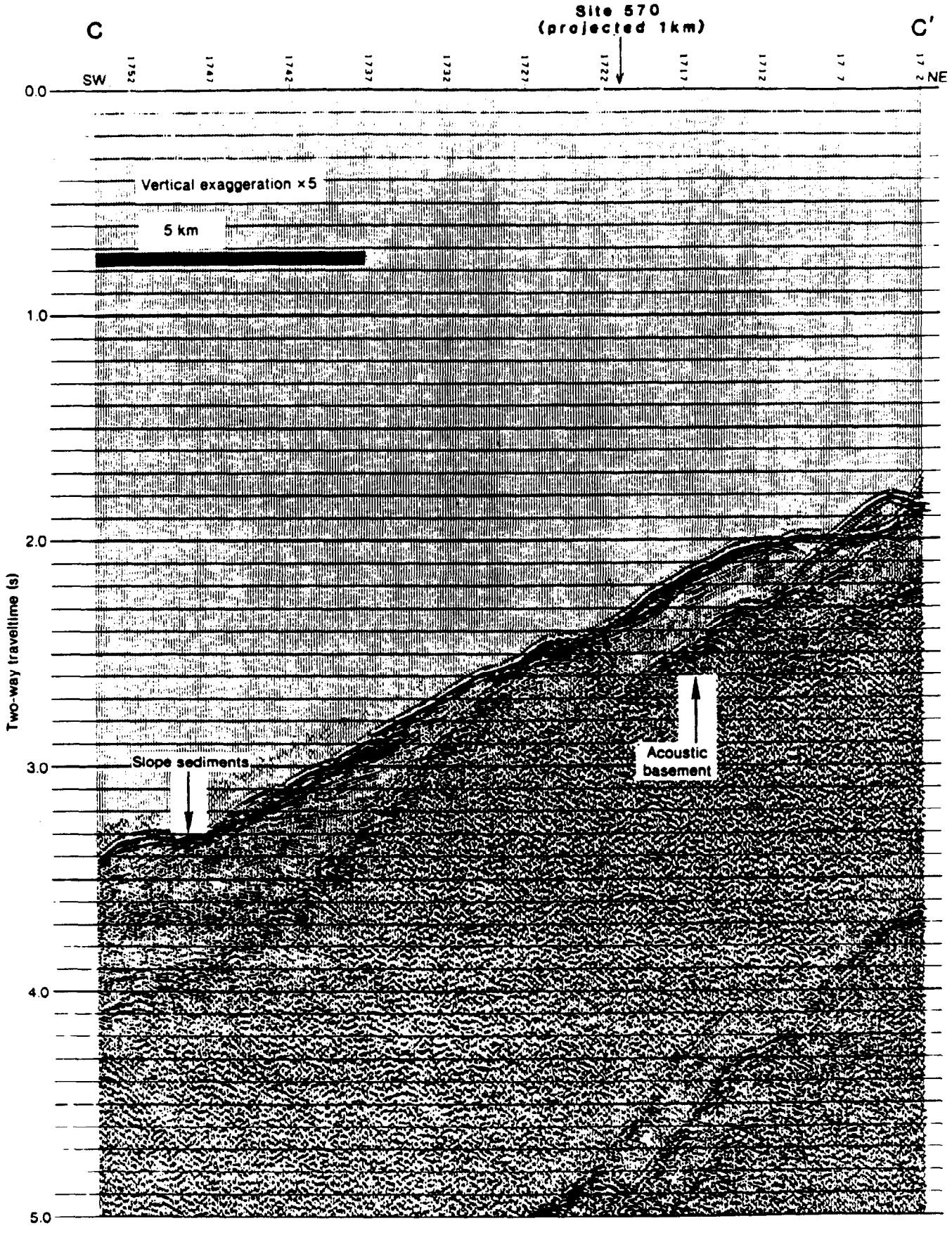

Figure 77. SEISMIC SECTION NEAR DSDP SITE 570

After Volpe et al., 1985

While admitting that simple sedimentary processes may be responsible for the massive gas hydrate interval, Mathews and von Huene (1985) were clearly in favor of a fault-controlled deposit:

> The geologic setting of the massive hydrate and Site 570--near a transverse furrow (Volpe et al., this volume), which is probably a fault, and at a hiatus in the sedimentary sequence--favors the association of this massive hydrate with a fault zone rather than with a layer along an unconformity. Presumably, the massive hydrate may have formed during a progressive movement along the fault and perhaps a rhombochasm opened incrementally. Any free-gas migration along the fault would hydrate as it filled the void left during fault movement. Other gas hydrate at Site 570 was observed to occupy fractures in the massive mudstone or pore space in vitric sand layers. However, so little is known regarding the emplacement of gas hydrate in the marine environment that a layer of fractured mudstone and dolomite filled with hydrate cannot be ruled out.

The fault-controlled massive hydrate formation mechanism proposed by Mathews and von Huene (1985) is apparently based only on seismic evidence for a possible fault. The fault cannot be traced from the canyon to its intersection with Site 570 at 250 m depth (about 0.3 sec subbottom). Nor do the originators of the seismic data (Volpe et al., 1985) identify faults in the sedimentary section at Site 570.

In spite of the limited data base upon which the fault-controlled massive gas hydrate formation model is based, it is attractive. The proposed scenario would explain how the massive gas hydrate could form without displacing large quantities of sediment. Also, migration of gas along the fracture network of the associated fault breccia would permit efficient delivery of the large quantities of methane necessary for massive gas hydrate formation without invoking regional uplift or an impermeable cap rock.

Geological evidence for faulting. Geochemical and geological data obtained at Site 570 and compiled into the Leg 84 Initial Reports volume (von Huene, 1984) can be interpreted to support the concept of massive gas hydrate formation along a fault zone.

The massive gas hydrate at Site 570 corresponds to an unconformity. Paleontological dating by Filewicz (1985), Baltuck et al. (1985), Glacon and Bourgois (1985) places the hiatus which coincides with the massive gas hydrate zone between the late Miocene and early Pliocene. The work of Stone and Geller (1985) restricts the unconformity to within late Miocene time. If a normal fault were assumed to be present in core 27, the reported unconformity may just represent the age relationship to be expected between the footwall and hanging wall rather than a depositional hiatus. It is also interesting to note that documented unconformities representing much larger time gaps are found above and below core 27; no anomalous gas hydrate development is noted along those features.

The sequence of types of gas hydrate found at Site 570 can also be interpreted to suggest faulting at core 27. Gas hydrates were first noted at 192 m depth in core 21. These hydrates were concentrated in a porous volcanic ash layer, a typical mode of occurrence of gas hydrates drilled along

the Middle America Trench during DSDP Legs 66, 67, and 84. Gas hydrates were next encountered in cores 23 - 26. These gas hydrates were developed exclusively in fractures in fine-grained mud and mudstone. The massive gas hydrate was recovered from core 27. Fracture-filling gas hydrates again appeared in cores 28 - 30. The gas hydrate occurrences deeper in the hole were reported to be associated with relatively coarse-grained lithologies, e.g. core 33, rather than fractures in mudstone. A sequence of hydrate type from dispersed hydrates in porous sediments, to fracture-filling hydrates, to massive hydrates, back to fracture-filling hydrates, and finally to dispersed hydrates in porous sediments is apparent from the core descriptions. This pattern is suggestive of brecciation of rocks near a fault producing an increasing density of fractures on approach to the fault.

Geochemical evidence for faulting. Several anomalous features of the geochemical data from Site 570 can be interpreted as indicating a fault coincident with the massive gas hydrate found in core 27. The bimodal distribution of the carbon isotope data from Site 570 compared to adjacent Leg 84 locations suggests normal faulting. Heavy hydrocarbons which indicate migration are orders of magnitude more abundant near the proposed fault zone than elsewhere in the hole.

The carbon isotope content of methane from core 27 of Site 570 is 10 to 14 per mil heavier than methane from core 26 (Claypool et al., 1985; Galimov and Shabaeva, 1985; Jeffrey et al., 1985). This distinct break from the gradual change of isotope values with depth contrasts with the smooth $\delta^{13}C$ vs. depth relationship evident in the rest of the hole (Figure 78). A similar sudden shift to heavier values at core 27 (250 m) is seen in the $\delta^{13}C$ profile for CO_2 recovered from Site 570 (Figure 78).

Comparison of ^{13}C values from Sites 570 and 568 indicates that the sudden shift to heavier values at Site 570 is not typical (Figure 78). The data for Site 568 define a smooth sigmoidal curve. The $\delta^{13}C$ values corresponding to the sudden shift at Site 570, -53 to -42 per mil, define a particularly smooth segment of the Site 568 curve. Other than this segment both sites have very similar isotopic signatures; $\delta^{13}C$ values of -44 to -39 for methane in the deepest 100 m of the hole is common to both sites, but unique among all other DSDP drill holes shown to contain biogenic gas.

As a thought experiment, one could duplicate the distinct isotopic shift seen in the Site 570 plot by "removing" a segment of the Site 568 plot from about 200 m subbottom to about 340 m, and juxtaposing the remaining two sections (Figure 79). With 140 m of section missing, the isotopic profile for Site 568 is strikingly similar to the profile for Site 570.

The removal of a portion of the original sediment column at Site 570 to produce the observed profile could have been accomplished by either a normal fault or an unconformity. An unconformity spanning over 10 m.y. existed at 195 m depth at Site 568 (von Huene et al., 1985). Methane from 10 m beneath the unconformity was 3.3 per mil (Jeffrey et al., 1985) or 3.1 per mil (Claypool et al., 1985) heavier in ^{13}C than methane from 10 m above the unconformity. Another major unconformity was located at 335 m depth at Site 570. This unconformity represents a hiatus of about 25 m.y. from the early Eocene to early Miocene. There was little expression of the unconformity in carbon isotope values; Claypool et al. (1985) showed a change of 0.3 per mil in ^{13}C values for methane across the unconformity while the data of Jeffrey et al. (1985) showed a change of 0.6 per mil.

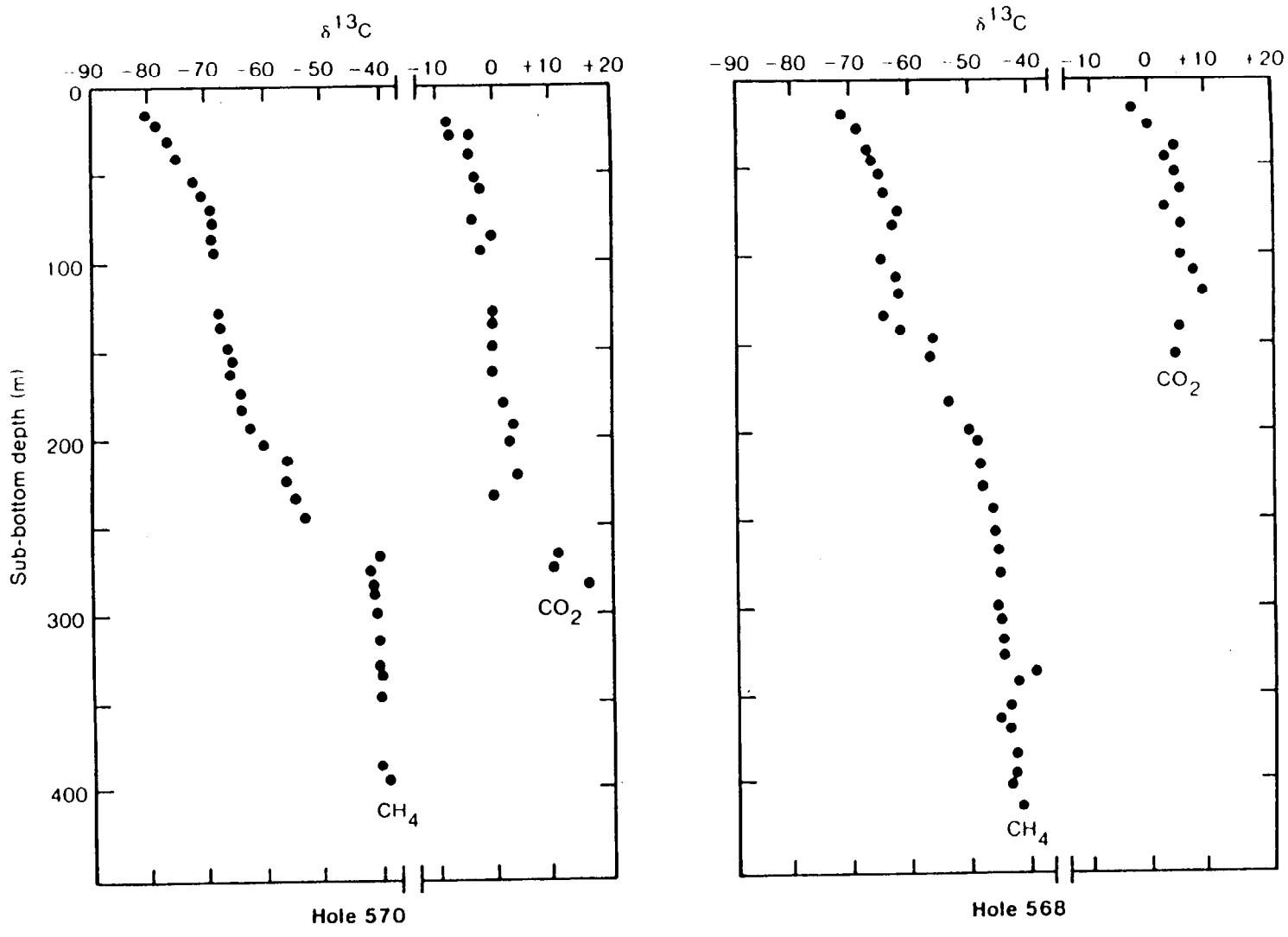

Figure 78. CARBON ISOTOPE CONTENT OF CORE GAS FROM DSDP SITES 568 AND 570

After Jeffrey et al., 1985

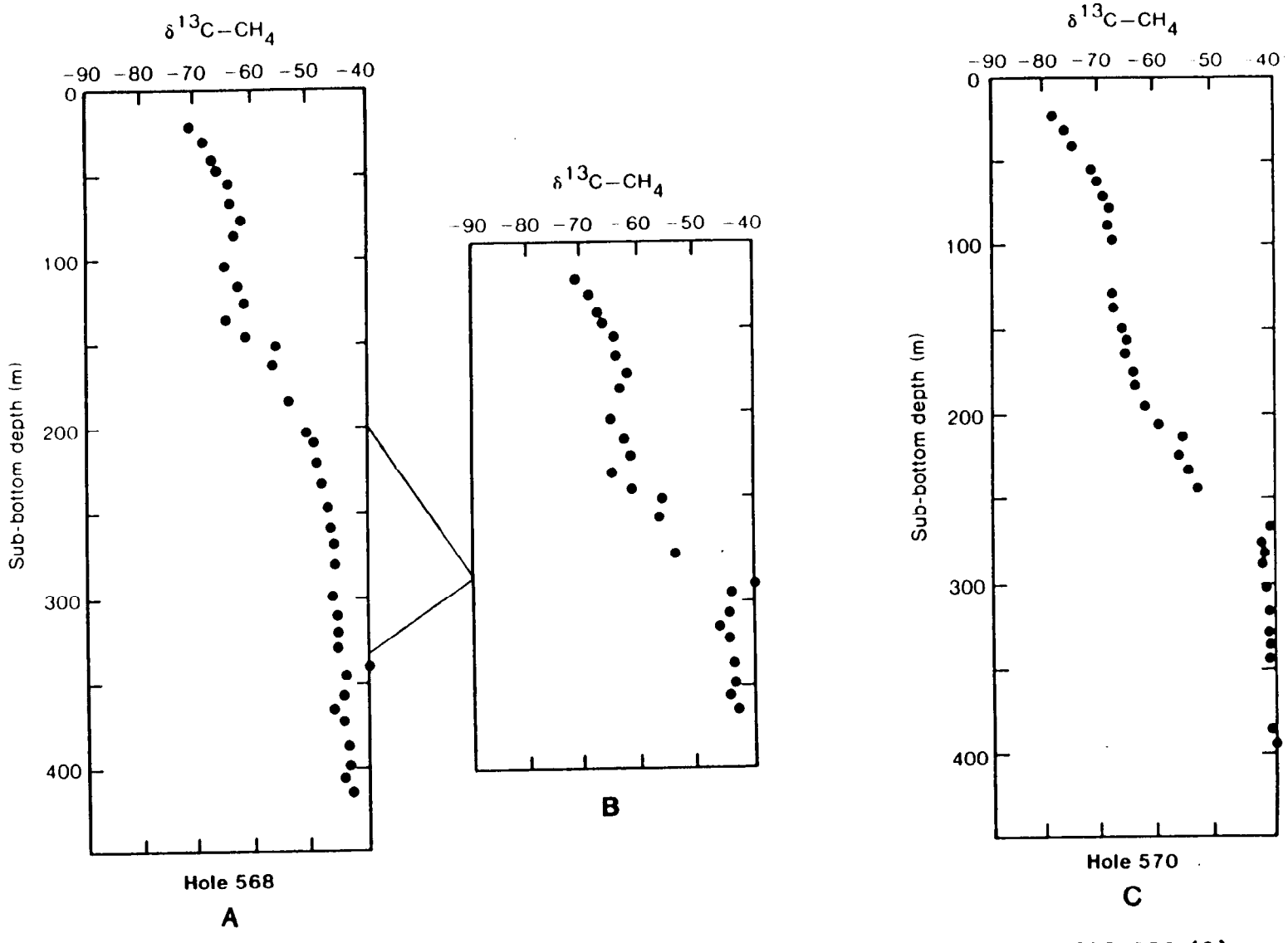

NOTE SIMILARITY OF PROFILE OF HOLE 568 AFTER FAULTING (B) AND PROFILE OF HOLE 570 (C)

Figure 79. HYPOTHETICAL EFFECT OF NORMAL FAULTING ON CARBON ISOTOPIC PROFILE

Data from Jeffrey et al., 1985

This relatively small change in carbon isotope values due to major unconformities at Site 568 and 570 indicates that the 10 to 15 per mil difference between methane from cores 26 and 27 is not due to a simple unconformity. If such a large isotope shift is expected from a hiatus of only 0.5 m.y. across the massive gas hydrate, then one would expect a huge change across the major documented unconformities at Sites 568 and 570 which span 10 and 25 m.y. respectively. A more reasonable mechanism for obtaining the shift in ^{13}C content at the massive gas hydrate zone would be relatively recent faulting which would remove some of the late Miocene and/or early Pliocene sedimentary section.

Another geochemical anomaly at Site 570 is the large relative increase in hydrocarbon gases heavier than methane in proximity to the massive gas hydrate zone. The hydrocarbon fraction of core gases recovered from Site 570 is principally methane (>99%). However, the content of propane, butane, and pentane rises sharply at core 26 and continues well above background through core 30. Below core 30 the heavier components reattain their low background levels which continue to the bottom of the sedimentary section (Figure 80). This zone of relative enrichment corresponds with the interval in which fracture-filling gas hydrates and the massive gas hydrates were found.

It could be argued that the increase in heavy hydrocarbons in this zone is the result of gas hydrate formation. Propane and isobutane could be preferentially trapped in the form of structure II hydrates. Since addition of these compounds permits hydrates to be formed at less severe conditions, it is reasonable that hydrates would scavenge all available propane and isobutane. Upon recovery, the structure II hydrates would be expected to dissociate. The gas collected from the core liners would then show higher than background levels of heavier hydrocarbons.

It can be shown that the exceedingly high relative concentrations of hydrocarbons heavier than ethane in cores 26 through 30 are not due to hydrate dissociation. Very high relative concentrations of n-butane and pentane are also found in cores 26 through 30 (Figure 81). These compounds show an even higher degree of enrichment through the fractured zone than do propane and isobutane. If the increased levels of heavier hydrocarbons were due to selective incorporation of these molecules into structure II hydrates, followed by dissociation, then the enrichment would only affect the concentrations of propane and isobutane. Isobutane and pentane, which are too large to form gas hydrates, would be expected to be depleted due to hydrate formation and subsequent dissociation. Since all measured heavier hydrocarbon species increase proportionately through the zone it can be concluded that the measured gas mixtures are indicative of composition of the core gas in situ.

The concentration of heavier hydrocarbons in the 50 m interval surrounding the massive gas hydrate is different from that expected of typical marine sedimentary environments. Based on the molecular distribution of the ethane through pentane fraction of the core gas from Leg 84, Jeffrey et al. (1985) concluded that the gases were formed by low temperature diagenetic processes of a nonbiological nature. These reactions are thought to be thermally controlled to a certain extent. Thus concentrations of these gases are typically increased exponentially with depth (Claypool and Kvenvolden, 1983). This is not always the case on the Guatemalan continental margin. The concentration of hydrocarbons heavier than ethane decreases slightly with

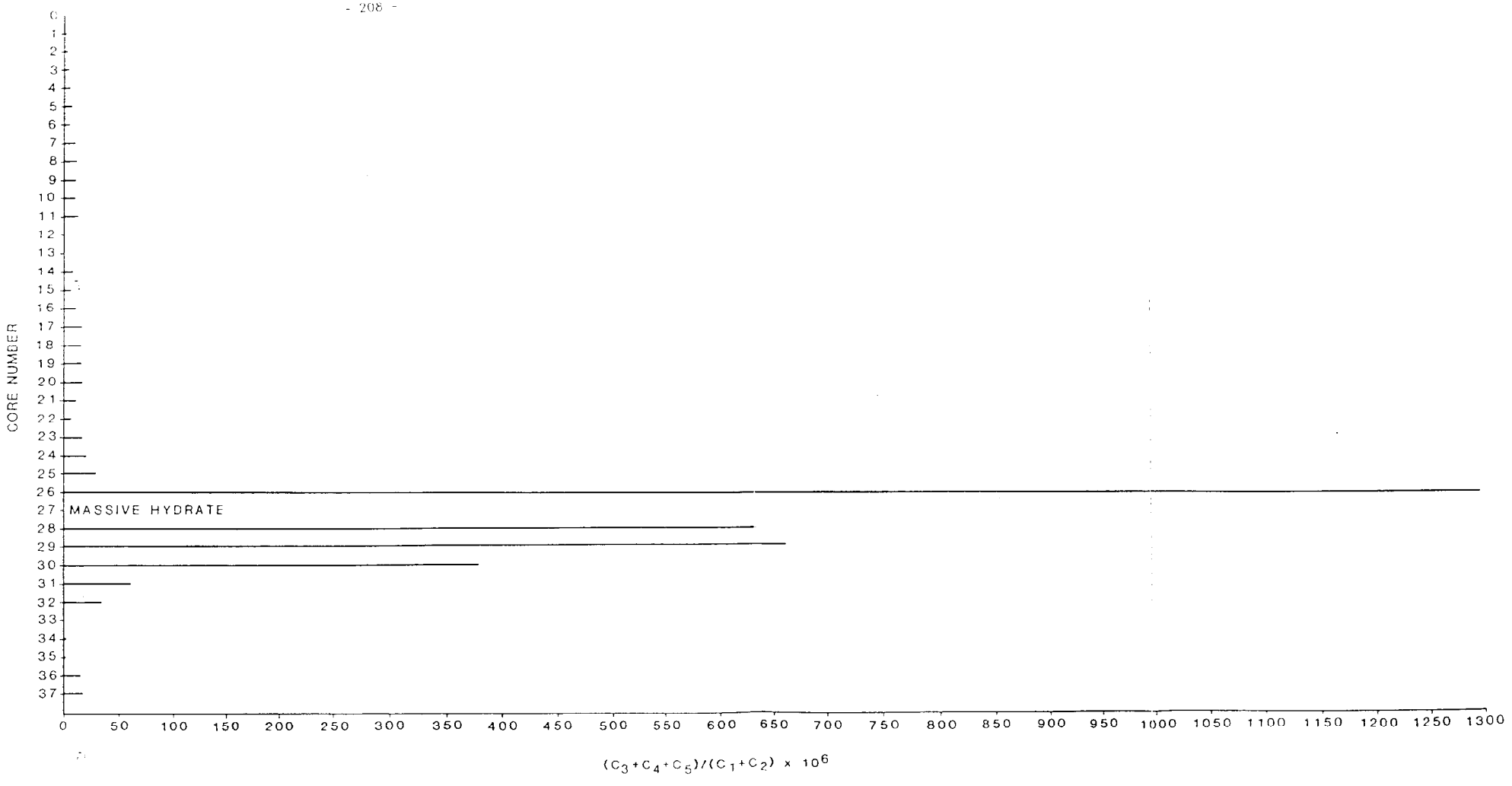

Figure 80. RATIO OF PROPANE, BUTANE, AND PENTANE TO METHANE AND ETHANE IN SEDIMENTS AT DSDP SITE 570

Data from von Huene et al., 1985

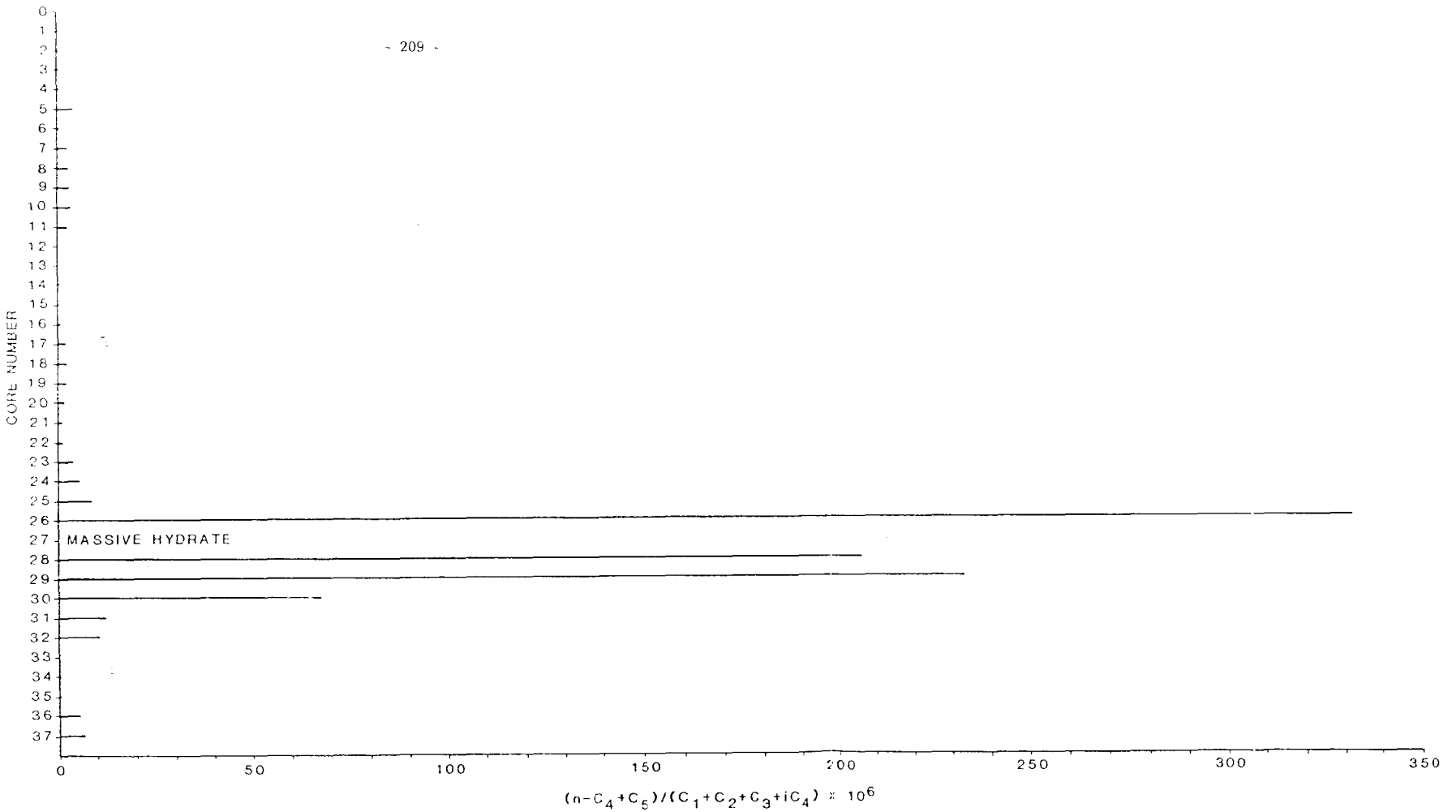

Figure 81. RATIO OF n-BUTANE AND PENTANE TO SMALLER HYDROCARBONS IN CORE GASES AT DSDP SITE 570

Data from von Huene et al., 1985

depth; however, ethane concentrations increase exponentially with depth as predicted by Rice and Claypool (1981) and Claypool and Kvenvolden (1983). At Site 570, all measured hydrocarbons from ethane through pentane increase 20 to 100 times over background in the interval which is highly fractured (cores 26 through 30), before dropping rapidly to expected levels in cores 31 through 37. No thermal anomaly was noted in the intervals in question at Site 570 (Mathews and von Huene, 1985).

One possible explanation for the relatively high concentrations of heavier hydrocarbons between cores 26 and 30 (246 to 284 m) is the concurrently high total organic carbon (TOC) content through the interval. The highest TOC value reported for Site 570 is 3.2% from core 29 (Kvenvolden and McDonald, 1985). However, TOC values of 2.2 and 2.5% are reported for cores 25 and 31 which are outside the zone of heavier hydrocarbon enrichment. The 45% increase in measured TOC values in core 29 relative to the mean of cores 25 and 31 corresponds to an 840% increase in hydrocarbons heavier than ethane and a 2,300% increase in hydrocarbons larger than isobutane in core 29. The poor correlation of TOC and heavier hydrocarbon core gases is further demonstrated by a high TOC value of 3.32% reported by Gilbert and Cunningham (1985) for core 32 which has low ethane, propane, butane and pentane contents. Thus it would appear that some factor other than elevated TOC content has increased the ethane through pentane concentrations near the massive gas hydrate.

The presence of heavy hydrocarbons is germain to the issue of a fault system facilitating gas hydrate formation at Site 570. Besides possibly forming open space for gas hydrates to occupy, a fault system with its concomitant fracturing provides a permeable conduit through which the large volumes of methane may have been delivered to the locus of hydrate formation. Thus, if a fault is responsible for the massive gas hydrate zone, as was suggested by Mathews and von Huene (1985), then one should expect to find evidence of mobilized hydrocarbons near the supposed fault. The presence of elevated levels of heavy hydrocarbons in cores 26 through 30 at Site 570 could be interpreted as suggestive evidence of past migration or diffusion.

Work by Whelan et al. (1984) demonstrated that hydrocarbons heavier than ethane are unlikely to diffuse for long distances in thermally immature sediments. Although methane and to some extent ethane are mobile in the pore fluid environment, heavier hydrocarbons are typically mobilized only in the more severe conditions of thermogenic hydrocarbon migration. A large concentration of these heavier hydrocarbons in thermally immature sediments implies some alteration of the sediment to promote more efficient diffusion and/or secondary migration.

The fracturing noted by Leg 84 personnel in the interval from 240 to 280 m at Site 570 could conceivably have enriched the pore fluid in heavier diagenetic hydrocarbons. Brecciation or fracturing would be expected to introduce a dual nature to the pore fluid system; the original intragranular pore fluid would be augmented by fluid in the fractures. The fluid in the fractures would be less restrictive to flow and diffusion than the fluid in the small pores of a mudstone. It is possible hydrocarbons would diffuse a shorter distance through the rock matrix to a nearby fracture, whereas long distance diffusion would be required in a nonfractured rock. Therefore, it could be argued that components with marginal diffusive capability within a matrix, such as propane, butane, and pentane would be enriched in the pore water of fractured intervals.

Gas analyses from other holes at Leg 84 do not support fracturing alone as a cause for high concentrations of propane through pentane. For example fractured intervals at Site 568 showed no systematic increase in heavier hydrocarbon content through four highly fractured intervals.

Once the fracture network along a fault is established, secondary migration of these components by hydrodynamic flow or diffusion could result in their anomalous enrichment. The migration of methane and heavier diagenetic hydrocarbons from a greater depth is an attractive solution for the unusual concentration of propane, butane, and pentane in the 40 m interval in which fracture filling and massive gas hydrates were found at Site 570.

One other portion of the drill hole at Site 570 had unusually large concentrations of heavy hydrocarbon gases in recovered cores. Cores 41 and and 42 (386 and 394 m) from the serpentinized peridotite basement showed even greater enrichment of ethane through pentane than cores 26 - 30. Although recent research indicates that the hydrocarbons in the basement could conceivably have been generated in place (Morency et al., 1986), conventional wisdom dictates that hydrocarbon gases must have migrated from sedimentary sources along faults and fractures (Galimov and Shabaeva, 1985; Jeffrey et al., 1985; Kvenvolden and McDonald, 1985).

By analogy with the migrated serpentinite hydrocarbons, it could be argued that migrated hydrocarbons are also present in cores 26 - 30. In both instances, the levels of hydrocarbons heavier than methane are far above the levels measured elsewhere in the hole. Both intervals contain very immature diagenetic gas as indicated by the high isobutane to normal butane and pentane ratios (Jeffrey et al., 1985). Both intervals are fractured, and possibly faulted. The hydrocarbons recovered from serpentinite cores show that migration of immature diagenetic gases can result in enrichment in heavier hydrocarbons in core gases similar to that seen surrounding the massive gas hydrates.

Although many of the geochemical data for Site 570 support the concept of Mathews and von Huene (1985) that a fault localized massive gas hydrate formation, there are some contradictions. The most glaring inconsistency is that in the $\delta^{13}C$ values for methane and the content of heavy hydrocarbon gas from core 26. A sharp increase in ^{13}C content of methane is clearly seen between core 26 (-53 per mil) and core 27 (-41 per mil). However the major break in the content of propane, butane, and pentane is seen between cores 25 and 26 with increases of 4,000%, 11,000%, and 3,000% respectively. It is a relationship which is opposite of that to be expected; the more mobile methane from core 27 should mix with the gases of core 26 more efficiently than the slower diffusing heavier hydrocarbons.

Summary

The mechanism of massive gas hydrate formation along a fault zone proposed by Mathews and von Huene (1985) is reasonable. It agrees well with available geological and geochemical data with the exception noted above. The process of migration along high permeability zones adjacent to faults is well proven with respect to both petroleum and mineralizing solutions. The fault zone hypothesis is particularly appealing because it does not involve the improbable simultaneous occurrence of a dolomite cap rock, a rapid 2,000 m uplift and unusually intense microbial methanogenesis as required by

Kvenvolden et al. (1984) and Kvenvolden and Claypool (1985). The fault zone model relies instead on a combination of probable, well understood processes of simple faulting and gas migration and/or diffusion.

The resource implications of determining which model is closer to the actual situation are significant. If the model of Mathews and von Huene (1985) is accurate, then massive gas hydrates may be more abundant than otherwise. The fault zone model incorporates commonly occurring geological processes; thus deposits of this type would be more common than those described by the model of Kvenvolden et al. (1984) which requires conditions that may be unique to Site 570. Additionally, the issue of which model is more accurate could eventually have exploration implications. Since massive gas hydrates are not resolved by seismic methods (Volpe et al., 1985) and high resolution sparker techniques are well suited to detecting faults in marine sediments (Bouma et al., 1983), it may be possible to delineate small areas most prospective for massive gas hydrate deposits using standard geophysical techniques if faults do indeed control massive gas hydrate distribution.

Factors Controlling Gas Hydrate Formation

Gas hydrates identified in the Middle America Trench study region vary in their geological setting and chemical and physical properties. Abundant hydrocarbon gas was found in all holes drilled on the continental slope of the Middle America Trench during DSDP Legs 66, 67, and 84. However, recovery of gas hydrate samples from sediment cores was relatively rare. Indirect evidence in the form of pore water salinity profiles and core gas composition suggest that the dispersed gas hydrates may occur in intervals from which gas hydrate samples were not recovered. Presence of proper host lithology, gas composition, structural deformation, and sedimentation rates may influence the distribution of gas hydrates in the Middle America Trench study region.

Host Lithologies

All proven gas hydrate occurrences in the Middle America Trench were recovered from permeable lithologies. The gas hydrate host sediments in the study region are either coarse-grained sediments or fine-grained sediments with abundant fracturing. The largest number of recovered gas hydrate samples occur in coarse-grained volcanic ash. These ash layers are typically described as "vitric sand" by the DSDP scientists. Rare occurrences have also been noted in coarse detrital sediments, for example the felspathic sand at Site 570 (core 35). Various terms were used to describe host lithologies: "sand", "sandstone", "ashy sand", "tuffaceous mudstone", "sandy mud"; but all consist of coarser than typical grains, very often with a volcanic ash component.

One possible exception to the coarse host sediment relationship for gas hydrates is the hydrate recovered at 192 m from Site 570. This occurrence was described as being laminated with ash. The grain size of the constituent

ash was not specified. The wording of the reports is not clear; it appears that the hydrates may have developed between bedding planes of the ash layer.

Gas hydrates were repeatedly found filling fractures in fine-grained muds or mudstones which were otherwise barren of gas hydrates. These occurrences occasionally were of sufficient size for post-recovery testing. At Site 570, the gas hydrates in fractures had different molecular distribution of hydrocarbons than did pore-space-filling gas hydrates from elsewhere in the hole.

Some sediment (5 - 7%) is mixed with the recovered massive gas hydrate from Site 570 in the form of stringers of mud, but the relationship of the gas hydrate to the enclosed sediment is unclear. The massive gas hydrate could conceivably have formed by filling an open cavity or developed from pore-filling or fracture-filling gas hydrates. Massive gas hydrate formed in an open cavity would be expected to have little if any included sediment. Pore-filling gas hydrate which developed into massive gas hydrate would be expected to contain some sediment well dispersed in the hydrate. The sediment trapped in massive gas hydrate formed from continued development of fracture-filling gas hydrate would be expected to be trapped as relatively intact relics of the fractured lithologies. The published photographs of the massive gas hydrate show discrete sediment pockets and irregular bands within the hydrate. This arrangement suggests a fracture-filling origin, but neither of the other possibilities is excluded.

Gas Composition

All gas hydrates recovered on Legs 66, 67, and 84 were composed principally of methane (generally greater than 99%). The remainder was typically composed of ethane, carbon dioxide, and trace amounts of heavier hydrocarbons. The massive gas hydrates from core 27 of Site 570 and fracture-filling gas hydrates from cores 26 and 28 contained heavier hydrocarbons in quantities two to three orders of magnitude greater than other hydrates from the Guatemala continental slope. Samples from Sites 490 and 491 from the Mexico continental slope contained 100 times the typical amounts of hydrocarbons heavier than ethane.

Sedimentation Rates

Sediments in the Middle America Trench study region were deposited at widely varying rates. Coring on DSDP Legs 66, 67, and 84 has shown that sedimentation in the Quaternary was more rapid than in the Tertiary. Overall rapid deposition of sediments has occurred on the continental slope. The high sedimentation rates may have promoted organic matter preservation as described by Muller and Seuss (1979).

Based on their work on the Middle America Trench, Kvenvolden and Claypool (1985) have observed that sedimentation rates between 30 and 300 m/m.y. are necessary for the biogenic methane generation needed for gas hydrate formation. However records from DSDP Legs 67 and 84 indicate that gas hydrates occur in sediments which accumulated at rates between 5 and 1,000 m/m.y. Indeed, the best developed gas hydrate samples from the Middle America Trench were recovered from intervals with sedimentation rates of less than 30 m/m.y. These data suggest that a wider range of sedimentation

rates than those proposed by Kvenvolden and Claypool (1985) can support methanogenesis sufficient for gas hydrate formation. Alternatively, gas hydrates from intervals with anomalously high or low sedimentation rates may have been formed from gas which has migrated from sections with sedimentation rates more amenable to methanogenesis.

DSDP Leg 66. Sedimentation rates measured offshore of Mexico varied greatly. For example, in one hole (Site 491) the rate changed from 5 m/m.y. at 30 m depth to 1,055 m/m.y. beneath 70 m. No distinct correlation of sedimentation rate and gas hydrate presence was seen in the Leg 66 data. Gas hydrates were recovered from four intervals at Site 490, all with sedimentation rates of about 80 m/m.y. At Site 491, gas hydrates were recovered from three intervals with sedimentation rates of 95 m/m.y. and greater than 1,000 m/m.y. Two gas hydrate samples were recovered from Site 492 in an interval with a mean sedimentation rate of 35 m/m.y.

Shephard and McMillen (1982) calculated the sediment accumulation rates for Leg 66 locations. Sedimentation rates are calculated by dividing the thickness of a drilled interval by the time span it represents. No correction is made for compaction of the sediments. By multiplying the sedimentation rate by the bulk density of the sediment, the sedimentation accumulation rate is obtained. The sediment accumulation rate, also known as the grain accumulation rate or sediment flux, measures the mass of sediment accumulating in a unit area per unit time span. As such it more closely represents the depositional characteristics at a site. Ibach (1982) has shown that the relationship between carbon preservation and sediment accumulation rate is more direct than that with simple sedimentation rates. The sediment accumulation rates for Leg 66 are diagrammed in Figure 82.

Gas hydrates occur in intervals with sediment accumulation rates of: 10 to 50 $g/cm^2/10^3$ y. at Site 490, 8 to 100 $g/cm^2/10^3$ y. at Site 491, and 1.5 to 7 $g/cm^2/10^3$ y. at Site 492. Correspondingly, other sites with sediment accumulation rates similar to the gas hydrate intervals are barren of gas hydrates.

DSDP Leg 67. Sedimentation rates for Leg 67 also varied widely among and within the holes. Pleistocene sedimentation rates were typically greater than 100 m/m.y. Deeper sedimentary sections were deposited more slowly and/or removed by erosion or faulting. Tertiary sedimentation rates ranged from 2 to 82 m/m.y.

Only two recoveries of gas hydrates were made during Leg 67 drilling (Harrison and Curiale, 1982). The interval from which gas hydrate sample was recovered at Site 497 accumulated at 32 m/m.y. The Miocene sediments from which gas hydrates were sampled at Site 498 accumulated at about 6 m/m.y.

DSDP Leg 84. High sedimentation rates in the Pleistocene (100 to 140 m/m.y.) and lower and more irregular rates in deeper sections (1 to 47 m/m.y.) characterize the sediments drilled on Leg 84.

Gas hydrates were recovered from Sites 565, 568, and 570. No consistent differences exist between the sedimentation rates at these sites and at nearby sites without gas hydrates (567 and 569). Even less correspondence exists among the sedimentation rates of the individual intervals from which gas hydrates were recovered. Gas hydrates were recovered from an interval at Site 565 with a sedimentation rate of 125 m/m.y. At Site 568, the only

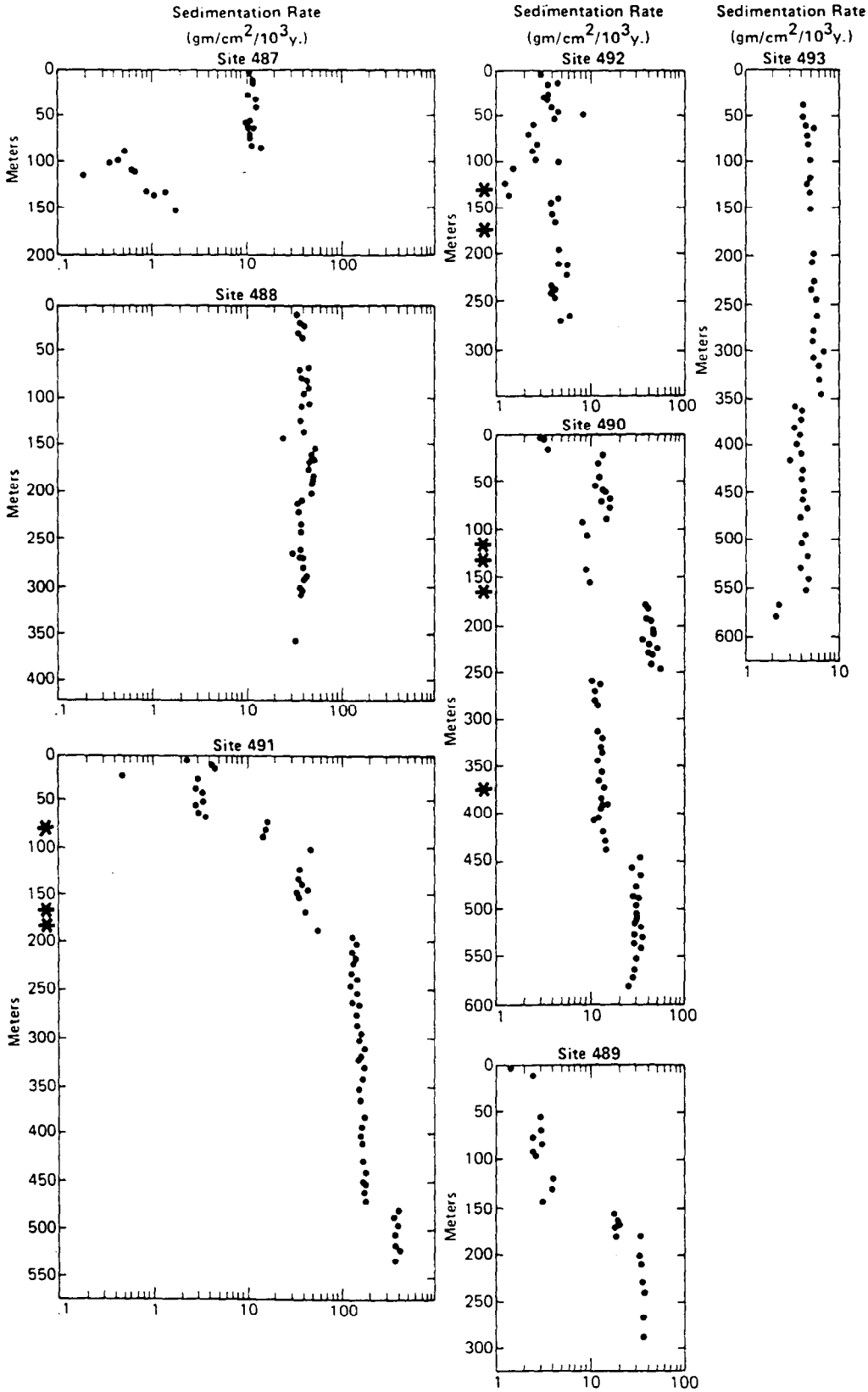

Figure 82. **MASS SEDIMENT ACCUMULATION RATES FOR DSDP LEG 66 SITES**

After Shephard and McMillen, 1982

gas hydrate recovery was from an interval of uncertain age; the site summary suggests a sedimentation rate of less than 3 m/m.y. Many samples of gas hydrates were recovered from Site 570. The Pliocene section from which the shallowest gas hydrate sample was recovered at 192 m accumulated at 130 m/m.y. The Miocene to Pliocene section from which massive and fracture-filling gas hydrates were recovered between 240 and 270 m have an average sedimentation rate of 13 m/m.y. Interstitial gas hydrates formed in late Miocene sediments which accumulated at 47 m/m.y. Gas hydrates were also found in Eocene sands which accumulated at 5.3 m/m.y.

Structural Geology

Gas hydrate recoveries and BSR development in a wide variety of structural settings permit an evaluation of the effect of structural deformation on gas hydrate presence in the Middle America Trench study region.

Geological structures could enhance gas hydrate formation primarily by providing routes by which large quantities of hydrocarbons can be delivered to sites where temperatures and pressures permit hydrate formation. Faults and fractures could serve as such migrational conduits. As pointed out by Mathews and von Huene (1985) faults can also provide open space in which massive gas hydrate can form without requiring the forming hydrate to push aside sediments. A conventional structural trap produced by faulting or folding could trap sufficient gas to initiate rapid gas hydrate formation.

In the previous examination of the proposed models for massive gas hydrate formation, we have implicitly endorsed the role of faulting in formation of the massive gas hydrate at Site 570. The available evidence suggests that the model of hydrate growth in a fault zone proposed by Mathews and von Huene (1985) is more plausible than that of Kvenvolden et al. (1984) and Kvenvolden and Claypool (1985) which required no structural deformation. At Site 570, the principal function of the fault was to provide the required permeability to deliver methane in large quantities to the site of gas hydrate formation. In this section the possible relationships of gas hydrate formation and geologic structure are examined.

Fractures. Gas hydrates were recovered from fractures in muds and mudstones drilled on DSDP Legs 66, 67, and 84. Indeed, the only reports of gas hydrates in fine-grained sediments were from fracture systems; dispersed interstitial gas hydrates were limited to coarse-grained volcanic ash and detrital sand layers. It appears that permeability in the form of intergranular porosity in coarse-grained sediments or in fracture systems is necessary for formation of gas hydrates which are sufficiently well developed to survive the coring and recovery processes.

Although fractures are necessary for gas hydrate formation in fine-grained sediments, fractures do not indicate gas hydrate presence. The reported occurrences of gas hydrates in cores from DSDP Legs 66, 67, and 84 are relatively rare. Fracturing is common in the sediments recovered from the Middle America Trench.

Vertical fractures filled with sediment were found in mudstone cored from the upper continental slope of Guatemala. These filled fractures were termed "veins" by DSDP scientists. Very similar veins were described from Sites 496 and 497 of Leg 67 (Cowan 1982) and Sites 568 and 569 of Leg 84 (Ogawa and Miyata, 1985). The veins occurred in mudstone between 200 and 400 m subbottom. The veins were typically vertical, subparallel, and occasionally anastomosed to form a network. Although the fillings were different colors and shades than the surrounding rock, the mineralogy of the fillings was similar to the surrounding rock. The principal difference in the material was the vertical orientation of platy minerals in the vein fillings compared to the horizontal orientation of platy minerals in the surrounding rock. The vein systems could be traced vertically across the bedding of the mudstone, but terminated at the contact of the mudstone with sand or ash layers.

Cowan (1982) interpreted the vein system to be tensional fractures through which water had been expelled during sediment compaction. Helm and Volbrecht (1985) and Ogawa and Miyata (1985) preferred to interpret the veins as shear features reflecting small-scale tectonic movement.

If the veins are dewatering features as suggested by Cowan (1982), they may affect gas hydrate formation. As water was being expelled through the fractures, any methane which had been formed would be carried along. Cowan's (1982) observation that amorphous organic material is depleted from the rock near the veins may indicate that the organic matter close to the veins was consumed by gas-producing microbes. Cowan (1982) contended that the direction of fluid flow in the vein system was toward the sand and ash layer. The flow of methane-laden pore water toward sand and ash layers from mudstones may present a partial explanation of a major paradox of Middle America Trench hydrates: gas hydrates are preferentially located in sands and coarse ash layers, but these lithologies lack sufficient organic matter to generate the large quantities of methane necessary to form the hydrates. The mudstones typically have high contents of organic matter and could generate large amounts of gas, but are barren of gas hydrates except in fractures. The situation is analogous in some ways to conventional hydrocarbons; gas hydrates are found in permeable reservoirs, but must have migrated somehow from organic-rich, impermeable source rocks. The anastomosing vein systems may function as short-range migrational pathways for transport of dissolved methane from the site of bacterial methanogenesis in mudstones to the ash and sands where hydrates preferentially form.

It is interesting that gas hydrates were recovered from two of the DSDP sites where the anastomosing sigmoid vein systems were noted (497 and 568). At the other two sites, 496 and 569, abundant circumstantial evidence of possible gas hydrate presence was found. The only confirmed recovery of gas hydrate from the upper continental slope on Leg 67 was from core catcher of core 39, Site 497 at a depth of 368 m (Harrison and Curale, 1982). Immediately above and below that depth in cores 39 and 40, well defined fractures and veins were present (Abouin et al., 1982). Gas hydrate was recovered only from one interval at Site 568, Leg 84. At a depth of 403 - 404 m, crystals of gas hydrate were found in fractures in a tuffaceous mudstone (von Huene et al., 1985). Veins and fractures were "abundant" (von Huene et al., 1985) immediately above and below the gas hydrate. It must be stressed that fractures and veins occur elsewhere in the cores where no hydrates were found. However, in both instances the gas hydrates

corresponded with intervals with high concentrations of particularly well formed veins.

Faults. Only for the massive gas hydrate recovered from Site 570 can the presence of gas hydrate in a fault zone be reasonably inferred. Faults were penetrated elsewhere during Legs 66, 67,and 84 without encountering gas hydrates.

The hydrocarbon gases found in the fractured serpentinite at Sites 566 and 570 may have been in the form of gas hydrates (Kvenvolden and McDonald, 1985). A fault zone was inferred in the serpentinite basement at Site 566 based on sharp increase in drilling rate and hydrocarbon gas content (von Huene et al., 1985). Baltuck et al. (1985) noted "vigorous degassing" from the core which had the possible fault (566C-6) and suggested that the hydrocarbons at the fault zone were in the form of gas hydrate. Hesse et al. (1985) concurred, noting that gas was released ". . . from chips of ice-like material from these fractures."

Although only one and possibly two instances of gas hydrate forming in a fault zone can be demonstrated, faults which were not loci for gas hydrate formation may have supplied the sand and ash beds with the necessary gas for hydrate formation. On DSDP Leg 66, increases in hydrocarbon gas content of recovered cores were used as indicators of fault zones (Watkins et al., 1982).

Large-Scale Tectonics. Major deformation of the continental margin landward of the Middle America Trench could affect gas hydrate formation potential by providing access to deep biogenic or thermogenic gas sources. The thick accumulation of sediments in the accretionary wedge offshore of Mexico and Costa Rica and the large volumes of trench sediments subducted all along the Middle America Trench are potential gas sources which have a high probability of being thermally mature. Based on the work of Morency et al. (1986) in producing a biogenic hydrocarbon gas from serpentinized peridotite, and the startling similarity in the molecular composition of that gas to gas recovered from the serpentinite basement at Site 570, it is also prudent to include the metamorphic basement of the Guatemala margin as a potential source for hydrate gas. Structures which promote migration could have a major effect on gas hydrate potential given the potentially large sources for hydrocarbon generation distant from the gas hydrate stability zone. In this section, a short review of the documented structures which could permit access to potential gas sources in the accretionary wedge, subduction zone, or metamorphic basement is presented.

Stoiber and Carr (1973) proposed that the subducting Cocos Plate is broken into discrete segments 80 - 250 km wide which have subducted at different angles. The subducted plate segments stressed the overriding continental plates above the segment boundaries and produced tear faults transverse to the plate boundary. Stoiber and Carr (1973) claimed that these weakened transverse structures could be mapped using shallow earthquake epicenters and lineaments defined by volcanic vents. The concept promoted much investigation toward determining the cause of lineaments normal to the trench on the North America and Caribbean Plates.

Recent work indicates that the descending Cocos Plate is probably not regularly segmented, and that segments that do exist probably do not effect the overriding plate. Other workers have found that lineaments are the extentions of long existing zones of weakness or have been caused by interaction of the Caribbean, North America, and Rivera Plates.

The Colima rift, a segment boundary proposed by Stoiber and Carr (1973), may mark a zone of structural deformation extending seaward to ocean depths at which hydrates could be expected. The Colima rift is a north-trending feature extending from near Guadalajara, Mexico south to near the Pacific coast southeast of Manzanillo (Allan, 1986). The rift appears to be caused by the subduction of the transform boundary between the Cocos and Rivera Plates. Since the plates are subducting at different rates, east to west tensional stress has been manifested in a complex of horst and graben structures in a 70 km wide band between 103° and 104°W (Figure 83).

BSRs can be resolved on single channel seismic profiles where they cross the seaward extension of the Colima rift (Figure 83). A particularly well developed BSR from seismic lines collected on the R/V Kana Keoki cruise 740109 is shown in Figure 84. The lines which indicate BSRs over the Colima rift were not run systematically along the margin across the structure; thus, it cannot be determined whether there is a direct link between BSR development and rift structure. However, it can be noted that the BSR pictured in Figure 84 and one nearby from the R/V Vema (not illustrated) are among the best defined BSRs recorded in each of the cruises.

Stoiber and Carr (1973) also proposed a transverse structural discontinuity in the crust of the North America Plate overlying the subducted trace of the Orozoco Fracture zone offshore of Mexico between Zihuaenejo and Acapulco. A major concentration of BSRs also overlies that projected segment boundary (Figure 50). Analysis of earthquake data by Nixon (1982) and Burbach et al. (1984) found no evidence of a tear in the descending Cocos Plate as was projected by Stoiber and Carr (1973). None of the maps or geological reports of on-land geology of Mexico landward of the BSR field reviewed for this report show structures which obviously extend seaward.

Burbach et al. (1984) report that the focal mechanisms of two earthquakes offshore of Acapulco indicate shallow strike-slip motion in the continental margin. These two earthquakes are unlike most others reported which typically record thrusting events at the subduction zone. The exact location of the epicenters of these anomalous earthquakes is unclear. Burbach et al. (1984) stated that they "occurred off the coast of Mexico just northwest of Acapulco." However the locations for the events in an accompanying table are 50 km southeast of Acapulco, one on the shoreline and one 100 km seaward on the Cocos Plate. In their text, Burbach et al. (1984) reported that the earthquakes were not associated with any known structure. They claimed that the event may reflect a tear in the subducted plate at the transition from a steeply northeast dipping subduction zone to a shallow north-northeast dipping subduction zone. Such a tear in a subducted plate may affect the structural continuity of the overriding plate in a manner suggested by Stoiber and Carr (1973). If so, a migrational path for deep gases may result. If the northern location mentioned in the text is correct, the tear fault could coincide with a zone with abundant BSRs. If the more southeasterly location from the table in the article by Burbach et al. (1984) is correct, then the tear fault is near the area drilled during DSDP Leg 66.

The Cocos-North America-Caribbean Plate triple junction at 15°15'N (Figure 6) has insufficient seismic coverage for determination of a possible correspondence with BSR distribution. The only high quality line to cross the area, TRM-5, is oriented along the strike of the continental margin. As such, BSRs are difficult to confirm on line TRM-5. However, an anomalous reflector

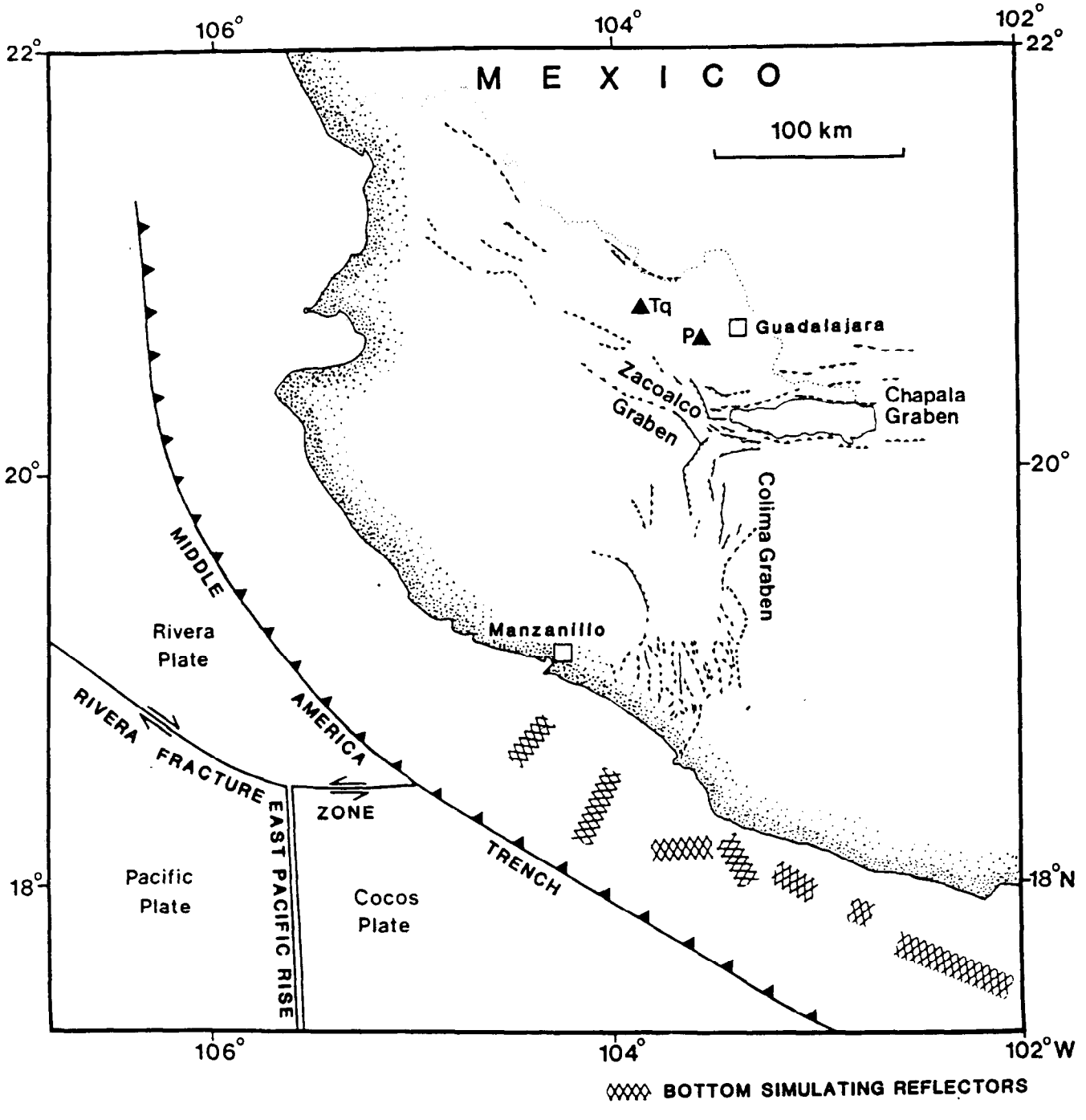

Figure 83. MAP SHOWING RELATIONSHIP OF COLIMA GRABEN, RIVERA FRACTURE ZONE AND BOTTOM SIMULATING REFLECTORS

After Allan, 1986

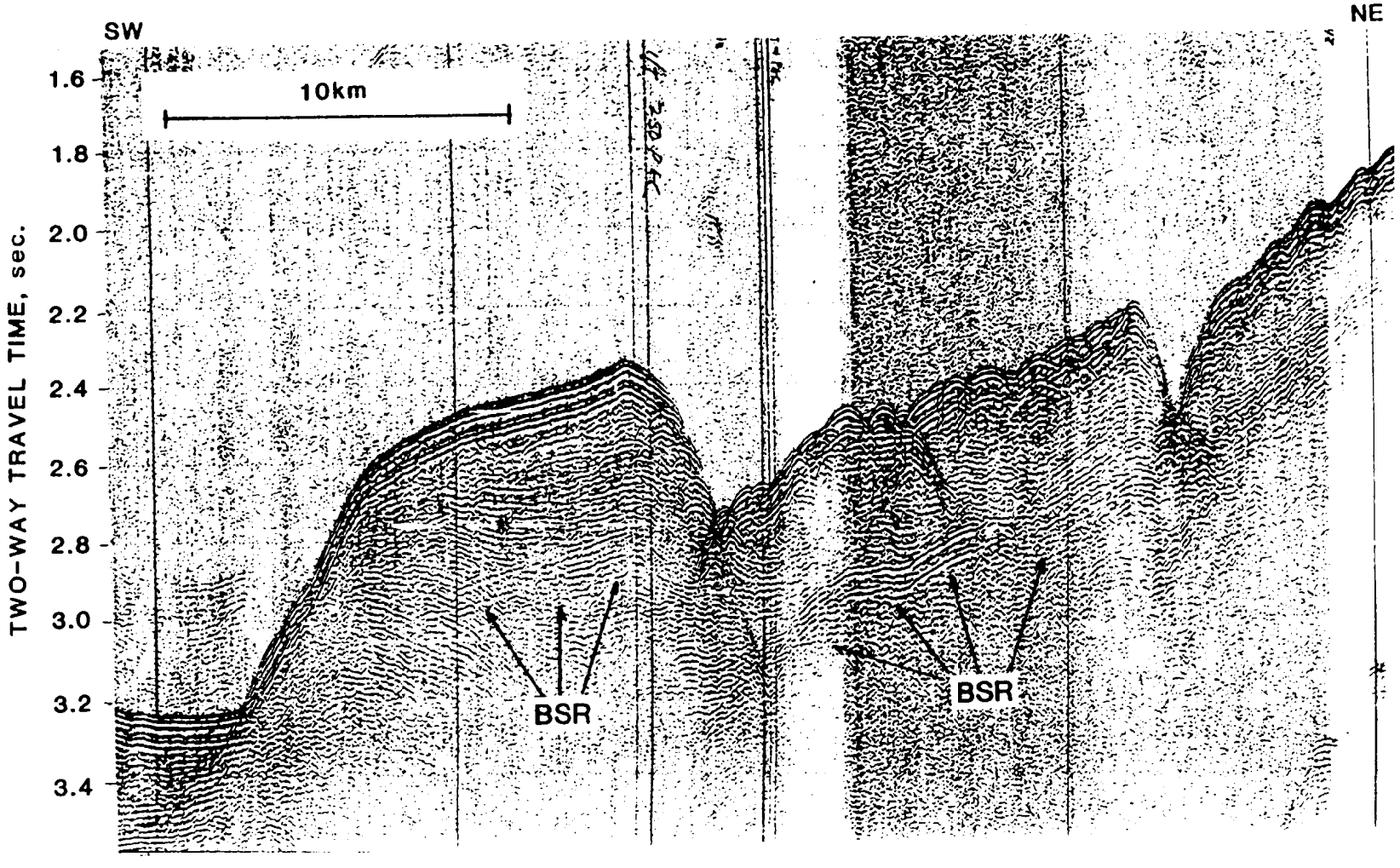

Figure 84. SEISMIC LINE FROM OFFSHORE MEXICO NEAR COLIMA GRABEN SHOWING BOTTOM SIMULATING REFLECTOR

which may be a BSR is found where line TRM-5 crosses the margin in the area of the triple junction mapped by Burkart (1983).

The continental margin offshore of Guatemala, which was drilled on DSDP Legs 67 and 84, shows evidence of recent structural activity. The San Jose Canyon, which dominates the topography of the area of the drilling transect, corresponds to a distinct break in continuity in linear magnetic anomalies which Ladd et al. (1982) attribute to a major transverse fault. Onshore numerous grabens (Burkart and Self, 1985) and strike-slip faults (Stoiber and Carr, 1973; Carr et al., 1976) can be projected offshore on trend with the San Jose Canyon and DSDP Sites 568 and 570.

Burkart and Self (1985) have indicated that the entire continental margin offshore of Guatemala is under extreme tensional stress. Only 135 km of sinistral movement since early Pliocene can be accounted for by the Polochic fault. The remaining 200 km of Pliocene to Holocene movement between the North America and Caribbean Plates must have occurred along other faults in Central America south of the Polochic fault. The Montagua and Jocotan absorbed some of the displacement. However, these faults are curved with the concave surface to the north (Figure 6). Thus, plate interaction requires that the movement of the Guatemalan margin is to the southeast in a curved path following the trace of Montagua and Jocotan faults. The net result is an high degree of tensile stress on the crust of southern Guatemala farthest from the faults, the offshore continental margin. This movement may be the cause of the extentional features noted in cores and on seismic sections from the offshore Guatemala area. It also fits in well with our assumption of a normal or strike-slip fault coincident with the massive gas hydrate zone of Site 570.

In summary, large- and small-scale extensional features exist in association with some gas hydrate deposits and BSRs in the Middle America Trench study region. With few exceptions, however, there is insufficient evidence to determine that tectonic deformation is related to the gas hydrate or BSR development, but the possible connection cannot be excluded.

Assessment of Gas Resources in Gas Hydrates

The potential gas resources associated with gas hydrates of the Middle America Trench cannot be assessed with high confidence in spite of the abundant evidence of gas hydrate presence. Drilling has proven the existence of gas hydrates at three widely separated areas of the study region: offshore of Mexico, offshore of Guatemala, and offshore of Costa Rica. No direct evidence of gas hydrate presence is known for parts of the continental slope between these sampled areas. These drilled areas are atypical of the continental margin as a whole. Drilling offshore of Mexico and Guatemala was concentrated alongside major submarine canyon systems, whereas the location offshore of Costa Rica is at the southern terminus of the trench. Within each drilled area, results indicate sporadic distribution of gas hydrates. Offshore of Mexico, probable gas hydrates were recovered from upper continental slope sites. However, offshore of Guatemala, gas hydrates were recovered from the lower slope (Site 498) and upper slope (Sites 497 and 568), but Site 569 on the middle slope was barren of hydrates. Gas hydrates were not recovered from holes drilled close to holes with hydrates, e.g. Sites 494, 496, and 567. The best developed gas hydrates offshore of Guatemala were drilled at Site 570 which is located 80 km from any other hole; the areal extent of the hydrate-rich zones cored at Site 570 is thus unknown. Only one hole was drilled offshore of Costa Rica, limiting the confidence with which the data from Site 565 can be extended.

Seismic evidence lends itself well to areal estimates of hydrate extent. The close spacing of high quality seismic lines in the three areas drilled by DSDP permits mapping of BSR distribution. Figures 38, 44,and 49 show that between 10 and 40% of the continental slope is covered by BSRs. Coverage is sparse between these well surveyed areas, however, and it is not known how representative the three small areas approximate conditions of the rest of the study region.

Evidence of gas hydrate presence from drilling and geophysics is not easily correlated. Gas hydrates were recovered from Sites 490, 498, 565, and 570 where no BSRs were present. Conversely, BSRs exist beneath DSDP Sites 496 and 569, but no hydrates were recovered by coring to within 200 m of the BSR. It is probable that the distribution of BSRs underestimates gas hydrate distribution offshore of Guatemala and Costa Rica. Gas hydrates were recovered from Site 565 near the only seismic line from the area which did not display BSRs (Figure 49), suggesting that hydrates are more plentiful than BSRs offshore of Costa Rica. No BSR existed beneath Site 570 because metamorphic basement rocks are found at shallower depths than the base of the gas hydrate stability zone. The thin slope sediments are common offshore of Guatemala and are probably a principal limit on BSR distribution offshore of Guatemala. Von Huene et al. (1982) and Ogawa et al. (1985) showed that most of the lower continental slope lacks sufficiently thick sediment for BSR development.

Offshore Mexico

Drilling indicates that the sediments covering the abyssal plain seaward of the trench have not generated hydrocarbon gas. Hence the gas hydrate potential of the large area of sea floor seaward of the trench is nil.

The trench floor sediments cored at Site 486 did not evolve gas. The coarse sand had been transported from the continental shelf to the trench in a turbidity flow. The trench floor sediments are young; subduction accretes or consumes older trench sediments. Although the sand should be a good hydrate host rock due to its permeability, adequate gas supply is lacking. The turbidity current or mass flow transport process probably leads to the escape of all gas which had been generated when the sediment was situated on the shelf. The well oxygenated water occupying the pores of the rapidly deposited material inhibits in situ bacterial methanogenesis. It is likely that the included sediment column does not have sufficient time to consume all included sulfate via microbial reduction and subsequently to generate methane during its short residence on the trench floor. With a low potential for gas generation, the trench axis has a correspondingly low potential for gas hydrate formation.

Shipley and Didyk (1982) mapped the BSR distribution of a small area of the Mexican continental margin. Their map (Figure 38) shows that BSRs cover about 900 km^2 or 15% of the 6,000 km^2 area mapped. All DSDP sites overlying the BSRs recovered frozen material that was probably gas hydrate, indicating that hydrates can be inferred to exist in sediments above BSRs in this area. However, the vertical distribution of recovered gas hydrates is discontinuous at these sites. Shipley and Didyk suggested that gas hydrates occupy much less than 1% of the sediment volume in this area based on identification of hydrates in cores. The sections drilled offshore of Mexico were terminated above the depth of the BSRs. Thus it is not known what amount of gas hydrate is causing the seismic response.

The area offshore of Acapulco mapped by Shipley and Didyk (1982) represents about 10% of the continental slope of Mexico within the study region. If the distribution of BSRs in the area offshore of Acapulco is typical, then about 9,000 km^2 of the continental slope of Mexico is underlain by BSRs. If it is assumed that the BSR is formed by interstitial gas hydrates occupying 50% of the available pore volume of a 50% porosity sediment, then gas content of the area underlain by BSRs can be roughly estimated. Although Kuuskraa et al. (1983) reported that 200 volumes of gas at standard temperature and pressure (STP; 0°C, 1 atm) can be trapped in a unit volume of methane hydrate, the theoretical maximum is near 180. Allowing for partial occupancy of the hydrate lattice by methane molecules, a volume factor of 150 is used for estimates for each meter thickness of hydrated sediment represented by the BSRs offshore of Mexico, and the contained gas volume would be:

$$9 \times 10^9 \text{ m}^2 \text{ area} \times 1 \text{ m thickness} \times 50\% \text{ pore occupancy} \times 50\% \text{ porosity} \times 150 \text{ volume gas:volume hydrate} = 3.4 \times 10^{11} \text{ m}^3 = 12 \text{ trillion cubic feet (TCF).}$$

The volume of gas contained in the gas hydrates composing the BSRs offshore of Mexico for various thicknesses of hydrate sediment corresponding to the BSRs is:

1 m =	3.4×10^{11} m^3	=	12 TCF
2 m =	7×10^{11} m^3	=	24 TCF
5 m =	1.7×10^{12} m^3	=	60 TCF
10 m =	3.4×10^{12} m^3	=	120 TCF

Based on the scarcity of gas hydrates recovered on Leg 66, as a fraction of core drilled, the gas hydrates contained in the sediments above the BSR would probably be less than the volume of hydrate causing the BSR. Results from Sites 490, 491 and 492 suggest that between 0.1 to 0.2% of the sediment above the BSR to a typical depth of 650 m is hydrated. Since Site 490 is not underlain by a BSR, the area with gas hydrates in sediment is larger than the areal extent of the BSRs. The areal extent of sediments above the BSR-forming gas hydrates is arbitrarily estimated at 150% of the BSR areal extent or 13,000 km^2. From hydrated sediment recovered at Site 492, Shipley and Didyk determined that 20 volumes of methane were released for each volume of pore water. That corresponds to about 13% pore occupancy of gas hydrate releasing 150 volumes of gas per volume of hydrate. Using these assumptions, the volume of gas in gas hydrates substantially above the base of the gas hydrate stability zone is this:

$$1.3 \times 10^{10}\ m^2 \text{ area} \times (650\ m \times 15\%) \text{ thickness} \times$$
$$13\% \text{ hydrates} \times 50\% \text{ porosity} \times 150 \text{ volume gas:volume hydrate} =$$
$$1.2 \times 10^{11}\ m^3 = 4 \text{ TCF}$$

Offshore of Guatemala

Coring at DSDP Site 495 on the abyssal plain of this Cocos Plate seaward of the Middle America Trench produced no evidence of hydrocarbons in the recovered cores. In contrast to the trench floor sediments offshore of Mexico, cores from Sites 499 and 500 offshore of Guatemala had measurable amounts of gas. The gas was composed almost entirely of methane. Shipboard scientists speculated that heavier hydrocarbons were removed during the downslope transport of sediment to the trench floor. No evidence of gas hydrates was noted. With no seismic or direct evidence of gas hydrates in trench floor or abyssal plain settings, no assessment of gas resources in gas hydrates can be made for these environments.

Von Huene et al. (1982) mapped the BSR distribution offshore of Guatemala in the area drilled on DSDP Legs 67 and 84. In this area, 1,500 km^2, about 17% of the 8,400 km^2 of the continental slope which was mapped, appears to be underlain by BSRs. The mapped area represents about 15% of the 1,000 km long continental margin. About 10,000 km^2 of the continental slope is thus underlain by BSRs. The gas contained in gas hydrates composing a BSR 1 m thick is:

$$1 \times 10^{10}\ m^2 \text{ area} \times 50\% \text{ hydrates} \times 50\% \text{ porosity} \times$$
$$150 \text{ volume gas: volume hydrates} = 4 \times 10^{11}\ m^3 = 13 \text{ TCF}$$

The volume of gas contained in BSR-producing gas hydrate layers of different mean thicknesses is:

$$1\ m = 4 \times 10^{11}\ m^3 = 13 \text{ TCF}$$
$$2\ m = 8 \times 10^{11}\ m^3 = 26 \text{ TCF}$$
$$5\ m = 2 \times 10^{12}\ m^3 = 65 \text{ TCF}$$
$$10\ m = 4 \times 10^{11}\ m^3 = 130 \text{ TCF}$$

The distribution of BSRs offshore of Guatemala is principally governed by the thickness of slope sediments (von Huene et al., 1982; Figure 44). The metamorphic basement underlying the continental slope is covered by only a thin layer of slope sediments. The mapped locations of BSRs correspond only to areas where slope sediments are deeper than the base of the gas hydrate stability zone. Von Huene et al. (1982) have shown that BSR occurrence requires not only that the base of the gas hydrate stability zone occur in sediments, but also that a sizable thickness of sediment must exist below the BSR, presumably to generate the gas from which the gas hydrate layer is formed. Since gas hydrates were recovered from Sites 498 and 570 where sediments were not sufficiently thick for BSR development, gas hydrates are probably more widespread than the 15% areal extent of BSRs would suggest.

Other workers have estimated the gas content of gas hydrates offshore of Guatemala. Claypool and Threlkeld (1985) claimed that the massive gas hydrate discovered at Site 570 would yield 5.2×10^8 m^3/km^2. Their method of estimation was not included in their publication. Mathews and von Huene (1985) obtained values ranging from 2.4×10^8 m^3/km^2 to 1.4×10^9 m^3/km^2 based on the response of well logs through the massive gas hydrate interval. Mathews and von Huene (1985) used the maximum theoretical volume conversion factor of 183 in their calculations.

Using the results of massive gas hydrate dissociation trials reported by Kvenvolden et al. (1984) estimates of the gas in massive gas hydrates can be derived. The empirically derived conversion factors of 62 to 82 with a mean of 71 measure not the volume of gas released from a unit volume of gas hydrate, but the volume of gas per unit volume of residual water after dissociation. Since gas hydrates are 10% less dense than water, the empirical value corresponds to a volume conversion factor of 64. Between 5% and 7% of the massive gas hydrate core is composed of sediment. For thickness of the section, the most optimistic value of 4 m from velocity logs can be used. With these assumptions, the amount of gas in the massive gas hydrate layer is:

$$10^6 \text{ m areal extent} \times 4 \text{ m thickness} \times 94\% \text{ hydrate} \times$$
$$64 \text{ volume gas: volume hydrate} = 2 \times 10^8 \text{ m}^3/\text{km}^2 = 0.008 \text{ TCF/km}^2$$

This estimate is about 50% of the value of Claypool and Threlkeld (1985) and is at the low end of the range of estimates provided by Mathews and von Huene (1985). All of these estimates are contingent on the massive gas hydrate layer being areally extensive. Without further drilling the extent of the massive gas hydrate remains unknown.

Estimates for gas hydrates dispersed in the slope sediments offshore of Guatemala are problematical due to the limited utility of BSRs as gas hydrate indicators in this area and the sporadic recovery of gas hydrates during DSDP Legs 67 and 84.

If pore water chemistry changes can be ascribed to gas hydrate presence as proposed by Hesse and Harrison (1981), Harrison et al. (1982) and Hesse et al. (1985) then gas hydrate volumes could be calculated directly from chemical data. In our previous examination of pore water chemistry of cores from offshore of Guatemala we concluded that the volumes obtained by that method were overly large. Estimates of gas content based on pore water chemistry at Site 568 indicated that 8×10^9 m^3/km^2 or 0.3 TCF/km of gas existed in interstitial gas hydrates. This represents 40 times the gas volume

reported for the massive gas hydrate from Site 570. Since these same anomalous pore water chemistry values also exist at Sites 496 and 497, it was calculated that the 400 km^2 area defined by these holes would contain 120 TCF of gas. We have concluded that pore water chemistry of DSDP Leg 67 and 68 holes was not a sufficiently accurate indicator to be used for volumetric assessments based on the disagreement of pore water chemistry data with geological data.

Although many holes were drilled offshore of Guatemala with no evidence of gas hydrates, the high concentration of gas hydrates raises our estimate of the probable occurrence of gas hydrates to higher values than assumed for offshore of Mexico. Averaged over the entire continental slope, we estimate that 2% of the sediment is occupied by gas hydrates. Using the same pore occupancy figures derived for offshore Mexico hydrates the quantity of gas in gas hydrates of the continental slope of Guatemala is estimated at:

$$5 \times 10^{10}\ m^2 \text{ area} \times 400 \text{ m sediment thickness} \times$$
$$2\% \text{ gas hydrate vertical extent} \times 13\% \text{ hydrates} \times 50\% \text{ porosity} \times$$
$$150 \text{ volume gas: volume hydrates} = 4 \times 10^{12}\ m^3 = 135 \text{ TCF.}$$

The figure derived for Guatemalan hydrates is much greater than for offshore Mexico based on the occurrence of gas hydrates where no BSRs are evident offshore of Guatemala, and the skewing of the probable vertical extent of gas hydrates based on the recovery of abundant gas hydrates of Site 570.

Offshore Costa Rica and Nicaragua

Seismic evidence for hydrates abounds in the sothern part of the study region, but only one hole has been drilled there. That hole (DSDP Site 565) did recover gas hydrates from three intervals.

Bottom simulating reflectors are common on the limited number of seismic lines available for offshore of Costa Rica and Nicaragua (Figure 49). About 35% of the 40,000 km^2 continental slope of this area is underlain by BSRs. The gas contained in a 1 m thick gas hydrate layer constituting the BSR offshore of Costa Rica and Nicaragua is:

$$1.3 \times 10^{10} \text{ m area} \times 1 \text{ m thickness} \times 50\% \text{ hydrates} \times 50\% \text{ porosity} \times$$
$$150 \text{ volume gas:volume hydrate} = 5 \times 10^{11}\ m^3 = 17 \text{ TCF}$$

The volume of gas represented by gas hydrate layers of various thicknesses coincident with the BSR is:

1 m =	$5 \times 10^{11}\ m^3$	=	17 TCF
2 m =	$1 \times 10^{12}\ m^3$	=	34 TCF
5 m =	$2.5 \times 10^{12}\ m^3$	=	85 TCF
10 m =	$5 \times 10^{11}\ m^3$	=	170 TCF

Drilling revealed gas hydrates at two intervals at Site 565. The nodular chunks are difficult to quantify in terms of percentage of core represented by hydrates. The occurrences appeared to be associated with ash layers 10 cm

thick. Considering the great uncertainty posed by only one sample hole and the similarity of the recovered hydrates with those from Leg 66, the same volume distribution of gas hydrates is assigned, 0.2%. Since no BSR is found at Site 565, gas hydrates are more widely distributed than BSRs; we estimate hydrates are in place over 150% of the BSR coverage. Thus the volume of gas contained in gas hydrates is:

$$1.3 \times 10^{10}\ m^2 \text{ BSR area} \times 1.5 \text{ hydrate to BSR} \times 600 \text{ m average thickness of gas hydrate stability zone} \times 0.2\% \times 13\% \text{ gas hydrates} \times 50\% \text{ porosity} \times 150 \text{ volume gas to volume hydrate} = 2.3 \times 10^{11}\ m^3 = 8 \text{ TCF}$$

Conclusions

Gas hydrates were recovered from sediments of the continental slope of the Middle America Trench. Their presence was confirmed by the quantity of gas released upon dissociation, their temperature, and physical properties. Recovered samples ranged from interstitial crystals, to chunks filling fractures in sediments, to one core of massive gas hydrate. Based on these recoveries the Middle America Trench study region presents the greatest quantity of direct information on the geological environments of offshore gas hydrates.

Offshore of Mexico gas hydrates were recovered as loose volcanic sediment cemented by interstitial gas hydrates. Additionally, chunks of gas hydrate were recovered from fractures. Frozen material which was not positively identified as gas hydrate was also recovered. Abundant hydrocarbon gas was found in cores with no gas hydrates.

Offshore of Costa Rica, a gas hydrate was recovered from a single drill hole. The material was associated with both fractures and a vitric sand.

Offshore of Guatemala, gas hydrates were drilled in the lower continental slope and upper continental slope. The lower slope location produced nodular samples from a sandy volcanic ash layer. On the upper slope gas hydrates were recovered as chunks apparently from fractures at DSDP Sites 497 and 568. These recoveries were isolated and restricted to 360 to 405 m depths, even though geochemistry suggested that hydrates should be found at shallower intervals. At Site 570, interstitial, fracture-filling, and massive gas hydrates were all recovered.

Seismic evidence indicates that gas hydrates are probably widespread throughout the study region. Bottom simulating reflectors (BSRs) are found in high quality seismic lines of the continental slope. Limited seismic coverage restricts mapping of BSR distribution to a few small areas. However, parts of the study region between areas surveyed probably also have abundant BSRs. A previously unreported area of abundant BSRs was discovered in this study.

Decreases in the chloride ion content and increases in ^{18}O content of pore water with depth is evident at some drill holes in the Middle America Trench study region. This pattern has been attributed to gas hydrate presence. Detailed analysis of the data suggests that only a portion of the observed chemical anomalies can be attributed to gas hydrate dissociation.

The massive gas hydrate recovered at Site 570 may require unusual geological conditions to form. One published model of massive gas hydrate

formation involves trapping methane by a lithological seal concurrent with rapid Tertiary uplift. Another theory holds that massive gas hydrate formed in open space and permeable fractures in and adjacent to a fault. The geological and geochemical evidence overwhelmingly supports the fault-controlled model.

Presence of permeable lithologies and abundant hydrocarbon supplies appear to control gas hydrate occurrences in the Middle America Trench study region. Sedimentation rate has no direct influence. There is evidence that structural deformation may enhance gas hydrate formation, but no clear link can be proven.

Estimates of gas resources in gas hydrates in the study region are speculative. Seismic evidence indicates widespread gas hydrate layers at the base of the gas hydrate stability zone. Lack of penetration of the base of the stability zone precludes accurate estimation of the degree of gas hydrate development. Drilling well above the base of the zone indicates that gas hydrates do not occur regularly. However, the abundant gas hydrates at Site 570 indicate that some areas of the study region have thicknesses and concentrations of gas hydrates that may have economic value in the future.

REFERENCES

Allan, J.F., 1986, Geology of the northern Colima and Zacoalco Grabens, southwest Mexico: Geol. Soc. Am. Bull., v. 97, p. 473 - 485.

Aubouin, J., Azema, J., Carfantan, J-Ch., Demant, A., Rangin, C., Tardy, M., and Tournon, J., 1982, The Middle America Trench in the geological framework of Central America, in Aubouin, J., von Huene, R., et al., Initial Reports of the Deep Sea Drilling Project, v. 67: U.S. Govt. Printing Office, Washington, p. 747 - 758.

Aubouin, J., and von Huene, R., 1985, Summary: Leg 84, Middle America Trench transect off Guatemala and Costa Rica, in von Huene, R., Aubouin, J., et al., Initial Reports of the Deep Sea Drilling Project, v. 84: U.S. Govt. Printing Office, Washington, p. 939 - 960.

Aubouin, J., von Huene, R., Azema, J., Coulbourn, W.T. Cowan, D.S., Curiale, J.A., Dengo, C.A., Faas, R.W., Harrison, W., Hesse, R., Ladd, J.W., Mazylov, H., Shiki, T., Thompson, P.R., Westberg, M.J., 1982, Initial Reports of the Deep Sea Drilling Project, v. 67: U.S. Govt. Printing Office, Washington, 799 p.

Azemà, J., Bourgois, J., Baumgartner, P.O., Tournon, J., Desmet, A., and Aubouin, J., 1985, A tectonic cross-section of the Costa Rican Pacific littoral as a key to the structure of the landward slope of the Middle America Trench off Guatemala, in von Huene, R., Aubouin, J., et al., Initial Reports of the Deep Sea Drilling Project, v. 84: U.S. Govt. Printing Office, Washington, p. 831 - 850.

Baltuck, M., von Huene, R., and Arnott, R.J., 1985, Sedimentology of the western continental slope of Central America, in von Huene, R., Aubouin, J., et al., Initial Reports of the Deep Sea Drilling Project, v. 84: U.S. Govt. Printing Office, Washington, p. 921 - 938.

Bouma, A.H., Stelting, C.E., and Feeley, M.H., 1983, High resolution seismic reflection profiles, in Bally, A.W., ed., Seismic expression of structural styles - a picture and work atlas: Am. Assoc. Petroleum Geologists Studies in Geology 15, v. 1, p. 2.1-1 to 2.1-23.

Brassell, S.C., Eglinton, G., and Maxwell, J.R., 1982, Preliminary lipid analyses of two quaternary sediments from the Middle America Trench, southern Mexico transect, Deep Sea Drilling Project Leg 66, in Watkins, J.S., Moore, J.C., et al., Initial Reports of the Deep Sea Drilling Project, v. 66: U.S. Govt. Printing Office, Washington, p. 557 - 580.

Brooks, J.M., Jeffrey, W.A., McDonald, T.J., Pflaum, R.C., and Kvenvolden, K.A., 1985, Geochemistry of hydrate gas and water from Site 570, Deep Sea Drilling Project Leg 84, in von Huene, R., Aubouin, J., et al., Initial Reports of the Deep Sea Drilling Project, v. 84: U.S. Govt. Printing Office, Washington, p. 699 - 704.

Burbach, G.V., Frohlich, C., Pennington, W.D., and Matumoto, T., 1984, Seismicity and tectonics of the subducted Cocos plate: Journal of Geophysical Research, v. 89, p. 7719 - 7735.

Burkart, B., 1978, Offset across the Polochic fault of Guatemala and Chiapis, Mexico: Geology, v. 6, p. 328 - 332.

Burkart, B., 1983, Neogene North American-Caribbean plate boundary across northern Central America: offset along the Polochic fault: Tectonophysics, v. 99, p. 251 - 270.

Burkart, B., and Self, S., 1985, Extension and rotation of crustal blocks in northern Central America and effect on the volcanic arc: Geology, v. 13, p. 22 - 26.

Case, J.E., and Holcombe, T.L., 1980, Geologic-Tectonic map of the Caribbean region; U.S. Geol. Survey map I-1100, Scale 1:2,500,000.

Chambers, R.L., and Erdman, J.G., 1982, Elemental composition and petroleum-generating potential of the methylene chloride extracts from Leg 66 samples, in Watkins, J.S., Moore, J.C., et al., Initial Reports of the Deep Sea Drilling Project, v. 66: U.S. Govt. Printing Office, Washington, p. 581 - 588.

Claussen, W.F., and Polglase, C.M., 1952, Solubilities and structures in aqueous aliphatic hydrocarbon solutions: J. Chem. Phys., v. 74, p. 4817 - 4819.

Claypool, G.E. Presley, B.J., and Kaplan, I.R., 1973, Gas analyses in sediment samples from legs 10, 11, 13, 15, 18 and 19, in Initial reports of the Deep Sea Drilling Project, v. 19: Washington, U.S. Govt. Printing Office, p. 879, 884.

Claypool, G.E., and Kaplan, I.R., 1974, The origin and distribution of methane in marine sediments, in Kaplan, I.R., ed., Natural Gases in Marine Sediments: Plenum Press, N.Y., p. 94 - 129.

Claypool, G.E., and Threlkeld, C.N., 1983, Anoxic diagenesis and methane generation in sediments of the Blake Outer Ridge, Deep Sea Drilling Project Site 533, Leg 76, in Sheridan, R.E., et al., Initial Reports of the Deep Sea Drilling Project, v. 76: 76: U.S. Govt. Printing Office, Washington, p. 391 - 402.

Claypool, G.E., and Threlkeld, C.N., 1985, Methane hydrate in slope sediments on west coast of Central America (Abs.): Amer. Assoc. Petroleum Geologists Bull., v. 69, p. 245.

Claypool, G.E., Threlkeld, P.N., Mankiewicz, P.N., Arthur, M.A., and Anderson, T.F., 1985, Isotopic composition of interstitial fluids and origin of methane in slope sediment of the Middle America Trench, Deep Sea Drilling Project Leg 84, in von Huene, R., Aubouin, J., et al., Initial Reports of the Deep Sea Drilling Project, v. 84: U.S. Govt. Printing Office, Washington, p. 683 - 692.

Claypool, G.E., and Kvenvolden, K.A., 1983, Methane and other hydrocarbon gases in marine sediment: Annual Reviews of Earth and Planetary Science, v. 11, p. 299 - 327.

Connard, G.G., Couch, R.W., Ness, G.E., Roy, J., Peper, J.S., Sanchez, O., 1985, Bathymetry Southern Mexico to Costa Rica margin, in Ladd, J.W., and Buffler, R.T., eds., Middle America Trench off western Central America, Atlas 7. Ocean Margin Drilling Program, Regional Atlas Series: Marine Science International, Woods Hole, MA, sheet 1.

Coulbourn, W.T., 1982, Stratigraphy and structures of the Middle America Trench: Deep Sea Drilling Project Leg 67 transect off Guatemala, in Aubouin, J., von Huene, R., et al., Initial Reports of the Deep Sea Drilling Project, v. 67: U.S. Govt. Printing Office, Washington, p. 691 - 706.

Coulbourn, W.T., Hesse, R., Azema, J., and Shiki, T., 1982, A summary of the sedimentology of Deep Sea Drilling Project Leg 67 sites: The Middle America Trench and Slope off Guatemala--an active margin transect, in Aubouin, J., von Huene, R., et al., Initial Reports of the Deep Sea Drilling Project, v. 67: U.S. Govt. Printing Office, Washington, p. 759 - 774.

Cowan, D.S., 1982, Origin of "vein structure" in slope sediments on the inner slope of the Middle America Trench off Guatemala, in Aubouin, J., von Huene, R., et al., Initial Reports of the Deep Sea Drilling Project, v. 67: U.S. Govt. Printing Office, Washington, p. 645 - 650.

Cross, T.A., and Pilger, R.H., 1982, Controls of subduction geometry, location of magmatic arcs, and tectonics of arc and back-arc regions: Geological Society of America Bull., v. 93, p. 545 -562.

Crowe, J.C., and Buffler, R.T., 1983, Regional seismic reflection profiles across the middle America trench and convergent margin of Costa Rica, in Bally, A.W., ed., Seismic expression of structural styles: Amer. Assoc. Petroleum Geologists Studies in Geology no. 15, v. 3.

Crowe, J.C., and Buffler, R.T., 1985, Multichannel seismic record across the Middle America trench and Costa Rica convergent margin, CR-7, 1985, in Ladd, J.W., and Buffler, R.T., eds., Middle America Trench off western Central America, Atlas 7. Ocean Margin Drilling Program, Regional Atlas Series: Marine Science International, Woods Hole, MA, sheet 10.

Culberson, O.L., and McKetta, J.J., 1951, Phase equilibria in hydrocarbon-water systems, III--The solubility of methane in water at pressures to 10,000 psia: Am. Inst. Mining Engineers Petroleum Transactions, v. 192, p. 223 - 226.

Curiale, J.A., and Harrison, W.E., 1982, Beta-sitosterol and stigmasterol in slope sediments, in Aubouin, J., von Huene, R., et al., Initial Reports of the Deep Sea Drilling Project, v. 67: U.S. Govt. Printing Office, Washington, p. 587 - 590.

Davidson, D.W., Leaist, D.G., and Hesse, R., 1983, Oxygen-18 enrichment in water of a clathrate hydrate: Geochimica et Cosmochimica Acta, v. 47, p. 2293 - 2295.

Davidson, D.W., and Ripmeester, J.A., 1978, Clathrate ices - recent results: Journal of Glaciology, v. 21, p. 33 - 49.

Dean, B.W., and Drake, C.L., 1978, Focal mechanism solutions and tectonics of the Middle America arc: Jour. Geol., v. 86, p. 111 - 128.

de Boer, R.B., Houbold, J.J.H.C., and Lagrand, J., 1985, Formation of gas hydrates in a permeable medium: Geologie en Mijnbouw, v. 64, p. 245 - 249.

Dengo, C.A., 1982, A structural analysis of cores from the Leg 67 transect across the Middle America Trench--offshore Guatemala, in Aubouin, J., von Huene, R., et al., Initial Reports of the Deep Sea Drilling Project, v. 67: U.S. Govt. Printing Office, Washington, p. 651 - 668.

Dominic, K.L, and Barlow, D.A., 1986, Geological occurrences of gas hydrates at the Blake Outer Ridge, Western North Atlantic: DOE-METC Research Report, 35 p.

Drummond, K.J., 1983, Geologic map of the Circum-Pacific region, northeast quadrant: Am. Assoc. Petroleum Geologists, Tulsa.

Drummond, K.J., 1985, Plate tectonic map of the Circum-Pacific region, northeast quadrant: Am. Assoc. Petroleum Geoloists.

Enns, T., Scholander, P.F., and Bradstreet, E.D., 1965, Effect of hydrostatic pressure on gases dissolved in water: J. Am. Chem. Soc., v. 69, p. 389 - 391.

Filewicz, M.V., 1985, Calcareous nannofossil biostratigraphy of the Middle America Trench and slope, Deep Sea Drilling Project Leg 84, in von Huene, R., Aubouin, J., et al., Initial Reports of the Deep Sea Drilling Project, v. 84: U.S. Govt. Printing Office, Washington, p. 339 - 362.

Finley, P., and Krason, J., 1986, Basin Analysis, Formation and Stability of Gas Hydrates in the Colombia Basin; Geological Evolution and Analysis of Confirmed or Suspect Gas Hydrate Localities, v. 7: U.S. Department of Energy, DOE/MC/21181-1950 (DE86006637), 132 p.

Fisher, R.L., 1961, Middle America Trench: topography and structure: Geol. Soc. Am. Bull., v. 72, p. 703 - 720.

Galimov E.M., and Shabaeva, I. Ju., 1985, Carbon isotope composition of CH_4 and CO_2 in sediments of the Middle America Trench, in von Huene, R., Aubouin, J., et al., Initial Reports of the Deep Sea Drilling Project, v. 84: U.S. Govt. Printing Office, Washington, p. 693 - 694.

Gieskes, J.M., Johnston, K., and Boehm, M., 1985, Appendix: Interstitial water studies, Leg 66, in von Huene, R., Aubouin, J., et al., Initial Reports of the Deep Sea Drilling Project, v. 84: U.S. Govt. Printing Office, Washington, p. 961 - 967.

Gilbert, D., and Cunningham, R., 1985, Organic facies variations in sediments from Leg 84, off Guatemala, in von Huene, R., Aubouin, J., et al., Initial Reports of the Deep Sea Drilling Project, v. 84: U.S. Govt. Printing Office, Washington, p. 739 - 744.

Glacon, G., and Bourgois, J., 1985, Upper Oligocene to recent planktonic foraminiferal remains in sediments of the inner wall of the Middle America Trench with special emphasis on Globorotalia, in von Huene, R., Aubouin, J., et al., Initial Reports of the Deep Sea Drilling Project, v. 84: U.S. Govt. Printing Office, Washington, p. 473 - 514.

Glew, D.N., 1960, The gas hydrate of bromochlorodifluoromethane: Canadian J. Chem., v. 38, p. 208 - 2212.

Glew, D.N., 1962, Aqueous solubility and the gashydrates. The methane-water system: J. Phys. Chem., v. 66, p. 605 - 609.

Harrison, W.E., and Curiale, J.A., 1982, Gas hydrates in sediments of holes 497 and 498A, Deep Sea Drilling Project Leg 67, in Aubouin, J., von Huene, R., et al., Initial Reports of the Deep Sea Drilling Project, v. 67: U.S. Govt. Printing Office, Washington, p. 591 - 594.

Harrison, W.E., Hesse, R., and Gieskes, J.M., 1982, Relationship between sedimentary facies and interstitial water chemistry of slope, trench, and Cocos Plate sites from the Middle America Trench transect, active margin off Guatemala, Deep Sea Drilling Project Leg 67, in Aubouin, J., von Huene, R., et al., Initial Reports of the Deep Sea Drilling Project, v. 67: U.S. Govt. Printing Office, Washington, p. 603 - 616.

Helm, R., 1985, Mineralogy and diagenesis of slope sediments offshore Guatemala and Costa Rica, Deep Sea Drilling Project Leg 84, in von Huene, R., Aubouin, J., et al., Initial Reports of the Deep Sea Drilling Project, v. 84: U.S. Govt. Printing Office, Washington, p. 571 - 594.

Helm, R., and Vollbrecht, A., 1985, Brittle-ductile shear zones in slope sediments off Guatemala, Sites 568 and 569, Deep Sea Drilling Project Leg 84, in von Huene, R., Aubouin, J., et al., Initial Reports of the Deep Sea Drilling Project, v. 84: U.S. Govt. Printing Office, Washington, p. 625 - 632.

Hesse, R., and Harrison, W.E., 1981, Gas hydrates (clathrates) causing pore-water freshening and oxygen isotope fractionation in deep-water sedimentary sections of terrigenous continental margins: Earth Planet. Sci. Lett., v. 55, p. 453 - 462.

Hesse, R., Lebel, J., and Gieskes, J.M., 1985, Interstitial water chemistry of gas-hydrate-bearing sections of the Middle America Trench Slope, Deep Sea Drilling Project Leg 84, in von Huene, R., Aubouin, J., et al., Initial Reports of the Deep Sea Drilling Project, v. 84: U.S. Govt. Printing Office, Washington, p. 727 - 738.

Hilde, T.W.C., 1983, Sediment subduction versus accretion around the Pacific: Tectonophysics, v. 99, p. 381 - 397.

Hunt, J.M., 1979, Petroleum geochemistry and geology: San Francisco, W.H. Freeman and Co.

Hunt, J.M., Huc, A.Y., and Whelan, J.K., 1980, Generation of light hydrocarbons in sedimentary rocks: Nature, v. 288, 670 - 688.

Ibach, L.E.J., 1982, Relationship between sedimentation rate and total organic carbon content in ancient marine sediments: Am. Assoc. Petroleum Geologists Bull., v. 68, p. 170 - 188.

Jeffrey, A.W.A., Pflaum, R.C., McDonald, T.J., Brooks, J.M., and Kvenvolden, K.A., 1985, Isotopic analysis of core gases at Sites 565-570, Deep Sea Drilling Project Leg 84, in von Huene, R., Aubouin, J., et al., Initial Reports of the Deep Sea Drilling Project, v. 84: U.S. Govt. Printing Office, Washington, p. 719 - 726.

Jenden, P.D., and Geiskes, J.M., 1983, Chemical and isotopic composition of interstitial water from Deep Sea Drilling Project Sites 533 and 534, in Sheridan, R.E., et al., Initial Reports of the Deep Sea Drillling Project, v. 76: U.S. Govt. Printing Office, Washington, p. 453 - 462.

Karig, D.W., 1974, Tectonic erosion of trenches: Earth Planet. Sci. Lett., v. 21, p. 209 - 212.

Karig, D.E., Cardwell, R.K., Moore, G.F., and Moore, D.G., 1978, Late Cenozoic subduction and continental margin truncation along the northern Middle America Trench: Geol. Soc. Am. Bull., v. 89, p. 265 - 276.

Kennicutt II, M.C., Brooks, J.M., McDonald, T.J., and Pflaum, R.C., 1985, Nonvolatile organic matter at Sites 565-570, Deep Sea Drilling Project Leg 84, in von Huene, R., Aubouin, J., et al., Initial Reports of the Deep Sea Drilling Project, v. 84: U.S. Govt. Printing Office, Washington, p. 705 - 718.

Kester, D.R., 19175, Dissolved gases other than CO_2, in Riley, J.P., and Skirrow, G., eds., Chemical Oceanography: New York, Academic Press, p. 498 - 556.

Klitgord, K.D., and Mammerickx, J., 1982, Northern East Pacific Rise: magnetic anomaly and bathymetric framework: Jour. Geophys. Research, v. 87, p. 6725 - 6750.

Krason, J., and Ciesnik, M., 1986, Basin Analysis, Formation and Stability of Gas Hydrates in the Panama Basin; Geological Evolution and Analyses of Confirmed or Suspected Gas Hydrate Locations, v. 7: U.S. Department of Energy, DOE/MC/21181-1950 (DE86001057), 85 p.

Krason, J., Finley, P., and Rudloff, B., 1986, Basin Analysis, Formation and Stability of Gas Hydrates in the Western Gulf of Mexico; Geological Evolution and Analysis of Confirmed or Suspected Gas Hydrate Localities, v. 3: U.S. Department of Energy, DOE/MC/21181-1950 (DE86001057), 168 p.

Kuuskraa, V.A., Hammershaimb, E.C., Holder, G.D., Sloan, E.D., 1983, Handbook of Gas Hydrate Properties and Occurrence: U.S. Department of Energy, DOE/MC/19239-1546, U.S. Govt. Printing Office, Washington, 234 p.

Kvenvolden, K.A., 1985, Comparison of marine gas hydrates in sediments of an active and passive continental margin: Marine Geology, v. 2, p. 65 - 71.

Kvenvolden, K.A., and Claypool, G.E., 1985, Geochemical and geological factors in the formation of marine gas hydrates, in Proceedings of the Unconventional Gas Recovery Gas Hydrates Program Peer Review Session, April 24 - 25, 1985, Bethesda, Maryland: U.S. Department of Energy, Office of Oil, Gas, and Shale Technology, p. 110 - 143.

Kvenvolden, K.A., Claypool, G.E., Threlkeld, C.N., and Sloan, E.D., 1984, Geochemistry of a naturally occurring massive marine gas hydrate: Organic Geochemistry, v. 6, p. 703 - 713.

Kvenvolden, K.A., and McDonald, T.J., 1985, Gas hydrates of the Middle America Trench--Deep Sea Drilling Project Leg 84, in von Huene, R., Aubouin, J., et al., Initial Reports of the Deep Sea Drilling Project, v. 84: U.S. Govt. Printing Office, Washington, p. 667 - 682.

Ladd, J.W., and Buffler, R.T., 1985, Introduction in Ladd, J.W., and Buffler, R.T., eds., Middle America Trench off western Central America, Atlas 7. Ocean Margin Drilling Program, Regional Atlas Series: Marine Science International, Woods, Hole, MA.

Ladd, J.W., Ibrahim, A.K., McMillen, K.J., Latham, G.V., and von Huene, R.E., 1982, Interpretation of seismic-reflection data of the Middle America Trench offshore Guatemala, in Aubouin, J., von Huene, R., et al., Initial Reports of the Deep Sea Drilling Project, v. 67: U.S. Govt. Printing Office, Washington, p. 675 - 690.

Ladd, J.W., and Schroder, S., 1985, Seismic stratigraphy of the continental shelf offshore of Guatemala: Implications for vertical tectonics related to subduction, in von Huene, R., et al., Ijnitial Reports of the Deep Sea Drilling Project, v. 84: U.S. Govt. Printing Office, Washington, p. 879 - 894.

Ladd, J.W., Truchan, M., Talwani, M., Stoffa, P.L., Buhl, P., Hontz, R., Mauffret, A., and Westbrook, G., 1984, Seismic reflection profiles across the southern margin of the Caribbean, in Bonini, W.E., Hargraves, R.B., and Shagam, R., eds., The Caribbean-South American Plate Boundary and Regional Tectonics: Geological Society of America Memoir 162, p. 153 - 160.

Lisitzin, A.P., 1972, Sedimentation in the world ocean. Soc. Econ. Paleontol. Mineral. Spec. Publ., 17.

Lundberg, N., and Moore, J.C., 1982, Structural features of the Middle America Trench Slope off southern Mexico, Deep Sea Drilling Project Leg 66, in Watkins, J.S., Moore, J.C., et al., Initial Reports of the Deep Sea Drilling Project, v. 66: U.S. Govt. Printing Office, Washington, p. 793 - 814.

Lynn, W.S., and Lewis, B.T.R., 1976, Tectonic evolution of the northern Cocos plate: Geology,v. 4, p. 718 - 722.

Makogon, Y.F., 1974, Hydrates of Natural Gas (Trans. from Russian by W.J. Cieslewicz): Geoexplorers Associates, Denver, 178 p.

Makogon, Y.F., and Koblova, I.L., 1972, Rastvorimost gazov v vode pri nalichii gidratov (The solubility of gases in water in presence of gas hydrates): E.I. VNII Gas Prom, no. 22, p. 3 - 11.

Makogon, Y.F., Tsarev, V.I., Cherskiy, N.V., 1972, Formation of large natural gas fields in zones of permanently low temperatures: Doklady of the Academy of Sciences USSR Earth Sciences section, v. 205, p. 215 - 218.

Manheim, F.T., Sayles, F.L., and Waterman, L.S., 1973, Interstitial water studies on small core samples, Deep Sea Drilling Project Leg 10, in Initial reports of the Deep Sea Drilling Project, v. 10: U.S. Govt. Printing Office, Washington, p. 615 - 623.

McDougall, K., 1985, Miocene to Pleistocene benthic foraminifers and paleoceanography of the Middle America Slope, Deep Sea Drilling Project Leg 84, in von Huene, R., Aubouin, J., et al., Initial Reports of the Deep Sea Drilling Project, v. 84: U.S. Govt. Printing Office, Washington, p. 363 - 418.

McMillen, K.J., and Bachman, S.B., 1982, Bathymetric and tectonic evolution of the southern Mexico active margin, Deep Sea Drilling Project Leg 66, in Watkins, J.S., Moore, J.C., et al., Initial Reports of the Deep Sea Drilling Project, v. 66: U.S. Govt. Printing Office, Washington, p. 815 - 824.

Mammerickx, J., and Klitgord, K.D., 1982, Northern East Pacific Rise: Evolution from 25 m.y.B.P. to the present: Journal of Geophysical Research, v. 87, p. 6751 - 6759.

Manheim, F.T., Sayles, F.L., and Waterman, L.S., 1973, Interstitial water studies on small core samples, Deep Sea Drilling Project Leg 10, in Initial reports of the Deep Sea Drilling Project, v. 10: U.S. Govt. Printing Office, Washington, p. 615 - 623.

Mathews, M.A., 1982, Logging characteristics of methane hydrate [paper presented at December 15, 1982 meeting of SPWLA Denver Well Logging Society Chapter].

Mathews, M.A., 1983, Logging characteristics and methane gas estimate of methane hydrate deposits [paper presented at September 28, 1983 meeting of SPWLA Four Corners Well Logging Society Chapter].

Mathews, M.A., and von Huene, R., 1985, Site 570 methane hydrate zone, in von Huene, R., Aubouin, J., et al., Initial Reports of the Deep Sea Drilling Project, v. 84: U.S. Govt. Printing Office, Washington, p. 773 - 790.

Miller, S.L, 1974, The nature and occurrence of clathrate hydrates, in Kaplan, I.R., ed., Natural Gas in Marine Sediments: Plenum Press, New York, p. 151 - 177.

Milton, D.J., 1976, Methane hydrate in the sea floor--a significant resource?, in Future supplies of nature-made petrolem and gas: proceedings of the First UNITAR Conference on Energy and the Future, and the Second IIASA Conference on Energy Resources, July 5 - 16, 1976, Luxemburg, Austria, p. 927 - 943.

Minster, J.B., and Jordan, T.H., 1978, Present-day plate motions: Jour. Geophys. Research, v. 83, p. 5331 - 5334.

Molnar, P., and Sykes, L.R., 1969, Tectonics of the Caribbean and Middle America regions from focal mechanisms and seismicity: Geol. Soc. Am. Bull., v. 80, p. 1639 - 1684.

Mook, W.G., Bommerson, J.C., and Staverman, W.H., 1974, Carbon isotope fractionation between dissolved bicarbonate and gaseous carbon dioxide: Earth and Planetary Science Lett., v. 22, p. 169 - 176.

Moore, G.F., Shipley, T.H., and Lonsdale, P.F., 1986, Subduction erosion versus sediment offscraping at the toe of the Middle America Trench off Guatemala: Tectonics, v. 5, p. 513 - 523.

Moore, J.C., Watkins, J.S., and Shipley, T.H., 1982, Summary of accretionary processes, Deep Sea Drilling Project Leg 66: offscraping, underplating, and deformation of the slope apron, in Watkins, J.S., Moore, J.C., et al., Initial Reports of the Deep Sea Drilling Project, v. 66: U.S. Govt. Printing Office, Washington, p. 825 - 836.

Morency, M., Mineau, R., Zeller, E., Dreschhoff, G., 1986, Are all fossil fuels really fossils: Oil and Gas Journal, June 2, 1986, p. 92 - 95.

Muehlberger, W.R., and Ritchie, A.W., 1975, Caribbean--Americas plate boundary in Guatemala and southern Mexico as seen on Skylab IV orbital photography: Geology, v. 3, p. 232 - 235.

Muller, P.S., and Suess, E., 1979, Productivity, sedimentation rate and sedimentary organic carbon content in the oceans: Deep Sea Research, v. 26, p. 1347 - 1362.

Nixon, G.T., 1982, The relationship between Quaternary volcanism in central Mexico and the seismicity and structure of subducted ocean lithosphere: Geological Society of America Bulletin, v. 93, p. 514 - 523.

Ogawa, Y. and Miyata, Y., 1985, Vein structure and its deformational history in the sedimentary rocks of the middle America Trench Slope off Guatemala, Deep Sea Drilling Project Leg 84, in von Huene, R., Aubouin, J., et al., Initial Reports of the Deep Sea Drilling Project, v. 84: U.S. Govt. Printing Office, Washington, p. 811 - 830.

Ogawa, Y., Fujioka, K., Nishiyama, T., Uehara, S., and Nakagawa, M., 1985, Ophiolitic rocks of the Middle America Trench landward slope off Guatemala: Deformational characteristics and tectonic significance, in von Huene, R., et al., Initial reports of the Deep Sea Drilling Project, v. 84: U.S. Govt. Printing Office, Washington, p. 791 - 810.

O'Neil, J.R., 1968, Hydrogen and oxygen isotope fractionation between ice and water: J. Phys. Chem., v. 72, p. 3683 - 3684.

Rice, D.D., and Claypool, G.E., 1981, Generation, accumulation, and resource potential of biogenic gas: Am. Assoc. Petroleum Geologists, v. 65, p. 5 - 24.

Ritter, U., 1984, The influence of time and temperature on vitrinite reflectance: Organic Geochemistry, v. 6, p. 473 - 480.

Schoell, M., 1983, Genetic characterization of natural gas: Am. Assoc. Petroleum Geologists Bull., v. 67, p. 2225 - 2238.

Schoell, M., 1984, Recent advances in petroleum isotope geochemistry: Organic Geochemistry, v. 6, p. 645 - 663.

Scott, M.I., Randolph, P.L., and Pangborn, J.B., 1980, Assessment of methane hydrates: Institute of Gas Technology Report No. GR1-79-0070.

Seely, D.R., 1979, The evolution of structural highs bordering major forearc basins, in Watkins, J.S., Montadert, L., and Dickerson, P.W., eds., Geological and geophysical investigations of continental margins: Amer. Assoc. Petroleum Geologists, Memoir 29, p. 245 - 260.

Seely, D.R., Vail, P.R., and Walton, G.G., 1974, Trench slope model, in Burk, C.A., and Drake, C.L., eds., The geology of continental margins: New York, Springer-Verlag, p. 249 - 260.

Shephard, L.E., Bryant, W.R., and Chiou, W.A., 1982, Geotechnical properties of Middle America Trench sediments, Deep Sea Drilling Project Leg 66, in Watkins, J.S., Moore, J.C., et al., Initial Reports of the Deep Sea Drilling Project, v. 66: U.S. Govt. Printing Office, Washington, p. 475 - 504.

Shephard, L.E., and McMillen, K.J., 1982, Sedimentation rates of the southern Mexico continental margin, Deep Sea Drilling Project Leg 66, in Watkins, J.S., Moore, J.C., et al., Initial Reports of the Deep Sea Drilling Project, v. 66: U.S. Govt. Printing Office, Washington, p. 445 - 452.

Shipley, T.H., 1982, Seismic facies and structural framework of the southern Mexico continental margin, in Watkins, J.S., Moore, J.C., et al., Initial Reports of the Deep Sea Drilling Project, v. 66: U.S. Govt. Printing Office, Washington, p. 775 - 792.

Shipley, T.H., and Didyk, B.M., 1982, Occurrence of methane hydrates offshore southern Mexico, in Watkins, J.S., Moore, J.C., et al., Initial Reports of the Deep Sea Drilling Project, v. 66: U.S. Govt. Printing Office, Washington, p. 547 - 556.

Shipley, T.H., Houston, M.H., Buffler, R.T., Shaub, F.J., McMillen, K.J., Ladd, J.W., and Worzel, J.L., 1971, Seismic evidence for widespread possible gas hydrate horizons on continental sloes and rises: Am. Assoc. Petroleum Geologists Bull., v. 63, p. 2204 - 2213.

Shipley, T.H., and Moore, G.F., 1986, Sediment accretion, subduction, and dewatering at the base of the trench slope off Costa Rica: J. Geophys. Research, v. 99, p. 2019 - 2028.

Shipley, T.H., and Shephard, L.E., 1982, Temperature data from the Mexico drilling area: report on logging and inhole temperature experiments, in Watkins, J.S., Moore, J.C., et al., Initial Reports of the Deep Sea Drilling Project, v. 66: U.S. Govt. Printing Office, Washington, p. 771 - 774.

Silver, E.A., Ellis, M.J., Breen, N.A., and Shipley, T.H., 1985, Comments on the growth of accretionary wedges: Geology, v. 13, p. 6 - 9.

Sloan, E.D., 1985, Shore-based laboratory experimental measurements on a gas hydrate sample recovered at Site 570, in von Huene, R., et al., Initial reports of the Deep Sea Drilling Project, v. 84: U.S. Govt. Printing Office, Washington, p. 595 - 598.

Stahl, W., 1977, Carbon and nitrogen isotopes in hydrocarbon research and exploration. Chem. Geol., v. 20, p. 121 - 149.

Stahl, W., and Carey, B.D., 1975, Source rock identification by isotope analyses of natural gases from fields in the Val Verde and Delaware basins, West Texas: Chem. Geol., v. 16, p. 257 - 267.

Stoiber, R.E., and Carr, M.J., 1973, Quaternary volcanic and tectonic segmentation of Central America: Bulletin Volcanologique, v. 37, p. 304 - 325.

Stoll, R.D., 1974, Acoustic waves in saturated sediments, in Hampton, L., ed., Physics of sound in marine sediments: Plenum, N.Y., p. 19 - 39.

Stone, S.M., and Keller, G., 1985, Planktonic foraminiferal biostratigraphy of the Middle America Trench Region, Deep Sea Drilling Project Leg 84, in von Huene, R., Aubouin, J., et al., Initial Reports of the Deep Sea Drilling Project, v. 84: U.S. Govt. Printing Office, Washington, p. 419 - 472.

Summerhayes, C.P., and Gilbert, D., 1982, Distribution, origin, and hydrocarbon potential of organic matter in sediments from the Pacific margin of Guatemala, in Aubouin, J., von Huene, R., et al., Initial Reports of the Deep Sea Drilling Project, v. 67: U.S. Govt. Printing Office, Washington, p. 595 - 600.

Summerhayes, C.P., and Gilbert, D., 1982, Distribution, origin, and hydrocarbon potential of organic matter in sediments from the Pacific margin of southern Mexico, in Watkins, J.S., Moore, J.C., et al., Initial Reports of the Deep Sea Drilling Project, v. 66: U.S. Govt. Printing Office, Washington, p. 541 - 546.

Taylor, E., and Bryant, W.R., 1985, Geotechnical properties of sediments from the Middle America Trench and Slope, in von Huene, R., Aubouin, J., et al., Initial Reports of the Deep Sea Drilling Project, v. 84: U.S. Govt. Printing Office, Washington, p. 745 - 766.

Tissot, B.P., and Welte, D.H., 1978, Petroleum Formation and Occurrence: Springer-Verlag, Heidelberg, 624 p.

Truchan, M., and Larson, R.L., 1973, Tectonic lineaments on the Cocos Plate: Earth and Planetary Science Letters, v. 17, p. 426 - 432.

Vail, P.R., and Mitchum, R.M., 1979, Global cycles of relative changes of sea level from seismic stratigraphy, in Watkins, J.S., Montadert, L., and Dickerson, P.W., eds., Geological and geophysical investiations of continental margins: Am. Assoc. Petroleum Geologists, Memoir 29, p. 469 - 472.

Vail, P.R., Mitchum, R.M., and Thompson, S., 1977, Seismic stratigraphy and global changes of sea level, in Seismic stratigraphy - applications to hydrocarbon exploration: Am. Assoc. Petroleum Geologists Memoir 26, p. 83 - 97.

Volpe, A.M., Shipley, T.H., and Moore, G.F., 1985, A high resolution geophysical survey of Deep Sea Drilling Project Leg 84 Site 570, in von Huene, R., Aubouin, J., et al., Initial Reports of the Deep Sea Drilling Project, v. 84: U.S. Govt. Printing Office, Washington, p. 851- 860.

von Huene, R., 1985, Direct Measurement of pore fluid pressure, Leg 84, Guatemala and Costa Rica, in von Huene, R., Aubouin, J., et al., Initial Reports of the Deep Sea Drilling Project, v. 84: U.S. Govt. Printing Office, Washington, p. 767- 772.

von Huene, R., and Aubouin, J., 1982, Summary--Leg 67, Middle America Trench transect off Guatemala, in Aubouin, J., von Huene, R., et al., Initial Reports of the Deep Sea Drilling Project, v. 67: U.S. Govt. Printing Office, Washington, p. 759 - 793.

von Huene, R., Aubouin, J., Arnott, R.J., Baltuch, M., Bourgois, J., Filewicz, M., Helm, R., Kvenvolden, K.A., Lienert, B., MacDonald, T.J., McDougall, K., Ogawa, Y., Taylor, E., Winsborough, B., 1985, Initial reports of the Deep Sea Drilling Project, v. 84: U.S. Govt. Printing Office, Washington, 967 p.

von Huene, R., Ladd, J., and Norton, I., 1982, Geophysical observations of slope deposits, Middle America Trench off Guatemala, in Aubouin, J., von Huene, R., et al., Initial Reports of the Deep Sea Drilling Project, v. 67: U.S. Govt. Printing Office, Washington, p. 719 - 732.

von Huene, R., Miller, J., Taylor, D., and Blackman, D., 1985, A study of geophysical data along the Deep Sea Drilling Project active margin transect off Guatemala, in von Huene, R., Aubouin, J., et al., Initial Reports of the Deep Sea Drilling Project, v. 84: U.S. Govt. Printing Office, Washington, p. 895 - 910.

Waples, D.W., 1980, Time and temperature in petroleum formation: application of Lopatin's method: Am. Assoc. Petroleum Geologists Bull., v. 64, p. 916 - 926.

Watkins, J.S., McMillen, K.J., Bachman, S.B., Shipley, T.H., Moore, J.C., and Angevine, C., 1982, Tectonic synthesis, Leg 66: transect and vicinity, in Watkins, J.S., Moore, J.C., et al., Initial Reports of the Deep Sea Drilling Project, v. 66: U.S. Govt. Printing Office, Washington, p. 837 - 852.

Watkins, J.S., Moore, J.C., Bachman, S.B., Beghtel, F., Butt, A., Didyk, B.M., Dmitriev, Y., Leggete, J.K., Lundberg, N.F., McMillen, K.J., Niitshma, N., Rodriguez-Torres, R., Shephard, L.E., Shipley, T.H., Stephan, J., Stradner, H., 1982, Initial Reports of the Deep Sea Drilling Project, v. 66: U.S. Govt. Printing Office, Washington, 864 p.

Weiss, R.F., 1970, The solubility of nitrogen, oxygen, and argon in water and sea water: Deep Sea Research, v. 17, p. 721 - 735.

Wetlaufer, D.B., Malik, S.K., Stoller, L., and Coffin, R.L., 1964, Nonpolar group participation in the denaturation of proteins: J. Am. Chem. Soc., v. 86, p. 508 - 512.

Whelan, J.K., Hunt, J.M., Jasper, J., and Huc, A., 1984, Migration of C_1-C_8 hydrocarbons in marine sediments: Organic Geochemistry, v. 6, p. 683 - 694.

Wigley, T.M.L., Plummer, L.N., and Pearson, F.J., 1978, Mass transfer and carbon isotope evolution in natural water systems: Geochimica et Cosmochimica Acta, v. 42, p. 1117 - 1139.

Winsborough, B., and Abbott, W.H., 1985, Cenozoic diatom biostratigraphy of the Middle America Trench and Slope, Deep Sea Drilling Project Leg 84, in von Huene, R., Aubouin, J., et al., Initial Reports of the Deep Sea Drilling Project, v. 84: U.S. Govt. Printing Office, Washington, p. 515 - 532.

Wolf, M., 1982, Coal petrological studies of sediments from Sites 496, 499, and 500, Deep Sea Drilling Project Leg 67, Middle America Trench and Slope off Guatemala, in Aubouin, J., von Huene, R., et al., Initial Reports of the Deep Sea Drilling Project, v. 67: U.S. Govt. Printing Office, Washington, p. 601 - 602.

Woodcock, S.F., 1975, Crustal structure of the Tehuantepec Ridge and adjacent continental margins of southwestern Mexico and western Guatemala, Masters Thesis, Oregon State University, Corvallis, Oregon, 183 p.

Yamano, M., Uyeda, S., Aoki, Y., and Shipley, T.H., 1982, Estimates of heat flow derived from gas hydrates: Geology, v. 10, p. 339 - 343.